Gene Therapy for Male Infertility

by

Chatchanan Doungkamchan

Doctor of Medicine, Chulalongkorn University, Thailand, 2012

Submitted to the Graduate Faculty of the

School of Medicine in partial fulfillment

of the requirements for the degree of

Doctor of Philosophy

University of Pittsburgh

2020

UNIVERSITY OF PITTSBURGH

SCHOOL OF MEDICINE

This dissertation was presented

by

Chatchanan Doungkamchan

It was defended on

March 26, 2020

and approved by

Neil Hukriede, Professor, Department of Developmental Biology

William H. Walker, Associate Professor, Department of Obstetrics, Gynecology and Reproductive Sciences

Gregg E. Homanics, Professor, Department of Anesthesiology and Perioperative Medicine

Aleksandar Rajkovic, Professor, Department of Pathology and Obstetrics/Gynecology and Reproductive Sciences, University of California San Francisco

Dissertation Director: Kyle E. Orwig, Professor, Department of Obstetrics, Gynecology and Reproductive Sciences

Gene therapy for male infertility

Chatchanan Doungkamchan, PhD

University of Pittsburgh, 2020

Single gene defects have been associated with non-obstructive azoospermia patients and confirmed in infertile mouse models. Those defects can impact the function of testicular somatic cells (e.g., Sertoli cells) or germ cells. In an infertile Sertoli cell androgen receptor knockout (SCARKO) mouse model, I used adenovirus for in vivo delivery of an androgen receptor (AR) expression vector into Sertoli cells. I retrieved sperm three months later for intracytoplasmic sperm injection (ICSI). Four babies were born from two surrogate mothers, all of which were fertile and transgene-free. For germline gene therapy, I generated a mouse model (*Tex11-D435fs*) with an analogous mutation to one of our human patients. I transfected *Tex11-D435fs* spermatogonial stem cell (SSC) culture with CRISPR/Cas9 and an oligonucleotide template to correct the mutated sequence back to the sequence that is common in the human and mouse genome. Gene-corrected SSCs were transplanted into the testes of infertile recipients and established complete spermatogenesis. Sperm were competent to fertilize eggs using ICSI or IVF and produced healthy offspring. For large deletions where insertion of a transgene cassette is required, I used *Sohlh1-KO* mice with a three-exon deletion. Since $Sohlh1^{+/-}$ mice are fertile, I hypothesized that introducing one normal allele of *Sohlh1* cDNA at the "safe harbor" *Rosa26* locus would restore spermatogenesis. Because the segregation outcome from $Rosa26^{Tg\text{-}Sohlh1/WT}$ $Sohlh1^{-/-}$ SSCs, would result in 50% transgene-free sperm, half of offspring will be transgene-free. I generated $Rosa26^{Tg\text{-}Sohlh1/WT}$ $Sohlh1^{-/-}$ SSCs and transplanted them into infertile recipients. In contrast, methods to culture and edit human induced pluripotent stem cells (iPSCs) are well established. I acquired the

expertise to produce iPSCs from wild type mouse fibroblasts and differentiated them into primordial germ cell-like cells (PGCLCs) that produced spermatogenesis in recipient males and an embryo from iPSC-derived sperm. I then established iPSC lines from *Sohlh1-KO* mice and used CRISPR/Cas9 gene editing to introduce the *Sohlh1* cDNA into the *Rosa26* locus. Studies are planned to differentiate those cells into PGCLCs and transplant. These studies demonstrate the feasibility of using somatic cell and germ cell gene therapy to treat male infertility.

Table of Contents

List of Tables

List of Figures

1.0 Introduction

1.1 Spermatogenesis

Spermatogenesis is a process by which sperm is produced. Proliferation and differentiation of spermatogonial stem cells (SSCs), the precursors of sperm, is tightly regulated by the microenvironment (niche) inside the testis and by hormonal regulation from the hypothalamus-pituitary-testis (HPT) axis [1]. Therefore, spermatogenesis is regulated by cell types inside and outside of the testis. Sperm production takes place inside the seminiferous tubules, which contain the germ cells and somatic Sertoli cells that support every stage of spermatogenic lineage development from stem cells to sperm. The seminiferous tubules are surrounded by peritubular myoid cells that are on the outside of the seminiferous tubule basement membrane. Sertoli cells and peritubular myoid cells are two important components of the SSC niche [1, 2]. The other cells in the niche including Leydig cells, fibroblasts, macrophages and blood vessels reside in the interstitial space between the seminiferous tubules [1-5]. SSCs are at the foundation of spermatogenesis and, in response to niche signals, must balance self-renewing divisions to replenish the stem cell pool with differentiating divisions that give rise to committed spermatogonia, spermatocytes, spermatids and sperm. Undifferentiated spermatogonia can undergo multiple rounds of transit-amplifying mitotic divisions before giving rise to spermatocytes that undergo meiosis. Once meiosis is completed, germ cells at this stage are defined as round spermatids. This process of differentiation starts from the basement membrane, moving along towards the lumen of the seminiferous tubules as germ cells differentiate. Round spermatids will then undergo spermiogenesis where the nucleus condenses, cytoplasm is eliminated to finally give

rise to elongate spermatids and sperm. Sperm, which is now on the adluminal aspect of seminiferous tubules will be released in the process called spermiation. Sperm will then be transported through the male reproductive tract through the rete testis, efferent ductules, head of epididymis (caput epididymis), tail of epididymis (cauda epididymis), vas deferens and urethra. The term germ cell is used to refer to cells with capability to become a gamete, including SSCs, spermatocytes, spermatids and sperm (reviewed in [6]).

In this chapter, I provide the definition of each germ cell species during the process of spermatogenesis, the changes and development, the important genes/markers involved in this process especially the ones that will be used in the following chapters.

1.1.1 **Interaction between germ cells and Niche cells especially Sertoli cells and hormonal controls from the Hypothalamus-Pituitary-Testis (HPT) axis in spermatogenesis**

The HPT axis plays a role in hormonal control for spermatogenesis. Gonadotropin-releasing hormone (GNRH) from the hypothalamus stimulates Follicle-Stimulating Hormone (FSH) and Luteinizing Hormone (LH) secretion from the anterior pituitary. In immature testis, FSH stimulates the proliferation of Sertoli cells, whereas in the adult, FSH stimulates Sertoli cells to produce growth factors such as glial cell line-derived neurotrophic factor (GDNF) that are required to maintain the SSC pool [7-12]. GDNF-haploinsufficient mice showed multiple empty seminiferous tubules with Sertoli cell only phenotype, indicating the inability to maintain the stem cell pool [10]. GDNF binds to a receptor complex composed of GFRα1/RET co-receptor, which are both markers for undifferentiated stem and progenitor spermatogonia [13-15]. Sertoli cells also provide differentiation signals for spermatogonia by expressing Retinoic acid (RA), Stem Cell Factor (SCF) or Kit-ligand (KITL) and Bone Morphogenic Protein 4 (BMP4) [16, 17]. Other

Sertoli cell function in spermatogenesis includes 1) providing the habitat and anchoring molecules for germ cells to adhere to while undergoing differentiation, 2) preventing immune attack by forming the blood-testis barrier, and 3) phagocytosing dead germ cells to recycle and prevent toxic debris being released into the lumen of seminiferous tubules [16].

While FSH from the pituitary is important for Sertoli cell regulation, LH from the pituitary stimulates production of testosterone by Leydig cells in the testicular interstitium [18]. Testosterone plays an important role for spermatogenesis by acting through androgen receptor (AR), which is expressed by Sertoli cells. Testosterone is essential for spermatogenesis but does not have receptors on germ cells. Therefore, testosterone regulation of spermatogenesis is mediated at least in part by Sertoli cells [18, 19]. The role of AR in Sertoli cells will be reviewed in Chapter 1.3.1.

1.1.2 **Germ cell stages during spermatogenesis and their molecular markers**

1.1.2.1 Spermatogonial stem cells and Spermatogonia

Undifferentiated stem and progenitor spermatogonia are located on the basement membrane of seminiferous tubules as single cells, in pairs or in chains of 4-16 cells, referred to A_{single}, A_{paired} and $A_{aligned}$, respectively. $A_{aligned}$ spermatogonia give rise to differentiated type A1 spermatogonia that through a series of transit-amplifying mitotic divisions give rise to A2, A3, ,A4, , intermediate and Type B with Type B being the most differentiated population. In rodents, $A_{singles}$ are believed to contain spermatogonial stem cells . Transit-amplifying spermatogonia are connected with intercellular bridges and share mRNA and proteins that regulate coordinated divisions [20-24]. The number of transit-amplifications species-specific (10 rounds in mice, 5 rounds from $A_{dark/pale}$ to Type B4 in non-human primates and 2 rounds from $A_{dark/pale}$ to Type B in

human) [3, 25-27]. While transit amplifying division happens, differentiation of spermatogonia also happens simultaneously by induction of *cKit* expression. *cKit* expression in spermatogonia is induced by exposure to All-trans retinoic acid (ATRA), the active metabolite of vitamin A, which will bind to the cytoplasmic receptor RAR and RXR heterodimer in spermatogonia [28]. Once *cKit* is expressed, the spermatogonia are considered differentiated and capable of binding to KIT ligand (KITL or SCF) from Sertoli cells. The binding of KITL/cKIT results in maintenance of proliferation and survival of already differentiated spermatogonia until meiosis is initiated [29-31].

Because cKIT is a marker of differentiated spermatogonia, cKIT expression is suppressed in undifferentiated spermatogonia. Several mechanisms are believed to play a role in the suppression of cKIT expression, and therefore the proteins involved in cKIT suppression or early cKit induction are among the markers used to identify undifferentiated/differentiating spermatogonia. For example, ZBTB16 (PLZF) a transcription factor that binds to the *cKit* promoter to prevent transcription of *cKit*, is among the markers for undifferentiated spermatogonia [32]. SALL4 can bind to ZBTB16 to open the promoter region of *cKit*, allowing expression of *cKit* to take place in the presence of ATRA [33-35]. PLZF and Sall4 are expressed in A_{single} to $A_{aligned}16$ [33]. *Sohlh1* is also believed to be upregulated under the influence of ATRA and directly binds to the *cKit* promoter to promote *cKit* expression [36, 37]. Other molecular markers are ID4, PAX7, BMI1, EOMES (seen in A_{single}); GFRa1, NANOS2, UTF1 (seen in A_{single}, $A_{paired\ and}$ $A_{aligned}4$); PLZF, SALL4, LIN28, FOXO (seen in A_{single} to $A_{aligned16}$); STRA8 (marks $A_{aligned}$ to A1 transition); NGN3, NANOS3, SOHLH1 (seen in A_{single} to Type B differentiated spermatogonia) (reviewed in [27, 38]).

Spermatogonial stem cells (SSCs) are germ cells with the ability to self-renew and differentiate into sperm [39]. SSCs are believed to belong to a population of A_{single} on the basement membrane of the seminiferous tubules. However, it is uncertain whether all A_{single} have stem cell potential or whether SSCs reside exclusively in the A_{single} population. There is still no definite set of markers to identify SSCs. Therefore, SSCs can only be definitively identified by their biological potential to produce and maintain spermatogenesis in vivo by 1) allotransplantation into germ cell-depleted recipients and 2) lineage tracing.

1.1.2.2 Spermatocyte

Spermatocytes are germ cells that have initiated the meiosis program. Meiosis is a process in which the cells that are diploid (2n) divide to give rise to daughter cells with a haploid set of chromosomes (1n). Meiosis consists of prophase (lysis of nuclear membrane, homologous chromosome pairing and exchange the genetic materials through crossover), metaphase (crossover complete and homologous chromosome pairs line up in the center of nucleus ready to be separate), anaphase (separation of homologous chromosome to the opposite side of the nucleus) and telophase (nuclear membrane synthesis and separation into 2 nuclei). The first meiosis (Meiosis I) results in 2 daughter cells with a haploid set of chromosomes, each set with 2 copies of chromosomes in a form of sister chromatids (1n, 2C). The second round of meiosis (Meiosis II) results in separation of sister chromatids and finally gives rise to 4 daughter cells, each with 1n (1n, 1C) [40, 41].

Crossover, which happens in prophase I, facilitates proper segregation of homologous chromosome and an adequate copy number of chromosomes in daughter cells [40, 42]. Several events happen in prophase I which results in products including leptotene, zygotene, pachytene and diplotene. Proteins involved in DNA double stranded break (DSB), crossover and resolution

of crossover are used as markers for primary spermatocytes. Table 1 shows prophase I products, important events that happen, and molecular markers involved in each step [6, 40, 43].

Table 1 Prophase I chromosome organization and molecular markers

Prophase I chromosome organization	Events	Molecular markers
leptotene	DSB formation	SYCP3, SPO11, MEI4, ATM, H2AX
zygotene	Recombination	SYCP3, H2AX, RAD51, DMC1
pachytene	Resolution of recombination, sex body	SYCP3, MLH1, MLH3
diplotene	Chiasma formation	SYCP3, H2AX at the sex body

PIWIL1 (MIWI), another spermatocyte marker used in this study, is a protein in the PIWI family which interact with piRNA. PIWIL1 expression can be seen at late pachytene spermatocyte to elongating spermatids [44, 45]. Failure of PIWIL1 expression in mice, as observed in *Miwi*-/- mice, results in arresting of germ cells at the beginning of the round spermatid stage [44].

1.1.2.3 Spermatids

The morphological change of round spermatids into elongated spermatids is known as spermiogenesis. Spermiogenesis includes 1) development of flagellum, 2) nuclear elongation, 3) cytoplasmic removal, 4) acrosome biogenesis, and 5) chromatin remodeling. [6]

Transition protein 1 (TP1), a spermatid marker used in this study, plays role in nuclear condensation. Histones will be first replaced by TPs and then by protamines (PRMs) during sperm chromatin condensation [46]. However, failure to express TP1 alone does not result in infertility [47], whereas deletion of both TP1 and 2 results in male infertility [48].

1.2 Definition, classification and epidemiology of Azoospermia

Infertility is a clinical diagnosis for couples who failed to conceive after 1 year of regular unprotected intercourse [49]. Infertility can be found in approximately 10-15% of couples. Male factors contribute to approximately 2/3 of all infertility cases [50]. The causes of infertility contributed from men can be defects in sperm quantity (e.g., azoospermia, no sperm in the ejaculates or oligozoospermia, some sperm in the ejaculates), or quality (e.g., teratozoospermia, abnormal morphology; asthenozoospermia, abnormal motility; or combination of both quality and quantity defects; oligoasthenoteratozoospermia (OAT) [51, 52]. Table 2 provides semen analysis parameters and the lower range limit of normal samples reported by the World Health Organization (WHO) [53]. Regardless of quantity or quality defects, infertile male patients can have their own biological children with assisted reproductive technology (ART), which includes In vitro fertilization (IVF) and intracytoplasmic sperm injection (ICSI) [54]. However, conditions such as azoospermia, where there is no sperm in the ejaculate, predict a poorer prognosis even with ART. Because of the rarity of sperm in azoospermic patients, azoospermia is considered the most severe form of male infertility.

Table 2 Parameters in semen analysis, WHO 2010

Parameter	Lower reference limit (range)
Semen volume (ml)	1.5 (1.4-1.7)
Total sperm number (10^6 per ejaculate)	39 (33-46)
Sperm concentration (10^6 per mL)	15 (12-16)
Total motility (Progressive+Non-progressive, %)	40 (38-42)
Progressive motility (%)	32 (31-34)
Vitality (live spermatozoa, %)	58 (55-63)
Sperm morphology (normal forms, %)	4 (3.0-4.0)

To be specific, azoospermia is a condition defined by the absence of sperm in at least 2 sedimented (preferably 3000 x g for 15 minutes) ejaculates [55]. Azoospermia affects approximately 1% of men worldwide [50, 52, 56, 57]. Azoospermia can be classified based on the site of lesion into obstructive azoospermia (OA, 15-20% of all azoospermic cases) and Non-obstructive azoospermia (NOA, 80-85% of cases) [52, 58, 59]. OA arises when there is a blockade in the reproductive tract preventing sperm release despite normal spermatogenesis, and non-obstructive azoospermia (NOA) is caused by primary or secondary failure of sperm production [52, 58, 59]. However, recent guidelines have revised classification based on pathophysiology into pre-testicular, testicular and post-testicular azoospermia [60, 61]. While the post-testicular azoospermia includes azoospermia that arise from pathology after sperm production, which is equivalent to obstructive azoospermia, testicular azoospermia includes azoospermia that arise from primary testicular dysfunction and pre-testicular azoospermia includes azoospermia from abnormal HPT axis that results in failure to produce sperm (secondary testicular failure). Pre-testicular and testicular azoospermia were therefore included in NOA.

Regardless of the causes of azoospermia, treatment is to surgically retrieve testicular sperm for ICSI [60, 62, 63]. This procedure is known as Testicular Sperm Extraction (TESE). Conventional TESE means to blindly and randomly take testicular biopsies from both testes from which sperm will be extracted in the laboratory for subsequent ICSI. Intracytoplasmic sperm injection (ICSI) is necessary because testicular sperm do not swim and therefore cannot fertilize by conventional IVF. In contrast to conventional TESE, microdissection-TESE or microTESE involves careful microscopic examination of all seminiferous tubules and selective biopsy of larger seminiferous tubules that are more likely to contain sperm [64-67]. The success rate from each technique will be reviewed extensively in Chapter 2. Consequently, the chance of having biological children in azoospermic patients depend largely on success rate of TESE (sperm recovery rate) in these patients.

1.2.1 **Histological classification of NOA**

There are multiple guidelines on how NOA histological classification is done [58, 68]. However, the main histological findings in NOA are 1) Sertoli cell only syndrome (SCO); 2) Maturation arrest (MA); 3) hypospermatogenesis (HS) and 4) tubular hyalinization [58]. Sertoli cell only syndrome is diagnosed when the tissue section is depleted of germ cells and only Sertoli cells are seen in the seminiferous cross section. Maturation arrest subtype is diagnosed when there are germ cells and Sertoli cells but no evidence of elongated spermatids because germ cells stop maturing at a certain step of development. Hypospermatogenesis is diagnosed when elongated spermatids are seen in the tissue but the degree of spermatogenesis is lower than normal. Tubular hyalinization is diagnosed when seminiferous tubules are empty with no evidence of either Sertoli cells or germ cells in the tubules. Although the classification criteria seem to be frank, more often

than not, the pathology of NOA is heterogeneous. This means that multiple biopsy tissues from the same patient might have multiple findings. When there is disagreement among histological findings from the same patient, the patient is diagnosed with the best readout [58].

As for the indications for testicular biopsy in NOA, biopsy of testis in NOA patients are not required before TESE [60]. Diagnostic biopsy is only done when the patients have normal FSH profile to differentiate with obstructive azoospermia [60]. Therefore, usually the histology result is often obtained alongside with first TESE operation.

1.3 Genetic causes of non-obstructive azoospermia

As mentioned above, proliferation of SSCs and spermatogonia, differentiation of spermatogonia, meiosis and spermiogenesis are specific phenomena that happen only in the gonads and there are several factors involving in supporting normal progression of those steps in spermatogenesis. Factors critical for normal spermatogenesis include 1) integrity of chromosome; 2) ploidy; 3) genes involved in spermatogenesis; 4) molecular cues from somatic cells; 5) hormonal axis from outside of the testis. If any of these factors do not function properly, spermatogenesis disruption or testicular failure or NOA will ensue.

The majority of the causes of NOA include chromosomal abnormality, as is observed in Klinefelter's syndrome (XXY) and Y-chromosome microdeletion of AZF-a, -b, and -c. These two conditions together make up 25% of all azoospermic cases [69, 70]. Therefore, genetic screening for NOA patients typically only covers karyotyping and/or FISH for Y-chromosome microdeletion [71]. The other known causes of azoospermia include infection, trauma, iatrogenic such as

chemotherapy, and exposure to gonadotoxin, which may be acquired from patients' history taking [72].

Nevertheless, up to 75% of azoospermic causes are unknown and consequently are categorized as idiopathic NOA [73]. Recent studies have identified single gene defects in idiopathic NOA patients both in germ cells or Sertoli cells such as SOHLH1 [74], TEX11 [73, 75, 76], AR [77] , NR5A1 [78, 79], SYCE1 [80], MEI1 [81] (for comprehensive lists, please see reviews [82-86]). More than 2,300 genes are believed to play a role in spermatogenesis [87, 88] and more than 380 genes are proven in the mouse models to play a role in spermatogenesis [71, 89]. These numbers were identified by comparing transcriptomes from different tissues in the mice and 2,300 genes were shown to have specific expression in the testis [88]. These genes are expressed by any cell type in the testis such as germ cells, Sertoli cells or Leydig cells. In this chapter, I will specifically review defects in AR, SOHLH1 and TEX11 since the knockout mouse models for these genes will be used in this thesis research.

1.3.1 *Ar* (Androgen receptor)

Androgen receptor (AR) is expressed in almost every tissue in the body. It is the receptor for testosterone, 5α-dihydrotestosterone (5α-DHT) and other androgens. In mice, the Ar gene is located on the X-chromosome, comprised of 8 exons, encoding a 10,048 base pair-long mRNA (MGI database). During sex organ development, testosterone binding to AR results in developmental progression of the Wolffian duct to become the epididymis, vas deferens and seminal vesicle [90]. Binding of 5α-DHT to AR results in development of male external genitalia [91]. Once AR binds to its ligand in the cytoplasm, the complex is transported into the nucleus where AR is bound to Androgen Responsive Elements (ARE) which is an AR-binding sequence

on the DNA, initiating transcription of genes downstream of the cascade (classical pathways). Alternatively, AR interacts with other proteins in the cytoplasm resulting in the phosphorylation and activation of other proteins such as Src in non-classical pathway (reviewed in [92, 93]).

1.3.1.1 Roles of androgen receptor in spermatogenesis

AR plays an important role in spermatogenesis as evidenced by its expression in Sertoli cells, peritubular myoid cells, vascular smooth muscle/endothelial cells and Leydig cells [94]. These somatic cells are, as mentioned earlier, important cells that make a niche for SSCs and spermatogenesis. There have been conflicting studies on the expression of AR in germ cells, However, lack of detectable AR in immunohistochemical analyses of germ cells and the absence of the infertility phenotype in germ cell-specific AR knockout mice indicates AR in germ cells (if any) is not necessary for spermatogenesis [95, 96]. .

The role of testosterone in spermatogenesis is therefore mediated by testicular somatic cells, such as Sertoli cells, that have the AR receptor. During normal spermatogenesis, FSH stimulates Sertoli cells to produce GDNF, which promotes proliferation of spermatogonia [7]. LH on the other hand, induces production of testosterone from Leydig cells, which binds to AR in Sertoli cells to increase expression of retinoic acid. Retinoic acid (RA) then induces differentiation of spermatogonia, initiating the process of spermatogenesis [97]. Sertoli cell-specific androgen receptor knockout (SCARKO) mice are infertile with meiotic arrest at diplotene stage of prophase I spermatocyte, progressive loss of spermatocytes, round spermatids and complete loss of elongated spermatids [98-100], indicating that Sertoli cell mediated androgen signaling is important for spermatogenesis. Further studies revealed that AR could act through classical and non-classical pathways to mediate four main functions 1) getting germ cells through their first meiosis 2) preventing premature release of germ cells by maintaining proper molecular adhesion

between Sertoli cells and germ cells, 3) maintaining blood-testis barrier integrity, and 4) ensuring normal spermiogenesis [101, 102].

1.3.1.2 *AR* mutations in human infertility phenotype

Abnormality in the AR gene can manifest in different clinical phenotypes that may or may not be associated with testicular dysfunction. These manifestations include Androgen Insensitivity Syndrome (AIS), prostate cancer, premature ovarian failure and Kennedy's disease (spinal-bulbar muscular atrophy, OMIM#313200) [103]. Among more than 1,100 human AR mutations identified, 90% of the cases are AIS [77]. AR mutations have been found in 2-3% of infertile men [104]. As mentioned previously, AR is also important for sex organ development, patients with AIS can present with having external female genitalia in complete AIS (CAIS), or with spectrum of ambiguous genitalia in partial AIS (PAIS) [105]. However, the presentation that is relevant to this study is mild AIS (MAIS), where the patients present with primary infertility with otherwise normal phenotype. The severity of AIS depends on where the mutation is and how deleterious the mutation is. For example, premature stop codon at exon 1 will result in CAIS, whereas the single base substitution in the same exon may instead result in MAIS. Additionally, mutation at different AR domains may result in different AR activity in different tissues despite the same mutation. For example, one patient with a mutation that prevents AR from interacting with Sertoli cell-specific co-activator TIF2 will result in Sertoli cell-specific AR dysfunction [106]. I used Sertoli Cell-specific Androgen Receptor Knockout (SCARKO) mice as a model for MAIS and infertility in my study due to Sertoli cell single gene defect to demonstrate gene therapy to restore spermatogenesis [104].

1.3.1.3 SCARKO mouse model

I picked SCARKO mice as a model of mild androgen insensitivity syndrome where patients present with azoospermia but an otherwise normal phenotype. There are 3 main SCARKO mouse models reported [98-100]. All of which have the same infertility phenotype with slightly different hormonal profiles. The model used in this study was from Braun's laboratory [98]. The mice were generated by crossing Art^{m2Reb} heterozygous female mice with Amh-Cre male mice, resulting in complete knockout of AR only in Sertoli cells. The phenotype reported in the original studies included 1) absence of AR expression in Sertoli cells, 2) azoospermia, 3) infertility with maturation arrest phenotype with complete absence of elongated spermatids, and 4) blood-testis-barrier integrity compromise [98]. Therefore, these are the phenotypes to be evaluated after the gene therapy treatment is delivered to the SCARKO mouse model.

1.3.2 *Tex11* (Testis -expressed gene 11)

Murine *Tex11* is an X-linked gene that is comprised of 31 exons which is transcribed into a 221 kb-long mRNA and 109,624 Da protein [107, 108]. TEX11 protein is expressed exclusively in the testis with abundant expression in the cytoplasm and nuclei of Type B spermatogonia up to pachytene spermatocyte stage [75, 109].

1.3.2.1 Roles of *Tex11* in spermatogenesis

TEX11 protein contains a trinucleotide repeat domain for protein-protein interaction [110] that was later found to be interacting with at least RPA (Replication Protein A) and SCYP2 (Synaptonemal complex protein 2), both of which are important in meiosis [107]. Immunostaining of nuclei showed colocalization of TEX11 along synaptonemal complex which become apparent

at the synapse region during zygotene to pachytene stage. *Tex11*$^{-/-}$ mice were therefore infertile and exhibited chromosomal asynapsis and reduced crossover formation [107]. The testis histology resembles those with meiotic arrest with aberrant chromosome segregation in anaphase spermatocytes. In conclusion, TEX11 is important for promoting chromosomal synapsis and meiotic crossover in males [107].

1.3.2.2 *TEX11* mutations in human infertility phenotype

Genes expressed in spermatogonia were reported in mouse to highly accumulate on the X-Chromosome [108]. The *Tex11* gene is among those X-link genes identified to associate with human idiopathic NOA [73, 75, 76]. Yatsenko and colleague reported the incidence of Tex11 mutations to be as high as 2.4% in idiopathic NOA, and 15% among those with meiotic arrest phenotype [76]. The mutations range from a large deletion of 99 kb to point mutations, indels that result in-frame, missense and frameshift mutations or alteration of splice site. The majority of these patients have meiotic arrest phenotypes, whereas some may exhibit mixed atrophy or tubular hyalinization mixed with foci of spermatogenesis [73, 75, 76].

1.3.2.3 *Tex11*-mutant (*Tex11-D435fs*) mouse model

The *Tex11-D435fs* mouse model was generated based on the mutation identified previously in a patient with idiopathic NOA [73]. The mutation is *Tex11-1126Ins(TT)*, described as substitution of GTAC sequence in WT exon 16 with TTGGTA, creating a frameshift mutation from the amino acid at position 435 (aspartic acid) (D435fs) [73]. The patient with this mutation had azoospermia with meiotic arrest phenotype. Since this is a small mutation that could be repaired using a single-stranded oligonucleotides (ssODN) without transgene selection cassette, I chose this mouse model to demonstrate a strategy to convert mutated sequence to WT sequence

without introducing new mutations to the genome of the offspring (footprintless gene therapy strategy). In this study, I aimed to establish a causal relationship between this mutation and azoospermic phenotype, and to demonstrate the feasibility of footprintless germline gene therapy to restore spermatogenesis in cases with germ cell-specific single gene defects. Detailed characterization of this newly generated mouse model will be described in Chapter 4.2.

1.3.3 ***Sohlh1*** **(Spermatogenesis/oogenesis helix-loop-helix (bHLH) 1)**

The *Sohlh1* is located on mouse chromosome 2, comprising 8 exons, encoding 1,314 kb-long mRNA and 38 kDa protein [36]. SOHLH1 is a transcriptional regulator identified to express in differentiating spermatogonia Aal, A1, A2, A3, A4, intermediate and type B spermatogonia [36].

1.3.3.1 Roles of *Sohlh1* in spermatogenesis

Sohlh1$^{-/-}$ mice exhibit an azoospermic phenotype with maturation arrest at the undifferentiated spermatogonia stage. Immunohistochemistry showed PLZF-positive cells on the basement membrane of the *Sohlh1*$^{-/-}$ testis. *Sohlh1*$^{-/+}$ mice are grossly normal and fertile, indicating that a single copy of the Sohlh1 is sufficient to support spermatogenesis. Gene expression profile in *Sohlh1*$^{-/-}$ mice showed downregulation of *Lhx8, Kit, Ngn3* and *Crabp1* and upregulation of *Sycp2* and *Sox30* [36]. The expression of genes involved in late meiosis and apoptosis remains unaltered, some of which are *Mlh1, Bcl2, Bax* [36]. Study of *Sohlh1*$^{-/-}$ mice also led to discovery of the *Sohlh2* gene, which is another gonad-specific bHLH protein sharing 50% homology with *Sohlh1* [36]. A subsequent study from the same group revealed co-expression between these SOHLH1/SOHLH2 in GFRA1-negative spermatogonia population [111]. SOHLH1 and SOHLH2 are believed to play

role in suppression of GFRA1 expression and acting downstream of retinoic acid to induce expression of *cKit*, a protein that is essential for spermatogonial differentiation [37, 111].

1.3.3.2 SOHLH1 mutations in human infertility phenotype

A study done in a Korean population identified *Sohlh1* mutations in idiopathic NOA patients [74]. *Sohlh1* exons were sequenced in 96 idiopathic NOA patients and were compared to the control sequence from 156 healthy individual [74]. Among 14 mutations identified in this study are single nucleotide changes that results in amino acid change and alteration of splice site [74]. No functional study was done in a mouse model to establish causality of mutations and the infertility phenotype in those patients.

1.3.3.3 *Sohlh1*-knockout (*Sohlh1-KO*) mouse model used in this study

The *Sohlh1-KO* mouse model used in this study was first published in 2004 [36]. The *Sohlh1* gene was knocked out by removing exons 2-8 along with 500 bp portion of promoter. The removed promoter-exons region was replaced by a PGK-HPRT selection cassette. Since the deletion spans approximately 3.5 kb length, it is not possible to replace the mutant allele with wild-type sequence without transgenic selection cassette. Characterization of this mouse model will be described in detail in chapter 4.3.

1.4 Gene editing techniques for mammalian cells

DNA double-stranded breaks (DSB), one of the most lethal forms of DNA damage, happen spontaneously or as a result of exposure to toxic environment [112]. DSB is always followed by

DNA damage response (DDR) which could lead to 1) cell cycle arrest, 2) apoptosis, 3) transcription and/or 4) DNA repair [113]. For DNA repair, there are two major pathways following DSBs, 1) Non-homologous end joining (NHEJ) where the break ends are trimmed and joined and often accompanied by small deletions/insertions (indels), or 2) homologous recombination (HR) where the homologous chromosome is utilized as the template for repair, resulting in retention of the same original sequence as the homology template [112]. Because DNA repair may lead to alteration of the original DNA sequence (mutations), gene editing has been achieved through induction of DSB using FokI endonuclease. FokI has been fused to different types of DNA-binding proteins, such as Zinc-finger and TALEs, (Transcription activator-like effectors) to direct the endonuclease to a specific place in the genome [114]. These DNA-binding protein/FokI endonucleases have been shown to successfully create targeted mutations, both indels and homologous recombination, at a reliable success rate. However, many laboratories still have to rely on the commercially available protein/endonucleases complex which could be time-consuming and expensive. Therefore, gene editing had been difficult not only because of the complicated nature of DNA repair itself, but also because of the hugely limited accessibility to the gene-editing tools.

After the introduction of CRISPR/Cas9 (Clustered Regularly Interspaced Short Palindromic Repeats) [115, 116], gene editing has been more easily accessed. CRISPR/Cas9 is easy to prepare and can be done in any laboratory [117]. Since then the tools for genome editing has largely shifted to CRISPR/Cas9 and is very readily accessible in a short amount of time. This chapter will be dedicated to reviewing the use of CRISPR/Cas9 in mammalian cells especially mouse spermatogonial stem cells (SSCs).

1.4.1 **Precise genome editing (gene targeting) using CRISPR/Cas9 system in mouse SSCs**

CRISPR/Cas9 system was first identified as a cluster of repetitive sequences in the bacterial genome, which was later proven to be an acquired immune system for bacteria [118-121]. When bacteria are infected with viruses, they utilize this cluster for storing parts of the infecting viral genomic sequence [118, 119, 122, 123]. When virus harboring the same sequence re-infected the bacterium, this cluster is transcribed into CRISPR RNA (crRNA), which when combined with transactivating RNA (transcrRNA) and Cas9 endonuclease is capable of searching and destroying the re-infecting viral genome [124, 125]. Genome editing applies the fact that these complexes can cleave DNA to create a double stranded break.

The engineered CRISPR/Cas9 system therefore is comprised of 2 components, 1) the guide RNA, and 2) Cas9 endonuclease [117]. While Cas9 functions in creating DNA double stranded breaks, guide RNA is responsible in landing Cas9 into a desired nucleotide sequence in the genome. The guide RNA is 20-nt RNA fused with transcrRNA [124]. The 20-nt sequence must be immediately followed by PAM sequence (NGG for spCas9) as a recognition site for Cas9 [123].

The definition of precise genome editing, or gene targeting, is to specifically edit or alter the sequence only at a desired locus in the genome. CRISPR/Cas9 can be delivered into the cells in many forms ranging from plasmids, sgRNA and Cas9 mRNA, or sgRNA/Cas9 protein (Ribonucleoprotein; RNP) with or without donor template DNA. The DSB will be induced at the target site (on-target DSB) and will be followed by NHEJ or HR if the donor DNA template is provided. When HR happens, the provided donor DNA will serve as a template for homology-directed repair and introduce desired sequence into the locus where DSB took place [117].

1.4.2 **CRISPR/Cas9 off-target activity and how to assess it**

The CRISPR/Cas9 complex is directed to the desired site with small RNA of only 20 base pairs. Therefore, it is reasonable to assume that parts of the genome, harboring similar sequence to these 20 nucleotides (nt), might also be the target of the CRISPR/Cas9 complex. Indeed, Fu and colleagues showed that the off-target activity from CRISPR/Cas9 can be as high as 40% (human cell lines) depending on the sequence of sgRNAs and the target sequences [126]. The mismatch tolerance is seen especially in the 5' side nucleotides distal to the PAM sequence [127]. In fact, there are only a few sequences upstream of the PAM sequence, known as seed sequences, that are important in target binding of the complex and are mismatch intolerant [128, 129]. There are a few strategies to avoid off-target activity of CRISPR/Cas9, 1) the mainstream sgRNA design software (reviewed in [130]) will calculate similarity of designed 20 nt and possible binding sites in the genome and will calculate the score accordingly. One might start from the sgRNAs with the lowest number of potential off-target sites, then validate the off-target activities later in vitro. 2) There are a number of in vitro tests that can be done to assess the precision of CRISPR/Cas9 of your choice. Examples of these methods are Integrase deficient lentiviral vector (IDLV) capture, genome-wide unbiased identification of DSBs evaluated by sequencing (GUIDE-seq), high-throughput genome-wide translocation sequencing (HTGTS), direct in situ breaks labeling, enrichment on streptavidin, next-generation sequencing (BLESS), and breaks labeling in situ and sequencing (BLISS) (reviewed in [131]). All of these share the same principle: to mark where DSBs happened in the cells and then sequence the genome to identify where the marks are. However, methods to retrospectively check the off-target activity of CRISPR/Cas9 in the final product is still important. The principle of this method is to compare genomic sequence from the cell before and after treatment with CRISPR/Cas9, where the sequence should be identical except for the gene targeted

locus. Although the whole genome sequencing might be too wasteful, focused sequencing can be performed by looking only at the high-risk (high similarity) loci [132]. The sequencing can be done in any fashion, from Sanger to next-generation sequencing. In this study, I plan to perform next generation whole genome sequencing and compared to the original parental sequence before CRISPR/Cas9 editing.

1.4.3 **Method of delivery into mouse spermatogonial stem cells**

As mentioned earlier, methods of CRISPR/Cas9 delivery is key to successful and precise gene targeting. In other words, the delivery/transfection methods used in gene targeting must not cause random genome integration. In rodent SSCs specifically, lentivirus was shown to deliver foreign DNA materials into the mSSCs at a very high efficiency and high survival rate [133, 134]. However, since lentivirus brings about random integration in the genome, it was not my first choice for introducing CRISPR/Cas9 elements into mSSCs. Non-integrative viruses, such as adenovirus [135] or adeno-associated virus [136], have been shown by some groups to successfully infect rat and mouse SSCs in vitro. However, transfection efficiency is low and adenovirus is toxic to mSSCs in our experience. For AAV, the viral genome size is too small that the Cas9 gene cannot be incorporated into the virus [137]. Additionally, Honaramooz and colleagues showed germline transmission with AAV, which may be undesirable [138]. Other transient transfection methods such as electroporation, lipid-based reagent or chemical cationic polymer are options for introducing CRISPR/Cas9 elements into SSCs with very low incidence of genomic integration. In this study, I explored transient transfection options such as lipofectamine, electroporation and chemical cationic polymer polyethylenimine (PEI). The detailed optimization methods can be found in Chapter 4.

1.5 In vitro germ cell generation from pluripotent stem cells (iPSCs)

Human embryonic stem cells (hESCs) were successfully derived by Thomson et al. in 1998 from inner cell mass (ICM) and were shown to retain pluripotency, which also means the ability to differentiate into germ cells were retained [139]. Indeed, ESCs kept in culture without the differentiation inhibitor, Leukocyte Inhibitory Factor (LIF), were shown to spontaneously differentiate into all lineages in vitro including cells positive for germ cell markers [140-143]. Early germ cell differentiation techniques from ESCs exploited this observation (that germ cells spontaneously arise in ESCs cultures), thus focusing on how to enhance/increase and how to efficiently isolate these rare events. This technique, which is hence referred to as direction-selection method, include supplementing the ESC culture (either 2D or 3D cultures) with different growth factors/hormones, inducing expression of the known germ cell markers such as Vasa [144], and later isolating these rare germ cells with germ cell markers. Details of example works can be found in table 3. The downside of this technique is low efficiency, and the overlapping of germ cell markers with pluripotency markers that results in a higher rate of pluripotent cell contamination and less-efficient isolation of germ cells [145]. More importantly, most studies failed to use the in vitro generated gamete-like cells to make live offspring [146]. This indicates that germ cells derivation by direction-selection methods still need improvement, especially in terms of efficiency.

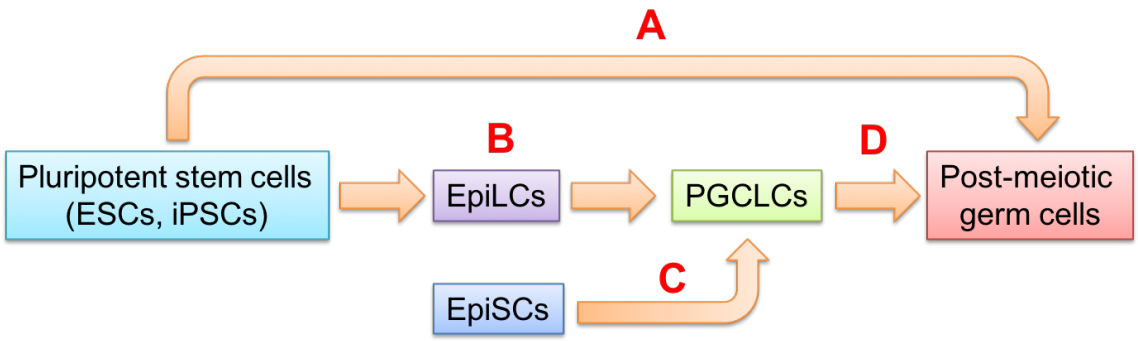

Figure 1 diagram showing different approaches to derive germ cells from pluripotent stem cells

Pathway A=ESCs directly to gamete/germ cell-like cells (Direction-selection method), pathway B=ESCs/iPSCs to EpiLCs to PGCLCs to gametes (by transplantation), pathway C=Epiblast cells or EpiSCs to PGCLCs to gametes (by transplantation), pathway D=Recapitulation of sex determination and meiosis *in vitro* from PGC/PGCLCs

Table 3 Examples of in vitro gemete derivation studies

First Author	year	organism	End product *in vitro*	Markers to identify/isolate germ cells	efficiency	Fertilizing capability	technique
Fig.1 pathway A; ESCs directly to gamete/germ cell-like cells (Direction-selection method)							
Male							
1. Toyooka et al. [140]	2003	mouse	Mvh-GFP positive PGCs from EB	Transgenic Mvh-GFP	2.9%	Sperm not used to fertilize	3D culture of Vasa-GFP-LacZ transgenic ES cells to obtain embryoid body (EB), cocultured with BMP4-producing M13 cells and selected for VASA-GFP+ cells, then cocultured with embryonic gonadal somatic cells prior to transplantation
2. Geijsen et al. [142]	2004	mouse	Haploid cells resemble round spermatids	FE-J1 and Hoechst 33342 to distinguish haploid chromosome	0.01% FE-J1-positive cells	Diploid blastocyst	3D culture of ES cells to obtain embryoid body (EB), selected SSEA-1+ cells and exposed to Retinoic acid. Selected for embryonic germ cells and cultured for 4 more weeks and selected for FE-J1-positive cells
3. Clark et al. [141]	2004	human	Germ cells undergone meiosis but no haploid detected	SCP1, SCP3, GDF9 and TEKT1	Not quantified	No haploid cells	Observe spontaneous germ cell differentiation and various markers expression temporally in

Table 3 continued

							human ES cell culture
4. Nayernia et al. [147]	2004	F9 teratocarcinoma cell line	Sperm	Stra8-GFP	86% of Stra8-GFP transfected cells are positive for GFP after induction with RA	embryo	Derive Stra8-GFP stable F9 teratocarcinoma cell line then induced Stra8 expression with RA and select for Stra8-GFP+ cells for transplantation
5. Nayernia et al. [148]	2006	mouse	haploid *in vitro*	Stra8-GFP then Prm1-dsRed sort	$2x10^6$ cells were used initially to establish double transgenic lines. Two clones were double transgenic, one of which could give rise to haploid cells.	Live offspring but a few carried Protamine-dsRed transgene	Mouse ES cells were transfected by Stra8-GFP. RA was added to culture and GP-positive cells were sorted. Prm1-dsRed were subsequently transfected into Stra8-positive cells and were induced by RA again. Prm1-dsRed positive cells were isolated for further haploid cells detection and analysis. Prm1-dsRed+ haploid cells were subsequently used for ICSI
6. Kee et al. [149]	2006	human	SYCP3 meiotic cells	VASA and SYCP3 staining to identify germ cells	10-14.5% VASA-positive cells from hESCs cell in the presence of BMPs.	No haploid cells	Adding BMPs into hESC culture could modestly but reproducibly induce PGCs.
7. West et al. [150]	2008	human	Meiotic germ cells	SYCP3 and MLH1	69% DDX4-and	No haploid cells	Human ESCs were cultured with mouse

Table 3 continued

					POU5F1-positive germ-like cell, among which 90% are positive for SYCP3 and MLH1		embryonic fibroblast (MEF) and bFGF (basic fibroblast growth factor) and spontaneously differentiated into SYCP3 and MLH1 positive meiotic germ cells.
8. Tilgner et al. [151]	2008	human	Meiotic germ cells	SSEA-1 sort for PGC-like cells SYCP3 to detect meiotic cells	5% of ESCs were positive for SSEA-1.	Not used to fertilize	The authors overcome the low efficiency problem by increase the ESC number to start with by culturing cells in gelatin-coated monolayer cells. Then the cells were sorted for SSEA-1 for further differentiation.
9. Bucay et al. [152]	2009	human	Acrosin - positive cells (RT-PCR, 0.1% positive from immunostaining) from CSXR4 Putative migratory PGCs. Sertoli cells were recognized by Sox9 and FSHR expression	CXCR4 for PGCs	Approximately 20% alkaline phosphatase positive cells/cluster of ES cells	Not used to fertilize	Germ cells spontaneously arise under regular condition used to expand ESCs but could be promoted by subculturing more frequently and breaking colonies into smaller size. Sertoli cells were seen to have formed structure surrounded germ cells.
10. Park et al. [153]	2009	human	PGC-like cells	cKIT/SSEA1/VASA or	8-10% of the hESC in culture	Not used to fertilize	Stain human PGCs to identify markers. Then used the markers

Table 3 continued

				PLAP/SSEA1/ VASA			to identify induced PGCs (iPGCs) from human ESC *in vitro*. iPGCs were obtained by co-culturing with human gonadal stromal stem cells.
11.Kee et al. [154]	2009	human	Vasa-GFP positive putative PGCs	Vasa-GFP for putative PGCs SYCP3, yH2AX for meiosis Propiodium iodide intensity for chromosome number	5% Vasa-GFP positive with BMP4 induction, of which 2.06% were haploid.	Haploid cells not used to fertilze	Human ES cells were transfected with Vasa-GFP and induced by BMP4. The expression pattern of Vasa-GFP was observed after silencing or overexpressing DAZ, DAZL and BOULE.
12.Aflatoonian et al. [155]	2009	human	Spermatid-like cells	Q-PCR and immunostaining for protamine 1 and protamine 1.97	1-5% of PRM1 or protamine 1.97-positive cells in EB	Not used to fertilize	Human ESCs were culture and gave rise to EBs spontaneously. The Q-PCR and immunostaining were performed to confirm the presence of post-meiotic PRM-positive spermatid-like cells.
13.West et al [156]	2010	human	Germ cell-like cells	DDX4+ POU5F1+ cells	When KITL was removed, DDX4+ POUF1+ germ cells decreased by 70.5%	Not used to fertilize	The authors cultured hESCs with bFGF and feeder compared with KITL-/- feeders to assess the importance of KITL in human germ cell development.

Table 3 continued

14.Tilgner et al.[157]	2010	human	Meiotic germ cells	VASA-GFP sort for postmigratory germ cells SYCP3 staining and RT-PCR to identify meiotic cells	0.8% of ESC in culture were positive for VASA-GFP. SYCP3-positive cells were not quantified.	Not used to fertilize	The authors made and characterized human embryonic stem cell lines stably expressed a VASA-pEGFP-1 reporter. Therefore, they used the same technique as their previous paper (shown above) but in the Vasa-GFP ESC line.
15.Eguizabal et al. [158]	2011	Human	Haploid cells	DNA content and FISH	0.4-2.3% haploid cells from iPSCs	Fertilizatio n not attempted	Human iPSCs were culture, exposed to RA, sorted for CD49f, CD9+, CD90-, SSEA4-. Then continue the culture with FGF2, Froskolin, hLIF, R115866 until meiosis is detected.
16. Medrano et al. [159]	2012	human	Haploid population	ploidy analysis e.g. FISH	1.5% haploid	Haploid cells not used to fertilize	VASA or DAZL were overexpressed in hESCs or iPSCs.
17.Easley et al. [160]	2012	human	Haploid spermatid-like cells	UTF1, PLZF and CDH1 for spermatogonia-like cells, HIWI and HILI-positive for spermatocyte-like cells, and Acrosin, TP1, PRM1 for spermatid-like cells	40-60% VASA-positive cells among 5,000 cells counted. 3.5 and 4.9% haploid cells by FACS ploidy analysis	Haploid cells not used to fertilize	Humam iPSCs/ESCs were cultured in the culture condition used for maintaining spermatogonial stem cells containing key growth factors bFGF, GDNF.

Table 3 continued

Fig.1 pathway C; Epiblast cells or EpiSCs to PGCLCs to gametes (by transplantation)							
male							
18.Ohinata et al. [161]	2009	mouse	Sperm from transplantation of PGCLCs	Blimp-Venus, Stella-ECFP, Stella-Venus transgenic lines to isolate PGC-like cells	1250 cells were positive for Blimp-venus (45% from total 300 cells at the time point evaluated) after growing 250 cells of E6.0 epiblast for 132 hours.	Live-born offspring	BMP4 alone can induce E6.0 epiblast to undergo PGC differentiation. The transcriptional regulators that were induced in response to BMP4 were Blimp1 and PRDM14. The epi-PGC (PGC that were induced from E6.0 epiblast) were either transplanted as is or after reagregate *in vitro* before transplantation.
female							
19.Hayashi, Surani et al. [162]	2009	mouse	Oocyte-like cells	Blimp1-GFP or Stella-GFP transgenic EpiSC lines to isolate PGC-like cells SYCP3, Ddx4 staining to identify oocyte-like cells	0.5% of Stella-GFP EpiSCs were positive for GFP after 5 days in culture. 0.6% oocyte-like cells from 3000 Stella-GFP cells	Not used to fertilize	The authors used EpiSC instead of ESC to derive PGC-like cells (PGCLCs). Stella-GFP positive cells were then cocultured with cells from E12.5 female genital ridge, including endogenous germ cells. Stella-GFP positive cells proceeded to form oocyte-like cell *in vitro*.
Fig.1 pathway B; ESCs/iPSCs to EpiLCs to PGCLCs to gametes (by transplantation)							
male							

Table 3 continued

20.Hayashi et al. [163]	2011	mouse	Sperm from transplantation of PGCLCs	Blimp1-Venus and Stella-EGFP mESC transgenic lines	40% of EpiLCs were positive for Blimp1-Venus (PGC marker) after BMP4 induction.	Live-born offspring	PGCLCs were derived from mESCs by inducing Epiblast-like cells (EpiLC), the *in vitro*-derived stem cells with the same pluripotent state as E6.0 epiblasts *in vivo*. BMP4 was used to induce PGC induction in EpiLCs. PGCLCs were then transplanted to the germ cell-depleted hosts to produce sperm. EpiLCs induction method was described in text.
21.Nakaki et al. [164]	2013	mouse	Sperm from transplantation of PGCLCs	Blimp1-Venus and Stella-EGFP mESC transgenic lines		Live-born offspring	PGCLCs could also be induced from EpiLCs by overexpressing Blimp1, Prdm14 and Tfap2c.
22.Sasaki et al. [165]	2015	human	PGCLCs (via iMeLCs)	PRDM1/ And surface marker EpCAM and ITGA6 to isolate the PGCLCs	32% of population were highly positive for EpCAM and ITGA6.	Not used to fertilize	Human iPSCs were obtained according to the established protocol. The human IPSCs were then induced to form incipient mesoderm-like cells (iMeLCs) bearing prime pluripotent state between mEpiLC and mEpiSCs, which expressed SP5, MIXL1, EOMES. Then BMP4, SCF, EGF

Table 3 continued

							and LIF were added to the culture to induce PGC fate. EpCAM and INTEGRIN-alpha 6 were used to isolate PGCLCs.
23.Irie et al. [166]	2015	human	PGCLCs	SOX17, BLIMP1, TFAP2C for human germ cell specifier	10-50% NANOS-mCherry positive cells per one embryoid body	Not used to fertilize	Conventional hPSCs culture was done in a medium with bFGF, TGF β, LIF, GSK3ß inhibitor (i), MEKi, p38i, and JNKi. To induce hPGCLC differentiation, BMP2 or BMP4, LIF, SCF, EGF, and ROCK inhibitor was added to the culture. NANOS-mCherry-positive hPGCLC cells emerged around day5.
Female							
24.Hayashi et al. [167]	2012	mouse	Mature oocyte from transplanting *in vitro* reconstituted ovaries	Blimp1-Venus and Stella-EGFP mESC transgenic lines		Live-born offspring	PGCLCs were also induced from ESCs through EpiLCs, using the same method as they previously described. The PGCLCs were then cocultured with female embryonic gonadal somatic cells to reconstitute ovary-like structure. The

Table 3 continued

							reconstituted ovaries were then transplanted to the bursa of recipients' ovary/kidneys. Mature ovaries were retrieved.
Fig.3 pathway D; Recapitulation of sex determination and meiosis *in vitro* from PGC/PGCLCs							
male							
25.Zhou et al. [168]	2016	mouse	Round spermatid-like cells	1. Meiotic marker staining 2. SYCP3 staining to show segregation 3. Q-PCR for meiotic markers 4. ICSI		Live offspring that could produce next generation fertile offspring	Coculturing PGCLCs with embryonic gonadal somatic cells, then treated with series of morphogens including pituitary extracts.
female							
26. Morohaku et al. [169]	2016	mouse	MII oocytes *in vitro*	Morphology and karyotype	50-58% number of MII oocyte/number of cultured follicles	Live-born offspring	E12.5 PGCs were cultured ex vivo with changing medium formula to support different growth phases of follicles.
27.Hikabe et al. [170]	2016	mouse	MII oocyte *in vitro*	Morphology, karyotype and gene expression profile	55.1 GV oocytes were obtained from one Reconstituted Ovary (rOvary). Approximately 28.9% extruded a	Live-born offspring	PGCLCs were derived from mouse ES via EpiLCs. The PGCLCs were co-culture with somatic cells from E12.5 gonads to obtain reconstituted ovary. The reconstituted ovary was then differentiated *in*

Table 3 continued

					1st polar body		*vitro* to obtain primary oocyte (step1 culture). The step 2 culture was done to obtain GV oocyte (*in vitro* growth). The GV oocyte was then matured in vitro to get MII oocyte (step 3; *in vitro* maturation).

In fact, to generate in vitro gametes from pluripotent stem cells, one needs to recapitulate the series of events that leads to the differentiation of embryonic cells into germ cells *in vivo*. These steps include 1) primordial germ cell (PGC) specification (pluripotent stem cells to PGC), 2) sex determination and gonocyte maturation (bipotential gonad to testis or ovary) and 3) gametogenesis (mature gonocytes undergoing spermatogenesis or oogenesis, which includes meiosis and maturation) [146, 171]. To increase efficiency in germ cell generation, the new approach is to mimic step 1, which is to induce PGC fate in pluripotent cells. Based on the *in vivo* observation that PGCs arises from epiblast cells, Hayashi et al. induced PGC fate with BMP4 in Epiblast stem cells (EpiSCs), a pluripotent stem cell line derived from the E5.5-6.5 epiblast of post-implantation embryo [162, 172]. However, instead of seeing robust induction of PGC fate, EpiSCs rarely responded to BMP4. This shows that; 1) EpiSCs are not the cells at the right pluripotent stage to respond to BMP4; 2) the derived pluripotent cell lines do not necessarily retain their *in vivo* pluripotent stage (as seen in *in vivo* epiblast versus EpiSCs) [173, 174]. To pinpoint the pluripotent stage with PGC competency, Ohinata et al. assessed responsiveness of ex vivo epiblast to BMP4 and found that it lost responsiveness to BMP4 (hence PGC competency) by E6.25, despite being fully responsive at E5.5-E6.0 [161]. However, EpiSCs, which were derived from E5.5-6.5

epiblasts, have already lost PGC competency in culture. Many groups therefore converted their interest to finding a subpopulation in ESC culture that is PGC-competent, including Hayashi et al. They reported that under regular culture with Leukocyte Inhibitory Factor (LIF), Fetal Calf Serum (FCS) on Mouse Embryonic Fibroblast (MEF) feeder [175, 176], there was a dynamic equilibrium between Stella-positive (expressing genes found in inner cell mass) and Stella-negative cells (expressing genes found in post-implantation epiblasts including *Fgf5*) [177]. Ultimately, this ICM-epiblast equilibrium can be shifted towards ICM if inhibitors for FGF4/MAPK pathway and GSK3 are added (2i) [178], whereas Activin A and bFGF cause the equilibrium to shift towards post-implantation epiblasts [172, 179, 180]. This means that these naïve and primed pluripotent stages of epiblast, found in ESC culture, are interchangeable when suitable pathway inhibitors/activators are applied. The pluripotency state that has PGC competency (equivalent to epiblasts at E5.5-6.0) is in between these two stages of pluripotency of ESC culture.

To capture the pluripotent stage with PGC potency (with pluripotent stage equivalent to E5.5-6.0 *in vivo*), Hayashi et al. experimented in ESC cultures that were kept in naïve stage (LIF+2i), then slowly induced into primed pluripotent stage with bFGF and Activin A. To capture the pluripotent stage that are fully PGC-competent, they added BMP4 at day 1, 2 and 3 after culturing in bFGF and Activin A and found that adding BMP4 at day 2 caused robust PGC differentiation (approximately 40% compared to 1.4% from EpiSC induction) [163]. This means that day 2 ESC culture in bFGF and Activin A may have comparable pluripotent stage as E5.5-6.0 epiblast *in vivo*, hence given the name Epiblast-like cells (EpiLCs) that efficiently give rise to primordial germ cell-like cells (PGCLCs). The same induction method is also applicable to iPSC, as shown by the same group. Later in 2013, Nakaki et al. identified sets of transcription factors used to induced ES cells to EpiLCs [164]. These PGCLCs were then transplanted into the testes

of infertile W/Wv mice and produced mature sperm, with no testicular tumors. Female PGCLCs could also be co-cultured with embryonic ovarian somatic cells to form “reconstituted ovary”, which can produce mature oocytes after transplanted into the ovarian bursa in mice [167]. This is the first demonstration that the *in vitro* derived germ cells (PGCLCs) from pluripotent stem cells could produce fertilization-competent gametes and offspring that developed normally to adulthood and could produce the next generation offspring [146, 171]. In addition to transplantation, Zhou et al. showed that mouse PGCLCs derived by Hayashi’s method, could be differentiated *in vitro* into spermatid-like cells, which could be used for round spermatid injection (ROSI) to produce offspring [168]. The female counterpart was demonstrated in the study by Hikabe et al [170].

Deriving PGCLCs in human from pluripotent stem cells has been shown successful by Sasaki and Irie et al. by a similar method to what has been done in mice. Since the success of human iPSCs (hiPSCs) derivation in 2007 by Yamanaka et al., human ESCs are no longer the obligated choice of pluripotent cells, thus hugely facilitating translation to clinic [166, 181, 182]. Sasaki et al. and Irie et al. identified the culture condition for hiPSCs in pre-formulated, commercially available medium, resulting in the appropriate pluripotent stage at which the cells can give rise to 40% PGCLCs after being exposed BMP4. These cells are called insipient mesoderm-like cells (hiMeLCs) [165].

Morohaku et al. in 2016 produced postmeiotic oocytes from E12.5 PGCs by using different media formula to support particular phases of follicular development [169]. Hikabe et al. also reported similar methods to derive fertilizable oocyte all *in vitro* from PGCLCs in 2016 [170]. Studies from Zhou et al. and Morohaku et al. and Hikabe et al. showed that the entire process of *in vitro* germ cell derivation from ESCs/PGCs, both in male and female, is possible now in mice. In human, even though the PGCLC-equivalent cells could be derived from iPSCs by Irie and

Sasaki et al., there were no studies, to our knowledge, that could derive sperm/oocyte *in vitro* from human PGCLCs or that PGCLCs can be transplanted to produce spermatogenesis or oogenesis. Monkey and human PGCLCs are transplantable (produce clusters of spermatogonia or oogonia) but there is no evidence yet that they can differentiate to produce oocytes or sperm, in vivo [183-185].

1.6 Ethical and society concerns over germline gene editing

The ethical concerns surrounding germline gene therapy were raised once more when a Chinese biophysicist used CRISPR/Cas9 to knock out *CCR5* in the embryos resulting in twin babies, in the hope to make them resistant to HIV infection [186]. This research has been widely condemned by the scientific society world-wide due to the following: 1) there are major safety issues regarding the off-target activity of CRISPR/Cas9, 2) mosaicism is known to occur as a result of injecting CRISPR/Cas9 into a zygote, making treatment efficacy questionable and germline transmission possible, and 3) the experiment itself was not well-documented or conducted with the appropriate ethical approvals. This study was the first clinical trial of CRISPR use in humans. Germline transmission is a particularly concerning issue, since it is not known how a transgene, or unoriginal sequence, may interact with the genome and influence the development of an embryo and health of the resulting offspring [187]. Based on these and other concerns (e.g., inability to consent the next generation) the first international summit on human gene editing (Washington DC, 2015) advised that it would be irresponsible to proceed with any clinical use of germline gene editing unless and until safety and feasibility issues have been resolved and there is broad societal consensus about the appropriateness of the proposed application. The committee did advise,

however, that “as scientific knowledge advances and societal views evolve, the clinical use of germline editing should be revisited on a regular basis” [188]. While many experts agree that germline gene therapy should be limited to life-threatening diseases with no cure, the decision on which diseases are severe or treatment-deprived enough to be eligible for germline gene therapy is not an easy task.

1.6.1 **Acceptable practices in gene therapy in germline**

Although major societies, including an interdisciplinary ethics consortium (the Hinxton Group) [189], the US National Academies of Science, Engineering, and Medicine (NASEM) [190], the American Society of Human Genetics (ASHG) Workgroup on Human Germline Genome Editing [191], and most recently, the UK Nuffield Council on Bioethics [192], agree that germline gene therapy in humans may move to clinical trial in the future within a robust and effective regulatory framework. Specifically, the US National Academy of Sciences, Engineering and Medicine Committee on Human Gene Editing recommended in 2017 [190] that clinical trials using heritable genome editing could be permitted within a robust and effective regulatory framework that encompasses:

- absence of reasonable alternatives;
- restriction to treating a serious disease or condition;
- restriction to editing genes that have been convincingly demonstrated to cause or to strongly predispose to that disease or condition;
- restriction to converting such genes to versions that are prevalent in the population and are known to be associated with ordinary health with little or no evidence of adverse effects;

- the availability of credible preclinical and/or clinical data on risks and potential health benefits of the procedures;

These societies have agreed that germline gene therapy in human embryos will be allowed as long as the gene-modified embryos are not transferred [187]. Since the duration that embryos can survive in vitro is approximately two weeks, it is acceptable to practice germline gene therapy in human embryos younger than two weeks of age in some countries; however, in the United States, germline gene therapy on human embryos is not allowed by law (consolidated appropriations act of 2016) or using federal funding. Nevertheless, the use of public research funding is still encouraged where allowed to establish the necessary safety and feasibility parameters and to avoid rogue research that could bring about more harm than good [191].

1.6.2 **This study complies with safety concerns surrounding germline transmission**

Using CRISPR/Cas9 in zygotes often creates mosaicism, precluding careful investigation of off-target, unintentional, additional mutations that might be passed on via the germline. In this study, I propose a mechanism of germline gene therapy that can be achieved with or without germline transmission, therefore potentially evading the concern of transgene transmission to future generations. The gene targeting was first performed in spermatogonial stem cells, enabling us to carefully investigate the consequences of CRISPR/Cas9 gene targeting. Second, I used SCR7, a DNA ligase VI inhibitor, to block the NHEJ pathways, which has been shown to minimize downstream, off-target mutations [132]. To address the question of off edits outside of the gene-targeted region, next-generation whole genome sequencing was used to compare the sequence of the gene-edited clones to the paternal sequence. Because of these measures, offspring are expected

to contain purely original sequences, as found in the father, while the infertility phenotype is corrected without transgene creation.

While these steps outlined above minimize the risk and address several of the concerns surrounding germline gene editing, it is important to note that for large deletions, where transgene insertion is crucial to reverse the phenotype and for colony selection, Prenatal Genetic Diagnosis (PGD) would be necessary to select against embryos carrying transgenes prior to implantation (detailed explanation in Chapter 4.3). This approach of germline gene therapy for large deletions without germline transmission will also be demonstrated in this study.

1.7 Introduction to the experimental chapters

As many as 75% of all NOA cases are predicted to be idiopathic [73], among which single gene defects in germ cells and Sertoli cells are constantly identified. While the success rate of TESE among NOA patients is approximately 50% (Chapter 2), there are no further options for those who fail TESE. Gene therapy in Sertoli cells and germ cells are promising approaches to improve sperm recovery rate, particularly when combined with TESE, to provide further options for those who fail TESE. In chapter 2, the first experimental chapter, I showed details of the sperm recovery rates by the two most-widely used TESE techniques, conventional and microdissection TESE, for each NOA histological subtype. The purpose of this experiment is to identify the magnitude and progression of standard treatment for idiopathic NOA over the last 20 years and to emphasize the need of novel treatment through germline gene therapy (see Chapter 2). The following chapters show gene therapy in both Sertoli and germ cells in the azoospermic mouse models with single gene defects that are associated with azoospermia in human patients. Figure 2

summarizes the approach of gene therapy for azoospermia due to single gene defects. If a single gene defect is identified as Sertoli cell-specific, in vivo adenoviral gene therapy can be used to introduce a therapeutic transgene to Sertoli cells and restore spermatogenesis (details in Chapter 3). Whereas, germ cell single gene defects will need to be approached via testicular biopsy, to determine the presence or absence of germ cells. If germ cells are present, gene targeting can be performed ex vivo in SSC culture (Chapter 4). Alternatively, gene targeting can be achieved through induced-pluripotent stem cells (iPSCs) derived from the patient's skin fibroblasts and later differentiated into primordial germ cell-like cells (PGCLCs) for transplantation (Chapter 5). This is to circumvent the problems regarding failure of human spermatogonial stem cell culture, and to provide an alternative approach for those whose testes are devoid of germ cells (such as in some SCO cases). To prevent transmission of transgenes to the next generation, prenatal genetic diagnosis (PGD) will be used to select against embryos with resultant transgenes (Chapter 4.3). In the case of gene targeting for small mutations where transgenic selection cassette is not needed, I demonstrate a footprintless gene editing using ssODN (Chapter 4.2). DNA delivery methods for SSCs will be systematically experimented and shown in Chapter 4.1.

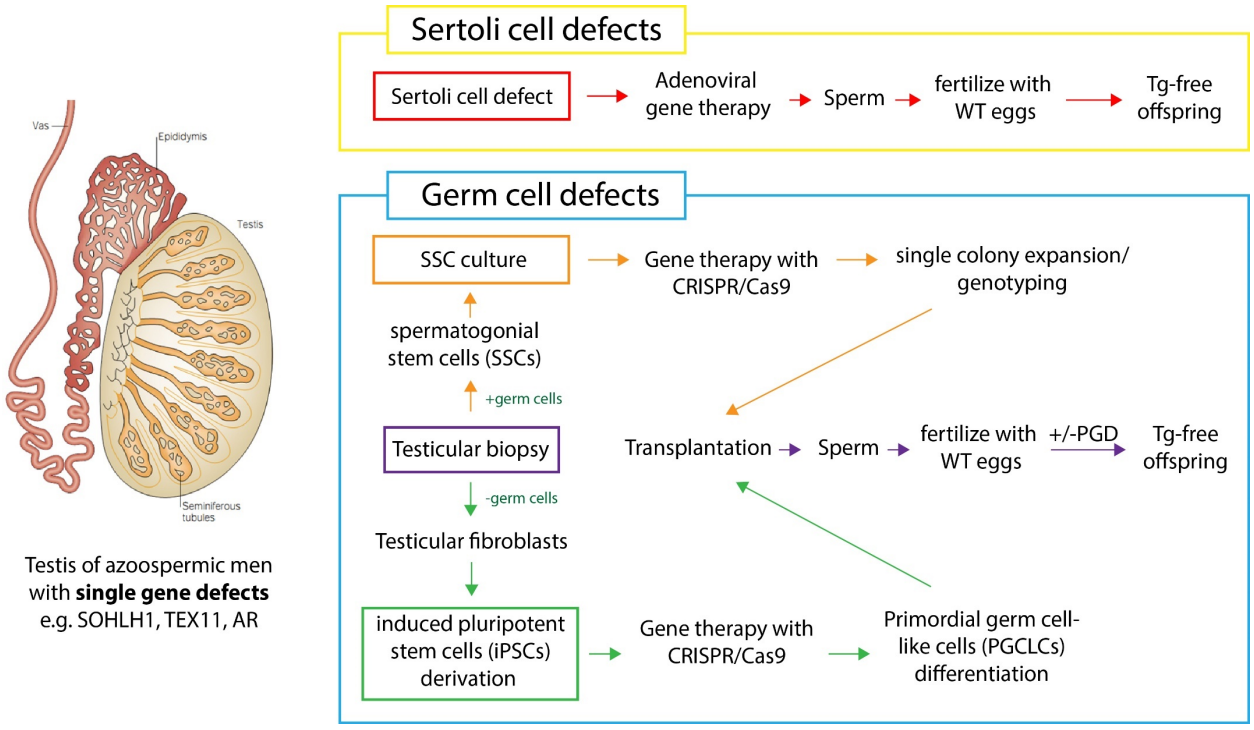

Figure 2 Gene therapy treatment approaches for male infertility related to single gene defects

Both for Sertoli cell defects or germ cells defects (WT=wild-type, Tg=transgene)

2.0 Identify treatment outcome in NOA by standard Testicular Sperm Extraction procedure to emphasize the need of novel therapy for NOA

2.1 Introduction

NOA patients do not have sperm in their ejaculates but many have pockets of spermatogenesis in the seminiferous tubules of their testes that can be extracted surgically and used to fertilize eggs by Intracytoplasmic Sperm Injection (ICSI); allowing NOA patients to have biological children [52, 58, 59]. The procedure of incisional testicular biopsy known as Testicular Sperm Extraction (TESE) is the standard approach to retrieve sperm from azoospermic men regardless of the causes of azoospermia [54, 60]. Therefore, the likelihood of an NOA patient having a biological child is primarily dependent on successful sperm recovery by TESE.

TESE is categorized into conventional TESE, where the biopsy is done by blind sampling while biopsy by microdissection TESE (microTESE) is performed with visualization under the microscope. MicroTESE therefore allows surgeons to identify seminiferous tubules with a larger diameter, which is associated with higher spermatogenesis activity [65, 193]. MicroTESE was first introduced in 1998 by Schlegel et al., who showed that microTESE increased sperm recovery rate (SRR) from 45% to 65% compared to conventional TESE [65, 66]. Thereafter independent studies in multiple centers have supported higher overall SRR from microTESE compared to conventional TESE in uncategorized NOA cases. A meta-analysis by Bernie et al., summarized this difference to be 1.5 times higher [194]. Nevertheless, microTESE is not as commonly performed as conventional TESE because it requires special equipment and setting, expertise, and a longer operation time per patient [195, 196]. Because it is currently not feasible

for microTESE to be provided to every NOA patient even in clinics where it is available, it is necessary to identify criteria for patient allocation based on need.

Multiple studies on conventional TESE uniformly reported higher SRR in hypospermatogenesis over Sertoli cell only syndrome (SCO) or maturation arrest (MA) subtypes, showing dissimilar nature among histological subtypes of NOA [64, 196-215]. There were limited numbers of studies that directly compared conventional and microTESE in individual histological subtypes and the results are conflicting [196, 205, 208, 209, 215, 216]. The apparent advantage of microTESE over conventional TESE is the ability to select larger seminiferous tubules by microscopic inspection; because not all NOA histological subtypes exhibit the same degree of heterogeneity in tubule size, I hypothesized that the benefit of microTESE is not uniform among NOA subtypes. I performed meta-analyses to identify which NOA histological subtypes may benefit more from microTESE over conventional TESE. Our analyses may be helpful in prioritizing patients for microTESE, especially in the settings where microTESE cannot be provided to every NOA patient and a diagnostic testicular biopsy can be performed before TESE procedures.

In this study, I sought to answer two questions. First, I aimed to determine the overall SRR for each NOA histological subtype by either conventional or microTESE. These findings provide general statistics on SRR for both techniques in all NOA histological subtypes, which can be used as reference standards for infertility clinics or conventional/microTESE studies to compare their performances to relevant studies that were published. The second aim was to ascertain whether microTESE has higher SRR over conventional TESE for each NOA histological subtype by directly comparing the subtype SRRs from microTESE and conventional TESE performed within the same study. This finding will uncover whether microTESE has benefit over

conventional TESE in all NOA subtypes or only certain subtypes, which may aid surgeons in prioritizing patients for microTESE based on histological subtypes.

2.2 Materials and methods

2.2.1 **Study design**

Because this meta-analysis aimed to 1) comprehensively estimate standard SRRs for each NOA histological subtype extracted from conventional or microTESE surgery, and 2) directly evaluate the surgery outcome of microTESE compared to conventional TESE for each subtype by calculating relative SRRs, this study was separated into two parts. The first part was to include studies that performed either conventional or microTESE in at least one histological subtype. The pooled (combined) SRRs were calculated separately for each technique and each histological subtype resulting in six statistical paradigms. The second analysis only included studies that performed both techniques in the same study in at least one histological subtype. I then calculated relative SRRs (SRR of microTESE over conventional TESE) from each study separated by histological subtype, resulting in three direct comparisons of both techniques.

Because histological classification and terminology varied across studies, I re-classified, if necessary, the histological subtypes to meet McLachlan's criteria [58]. In brief, after any tissue biopsy (obtained before or after surgery) if no germ cells of any stage of development were seen, then the subtype was classified as SCO. MA was diagnosed if both germ and Sertoli cells were present, but no elongated spermatids were seen in any tissue biopsy obtained before or during TESE. Lastly, hypospermatogenesis was classified when elongated spermatids/mature sperm were

found in any tissue biopsy, but the degree of spermatogenesis was less than normal. If multiple biopsies were performed the most advanced stage was used to classify the patient.

The authors followed the Preferred Reporting Items for Systematics Reviews and Meta-Analyses (PRISMA) guideline in writing the protocol for study design, search strategy, inclusion/exclusion criteria, outcomes, statistical analysis, and bias assessment [217].

2.2.2 **Literature search**

I searched MEDLINE via Pubmed for studies that were published in English between 1988 to 2019. The search terms were "Azoospermia AND TESE OR microTESE AND (SCO OR MA OR Hypospermatogenesis)" and yielded 230 results. An additional manual search was done by scanning reference lists of review articles and related studies. Subsequently, 21 more studies were identified. After duplications were removed, 228 abstracts were screened, and 174 studies were excluded by exclusion criteria (detailed in the "Study selection" section). Full text of 54 studies were assessed and an additional 16 studies were excluded (reasons provided in table 4). Overall, 38 studies were included in this meta-analysis (Fig. 3).

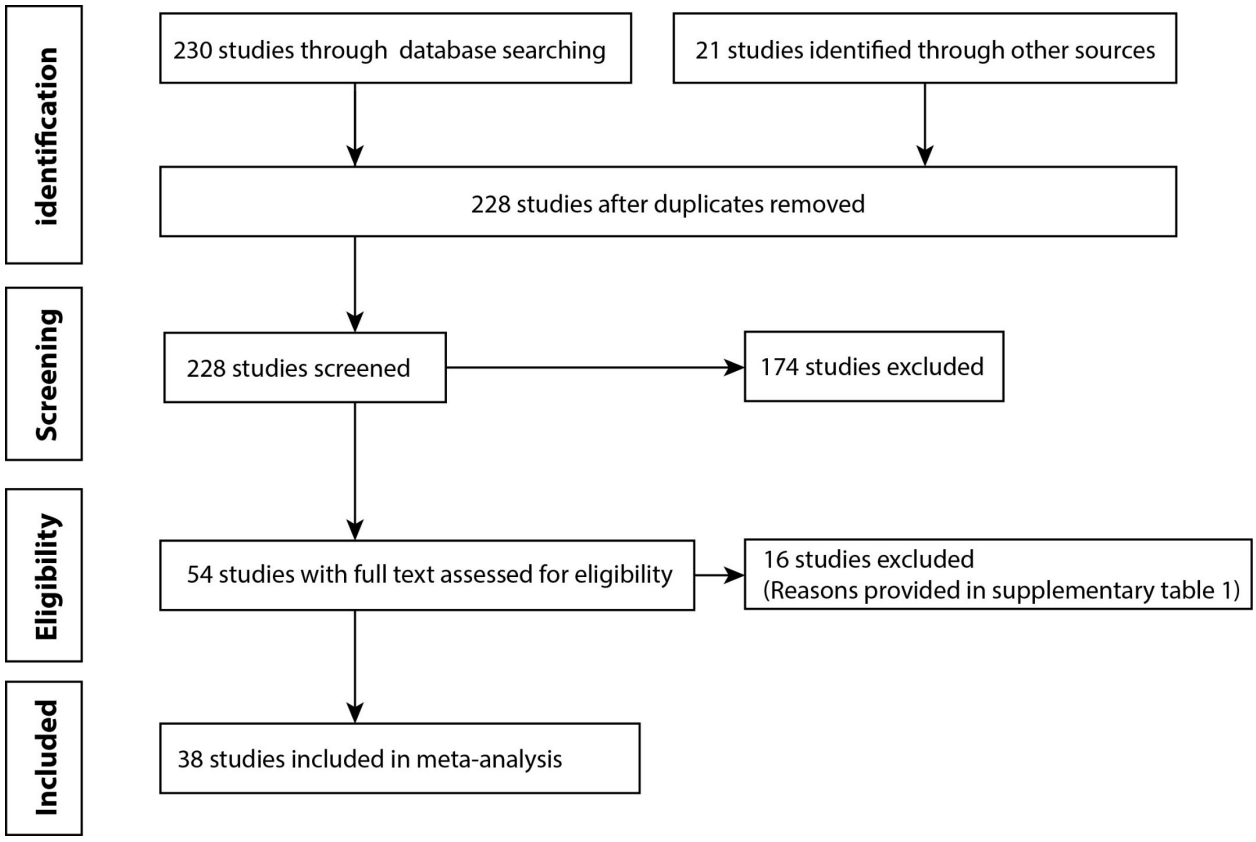

Figure 3 PRISMA-formatted study selection

Both a database search and literature review were done to identify studies and after duplications were removed a total of 228 studies were screened. All studies were screened by reading abstracts and 54 studies were included for full-text assessment. Sixteen studies were excluded with reasons given in table 4. Finally, 38 studies were included for the first meta-analysis and six were included for the second.

Table 4 Studies that were excluded from the meta-analysis and reasons

No	Study	Year	Reasons
1	Friedler	1997	Potentially overlapped group of patients with later study
2	Tournaye	1999	No histology definition was given, cannot be re-categorized
3	Jezek	1998	Did not report SRR for each histology
4	Amer	2000	Histology not classified
5	Mesequer	2003	Post-chemotherapy patients
6	Mulhall	2005	Did not report SRR for each histology
7	Ramasamay	2006	All patients had a history of failed TESE
8	Haimov-Kochman	2009	All patients had a history of failed TESE
9	Tarunc	2010	MicroTESE was done after a failed conventional TESE
10	Abdel	2012	Did not specify the type of procedure, between conventional or microTESE, that was used in each case
11	Schwarzer	2013	MicroTESE was done after a failed conventional TESE
12	Kalsi	2015	All patients had a history of failed TESE
13	Ramasamay	2015	Did not report SRR for each histology
14	Vloeberghs	2015	SRR reported were mixed between conventional and microTESE
15	Franco	2016	All patients had a history of failed TESE
16	Gnessi	2018	Oligozoospermia patients were included in the analysis

2.2.3 **Study selection**

For the first meta-analysis, I included the microTESE/TESE studies which met all the following criteria: 1) had non-obstructive azoospermic patients with either SCO, MA, or hypospermatogenesis histological subtypes identified or described, 2) patients had no prior history of conventional or microTESE surgery, and 3) SRRs were reported as the surgery outcome. In the second analysis, only studies that compared conventional and microTESE within the same study were included to calculate relative SRR for each histological subtype. I excluded studies if they met any of these conditions: 1) the study did not report histology, 2) chemotherapy or other toxic

agents were the likely cause of NOA, 3) oligozoospermic or obstructive azoospermic patients were included, 4) patients had undergone and failed TESE prior to recruitment, 5) microTESE was performed after a failed conventional TESE within the study, 6) SRRs were not specific to individual histological subtypes, or 7) studies that reported patients from the same center within an overlapped period of time.

2.2.4 **Data collection**

The studies' location, sample size, surgical technique (and description), and the SRR for each histological subtype were collected and recorded in a standardized form, along with patient demographic data including: age, hormonal profile (testosterone, FSH, LH, prolactin), testicular size, and histological subtypes when available.

2.2.5 **Data synthesis**

All data syntheses were performed using STATA software (STATA corp. version 15.1). Pooled SRRs were calculated using the *metaprop* command based on a random effect model [218]. For pooled relative SRRs, the SRR for individual study were calculated and the pooled SRR and heterogeneity test were generated by the *metan* command. Consistency of finding across studies was assessed by T- and I-square statistics. Publication bias was assessed by funnel plots using the *metafunnel* command. Statistical significance was determined by a two-tail p-value less than 0.05.

2.3 Results

2.3.1 **Studies included in the meta-analysis and demographic results**

Overall, 38 studies and 6,528 patients (ranging from 31-191 patients per study) were included in this meta-analysis. Among these studies, 26 studies with 4,020 patients were used for pooled SRR synthesis for conventional TESE (26 studies with 2,101 patients for SCO, 25 studies with 932 patients for MA, and 22 studies with 937 patients for hypospermatogenesis). Whereas, 18 studies with 3,861 patients were used for synthesis of pooled SRR for microTESE (17 studies with 3,218 patients for SCO, 16 studies with 1,194 patients for MA, and 15 studies with 466 patients for hypospermatogenesis). For the second meta-analysis, six studies with 1,027 patients were used for synthesis of pooled relative SRRs (6 studies with 620 patients for SCO, 6 studies with 165 patients for MA and 5 studies with 242 patients for hypospermatogenesis) because each study performed both conventional and microTESE surgeries.

The studies were published in English between 1996 to 2019. There were 6 studies from North America, 17 from Asia, 13 from Europe and 2 from Africa. The details of patient characteristics such as age, testicular volume, testosterone, FSH, LH, Prolactin level, as well as the details of surgical techniques were summarized in Table 5.

Table 5 Demographic data and details of surgery

No.	First author	Study design	Year	Number of patients	Age (year)	Testosterone (ng/mL)	FSH (mIU/mL)	LH (mIU/mL)	Prolactin (ng/dL)	Testicular volume (mL)	Place	Surgical technique	Year of surgery
Conventional TESE													
1	Kahraman [197]	Retrospective study	1996	27	34.0 ± 4.2	-	13.2(9.6)	-	-	9.8 (3.2)	Belgium	-	1995
2	Mulhall [198]	Prospective study	1996	30	34±5 (24-58)	-	10.9±6.8	-	-	-	MA, USA	TESE: single open biopsy of 1-mL size ± contralateral side	-
3	Tournaye [219]	Retrospective study	1997	204	37.5 ± 7.3 (23-70)	-	-	-	-	-	University Hospital Dutch-speaking Brussels Free University Brussels	TESE: multiple random biopsy	-
4	Silber [220]	Case series (prospective study)	1997	35	-	-	-	-	-	-	Belgium	Multiple TESE from all over the region of testicle	-
5	Ezeh [199]	Prospective study	1998	33	-	-	18.5±12.5	-	-	30.4±12.4	UK	cTESE: single biopsy of 0.5x1.0x0.5 cm to 1.0x1.5x1.5 cm in size	-
6	Su [64]	Case series	1999	79	38±6 (26-63)		20 ± 13	-		10 ± 5	Cornell, NY	-	-

Table 5 continued

7	Seo and Ko [200]	Retrospective cohort(?)	2001	178	35.4± 2.7 years (26-45).	-	-	-	-	-	Korea	TESE: multiple TESE	June 1996 to February 1999
8	Friedler [201]	Retrospective study	2002	83	33.5±6.3	11.7±7.6 nmol/L	23.4±12.1	-	-	-	Assaf Harofeh Medical center, Israel	TESE: multi-site Biopsy	1995-1999
9	Ferras [221]	Case series	2004	91	-	-	-	-	-	-	France	-	-
10	Betella [202]	retrospective	2005	125	37.6 ± 3.3 (28-43)	3.9 ± 1.1 4.2 ± 0.8 4.3 ± 0.8	22.1 ± 6.3 17.7 ± 3.9 17.9 ± 1.7	5.0 ± 1.5 4.7 ± 1.0 4.2 ± 0.9	-	10.8 ± 1.7 11.4 ± 1.6 11.9 ± 0.9	University of Padova, Italy	TESE: bilateral open biopsy with 2 pieces of tissues with 5mm in diameter	March 1999 and April 2004
11	Nagata [204]	Retrospective cohort	2005	62	35(26-52)	-	-	-	-	-	Niigata University Hospital, Niigata, Japan	TESE: three biopsies taken randomly from each side	2000 - 2004
12	Koscinski [203]	Case series?	2005	37	32.9 ± 4. 6 (23–42)	-	22.9 ± 18.6 (1.9–89.4)	-	-	16.1 ± 8.1 (2.7–33.0)	France	TESE: A single large biopsy was taken from each testis	-
13	Vernaeve [207]	Retrospective study	2006	612	-	-	-	-	-	-	Belgium	TESE: multiple serial biopsies of 150 mg in size	1995-2003
14	Hauser [206]	Prospective	2006	86	21-47	-	-	-	-	-	Israel	TESE: multifocal TESE 3	-

Table 5 continued

												sites, 50mg each	
15	Weedin [211]	Retrospective study	2011	215	34.8±6.4	3.301+1.410	-	6.7±4.9	11±9.4	14.2±4.1	Baylor, Tx	TESE: 6 tissues taken from specific sites	2002-2009
16	Dadkhah [212]	Retrospective cohort	2012	440	-	-	-	-	-	-	Iran	Multiple TESE (the second and the following biopsy upto 5 was performed if the first biopsy yielded no sperm)	2007-2010
17	Nowroozi [210]	Single center controlled cross sectional study	2012	385	33±7.6 (22-65)	4.5±1.2	21.7±15.5	12.7±7	8.3±4.9	14.8 ±5.8	Vali-e-Asr infertility center Tehran, Iran	TESE: multi-site TESE (3 cuts on both sides)	2004-2010
18	Gul [222]	retrospective	2012	543	-	-	-	-	-	-	Turkey	TESE: multi-site biopsy started with one near upper pole ±middle or lower pole or opposite site	2003-2011
19	Sacca [213]	Descriptive study	2015	63	37.31±14.69	4.48±1.85	17.77±11.94	6.49±5.89	11.12±4.7	-	Italy	cTESE: 1 incision, multiple biopsy	2012-2015
20	Caroppo [214]	Retrospective cohort	2018	356	36.8	-	-	-	-	-	Italy	TESE: single open biopsy for a	2004-2009

Table 5 continued

												piece of ~8 × 4 × 3 mm	
microTESE studies													
21	El-Hagger [223]	Prospective study (not declared)	2007	48	-	-	-	-	-	-	University Hospital, Cairo Egypt	-	-
22	Song [224]	Retrospective cohort	2010	3	-	-	-	-	-	-	Korea	-	2002-2007
23	Ishikawa [195]	Retrospective	2010	150	34.7±6.8 (24-57)	-	-	-	-	-	Male infertility center	-	2006-2008
24	Kalsi [225]	Retrospective cohort	2011	100	37.25 (29-56)	-	21.3 IU/L (SCO) 16.18 IU/L (MA) 18.71 ± 1.37 (hypospermatogenesis)	-	-	-	UK	-	2005-2010
25	Berookhim [226]	Retrospective cohort	2014	640	34.0 ± 6.5	-	25.2 ± 14.2	-	-	8.3 ± 4.7	Tertiary referral center, Cornell	-	-
26	Cetinkaya [227]	Retrospective cohort	2015	191	34.4 ± 5.6	4.203 ± 2.65	21.1 ± 15.1	8.9 ± 6.5	13.2 ± 18.1	9.74 ± 8.09	Turkey	mTESE: 20 to 40X to identify. 15-20 mg from each testis were removed.	2006-2009
27	Bernie [194]	Retrospective cohort	2015	211	36 ± 7	4.08	21	-	-	10 ± 5	Cornell, NY	-	1995-2014
28	Enatsu [228]	Retrospective study	2015	329	33.9 ± 5.3	4.3 ± 1.9	22.5 ± 12.2	8.9 ± 6.1	-	10.9 ± 5.1	Japan	mTESE: under 20x microscope	-

Table 5 continued

29	Binsaleh [229]	Retrospective cohort	2017	255	35.8 ± 7.2	-	-	-	-	13.1 ± 5 ml, and left testicular volume 12.9 ± 5 ml	King Saud University, Saudi Arabia	-	2011-2014
30	Eken [230]	Retrospective study	2018	100	33.40 ± 5.73	3.6802 ± 1.4108	19.04 ± 7.64	9.39 ± 4.15	-	10.42± 3.76	Acibadem Adana Hospital, Adana, Turkey	-	2013-2016
31	Yu [231]	Retrospective study	2018	72	31 (23–46)	-	-	-	-	6.3 ± 3.3	Reproductive Medicine Center of the First Clinical Hospital of Jilin University, China	-	2016-2017
32	Amer [232]	Retrospective study	2019	1,191	successful mTESE cases: 37. 21 ± 9.71 failed mTESE cases: 36.38 ± 7. 62	-	successful mTESE cases: 19. 52 ± 13.08 failed mTESE cases: 19. 81 ± 14.21	-	-	-	Adam International Hospital, Giza, Egypt	-	January 2010 to May 2013
Conventional TESE and microTESE studies													
33	Tsujimura [196]	Comparative study?	2002	37 (cTESE) 56 (mTESE)	32.4±4.6 (cTESE) 33.9±5.4 (mTESE)	4.4±1.7 (cTESE) 3.7±1.7 (mTESE)	22.6±10.6 (cTESE) 24.0±14.6 (mTESE)	11.3±8.6 (cTESE) 8.3±7.1	12.3±9.3 (cTESE) 9.4±9.8 (mTESE)	7.2±3.7 (cTESE) 8.6±4.9 (mTESE)	Osaka University Hospital (Japan)	TESE: ~4mm near upper pole ±middle or lower pole or opposite	-

Table 5 continued

								(mTESE)				site (50mg/piece) mTESE: cTESE was performed if no sperm were retrieved by mTESE	
34	Okada [216]	Retrospective study	2002	24 (cTESE) 74 (mTESE)	-	-	-	-	-	-	Japan	TESE: multi-site biopsy	TESE: 1997-1998 microTESE:1999-2001
35	Ramasamy [205]	Retrospective	2004	48 (cTESE) 372 (mTESE)	38±1 (cTESE) 36±0.3 (mTESE)	3.16 (cTESE) 3.03 (mTESE)	-	-	-	-	New York Presbyterian Hospital Weill Cornell MC, NY	TESE: single incision, multiple biopsy upto 2 from the same side ± additional 2 form the contralateral side	-
36	Colpi [208]	Randomized controlled trial	2009	69 (cTESE), 69 (mTESE)	36.69 (19-57)	-	-	-	-	-	San Paolo Hospital, University of Milano, Italy	TESE: a single biopsy of 8x4x3 mm in size	2004-2006
37	Ghalayini [209]	Case series	2011	68 (cTESE), 65 (mTESE)	cTESE: 35.4±7.1 mTESE: 34.8±8.5 (p=0.4)	cTESE: 3.9±2.2 mTESE: 4.32.2 (p=0.3)	cTESE: 16.7±14.2 mTESE: 19.7±12.5(p=0.06)	11.1±8 11.1±7.6 (p=0.8)	8.7±4.1 8.7±2.9 (p=0.4)	11.9±4.6 11.8±4.1 (p=1.0)	Jordan	TESE: ~4mm near upper pole ±middle or lower pole or opposite site	-

Table 5 continued

												mTESE: cTESE was performed if no sperm were retrieved by mTESE	
38	Maglia [215]	Cross-sectional study	2018	96 (cTESE), 49 (mTESE)	Overall: 35.4 (21-54) cTESE: 35.6 (21-54) mTESE: 34.9 (23-48)	Overall: 5.0 (1.17-24.1) cTESE: 5.4 (1.17-24.1) mTESE: 3.6 (2.16-7.58)	Overall: 14.8 (1.71-59) cTESE: 12.8 (1.71-52.3) mTESE: 20.9 (1.81-59)	Overall: 5.7 (1.91-18.5) cTESE: 5.3 (1.91-18.5) mTESE: 7.2 (2.55-17.7)	Overall: 26.3 (4.6-68.1) cTESE: 30.1 (4.6-68.1) mTESE: 11.7 (5.0-26)	-	A single academic center for primary couple's infertility	cTESE: 5mm horizontal incision at the right median part of scrotum. If no sperm, upper and lower pole parts will be incised for more tissue. mTESE: Schlegel's method [66]. If no sperm, the same procedure were performed on the contralateral site	January 2012 – April 2017

2.3.2 **Meta-analysis for pooled SRR**

To acquire overall SRR for conventional and microTESE for each subtype, I calculated pooled (combined) sperm recovery rates from 38 studies. For conventional TESE, SCO had a 27% recovery rate (95% confidence interval (CI) =21-34%, p=0.00; T^2= 0.02, d.f.=25, p=0.00, I^2= 90.62%), MA had a 44% SRR (95% CI =35-52%, p=0.00; T^2= 0.04, d.f.=24, p=0.00, I^2= 86.80%), and hypospermatogenesis had a 82% SRR (95% CI =75-92%, p=0.00; T^2= 0.03, d.f.=21, p=0.00, I^2= 90.27%). For microTESE, the pooled sperm recovery rate for SCO was 32% (95% CI =27-37%, p=0.00; T^2= 0.01, d.f.=16, p=0.00, I^2= 84.27%), while MA was 44% (95% CI =35-52%, p=0.00; T^2= 0.02, d.f.=15, p=0.00, I^2= 77.13%), and hypospermatogenesis was 91% (95% CI =87-96%, p=0.00; T^2= 0.00, d.f.=14, p=0.00, I^2= 73.69%) (Fig. 4). This analysis showed nearest estimates of SRRs of either conventional or microTESE for each histological subtype by summarizing SRR from all relevant studies. However, it is not appropriate to directly compare the six statistical SRR estimates because each analysis had a different set of relevant studies included.

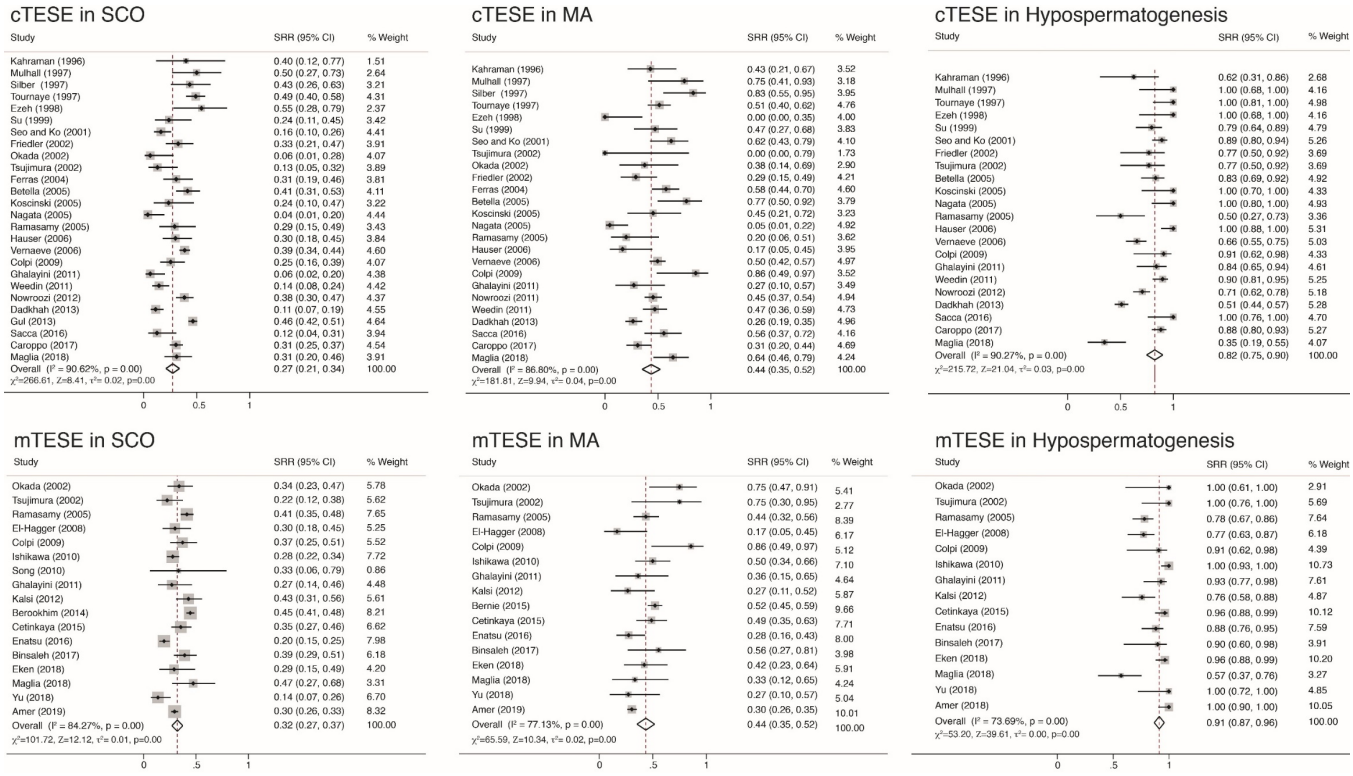

Figure 4 Pooled SRR for conventional TESE and microTESE in each histological subtype of NOA

Pooled SRR for conventional and microTESE for each histological subtype of NOA. The pooled SRR were calculated based on a random-effects model. SCO=Sertoli cell only syndrome, MA=maturation arrest, cTESE=conventional TESE, mTESE=microTESE.

2.3.3 **Meta-analysis for pooled relative SRR**

To directly compare the SRR between microTESE and conventional TESE within histological subtype, I calculated relative SRR (microTESE SRR divided by conventional TESE SRR) from the six studies that performed both techniques; I calculated pooled (combined) relative SRR results for each subtype based on a random-effects model. The pooled relative SRR for SCO was 1.48 (95% CI =1.04-2.10, p=0.028; $T^{2=}0.00$, d.f.=5, p=0.706). The pooled relative SRR for MA was 1.24 (95% CI =0.77-1.99, p=0.39; T^2=0.08, d.f.=5, p=0.259). For hypospermatogenesis, the pooled relative SRR was 1.07 (95% CI

=0.83-1.37, p=0.58; T^2=0.01, d.f.=4, p=0.95,) (Fig. 5). This showed that SCO had a higher SRR from microTESE compared to conventional TESE by 1.48-fold (p=0.028). However, there was no statistical significance between techniques for MA or hypospermatogenesis subtypes.

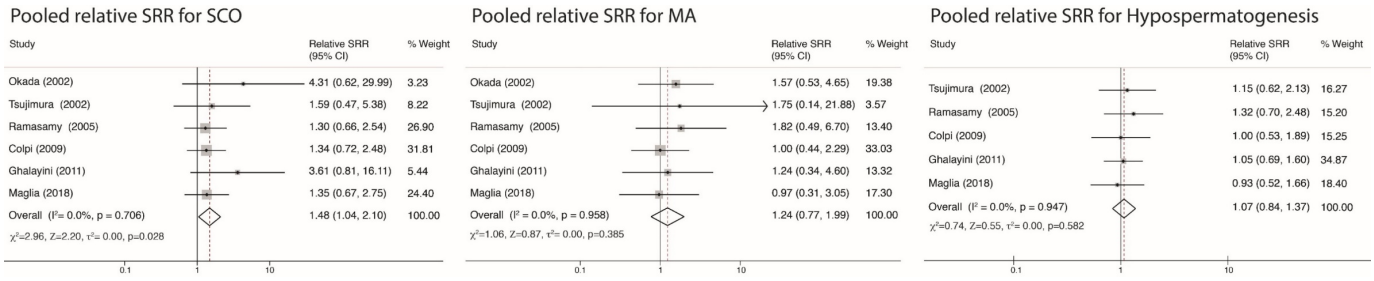

Figure 5 Pooled relative SRR of microTESE compared to conventional TESE

Relative SRRs were calculated from SRR $_{\text{microTESE}}$/ SRR $_{\text{conventional TESE}}$. SRR= sperm recovery rate, SCO=Sertoli cell only syndrome, MA=maturation arrest, D+L= DerSimonian-Laird random-effects model

2.4 Discussion

In this study, our first meta-analysis systematically combined SRRs for all three NOA histological subtypes from either conventional or microTESE surgeries. These pooled SRRs separated by histological subtype and surgery technique can be used as reference points to compare the outcome of a new center/study to the performance of multiple centers from 1997-2019. The strength of the first analysis is the large sample size, which provides a comprehensive estimate of SRR for each technique and individual subtype. The pooled SRRs from microTESE were 32% for SCO, 44% for MA, and 91% for hypospermatogenesis subtypes. SCO and hypospermatogenesis subtypes appeared to benefit from microTESE surgery compared to TESE, as conventional TESE pooled SRRs were 27% (SCO), 44% (MA), and 82% (hypospermatogenesis). However, these pooled SRRs cannot be used to directly compare

between microTESE and conventional TESE in the same subtype because the studies included in each analysis were different.

Therefore, I included a second meta-analysis to directly compare surgical outcome of microTESE to conventional TESE by calculating relative SRRs (the SRR from microTESE divided by the SRR from conventional TESE) for each NOA subtype. Thus, only the six studies that reported both microTESE and conventional TESE within the same study were included in this consecutive analysis. I found that the pooled relative SRR for SCO was 1.48 with a 95% CI of 1.04-2.10 and a significant p-value of 0.009, indicating that microTESE is superior in sperm recovery compared to conventional TESE for SCO patients. However, I did not observe a significant difference between pooled relative SRRs between surgical technique for either MA or hypospermatogenesis subtypes (1.38, p=0.210 for MA and 1.14, p=0.117 for hypospermatogenesis). Our second meta-analysis showed that patients with the SCO subtype significantly benefited from microTESE compared to conventional TESE, while patients with other histological subtypes did not. Therefore, from these analyses, patients with SCO subtypes should be prioritized for microTESE over the patients with the other two subtypes, especially in the setting where microTESE cannot be provided to all patients and a diagnostic testicular biopsy is performed prior to sperm recovery. However, it is noteworthy that MA and hypospermatogenesis subtypes had a smaller sample size compared to SCO (133 and 187 compared to 556, respectively), which may have contributed to inaccurate significance assessments.

Since the advantage of microTESE is that it allows the surgeon to visualize the different sizes of seminiferous tubules which enables us to identify the larger ones for sperm extraction, I hypothesized that microTESE should have more benefit in the histological subtypes with more heterogeneity (difference in size of the seminiferous tubules) than those that are homogeneous. The MA subtype has the lowest heterogeneity with 22.4% of MA cases reported to be uniform homogeneous phenotype [211]. Although

the percentage of homogeneity among SCO patients was not formally assessed, Berookim et al., reported that 2.34% (15/640) of SCO patients with lower SRR from microTESE compared to the rest of SCO patients (6.7% versus 31-49.5%) may associate with less heterogeneity in this subgroup [226]. The higher degree of heterogeneity among SCO patients may contribute to the fact that SCO is the only subtype with significantly higher SRR from microTESE compared to conventional TESE. The hypospermatogenesis subtype already has a high SRR from conventional TESE (95%CI= 76-91%). This is likely due to a high frequency of active seminiferous tubules in this subtype, increasing the chance of retrieving sperm from blind sampling. Therefore, it is unsurprising that the relative increase in SRR from microTESE compared to conventional TESE was not significant compared to SCO.

The largest limitation of this study is due to the inevitable variation across studies. Factors such as surgeon experience, pathologists who made the diagnosis, laboratory techniques to extract sperm, differences in surgery details (number of tissues taken, size of tissue, the site where the tissue was taken) and even the number of cases that underwent surgery/pathological diagnosis per day, can contribute to a wide range of SRRs. However, funnel plots showed symmetrical and pyramidal-shaped distribution, indicating minimal publication bias of the studies included in each analysis (Fig. 6, 7).

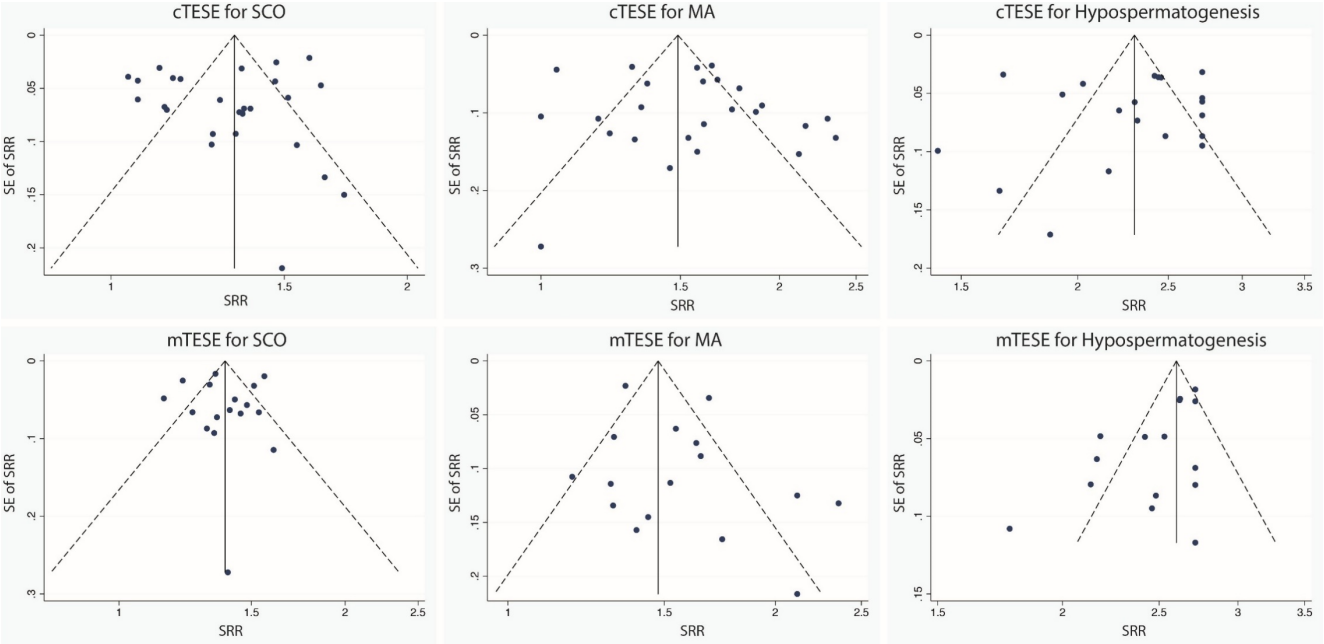

Figure 6 Funnel plot with pseudo 95% confidence limits for pooled SRR

Funnel plot for pooled SRR for conventional and microTESE for each histological subtype of NOA. SCO=Sertoli cell only syndrome, MA=maturation arrest, cTESE=conventional TESE, mTESE=microTESE, SRR=sperm recovery rate, SE= standard error of means

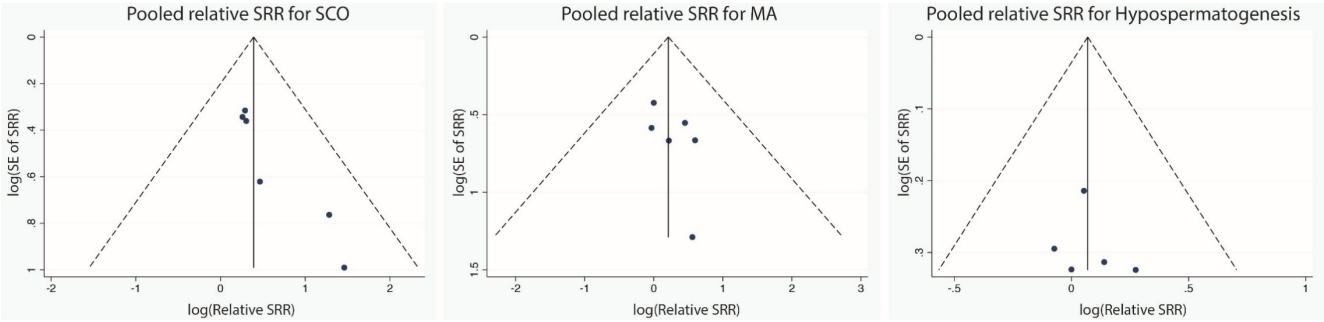

Figure 7 Funnel plot with pseudo 95% confidence limits for pooled relative SRR

Funnel plot for pooled relative SRR for each histological subtype of NOA. SRR = sperm recovery rate, Relative SRR = SRR microTESE/ SRR conventional TESE. SE=standard error of means

2.5 Conclusions

In conclusion, this study provided comprehensive statistics for SRR from conventional and microTESE separated by NOA histological subtype from relevant studies, which could be used as a reference for infertility centers and new studies to compare their performances. The second meta-analysis provided a direct comparison of surgical techniques across NOA histological subtypes and suggested that patients with the SCO subtype benefit the most from microTESE compared to TESE than the other subtypes. Therefore, centers that only can perform microTESE for a subset of patients and are also able to take a testicular biopsy prior to surgery should prioritize SCO patients for microTESE.

2.6 Acknowledgements

Chatchanan Doungkamchan planned, did the experiment, and prepare manuscript. Evelyn Talbot and Tianjiao Chu advised on statistics. Sarah Munyoki advised on STATA software coding. Amanda Zielen edited the manuscripts. Kyle E. Orwig advised on the study.

3.0 Sertoli cell gene therapy

3.1 Introduction

Azoospermia is defined by the absence of sperm in the ejaculate and hence considered the most severe form of male infertility [52]. Azoospermia affects approximately 10-15% of infertile men or 1% of men in their prime reproductive years of 20-50, which could be translated into 645,000 men in the United States alone [56, 57, 211]. The same incidences have also been reported worldwide, making this problem globally significant [50, 60].

To restore fertility in azoospermic patients, testicular sperm are retrieved surgically by a procedure known as Testicular Sperm Extraction (TESE). Testicular sperm are subsequently used for intracytoplasmic sperm injection (ICSI), thus allowing the patient to have their own biological child [59, 233, 234]. This entire process of TESE followed by ICSI is considered the standard measure to restore fertility in azoospermic patients [54, 60]. The success rate of TESE is highly associated with the type of azoospermia, Obstructive or Non-obstructive azoospermia. Obstructive azoospermia (15-20% of all azoospermia cases), where azoospermia happens because of an obstruction or malformation of the genital tract, has close to 100% sperm recovery rate (SRR) by TESE because spermatogenesis is still intact. On the other hand, non-obstructive azoospermia (NOA; 80-85% of all azoospermia cases), where pathology arises from inability to produce sperm, has only approximately 50% SRR by TESE [56, 58, 59]. To date, there are no further treatment options for those NOA patients who failed TESE to have their own biological children.

To improve the prognosis of NOA patients, I aim to seek a treatment method that improves sperm recovery rate or ultimately restores natural fertility in NOA patients, especially for those who failed TESE.

Among the three subtypes of NOA, which are hypospermatogenesis, Sertoli cell-only syndrome (SCO) and maturation arrest phenotype (NOA-MA), multiple studies consistently reported low TESE SRR in SCO (0-40% SRR) and Maturation arrest (30-50% SRR) compared to hypospermatogenesis (80-95% SRR) [58, 211]. While SCOs were diagnosed when no germ cells were spotted in the testicular biopsy, and therefore the treatment might have to rely on replenishing the germ cell pool with germ cells from any sources, maturation arrest testes already contain pre-existing non-maturing germ cells that might resume spermatogenesis once the causes of maturation arrest are corrected. Some causes of maturation arrest are reported to involve single gene defects related to Sertoli cells (e.g. *AR*, *NR5A1*, *WT1*) [79, 235-238] or germ cells (e.g. *SOHLH1*, *TEX11*) [73, 74, 76]. Therefore, I hypothesized that resumption of spermatogenesis in maturation arrest germ cells is possible if the expression of the defective gene is restored.

In this study, I focus on Sertoli cell defects because; 1) Sertoli cell defects have already been confirmed as a cause of human NOA-MA, as mention previously; 2) it is still ethically unacceptable to modify the germ line in cases where pathology arises from germ cell-specific single gene defects [239, 240]; 3) there have been studies reporting successful *in viv*o Sertoli cell transduction without evidence of modifying the germline [241-243]. These studies, conducted in 2002, independently used adenovirus, lentivirus and electroporation to deliver Kit ligand cDNA into Sertoli cells of Steel mice *(Kit*$^{l-/}$-), which lack the Kit ligand and were azoospermic from Sertoli cell defect. As a result, Kit ligand expression and spermatogenesis was partially restored. The sperm from lentivirus and adenovirus treatment were also used to fertilize eggs by ICSI and subsequent embryo transfer, resulting in live-born offspring that did not have the transgene in their genome. However, the combined results of 33 offspring were assessed in those two studies to address the risk of germline transmission; more rigorous assessment of germline transmission risk is needed. Additionally, *KITL*G mutation in humans results in deafness (loss of function

mutation) [244] or Familial Progressive Hyperpigmentation with or without Hypopigmentation (gain of function mutation) [102], neither of which is associated with infertility. Loss-of-function mutations of c*Kit, t*he receptor for KIT ligand results in Piebald trait described as hypopigmentation of hair or skin, but not infertility [245]. In this study, I used Sertoli Cell Androgen Receptor Knockout (SCARKO) mice, which exhibit NOA-MA phenotype [98] and model the Mild Androgen Insensitivity Syndrome phenotypes associated with human Androgen Receptor (AR) mutations observed in some infertile patients who are otherwise healthy. Adenovirus was used in this study because it was shown to specifically deliver a transgene to Sertoli cells *in vivo* [241] and does not integrate into the genome [246]. I aim to correct the NOA-MA phenotype in SCARKO mice by using an adenovirus vector to deliver a functional AR cDNA to defective Sertoli cells *in vivo.* I hypothesize that this can be achieved without transmitting the transgene to progeny.

3.2 Materials and methods

3.2.1 **Animals**

For adenoviral studies, SCARKO mice were the generous gifts from Dr. Robert Braun's laboratory. The generation of this line and phenotypic characterization was done and described previously [98]. In brief, flox-AR exon1 (Ar^{tm2Reb}) heterozygous female mice were bred with Anti-Müllerian Hormone (Amh)-Cre male mice, resulting in the Sertoli cell-specific removal of AR exon1 in offspring. Mice were 2-4 months old at time of adenoviral injection. The flox-negative Amh-Cre littermates were used as controls. The female mice used to test SCARKO fertility after treatment were C57BL/6J that were

8 weeks to 3 months old. Animal care and sacrifice protocol were approved by University of Pittsburgh IACUC committee (Assurance # A3654-01).

3.2.2 **Adenoviral vector**

To generate hAR adenoviral vector, the flag-hAR cDNA was amplified from pcDNA3 –flag-hAR (gift from Dr. William Walker) using primer pair: forward 5' CATTGTCGACATGGACTACAAGGACGACGA-3' and reverse 5'-GCATTCTAGATCACTGGGTGTGGAAATAGAT, digested by SalI/XbaI, then inserted into pENTR-EF-EGFP-2A plasmid. EGFP and hAR are under control of human EF1a promoter. The Gateway® LR recombination system (12535-019, ThermoFisher Scientific, PA, USA) was used to transfer EGFP-2A-hAR into pAd/PL-DEST. Adenoviral vectors were produced in 293A cells according to the user manual of ViraPowerTM Adenoviral Expression System (K4940-00, ThermoFisher Scientific, PA, USA).

3.2.3 **Adenoviral injection**

Adenoviral titer for both therapeutic and empty vector types was 4.2 x 10^6 ifu/mL. Adenovrial mixture was prepared for the injection by adding trypan blue to make adenoviral solution with 10% v/v trypan blue [247]. Approximately 6.5-7 µL of Trypan blue-adenovirus mixture was used for a SCARKO testis, whereas 10 µL was used for an Amh-Cre testis because Amh-Cre testes are larger and can accommodate a larger volume. The virus was introduced into the recipient mouse testes by efferent duct injection using an Eppendorf Femtojet microinjector and a pulled glass capillary pipette as described previously [248].

3.2.4 **Histology and Immunohistochemistry**

For fluorescence immunohistochemistry, testes were fixed in 4% paraformaldehyde (PFA) solution overnight followed by 3 washes in 1X PBS solution (10 mM PO_4^{3-}, 137 mM NaCl, and 2.7 mM KCl) every hour. The fixed testes were then sent to the Histology Core, University of Pittsburgh for sectioning. Prior to staining, deparaffinization was done in 100% acetone for 15 minutes twice. Rehydration was performed with serial diluted ethanol solutions starting from 100% Ethanol twice, then 95%, 75%, 55%, 25% and 1X PBS solution for 3 minutes each. Antigen retrieval was done using citrate buffer at 97°C for 30 minutes. Antigenic blocking was done prior to primary antibody staining with donkey blocking buffer (5% normal Donkey serum, 3% BSA, 0.1% Triton X-100 in 1x PBS) for 3-4 hours. Sections were incubated with primary antibody overnight and washed 3 times in 1xPBS, 3 minutes each. Secondary antibody incubation was for 45 minutes the following morning and washed 3 times in 1xPBS, 3 minutes each. Mounting medium used in this experiment was Vectashield (Vecterlab, USA) which has DAPI staining. Antibodies and concentrations used in this experiment are summarized in supplementary Table 1. Visualization and image collection were done with Zyla sCMOS camera (Andor technology, Belfast, UK) with NIS-elements Eclipse 90i software (Nikon, Tokyo, Japan).

For hematoxylin and eosin (H&E) staining, I fixed the tissue with Bouin's solution overnight followed by washing with 100% methanol 6 times every hour for 6 hours. The sixth wash was left overnight, and the tissues were sent to the histology core the following morning for sectioning and H&E staining. Analysis was performed with the microscope and Nikon NIA-elements Eclipse analysis (Nikon, Tokyo, Japan). Image collection was done using Nikon DSFi2 camera and NIS-elements Eclipse 90i software (Nikon, Tokyo, Japan).

3.2.5 **Intracytoplasmic Sperm Injection (ICSI)**

Superovulation of oocytes from female C57BL/6 x DBA/2 (B6D2 F1, 7-8 weeks old) mice was performed by intraperitoneal injection of 5 IU PMSG (Pregnant Mare Serum Gonadotropin) (HOR-272, ProSpec-Tany TechnoGene Ltd, Rehovot, Israel), followed 48 hours later by 5 IU hCG (human Chorionic Gonadotropin) (CG5-1VL, Sigma-Aldrich, MO, USA). Fourteen to fifteen hours after hCG injection, the oocyte-cumulus complexes were collected from oviducts, then treated with hyaluronidase to release eggs. The eggs were washed using M2 and KSOM media, then transferred into the dishes of KSOM drops covered with mineral oil. The dishes were placed in an incubator containing humidified 5% CO_2/air at 37°C.

Sperm were collected from the cauda epididymides of treated mice by dicing with fine scissors in a drop cryoprotective agent medium (18% raffinose and 3% skim milk) covered with mineral oil, then incubated at 37°C for 3-5 min. Sperm were collected, aliquoted, and frozen in liquid nitrogen. ICSI was performed by Piezo-actuated micromanipulation as previously described [249]. The injected eggs were cultured in KSOM medium to 2-cell or morula/blastocyst stage before transfer to pseudopregnant CD-1 females.

3.2.6 **Blood-testis barrier integrity assessment**

The integrity of the blood testis barrier was evaluated three weeks after virus injection. Amh-Cre and SCARKO mice were anesthetized and 30 µL of EZ-Link™ Sulfo-NHS-LC-Biotin tracer (30 µg/µL, 21335, Thermo-Fisher, PA, USA) were injected via the efferent ductules into the interstitial space (between seminiferous tubules). The testes were placed back into the abdominal cavity for 30 minutes before the animals were euthanized. Testes were then removed and immediately placed in 4% PFA

overnight as described previously [250]. The fixation, sectioning and staining protocols were the same as mentioned in the Histology and immunohistochemistry section. Antibody used to visualize tracer protein was streptavidin-conjugated Alexa 488. The tissues were stained for 45 min, washed 3 times each for 3 minutes in 1x PBS before visualization. Quantification was done by grading the severity of infiltration into three degrees; normal (no tracer inside the lumen of the seminiferous tubule), mild (tracer seen inside the lumen of seminiferous tubule) and moderate-to-severe (highly fluoresced particle in the lumen of seminiferous tubule) as described previously [251]. All seminiferous tubules (approximately 120-250 tubular cross sections) in a testicular cross section/testis were graded. The number of tubules with normal, mild and moderate-to-severe levels of infiltration were reported as a percentage of total tubules in that testis cross section.

3.2.7 **PCR for EGFP**

Pup tails born from ICSI using SCARKO sperm and natural breeding from Amh-cre mice treated with either Adeno-EGFP-hAR or -empty virus, were used for DNA extraction, which was done using DNA extraction buffer (40mM TrisHCl, 200mM NaCl, 20mM EDTA, 0.5% SDS, 0.5% β-ME, pH 8.0) and ethanol precipitation. Nuclease-free water was used to resuspend DNA precipitates. The DNA was then subjected to Nanodrop to determine concentration and quality of the DNA. PCR was performed using LongAmp® Taq 2X Master Mix (m0287, New England Biolabs, MA, USA). The forward primer sequence (EF1a-7) is ACGTGAGGCTCCGGTGCCCGTCAG, which will bind at EF1a region. The reverse primer sequence (GFP-6) is CGCTTTACTTGTACAGCTCGT, binding at the EGFP region. The PCR cycle was 95ºC for 10 minutes then 95ºC for 30s, 60ºC for 20s, 72ºC for 50s for 30 cycles, then 72ºC for 10 minutes. Positive control for EF1-EGFP PCR was pEF1-EGFP plasmid. Final concentrations of DNA were 100-400 ng/25 μL. All DNA were used for PCR for Rosa26 gene (Rosa26-F:

GTGTTCGTGCAAGTTGAGTCCAT and Rosa26-R: TAAAGACATGCTCACCCGAGTTTTA). PCR genotyping for Artm1Rb-flox allele and Cre allele were done as described previously [98].

3.2.8 **Statistical analysis**

Statistical analyses were done using Graphpad Prism 7 software (Graphpad Software, CA, USA). Statistical tests and numbers of samples (n) for each experiment were indicated separately in the results section.

3.3 Results

3.3.1 **SCARKO mice are infertile with an azoospermia maturation arrest phenotype**

The SCARKO mice were made and characterized by Braun and colleagues in 2014 [98]. To confirm the phenotypes of SCARKO mice I evaluated 1) spermatogenesis status by histology; 2) AR expression in the testis, and specifically Sertoli cells by immunohistochemistry; and 3) fertility status by breeding. A testis retrieved from an Amh-Cre control mouse (Fig. 8A, Left) is bigger than that of a SCARKO mouse (Fig. 8A, Right) (Amh-Cre-control: 118.10±16.2 mg versus SCARKO: 46.25±3.3 mg). To assess fertility status, SCARKO mice were bred with female mice and did not produce pups (0 pups/42 breeding attempts), compared to Amh-Cre mice that produced 33 litters/38 breeding attempts with an average litter size of 5.41 ± 3.0 pups/litter (Fig. 8B). To assess spermatogenesis, H&E staining was performed. Histological analyses in Amh-Cre mice revealed complete spermatogenesis in all seminiferous tubules with multiple layers of germ cells and a central lumen with spermatids or sperm (Fig. 8C). In

contrast, SCARKO testes were significantly smaller than wild type testis and histological analyses revealed an NOA-MA phenotype with uniform meiotic arrest. Round spermatids were rarely observed, and elongated spermatids and sperm were never observed (Fig. 8D). Immunohistochemistry for the AR protein confirmed AR expression in Leydig cells, peritubular myoid cells and Sertoli cells of Amh-Cre (control) testes (Fig. 8E). For SCARKO mice, AR was expressed in Leydig cells and peritubular myoid cells but was absent from Sertoli cells (Fig. 8F). The Sox9-positive Sertoli cell numbers were similar in SCARKO seminiferous tubules compared to the Amh-Cre controls (Fig. 8G, H), which means that Sertoli cells were present inside SCARKO testes but did not express AR. These SCARKO phenotypes are consistent with that previously reported by Braun and colleagues [98].

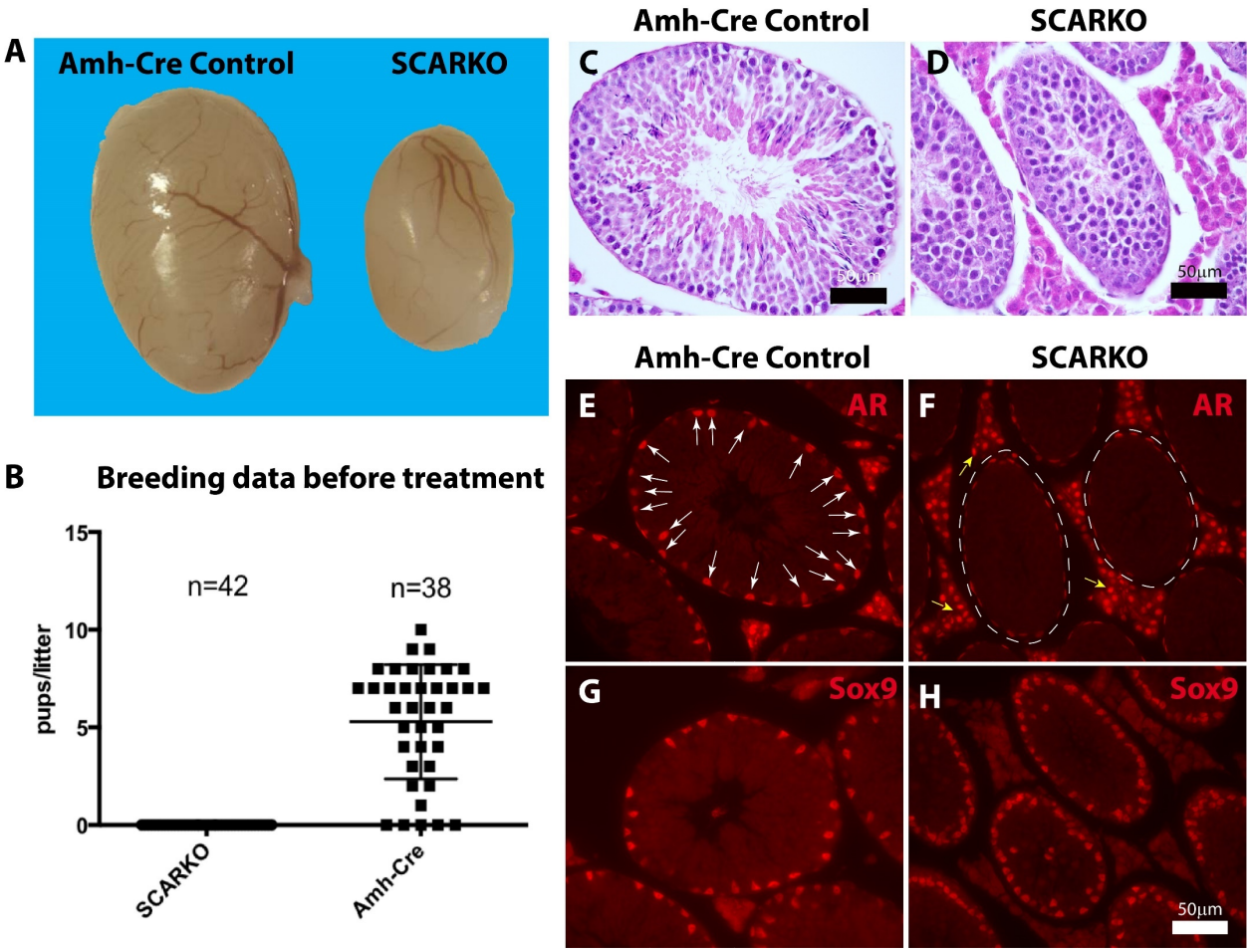

Figure 8 Phenotype of SCARKO mice compared to the Amh-Cre control

A testis retrieved from an Amh-Cre control mouse (A, Left) compared to that of a SCARKO mouse (A, Right). Breeding data before adenoviral treatment where 19 Amh-Cre mice and 21 SCARKO mice were individually bred with a female mouse for 2 cycles to make 38 breeding cycles for Amh-Cre mice and 42 breeding cycles for SCARKO mice (B). H&E staining in Amh-Cre mice (C), and in SCARKO mice (D). Immunohistochemistry using AR antibody in Amh-Cre (E) and SCARKO mice (F). Arrow indicates expression of AR in the cells on the basement membrane of seminiferous tubules in Amh-Cre testes (E, arrow), while no cells inside the seminiferous tubules of SCARKO mice were positive for AR (F). AR expressing cells such as peritubular myoid cells (F, dash line) and Leydig cells (F, yellow arrow) were normally expressing AR in SCARKO seminiferous tubules. Immuno-staining for Sox9 antibody in Amh-Cre testis (G) and SCARKO (H). (AR = Androgene Receptor, Sox9 = Sertoli cell marker, *scale bar = 50µm*)

3.3.2 **Adenovirus successfully restored AR expression in Sertoli cells**

To restore AR expression in Sertoli cells *in vivo*, I used adenovirus serotype 5 (Ad5) as a vector, separately packaged with two different types of transgenes, Adeno-EGFP-hAR (Fig. 9A) and Adeno-EGFP-empty plasmids (Fig. 9B). Adeno-EGFP-hAR plasmid includes EGFP-T2A-hAR expressed under EF1a ubiquitous promoter (Fig. 9A). Adeno-EGFP-Empty does not contain hAR (Fig. 9B). To test whether Adenovirus can successfully transduce seminiferous epithelium when injected into the seminiferous tubules, I injected Adeno-EGFP-Empty adenovirus into the lumen of seminiferous tubules of control mice via efferent ductules as previously described by Brinster and colleagues [248, 252, 253] and assessed for EGFP expression under the fluorescence microscope and by immunohistochemistry at 3 weeks after injection. To test whether Adeno-EGFP-hAR adenovirus can successfully restore AR expression, I injected Adeno-EGFP-empty (Fig. 9C-G) or Adeno-EGFP-hAR adenovirus (Fig. 9H-L) into seminiferous tubules of SCARKO mice. AR expression was detected by immunohistochemistry at 3 week after injection in SCARKO seminiferous tubules injected with Adeno-EGFP-hAR (Fig. 9J) but not in SCARKO seminiferous tubules injected with Adeno-EGFP-empty (Fig. 9E). AR expression was entirely localized with EGFP that was expressed from the same vector, confirming that successful AR expression was a result of transgene expression (Fig. 9L).

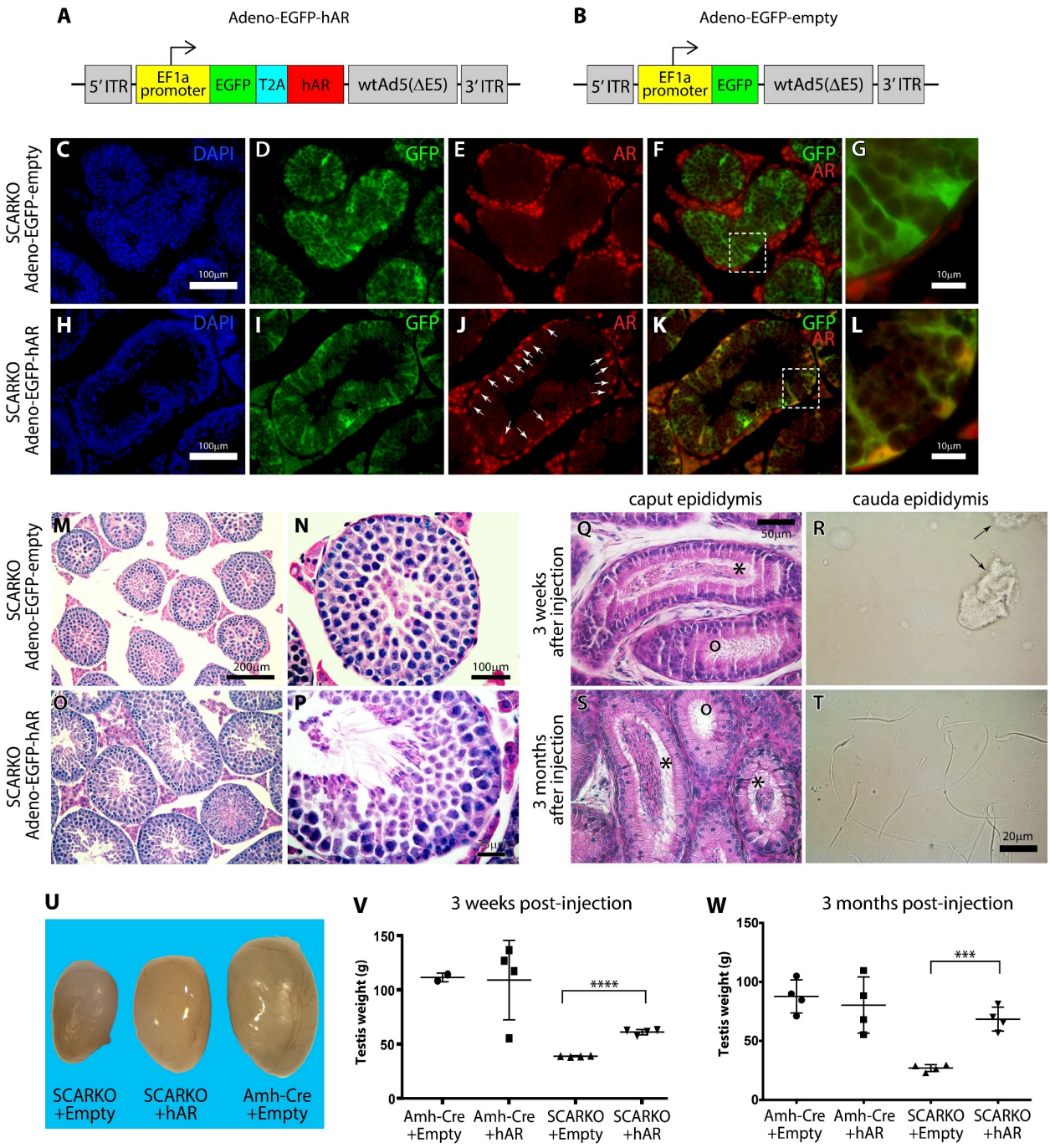

Figure 9 Adenovirus successfully restored AR expression and normal spermatogenesis in SCARKO mice

The plasmid constructs of the therapeutic vector (Adeno-EGFP-hAR, A) and control vector (Adeno-EGFP-empty, B). Testis from SCARKO mice injected with Adeno-EGFP-empty (C-G) or Adeno-EGFP-hAR adenovirus (H-L) co-stained with antibodies against EGFP (D, I) and AR (E, J). H&E staining of SCARKO mice treated with Adeno-EGFP-empty (M, N) versus Adeno-EGFP-hAR adenovirus (O, P). H&E section of head of the epididymis of SCARKO mice treated with Adeno-EGFP-

hAR adenovirus at 3 weeks (Q) and 3 months (S) after treatment. Star (*) indicates epididymis cross sections with mature sperm compared to empty tubules indicated by the letter o. Cauda epididymal sperm retrieved from SCARKO mice treated with Adeno-EGFP-hAR adenovirus at 3 weeks (R, arrow=pieces of cauda epididymis) and 3 months (T) after treatment. Scale bar = 20 µm. SCARKO testis size at 3 weeks after injection with Adeno-EGFP-hAR (U, V) and 3 months after injection (W). Graph bars represent means and SD. *(scale bar=100 µm for C-F, H-K; 10 µm for G, L; 200 µm for M, O; 100 µm for N; 25µm for P; 50µm for Q, S; 20µm for R, T)*

3.3.3 **Restoration of normal spermatogenesis was observed in SCARKO testis after treatment with Adeno-EGFP-hAR adenovirus**

To assess spermatogenesis, I examined testis histology of SCARKO mice treated with Adeno-EGFP-hAR and Adeno-EGFP-Empty adenovirus 3 weeks after injection. Mature sperm and elongated spermatids were found in the testis of SCARKO mice injected with Adeno-EGFP-hAR adenovirus (Fig. 9O, P) but not in the testes of mice that were injected with Adeno-EGFP-Empty adenovirus (Fig. 9M, N). Mature sperm were also found in the head of epididymis at 3 weeks after treatment (Fig. 9Q, S) and in the tail of epididymis at 3 months after injection (Fig. 9R, T), showing that the maturation arrest phenotype was relieved and mature sperm could be obtained from resident germ cells following the treatment. At 3 weeks after injection, the weights of SCARKO testes treated with Adeno-EGFP-hAR was significantly different than the group treated with Adeno-EGFP-empty vector (Fig. 9U, V) (SCARKO+hAR: 61 ± 2.4 g versus SCARKO+empty: 38.83 ± 0.4 g, unpaired t-test $p<0.0001$; Amh-Cre+empty: 111.4±4.0 g, Amh-Cre+hAR: 109.0±36.7 g). The same observations were made at 3 months after injection (SCARKO+hAR: 68.54±5.1 g versus SCARKO+empty: 27.00±1.5 g, unpaired t-test $p=0.002$). The weights of SCARKO testes treated with Adeno-EGFP-hAR were not significantly different compared to those of Amh-Cre mice treated with either types of adenoviruses (Fig. 9W) (Amh-Cre+empty: 87.73±14.0g, SCARKO+hAR:

68.54±5.1 g (p=0.691, unpaired t-test); Amh-Cre+hAR: 80.4±23.8 g, SCARKO+hAR: 68.54±5.1 g (p=0.395, unpaired t-test).

3.3.4 **Natural fertility status was not restored in SCARKO-mice treated with Adeno-EGFP-hAR adenovirus**

To evaluate fertility status after treatment, SCARKO mice treated with Adeno-EGFP-hAR adenovirus were bred with C57 female mice starting at 5 weeks after injection. Breeding was done every 4-5 weeks. In each breeding attempt, one to two female mice were left with one SCARKO mouse for 2 weeks. No pups were produced following the breeding, which means that despite the presence of complete spermatogenesis in some tubules, the adenoviral treatment was not enough to restore natural fertility. To identify the cause of failure to restore natural fertility, I assessed tubular differentiation index (number of tubules with elongated spermatids or sperm per 100 tubules counted) in all treatment groups from all time points. The mean tubular differentiation index for both Amh-Cre treated with Adeno-EGFP-empty and -hAR were 100% across all the time points (Fig. 10A). Whereas the tubular differentiation index for SCARKO mice treated with Adeno-EGFP-empty adenovirus were 0 across all time points (Fig. 10A). For SCARKO mice treated with Adeno-EGFP-hAR adenovirus, the tubular differentiation indices were 93.05±4.78 at 3 weeks, 90.07±8.56 at 3 months, 69.99±13.61 at 6 months and 64.63±2.36 at 1 year after injection (Fig. 10A). Significant differences were found among time points and treatment groups (2-way ANOVA; $p<0.0001$ for both factors). When comparing tubular differentiation indices within the same time point, we found significant differences in Amh-Cre+empty vs SCARKO+empty, Amh-Cre+hAR vs SCARKO+empty and SCARKO+empty vs SCARKO+hAR (Tukey's multiple comparisons for 2-way ANOVA, $p<0.00005$ for all pairs) at 3 weeks after treatment; Amh-Cre+empty vs SCARKO+empty

(Tukey's multiple comparisons for 2-way ANOVA $p<0.00005$), Amh-Cre+empty vs SCARKO+hAR ($p<0.05$), Amh-Cre+hAR vs SCARKO+empty (Tukey's multiple comparisons for 2-way ANOVA $p<0.00005$), Amh-Cre+hAR vs SCARKO+hAR Tukey's multiple comparisons for 2-way ANOVA (Tukey's multiple comparisons for 2-way ANOVA $p<0.05$) and SCARKO+empty vs SCARKO+hAR (Tukey's multiple comparisons for 2-way ANOVA $p<0.00005$) at 3 months after treatment; Amh-Cre+empty vs SCARKO+empty, Amh-Cre+empty vs SCARKO+hAR, Amh-Cre+hAR vs SCARKO+empty, Amh-Cre+hAR vs SCARKO+hAR and SCARKO+empty vs SCARKO+hAR at 6 months and 1 year after treatment; (Tukey's multiple comparison for 2-way ANOVA, $p<0.00005$ for all pairs). This showed that SCARKO+hAR had significantly higher tubular differentiation indices compared to SCARKO+empty at all time points. Significant differences were observed between SCARKO+hAR and Amh-Cre+empty or Amh-Cre+hAR at all time points except at 3 weeks time point (Fig. 10A). I performed epididymal sperm analysis to assess the quantity (concentration, absolute count per epididymis) and quality of sperm (morphology). The percentage of sperm with normal morphology were not significantly different between the Amh-Cre control groups and SCARKO mice treated with Adeno-EGFP-hAR (Fig. 10B; at 3 months: Amh-Cre+empty 29.73±9.4%, Amh-Cre+hAR 59.12±14.2%, SCARKO+hAR 50.73±7.1%, one-way ANOVA $p=0.14$; at 6 months: Amh-Cre+empty 51.63±5.6%, Amh-Cre+hAR 53.18±21.2%, SCARKO+hAR 46.88±1.3%, one-way ANOVA $p=0.88$; at 1 year: Amh-Cre+empty 66.13±5.6%, Amh-Cre+hAR 61.21±19.7%, SCARKO+hAR 69.0±1.4%, one-way ANOVA $p=0.82$). However, the mean sperm counts were much lower in SCARKO mice treated with Adeno-EGFP-hAR compared to Amh-Cre treated with both types of viruses regardless of time points (Fig. 10C; at 3 months: Amh-Cre+empty 4.98±0.42 million sperm/epididymis, Amh-Cre+hAR 5.23±1.94 million sperm/epididymis, SCARKO+hAR 0.78±0.18 million sperm/epididymis (one-way ANOVA $p=0.0.119$); at 6 months: Amh-Cre+empty 5.65±8.00 million sperm/epididymis, Amh-Cre+hAR 5.72±2.10 million

sperm/epididymis, SCARKO+hAR 0.137±0.00297 million sperm/epididymis (one-way ANOVA p=0.37); at 1 year: Amh-Cre+empty 1.931±2.550 million sperm/epididymis, Amh-Cre+hAR 0.487±0.610 million sperm/epididymis, SCARKO+hAR 0.0195±0.0255 million sperm/epididymis (one-way ANOVA p<0.0001).

3.3.5 **Live pups were born from Intracytoplasmic Sperm Injection using sperm from adeno-EGFP-hAR treated SCARKO mice**

To assess the function of sperm generated by this treatment, I performed Intracytoplasmic Sperm Injection (ICSI) with epididymal sperm retrieved from Adeno-EGFP-hAR treated SCARKO mice 6-months after treatment. The sperm were cryopreserved for 3-years before ICSI. I injected 76 eggs with frozen/thawed sperm from SCARKO mice. Among 76 injected eggs, 63 developed into 2-cell embryos (82.9%), which I transferred into 2 pseudopregnant mothers and both became pregnant. One mother gave birth to a litter of 2 male mice, one as Amh-Cre mice and one as WT. The other mother canabilized the litter of at least 2. I also injected another set of 85 eggs with sperm from another adeno-EGFP-hAR treated SCARKO mouse at 6 months after treatment. Among 85 eggs injected, 50 developed into 2-cell embryos (58.8%) (Fig. 10D-F). These were transferred to one pseudopregnant mother who later gave birth to a litter of two pups (Fig. 10G). Both are female and are heterozygous for the mutant $Ar^{tm1Rb\text{-}flox}$ allele. All the offspring genotyping showed agreeable results with Mandelian inheritance (0% $Ar^{tm1Rb\text{-}flox}$ in male and 100% heterozygote for $Ar^{tm1Rb\text{-}flox}$ in female, 50% chance of Amh-Cre heterozygotes among all offspring) (Fig. 10I). The PCR genotyping result was done as described previously [98]. This showed that sperm produced from SCARKO mice with this treatment can fertilize and result in embryos that can undergo normal development and produce offspring.

To assess fertility status of the F1 offspring, I bred the 2 males (Amh-cre and WT) to C57 female (2 rounds with 2 female each round). From WT male, litters of 8 and 9 were born to each mother. From Amh-Cre mice, litters of 6 and 10 were born to each female. For female F1, I did 2 rounds breeding with C57 male mice, I obtained two litters of 7 and 11 from one mother and two litters of 8 and 13 from the other mother (Fig. 10H). These showed normal fertility status of the F1 offspring that were born from gene therapy treated SCARKO mice.

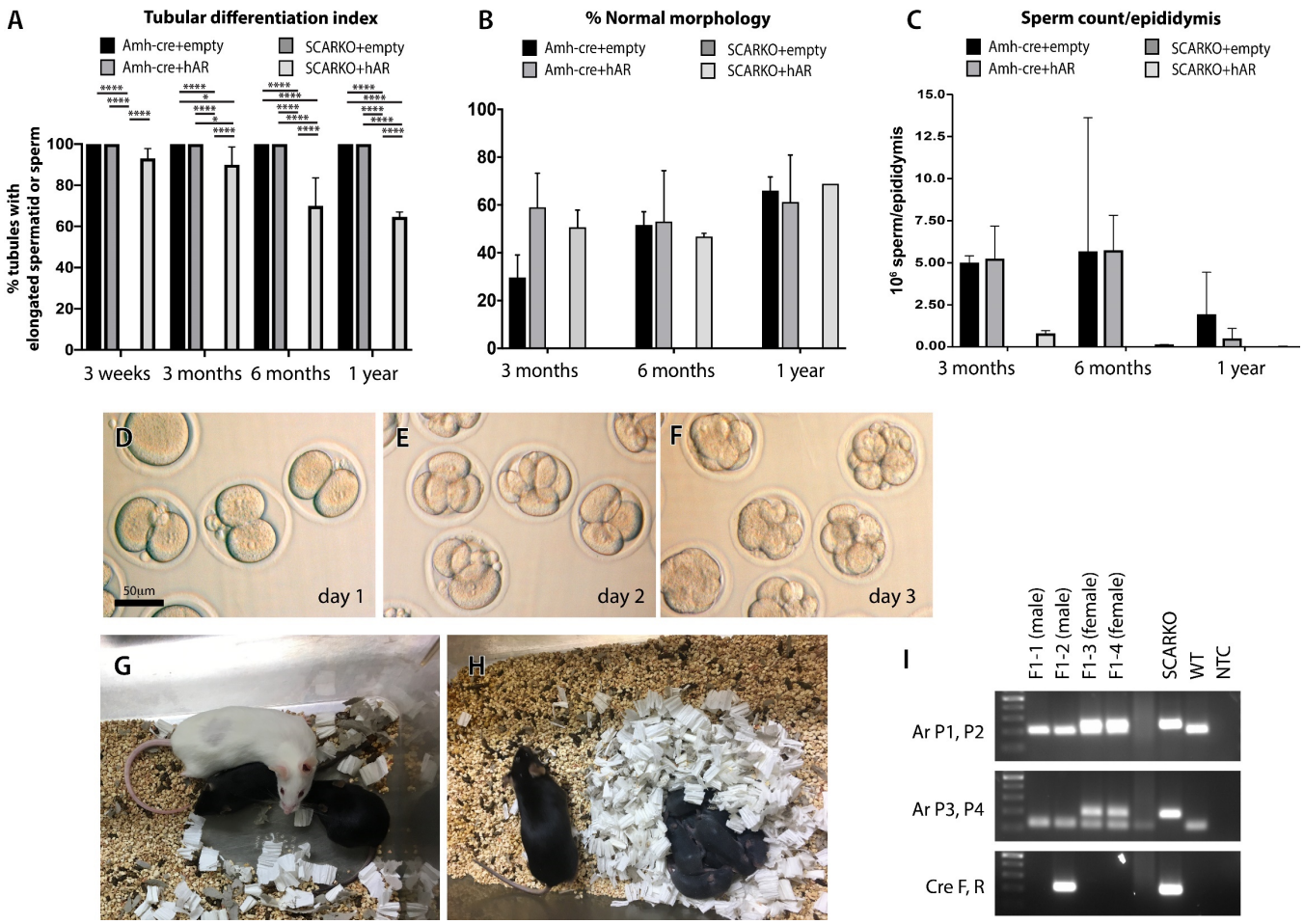

Figure 10 Sperm analysis from SCARKO mice after treated with adenoviruses

Tubular differentiation index as in % tubules with elongated spermatids or sperm (A). Sperm analysis from the tail of epididymis of Amh-Cre control and SCARKO mice treated with adenoviruses in terms of morphlogy (B) or sperm count per epididymis (C). Four testes from two mice were analyzed per group per time point. Embryo development was shown from 24 hours after ICSI (2-cell stage) (D), 2 days and 3 days after ICSI (E, F), A litter containing F1-1, F1-2 from SCARKO mouse-1 (sperm from 6-month time point after injection, 2.5 years cryopreserved) (G), A litter of F2 from breeding F1-1 mouse with a WT female (H). PCR genotyping to confirm genetic hereditary from SCARKO mice (I). *(scale bar = 50 µm for C-E)*

3.3.6 **Adenoviral infection was shown to be specific to Sertoli cells with no evidence of infection in germ cells or germline transmission**

To assess the risk of germline transmission, I performed immunohistochemistry to identify the cellular target of adenovirus transduction. Testes from SCARKO and Amh-Cre control mice treated with either Adeno-EGFP-hAR or Adeno-EGFP-empty adenovirus were co-stained with EGFP antibody, which marks the target of adenovirus transduction, and SOX9 or VASA, which mark Sertoli cells and germ cells, respectively. Immunohistochemistry of the testes obtained at 3 weeks after injection showed co-localization of EGFP and SOX9 in SCARKO mice (Fig. 11A-D). In contrast, EGFP did not co-localize with Vasa (Fig. 11E-H). The same observations were made in Amh-Cre mice treated with Adeno-EGFP-hAR or Adeno-EGFP-empty (Fig. 11I-P, Q-X, respectively), SCARKO mice treated with Adeno-EGFP-empty adenovirus and all other samples from 3 months, 6 months and 1 year after injection (data not shown). To directly assess risk of germline transmission, I performed polymerase chain reaction (PCR) to determine whether EGFP was transmitted to progeny. Because no pups were born from natural breeding of SCARKO mice treated with Adeno-EGFP-hAR adenovirus, I examined the pups born from Amh-Cre mice treated with either Adeno-EGFP-empty or Adeno-EGFP-hAR adenovirus for genotyping (Fig. 11Y). Among 408 pups born from Amh-Cre control fathers (8 representative samples shown in Fig. 11Z for Amh-cre controls, top half) and 4 from SCARKO mice treated with Adeno-EGFP-hAR adenovirus (Fig. 11Z, bottom half), none tested positive for the EGFP gene. Taken together, I showed that adenoviral transduction by intratubular injection was specific to Sertoli cells and there was no evidence of germline transmission.

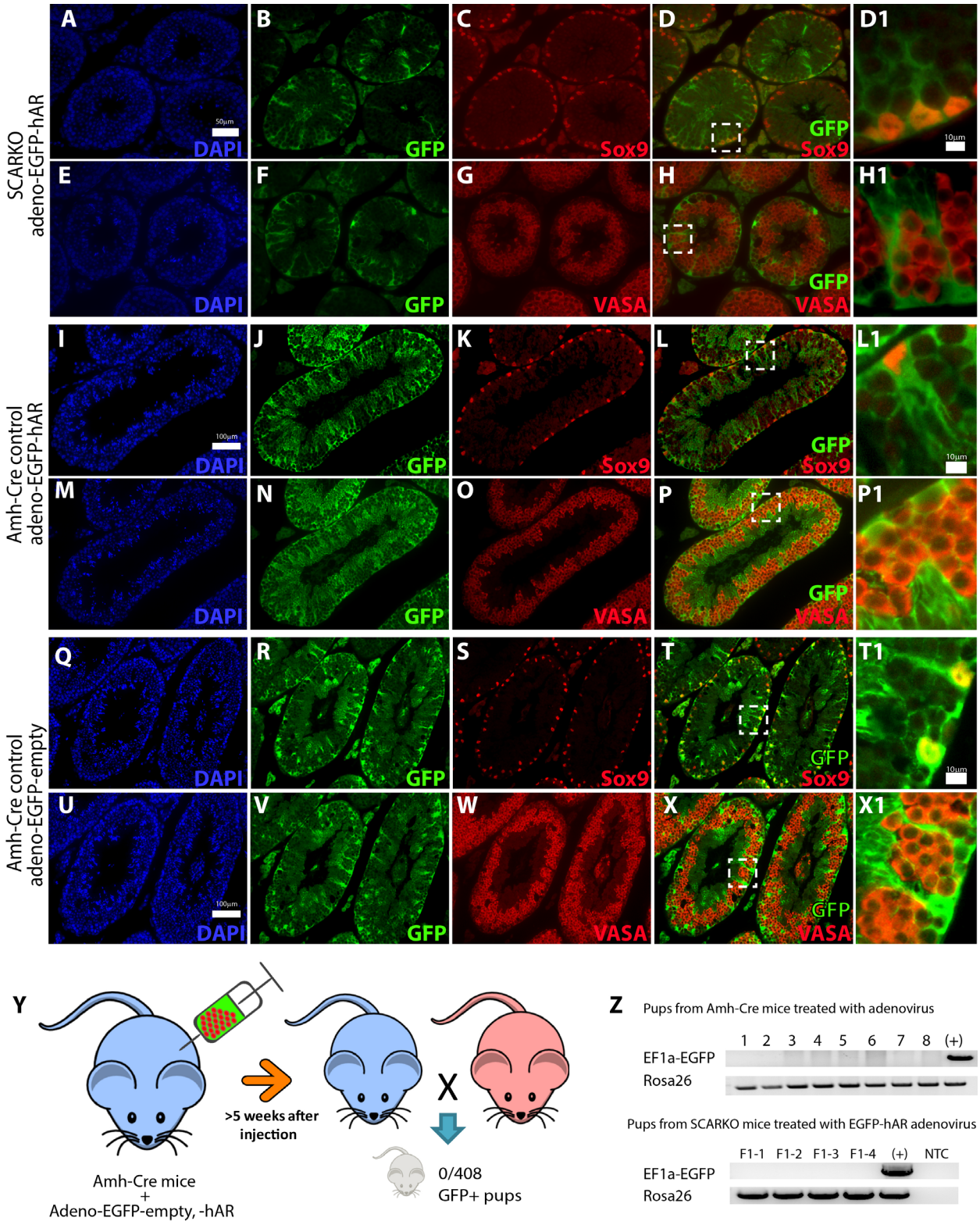

Figure 11 Adenoviral transduction was specific to Sertoli cells with no evidence of germline transmission

SCARKO testes at 3 weeks after treated with Adeno-EGFP-hAR adenovirus co-stained with EGFP and Sox9 antibodies (A-D). Dapi stains all cell nuclei (A, E, I, M, Q, U). GFP marks cells that were transduced and express the viral EGFP transgene (B, F, J, N, R, V); SOX9 marks Sertoli cells (C, K, S); VASA marks germ cells (G, O, W); co-staining is shown in D, H, L, P, T and X. To emphasize the co-localization between EGFP and Sox9 or VASA staining, boxed areas in D, H, L, P, T and X are shown at higher magnification in D1, H1, L1, P1, T1 and X1. Staining for EGFP, SOX9 and VASA were performed on the same sections. A Total of 408 offspring from Amh-Cre mice treated with either Adeno-EGFP-empty or Adeno-EGFP-hAR adenoviruses were tested for presence of the EF1a-EGFP transgene by Polymerase chain reaction (PCR) (Y, Z). The breeding occurred between 5 weeks and approximately 4 months after injection. DNA was obtained from the tails of the offspring. All 4 pups born from SCARKO sperm after treating with Adeno-EGFP-hAR adenovirus were also tested for EF1a-EGFP insertion in the genome (Z). *(scale bar=100 µm for A-X and 10 µm for D1, H1, L1, P1, T1 and X1)*

3.3.7 **Complete spermatogenesis and AR expression in Sertoli cells can be observed in SCARKO testis for at least 1 year after treatment**

To evaluate persistence of desired phenotypes, which are 1) the presence of mature sperm in the testis or 2) epididymis and 3) the expression of AR from Sertoli cells, at 3 weeks, 3 months, 6 months and 1 year after treatment, I assessed histology for testicular mature sperm, immunohistochemistry for AR expression, and epididymal sperm count from SCARKO mice treated with Adeno-EGFP-hAR adenovirus. Because mature Sertoli cells rarely divide, I hypothesized that expression of non-integrated transgenes will persist long-term in Sertoli cells, as well as the sperm count. However, sperm count per epididymis from SCARKO+hAR mice gradually decreased from SCARKO+hAR 0.78±0.18 million sperm/epididymis at 3 months, 0.137±0.00297 million sperm/epididymis at 6 months, and 0.0195±0.0255 million sperm/epididymis at 1 year after treatment (Fig. 12A; ordinary one-way ANOVA $p<0.005$). Sperm counts showed significant increase from 3 weeks to 3 months (Tukey multiple comparisons for ordinary

one-way ANOVA $p<0.005$), but significant decline between 3 months and 6 months, and 6 months and 1 year ($p<0.005$) (Fig. 12A). The sperm counts were also shown to be significant differences among time points. This showed that sperm counts significantly changed over time (Fig. 12A). Tubular differentiation indices (the percent of tubules positive for elongated spermatids or sperm) for SCARKO+hAR were 93.0±4.9% at 3 weeks after injection, and gradually decreased to 89.9±8.8%, 70.0±13.6% and 64.6±2.4% at 3 months, 6 months and 1 year, respectively. The tubular differentiation indices also showed significant different among time points (one-way ANOVA $p<0.005$) with 3 weeks being significantly different than 6 months and 1 year (Tukey's multiple comparisons $P<0.005$ for both pairs) and 3 months being significantly different than 6 months and 1 year (Tukey's multiple comparisons $P<0.05$ for both pairs) (Fig. 12B). Testis weights increased from 61.00±2.4 g at 3 weeks after injection to 68.54±10.2 g at 3 months after injection and then decreased to 50.13±2.4 g and 45.91±3.9 g at 6 months and 1 year after injection, respectively (Fig. 12C; ANOVA $p=0.0005$; Tukey's multiple comparisons; $p<0.005$ for 3 weeks vs 6 months, $p<0.0005$ for 3 weeks vs 1 year, and $p<0.05$ between 3 months and 1 year). The AR expression, quantified as the percent of AR-positive Sertoli cells, gradually decreased over time (Fig. 12D; 44.5±1.1% at 3 weeks after injection, 32.1±3.0% at 3 months after injection, 14.0±2.4% at 6 months after injection, and 15.9±0.8% at 1 year after injection (ANOVA $p<0.0001$; Tukey's multiple comparisons $p<0.00005$ for 3 weeks vs 3 months, 3 weeks vs 6 months, 3 weeks vs 1 year, and between 3 months vs 6 months and 3 months vs 1 year). These data indicated that treatment with the non-integrating adeno-EGFP-hAR vector produced AR expression and spermatogenesis phenotypes persisted for a long time, but gradually declined over time.

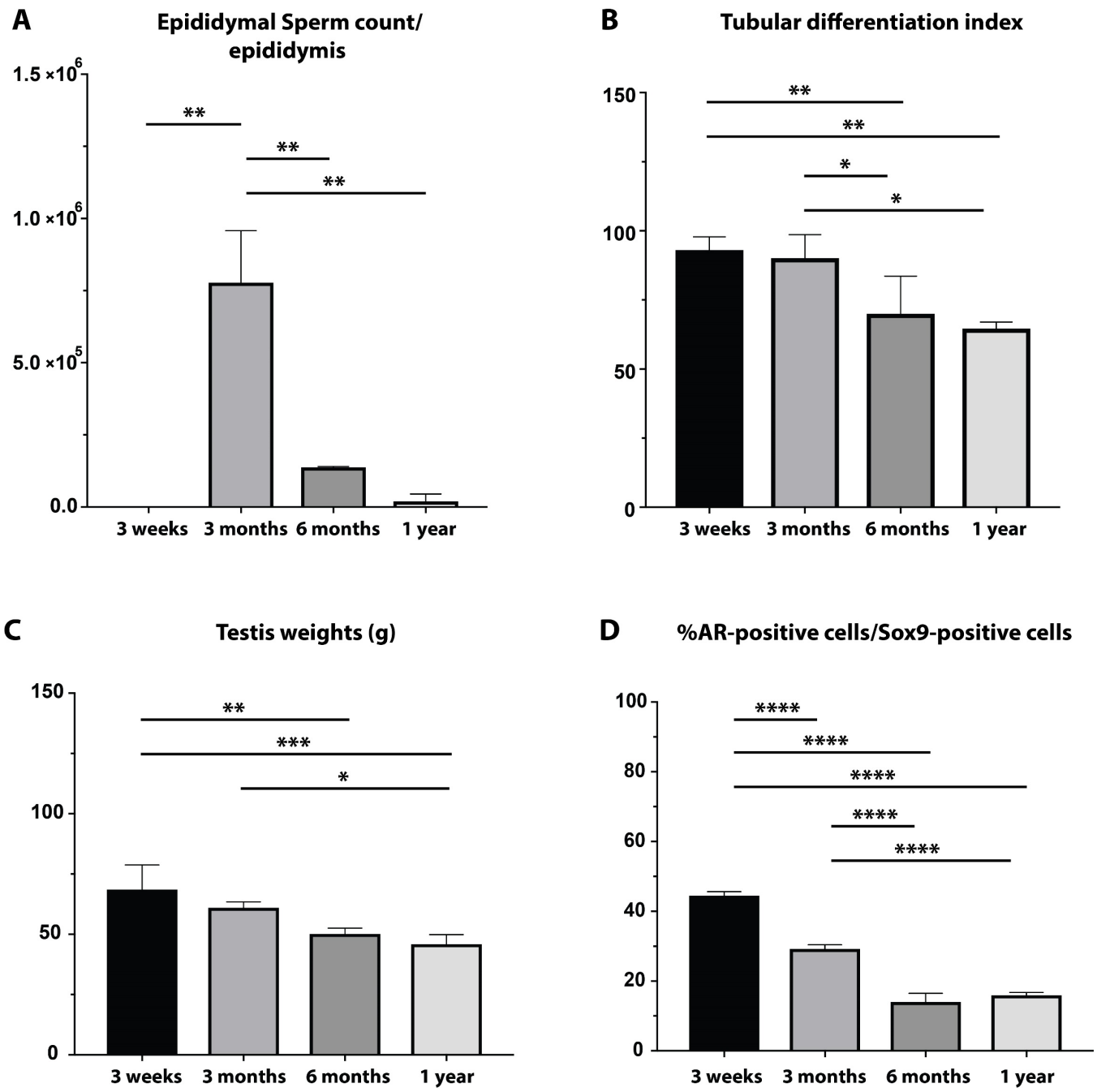

Figure 12 Mature sperm were detected in Adeno-EGFP-hAR treated SCARKO testes up to at least one year after treatment

Testes and sperm from SCARKO mice treated with Adeno-EGFP-hAR adenovirus at 3 weeks, 3 months, 6 months and 1 year after injection assessed for sperm count/epididymis (A), tubular differentiation index (% elongated spermatids or sperm) (B), tubules with testis weights (C) and %AR-positive Sertoli cells (D). Two animals from each experiment group were sacrificed at each time point. (*Statistical significance: * ($p<0.05$), ** ($p<0.005$), ***($p<0.0005$))*

3.3.8 **Blood-testis barrier disruption was a side effect from intratubular adenoviral injection**

Decreasing Adeno-hAR expression over time may explain the decline in sperm count, but other explanations are possible. To determine why the desired phenotype regressed over time, I assessed testicular histology for abnormalities. Compared to the non-treated control of the same age (Fig. 13A, D), I noticed vacuolation in seminiferous tubules (Fig. 13B-C, E-F asterisks and black arrows) and detachment of germ cells into the seminiferous lumens (Fig. 13B-C, E-F blue arrow). Empty tubules were also occasionally noted (Fig. 13B-C, E-F star) compared to normal-looking tubules (Fig. 13B n). These findings together were the pattern of Sertoli cell injury, previously described as Sertoli cell vacuolation, which is usually associated with Blood-Testis Barrier (BTB) disruption and germ cell exfoliation [254, 255]. Sertoli cell vacuolation were found as early as 3 weeks after injection, whereas the empty tubules were seen starting from 3 months after injection. To determine whether BTB disruption was associated with the vacuolization and adenoviral treatment, I compared the BTB integrity between the mice injected with both adenoviruses (Adeno-EGFP-hAR or Adeno-EGFP-Empty) and the non-injected group. To examine BTB integrity, I injected EZ-Link™ Sulfo-NHS-LC-Biotin tracer protein into testicular interstitium of Amh-Cre and SCARKO testes 3 weeks after adenovirus treatment. Testes were collected 30 minutes after biotin tracer injection and immediately fixed in 4% PFA for histology. The tissues were stained with Alexa fluoro 488 to visualize the biotin tracer. The presence of biotin tracer beyond the first layers of germ cells on the seminiferous tubule basement membrane are considered abnormal. I graded the degree of BTB disruption into three categories: none; mild (tracer seen inside the lumen of seminiferous tubules) and moderate-to-severe (very bright fluoresced particle seen in the lumen of the seminiferous tubules), as described previously [256]. While no biotin tracer was found beyond the first layer of germ cells in the non-adenoviral treated Amh-Cre control group (Fig. 13G), the biotin tracer was found in the lumen of seminiferous tubules of the Amh-Cre mice treated with adenovirus, regardless of

the types of transgenes the adenovirus carries (Fig13H, I). Quantification of 2 testes from 1 animal with average of 360 cross sections per treatment group was performed. Tubules with intact BTB were 99.43±0.81% for untreated Amh-Cre, 7.20±0.00% for Amh-Cre+empty, 25.65±9.55% for Amh-Cre+hAR, 68.35±12.37% for untreated SCARKO, 25.45±35.98% for SCARKO+empty, 65.00±12.86% for SCARKO+hAR (ordinary one-way ANOVA $p<0.05$) (Fig. 13M). Tubules with mildly disrupted BTB were 57.57±0.81% for untreated Amh-Cre, 60.40±0.00% for Amh-Cre+empty, 60.10±2.83% for Amh-Cre+hAR, 31.85±12.09% for untreated SCARKO, 58.60±26.74% for SCARKO+empty, 34.89±14.16% for SCARKO+hAR (ordinary one-way ANOVA $p=0.0538$) (Fig. 13M). Tubules with severely disrupted BTB were 0.00±0.00% for untreated Amh-Cre, 32.40±0.00% for Amh-Cre+empty, 19.14±19.29% for Amh-Cre+hAR, 0.00±0.00% for untreated SCARKO, 16.72±8.17% for SCARKO+empty, 0.52±0.73% for SCARKO+hAR (ordinary one-way ANOVA $p=0.124$) (Fig. 13M). Therefore, this experiment confirmed that adenoviral injection disrupted BTB integrity in the Amh-Cre control mice.

The same experiment was performed to assess blood-testis barrier integrity in SCARKO mice, with and without adenovirus injection. Untreated SCARKO mice had fewer intact BTB tubules than Amh-Cre controls and this is consistent with the known BTB phenotype of SCARKO mice (Fig. 13M). Treatment of SCARKO mice with Adeno-EGFP-Empty led to an increased disruption of BTB at 3 weeks after injection. Treatment of SCARKO mice with Adeno-EGFP-hAR appeared to improve BTB integrity to a level similar to untreated SCARKO mice (Fig. 13J-M). This confirmed that adenovirus also causes BTB disruption in SCARKO animals, that deficit may be compensated by the expression of AR.

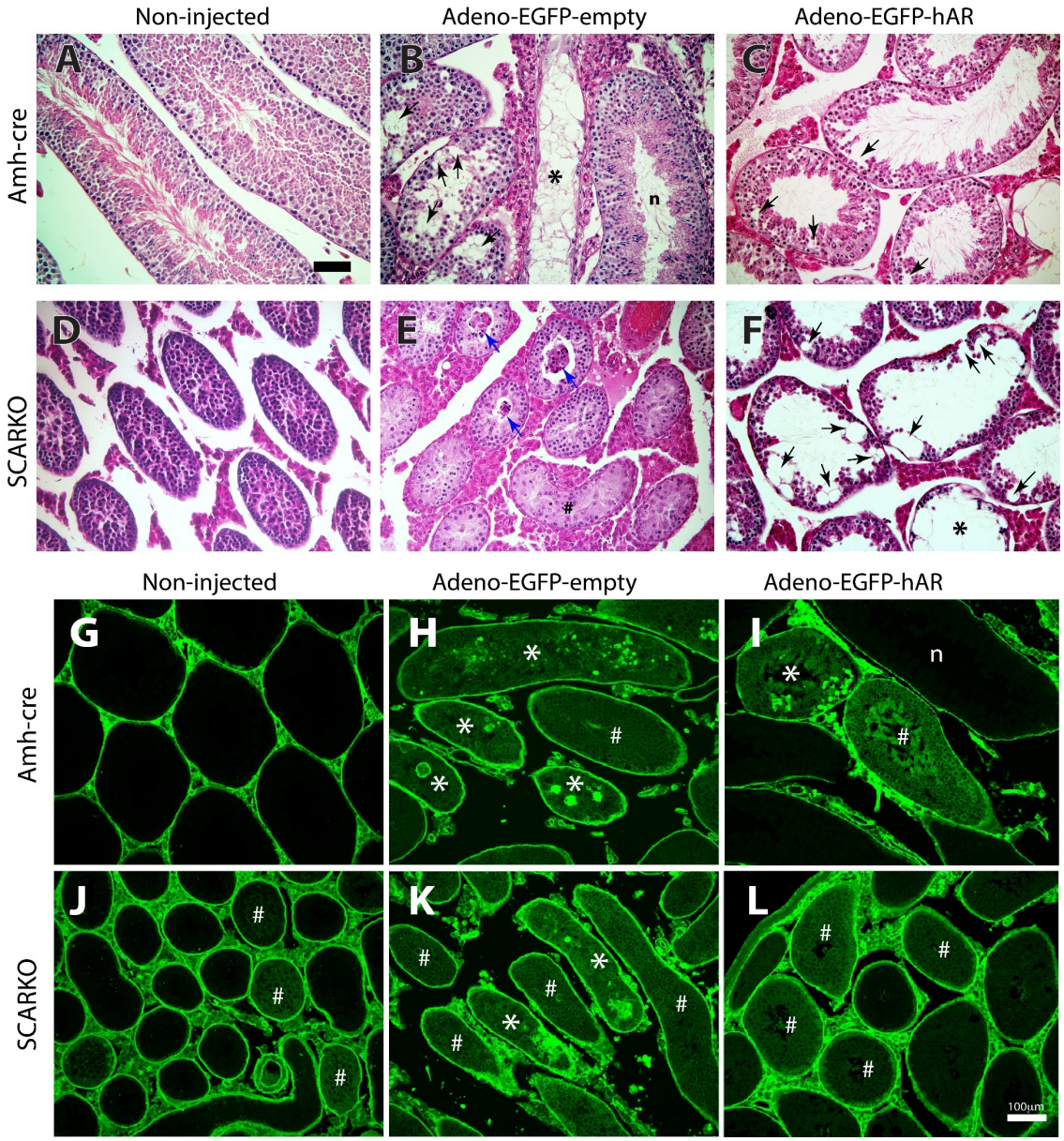
Non-injected
Adeno-EGFP-empty
Adeno-EGFP-hAR
Amh-cre
SCARKO
A
B
C
D
E
F
G
H
I
J
K
L
n
100μm

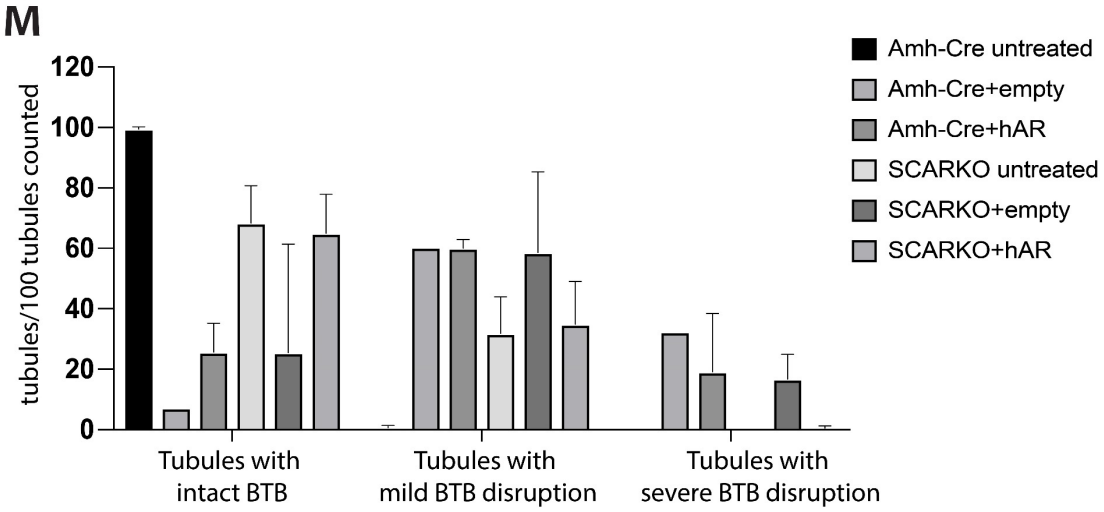
M
tubules/100 tubules counted
120
100
80
60
40
20
0
Tubules with intact BTB
Tubules with mild BTB disruption
Tubules with severe BTB disruption
Amh-Cre untreated
Amh-Cre+empty
Amh-Cre+hAR
SCARKO untreated
SCARKO+empty
SCARKO+hAR

Figure 13 Adenovirus associated with Sertoli cell toxicity and decreased blood-testis barrier integrity

Testis histology of Amh-Cre and SCARKO mice untreated (A, D, respectively), Amh-Cre and SCARKO mice treated with either Adeno-EGFP-empty (B, E, respectively) or Adeno-EGFP-hAR adenoviruses (C, F, respectively) 6 months after injection. Star (*) indicates empty tubules compared to the normal tubules (n), while Sertoli cell vacuolation were shown by black arrows. The blue arrows showed exfoliation of germ cells into the seminiferous lumen. The BTB integrity was assessed at 3 weeks after treatment by injecting EZ-Link™ Sulfo-NHS-LC-Biotin tracer (G-L). The tracer protein in the seminiferous lumen of Amh-Cre mice treated with Adeno-EGFP-empty (H) or Adeno-EGFP-hAR (I) and SCARKO mice treated with Adeno-EGFP-empty (K) or Adeno-EGFP-hAR (L) compared to the non-injected control (G, J). Severity of BTB disruption was graded by leakage of tracer into seminiferous lumen; mild (#) if the outline of germ cells in the seminiferous tubules can be observed; moderate to severe (*) if the outline of the seminiferous tubules is visualized or highly fluoresced particle was seen in the lumen compared to normal. Each BTB integrity category was quantified per 100 tubules (M). *(scale bars = 100 μm)*

To examine the presence of local immune reaction to adenovirus, I examined testicular histology for infiltration of inflammatory cells (neutrophils, macrophages and lymphocytes) to cover both innate and acquired immune response. I examined 5 cross-sections per testis and did not see any inflammatory cells infiltration from histology. I confirmed the findings by immunohistochemistry with antibody to CD66b, CD68 and CD3, which are markers for neutrophils, macrophages and T-lymphocytes, respectively [257-259]. Splenic tissue was used as the positive control for the antibodies while the testicular tissue from non-adenoviral injected Amh-Cre and SCARKO mice were used as negative controls. No SCARKO and Amh-Cre testes treated with adenoviruses from any time points were positive for CD66b and CD3 by immunohistochemistry, whereas there was a slight increase of CD68-positive cells (macrophages) in the interstitial space of some samples from 3 months after treatment. No CD66b-, CD68- or CD3-positive cells were seen inside the lumen of seminiferous tubules (Fig. 14). Therefore, this study

showed that local immune response played minimal to no role in alteration of seminiferous tubule architecture or BTB function.

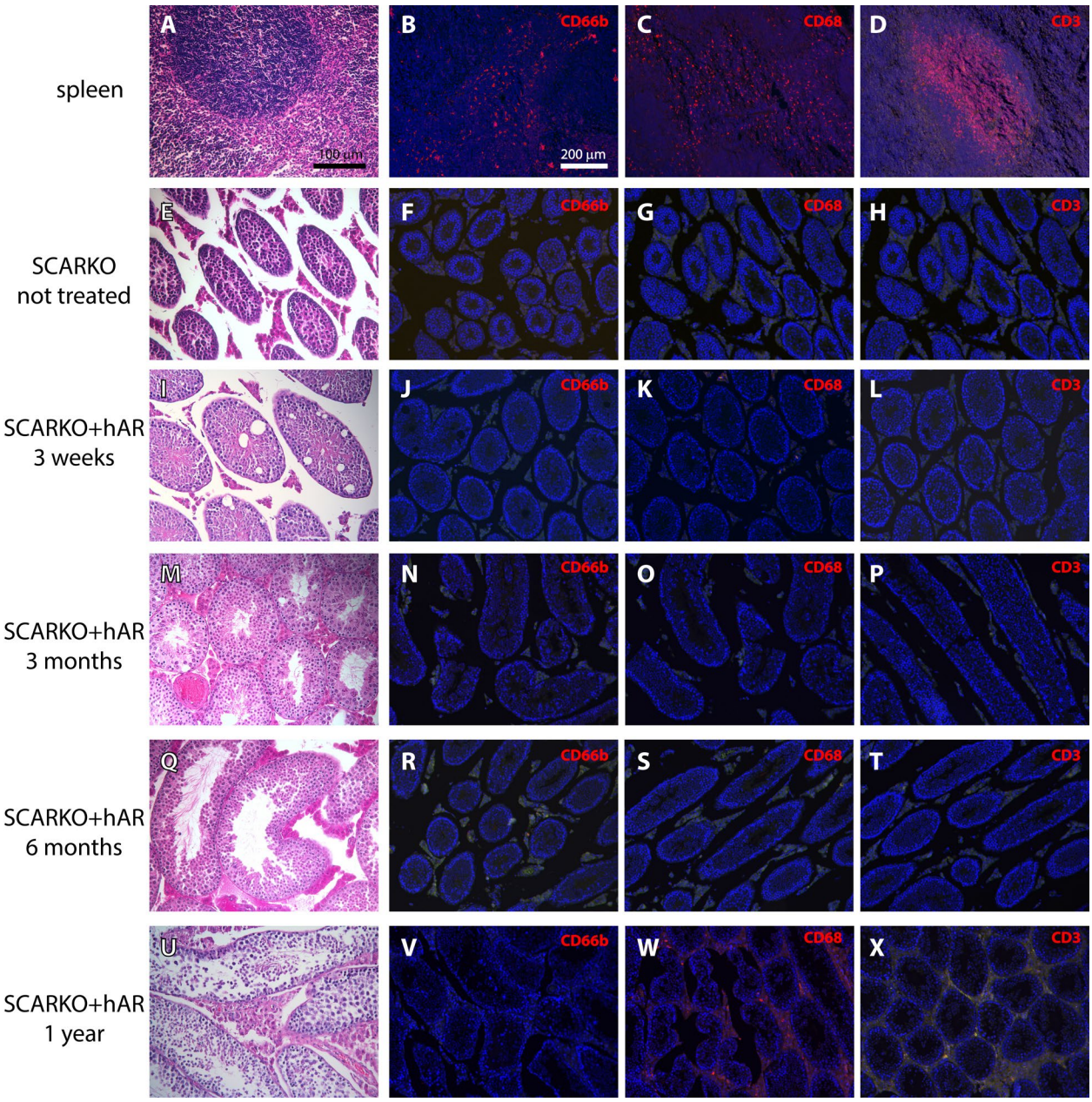

Figure 14 Testis section from SCARKO mice treated with Adeno-EGFP-hAR adenovirus

At 3 weeks (I-L), 3months (M-P), 6 months (Q-T) and 1 year after injection (V-X). Untreated SCARKO mice was used as negative control (E-H), whereas spleen was used as the positive control (A-D). CD66b staining (red) was shown in the column 2 (B, F, J, N, R and V). CD68 staining (red) was shown in column 3 (C, G, K, O, S and W) and CD3 staining (red) was shown in column 4 (D, H, L, P, T and X). *(Scale bar = 100 µm for A, E, L, M, Q and U; 200 µm for the rest of the panel)*

3.4 Discussion

I demonstrated that injecting a gene therapy vector, adeno-EGFP-hAR, into the seminiferous tubules of infertile SKARKO mice resulted in specific Sertoli cells transduction and subsequent AR expression and induction of spermatogenesis from resident germ cells. The specific Sertoli cell transduction by adenovirus has been consistently reported among similar independent studies [145, 241]. There were no reports regarding why adenovirus is specific to Sertoli cells. However, prime factors determining tropism for adenoviral type 5 (Ad5), which I used in this study, is the presence of the attachment receptor Coxsackie Adenoviral Receptor (CXADR, CAR) [247, 260-262]. Previous studies of rats and mice indeed showed that CAR is a component of blood-testis barrier and is expressed mainly in Sertoli cells [263, 264]. Because CAR was also found to be expressed in some degree in germ cells especially spermatocytes and spermatids [263, 264], other unknown determinants such as the amount of CAR on the surface of germ cells for efficient adenoviral transduction, the presence of other adenoviral receptors downstream to CAR such as αv-Integrins, CD46 and CD80/86 might also contribute to the low susceptibility of germ cells to adenovirus transduction [265-267]. This topic needs to be examined. It was also possible that adenovirus was initially taken up by germ cells but no longer detectable by the time of assessment (from 3 weeks to one year after injection) because of the germ cell turnover. Nevertheless, our data showed that the specificity of Sertoli cell transduction by adenovirus was observed as early as 5 days after injection, which is less than the duration of 1 seminiferous cycle (8.6 days) (Doungkamchan C and Orwig KE unpublished data). This means that the germ cell transfection was not observed even at the earliest timepoints. Promoter suppression in germ cells is also unlikely because the EF1a promoter is a ubiquitous promoter and was tested to drive EGFP expression in mouse spermatogonial stem cells *in vitro* (Doungkamchan C and Orwig KE unpublished data). Additionally, two independent studies reported the same specificity with CMV promoter plasmids [145, 241], indicating that the specificity has been

consistently observed regardless of which types the promoter used. The other explanation for specificity could be because Sertoli cells were capable of phagocytosing particles presented in seminiferous lumen whereas the germ cells cannot. This explanation is again less likely because there were no EGFP expression when naked EGFP plasmids (pEGFP C1, Takara Clontech, Japan) were injected into seminiferous lumen the same way adenovirus was delivered (Doungkamchan C and Orwig KE unpublished data). This showed that the adenovirus is necessary as a vector to deliver plasmid to the Sertoli cells and the most likely explanation to the specificity might be the presence of adenoviral receptors on the membrane of Sertoli cells.

I observed no evidence of germline transmission from genotyping 408 pups. This finding could be explained by the adenovirus being highly unlikely to integrate, which is required for germline transmission (6.72×10^{-5} per transduced hepatocyte for heterologous recombination and 3.88×10^{-7}per transduced hepatocyte for homologous recombination) [268]. Furthermore, I detected no transduced germ cells by immunohistochemistry, suggesting that the virus failed to even enter the cells.

I reported potential toxicity from adenoviral injection, which was indicated by seminiferous epithelial vacuolation and BTB disruption. However, at this viral dosage, I did not observe inflammatory cell (neutrophil, macrophage and lymphocyte) infiltration, which was previously shown to exhibit dose-dependent relationship with the dosage of adenovirus [145]. The vacuolation associated with intra-tubular adenoviral injection was consistent with the report by Hooley and colleagues in 2009 [145], and is a histopathologic pattern of Sertoli cell injury which often results in secondary germ cell exfoliation and BTB disruption [254, 255], all of which were observed in this study. The mechanism behind Sertoli cell injury from intratubular adenoviral injection is still unknown but it is possible that the viral vector infection could either directly trigger the apoptosis pathway by decreasing anti-apoptotic effect from the lack of functioning E1B 19K gene that binds to BAX to prevent apoptosis in the target cells, or indirectly from

the infected cells presenting viral antigen by MHC class I, triggering downstream immune response, or both [269-271]. Several studies also suggested that downregulation of CAR (adenovirus receptor), which could be the side effect from adenoviral internalization following adenoviral infection, directly disrupted BTB integrity *in vitro*. However, conditional knockout of CAR in Sertoli cells in mice showed neither spermatogenesis abnormality nor BTB disruption, making the contribution from CAR downregulation less likely [272, 273].

I followed the persistence of the phenotypes, AR expression, normal spermatogenesis in the testis and mature sperm in the cauda epididymis, for 1-year post-injection. Restorations of AR expression and spermatogenesis peaked at 3 weeks, whereas sperm counts, and testis weights reached their peak at 3 months before starting to decline. Factors contributing to persistence of adenoviral transgene include 1) the stability of episomal DNA; 2) slow turnover of Sertoli cells in adult animals and 2) the survival of the infected cells from adenoviral toxicity or immune effector cells after infection [274]. The observed decreases in AR expression and sperm production over time likely reflect the degradation of the episomal adenoviral transgene. Deterioration of sperm production can also be caused from Sertoli cell toxicity as detailed above. Additionally, the use of EF1a promoter, which is a ubiquitous promoter, results in persistent expression that did not mimic natural periodic expression of AR during the cycle of the seminiferous epithelium. Study from Hazra and colleagues indeed showed that constant overexpressing AR in Sertoli cells of SCARKO mice ($TgSCAR^{h}$) disturbed spermatogenesis and caused infertility [275]. In conclusion, many factors may contribute to the decline in adenovirus transgene expression and spermatogenesis over time.

3.5 Conclusions

Sertoli cell gene therapy may have application for treating some cases of male infertility. I confirmed that non-integrating adenoviral vectors could introduce a therapeutic hAR transgene into Sertoli cells and relieve the spermatogenesis blockade caused by Sertoli cell-specific single gene defect. This approach dramatically increased sperm recovery rate in SCARKO mice from 0% to 100% (n=21). Although natural fertility was not restored in this study, epididymal sperm recovered from treated SCARKO mice could be used with intracytoplasmic sperm injection to fertilize and produce offspring. These outcomes occurred without apparent transduction of germ cells or transmission of the adenoviral transgene to progeny, which may be an important considering the current moratorium on clinical application of germline gene editing in the United States. Although AR expression and spermatogenesis recovery appeared transient in this study, this could be desirable for first applications in the clinic. Further studies are needed to elucidate the mechanism(s) that mediate Sertoli cell-specific transduction and comprehensively examine the risk of germline transmission using single cell technique. Finally, to enable application of in vivo Sertoli cell gene therapy in the clinic, it will be necessary to discover the genes expressed by Sertoli cells that are associated with human male infertility.

3.6 Acknowledgements

Kyle E. Orwig, Chatchanan Doungkamchan planned the experiments. Chatchanan Doungkamchan made the adenovirus and measure the titer of the virus, maintained the animal colony, performed histology and immunohistochemistry, sperm analysis, spermatogenesis assessment and BTB integrity assessment. Yi Sheng made the plasmids, viruses and performed ICSI. Meena Sukhwani injected the virus and biotin

tracer into the testes. William H. Walker assisted with BTB integrity experiments and provided expertise related to Sertoli cell biology. Chatchanan Doungkamchan, Kyle E. Orwig analyzed data. Chatchanan Doungkamchan and Kyle E. Orwig prepared the manuscript, which was reviewed and edited by all authors.

4.0 Technology development for Germline gene therapy

4.1 Transfection of mSSCs using polyethylenimine (PEI)

4.1.1 **Introduction**

Mouse spermatogonial stem cell (mSSC) culture is an essential tool to study spermatogenesis in mammals. Because culturing of human spermatogonial stem cells is not yet feasible, mSSC culture is currently the best tool in studying gene functions associated with stem cell maintenance and spermatogenesis [9, 276]. In conjunction with gene manipulation techniques and stem cell transplantation [277], mSSC culture can generate offspring with specific mutations to evaluate their effect on infertility or other disease phenotypes in mice. Gene targeting, which is to precisely edit the genome at a desired locus, allows us to study specific variants such as single nucleotide polymorphisms (SNPs), point mutations, insertions/deletions, or copy number variants that are recently and increasingly identified in men with abnormal spermatogenesis [73-76, 80, 81, 236, 278-287].

Combining established mSSC culture methods [9, 276, 288, 289] with new robust CRISPR/Cas9 gene editing technologies [117] and transplantation [290] provides unprecedented opportunities for mouse genome manipulation, including germline gene editing. A major hurdle in germline gene editing using mSSCs is the efficiency of getting the gene editing reagents into the target cells. Mouse SSC cultures are known to be resistant to transfection [291-293]; consequently only gene transfer methods using lentivirus, adenovirus, adeno-associated virus (AAV) and electroporation have been proven successful. Additionally, when precise genome editing is required, where random genome integration is undesired, it further limits the transfection choices to AAV, Adenovirus, lipofectamine, and electroporation. Adenovirus [135]

showed high toxicity to mSSCs resulting in low viability after transfection. AAV was shown to result in less toxicity but it's small genome size limits that transgene cargo capacity [136-138]. In this study, I explored Polyethylenimine (PEI), a cation polymer, as a non-viral method to introduce large DNA constructs into mSSCs. My objective is to achieve efficient transient transfection of mouse SSCs using a method that has low probability of integration in the genome. PEI has been widely used to transfect a broad range of mammalian cells [294-297], but to our knowledge, there were no studies to report successful PEI transfection in mSSCs.

The mechanism of action for PEI is to form a positively charged complex when bound to DNA. The DNA-PEI complex will subsequently bind to the negatively-charged cell surface and will be phagocytosed [298-301]. The DNA/PEI complex then escapes the lysosome by a "proton sponge" mechanism [298, 302] and enters the nucleus where the DNA is dissociated from the complex to perform its function [300, 303]. The ability of PEI to form and dissociate from the DNA complex determines transfection efficiency [304, 305]. The mid-ranged 25 kilodalton (kDa) branched or linear PEIs are the most widely used in mammalian cells because of their low toxicity and balanced binding-dissociation from the complex, resulting in highest transfection efficiency [294, 296, 297, 306, 307]. In this study, I used linear 25 kDa PEI to optimize for mSSC transfection.

The proficiency of the DNA-PEI complex formation affects transfection efficiency (% transfected cells/total cells); it is very sensitive to the environment in which the complexes are formed and may vary across cell types [295]. The parameters that determine DNA-PEI complex formation efficiency are 1) PEI concentration and its effects on cell viability (PEI concentration); 2) the duration that the complex is incubated with cells (incubation time); 3) the nitrogen molecules in PEI per phosphorus molecules in DNA ratio (N:P ratio); 4) the solution/concentration of salt in which the complexes are formed (salt solution/concentration); 5) time in which the complex is allowed to form (complex formation time); and

6) the volume in which the complexes are formed (complex formation volume) [295]. In this study, I optimized these parameters individually and stepwise to learn the optimal PEI/DNA complex formation condition for mSSCs transfection.

I report an optimized PEI transfection condition for mSSCs that can be used to introduce CRISPR/Cas9 reagents for precise genome editing without evidence of random plasmid integration. PEI-transfected mSSCs retained the ability to colonize when transplanted into germ cell-depleted recipient mice.

4.1.2 **Materials and methods**

4.1.2.1 Animal model

DBA/2J wildtype (The Jackson Laboratory: 000671) and B6-CAG-EGFP (The Jackson Laboratory: 003291) mice were back crossed more than 6 times in our animal facility to produce male pups for EGFP-positive mouse spermatogonial stem cell culture with DBA/2J background (DBA/2J-CAG-EGFP). All animal experiments were conducted in compliance of the Guide for the Care and Use of Laboratory Animals and was approved by the Institutional Animal Care and Use of Committees of Magee-Womens Research Institute and the University of Pittsburgh (Assurance # A3654-01).

4.1.2.2 Spermatogonial stem cell culture

Mouse spermatogonial stem cells (mSSCs) were isolated from seven-day-old DBA/2J wildtype or DBA/2J-CAG-EGFP male pups using our lab's standard isolation protocol based on methods previously described [9, 288, 289]. In brief, testes were dissected, the tunica was removed, and the seminiferous tubules were digested with 0.25% Trypsin-EDTA and DNAse1 (3.5mg/mL). SSCs were further isolated with 30% Percoll and the pelleted fraction was sorted to enrich SSCs using MACS® THY1+ beads

(CD90.2 MicroBeads, Miltenyi Biotech) before plating onto a 20μg/mL mouse laminin-coated plate in Iscove's Modified Dulbecco's Medium (IMDM)/mouse serum free media (IMDM/SFM) [289]. The first few passages contained a mixture of germ and somatic cells but contaminating somatic cells were gradually reduced to low levels by passage four or five based on differential attachment characteristics. Somatic cells attach rapidly and tightly to the culture substrate while germ cells are loosely adherent and can be dislodged by gentle pipetting for passaging. Once cultures were established, passaging was done every week using 0.05% Trypsin-EDTA. All experiments in this study were performed on mSSCs with passage numbers between 6 and 14.

4.1.2.3 Transfection of mCherry expression vector in SSCs

A pAAV-CAG mCherry expression vector (Addgene#100054), which is a plasmid for AAV backbone expressing mCherry under CAG promoter, was used for optimizing PEI transfection and for comparison of four transfection methods: standard PEI, optimized PEI, lipofectamine, and electroporation.

The standard PEI protocol for one 24-well is described here. In one 1.5 mL tube, 10 μL of 7.5 mM PEI and 40 μL of 150 mM NaCl were combined and in another tube 1-2 μg of pAAV-CAG mCherry purified DNA (the plasmid concentration is preferred at higher than 1 μg/μL) and 50 μL of 150 mM NaCl were combined. Each tube was vortexed and incubated at room temperature for three minutes. The second tube with DNA/NaCl was added to the first PEI/NaCl tube and incubated at room temperature for 30 minutes. Approximately 5 minutes before the incubation time was over, mSSCs (at ~80% confluency) were washed twice with warm IMDM and replaced with 400 μL of IMDM. Then 100 μL of the pre-incubated PEI/DNA/NaCl mixture was added dropwise to a single well. Cells were incubated with the transfection mixture for 12 hours and then washed twice with IMDM and replaced with IMDM/SFM media.

I tested six parameters of the standard PEI protocol (PEI concentration, incubation time, N:P ratio, salt solution/concentration, complex formation time, and complex formation volume), to develop our optimized protocol. Our optimized protocol for one 24-well is as follows: 5 μL of 7.5mM PEI and 20 μL Opti-MEM were combined in one 1.5mL tube, while 2 μg of pAAV-CAG mCherry DNA and 20 μL of Opti-MEM were combined in a second. Tubes were vortexed and incubated at room temperature for three minutes and then the second tube with DNA/Opti-MEM was added to the first PEI/Opti-MEM. The PEI/DNA/Opti-MEM transfection mixture was incubated at room temperature for ten minutes and then added dropwise to washed mSSCs (~80% confluency) with 400 μL warm IMDM. Cells were incubated with the transfection mixture for six hours and then were washed twice with IMDM and replaced with IMDM mouse serum free media.

Transfection using Lipofectamine stem cell reagent was performed following the manufacturers protocol (Thermofisher scientific) but is briefly described here. For one 24-well, 4 μL of Lipofectamine and 25 μL Opti-MEM were combined in one 1.5 mL tube, while 2 μg of pAAV-CAG mCherry DNA and 25 μL of Opti-MEM were combined in a second. Tubes were vortexed and incubated at room temperature for three minutes and then the second tube was added to the first. The Lipofectamine/DNA/Opti-MEM transfection mixture was incubated at room temperature for ten minutes and then added dropwise to washed mSSCs (~80% confluency) that already had 400 μL warm IMDM. Cells were incubated with the transfection mixture overnight and then washed twice with IMDM and replaced with IMDM/SFM media.

Electroporation of mSSCs required ~$1x10^6$ cells per condition. For the transfection comparison experiment, the standard PEI, optimized PEI, and lipofectamine stem cell reagent protocols were modified for 6-well transfections. For electroporation, mSSCs were harvested (600xg for 5 minutes) after incubation with 0.05% Trypsin-EDTA and then Knockout Serum replacement. Cells were washed twice with Opti-MEM and then counted. Cells ($6x10^5$-$1.4x10^6$) were resuspended in 90 μL of Opti-MEM and mixed with

8μg of pAAV-CAG mCherry purified DNA, and the volume was adjusted to 100 μL. Cells were transferred to a NEPA electroporation cuvette with a 2 mm gap. The cuvette was placed into the cuvette chamber (CU500) and electroporated using the NEPA21 electroporator under the following conditions: 125 volts, 5 ms length, 50 ms interval, 2 pulses, a 10% D.Rate with a + polarity for the poring pulse; 20 volts, 50 ms length, 50 ms interval, 5 pulses, a 40% D.Rate with a +/- polarity for the transfer pulse. Quickly 500 μL of IMDM mouse serum free media was added to the cuvette after electroporation and cells were transferred to a 1.5 mL tube. Another 500 μL of IMDM mouse serum free media washed the cuvette. Cells were thoroughly mixed to avoid clumps and plated on mouse embryonic fibroblast (MEF) feeders to aid in recovery.

4.1.2.4 FACs sorting

Transfection efficiency was measured using flow cytometry. Cells were harvested in 1x PBS by mechanical dispersal of mSSCs. Cells were counted, pelleted (600 g for 5 minutes), and resuspended in 400 μL of 0.1% BSA. Cells were strained into a 5 mL FACs tube (Corning Science: 352235) and then 2 μL of DAPI (5 μg/mL) was added. The gates were set based on non-transfected mSSCs. The live cell gate was set based on forward and size scatter and DAPI staining. DAPI-positive cells were marked as dead cells and were therefore excluded. DAPI-negative and mCherry positive cells were collected for transplantation. None of the cells in the control group were designated as mCherry-positive. Non-transfected mSSCs from DBA/2J-CAG-EGFP mice were FACs sorted for GFP and used as a control for transplantation studies. Optimized PEI transfected DBA/2J-CAG-EGFP mSSCs were sorted for mCherry positive cells and used for transplantation.

4.1.2.5 Transplantation

Six wild-type nude recipient mice (Taconic: NCRNU-M) were treated with Bulsulfan to deplete endogenous spermatogonial stem cells. I injected non-transfected mSSCs that were GFP-positive into the right testis and sorted DBA/2J-CAG-EGFP mCherry-positive mSSCs that were transfected by our optimized PEI protocol into the left testis of each mouse. I transplanted $20x10^6$ cells per testis. Two months after injection, mice were euthanized and testes were collected for histology (H&E), colony counting, and immunohistochemistry. I only counted EGFP-positive colonies, which confirmed the origin came from cultured mouse SSCs.

4.1.2.6 Immunohistochemistry

Testicular tissue sections (5μm) were deparaffinized in xylene (2x 15 mins) and rehydrated in a graded ethanol series (100% for 10 mins x2, 95% for 5 mins, 80% for 5 mins, 70% for 5 mins, 50% for 5 mins, 25% for 5 mins) and washed in 1x PBS for 3 mins. Then sections were incubated in sodium citrate buffer (10 mM Sodium Citrate, 0.05% Tween-20, pH 6) at 97.5°C for 30 minutes. Slides were cooled and washed twice with 1x PBST (0.01% Tween-20) for two minutes. Sections were blocked with Donkey buffer (1x PBS with 3% bovine serum albumin, 0.1% Triton X-100, and 5% normal donkey serum) for 30 minutes at room temperature. Primary antibodies (Rabbit anti-VASA, 1:200, Abcam, ab13840; Goat anti-GFP, 1:200, Novus Biologicals, NB100-1770) were diluted in Donkey blocking buffer and incubated overnight at 4°C. Sections were washed with 1x PBS (3x 5 mins). Secondary antibodies (Alexa fluoro® Donkey anti-goat 488 (A11055) or Alexa fluoro® Donkey anti-rabbit 568 (A10042), Invitrogen) were diluted (1:200) in donkey blocking buffer. Sections were incubated with secondary antibody for 45 minutes at room temperature and then washed in 1x PBST (3x 5 mins) and 1x PBS (once for 5 mins). Sections were mounted with DAPI-containing Vectashield® mounting medium (Vector Laboratories, H-1200), and imaged within 48-72 hours.

4.1.2.7 Statistical analysis

Each dot represented a biological replicate, which is the mean of 2-4 internal replicates per each experiment. RM one-way ANOVA with multiple comparisons were performed in the experiment to optimized for PEI transfection condition for mSSCs shown in figure 22. Friedman test was used in the experiment to compare all transfection methods in figure 23. All statistical analyses were performed using Graphpad Prism 8 (California, USA).

4.1.3 **Results**

Linear PEI with a molecular weight of 25 kDa (CAS number 9002-98-6, 26913-06-4) was used for this study (chemical formula, Fig. 15A). Initially to assess the ability of PEI to transfect mSSCs, I followed our laboratory protocol for HEK293T transfection with PEI (standard PEI; Fig.15B). Briefly, an established DBA/2J-CAG-EGFP mSSC culture was trypsinized and plated into a 24-well, 1-2 days prior to transfection to achieve an 80-90% confluency. In one tube, 1μg of pAAV-CAG-mCherry plasmid was resuspended in 50 μL of 150 mM NaCl. In a separate tube, 10 μL of 7.5 mM PEI (0.323 mg/mL) was resuspended in 50 μL of 150 mM NaCl. After 3 minutes, the DNA solution was transferred to PEI solution, mixed and incubated for 30 minutes. The transfection mix was then put dropwise onto mSSCs with 150 μL Iscove's Modified Dulbecco's Media (IMDM) plain medium (PEI 0.3 mM final concentration). Then, the cells were incubated overnight at 37°C. The culture was washed and replaced with fresh complete medium. Three days after transfection, successful transfection of mSSCs was revealed by the presence of mCherry positive cells (Fig. 15C).

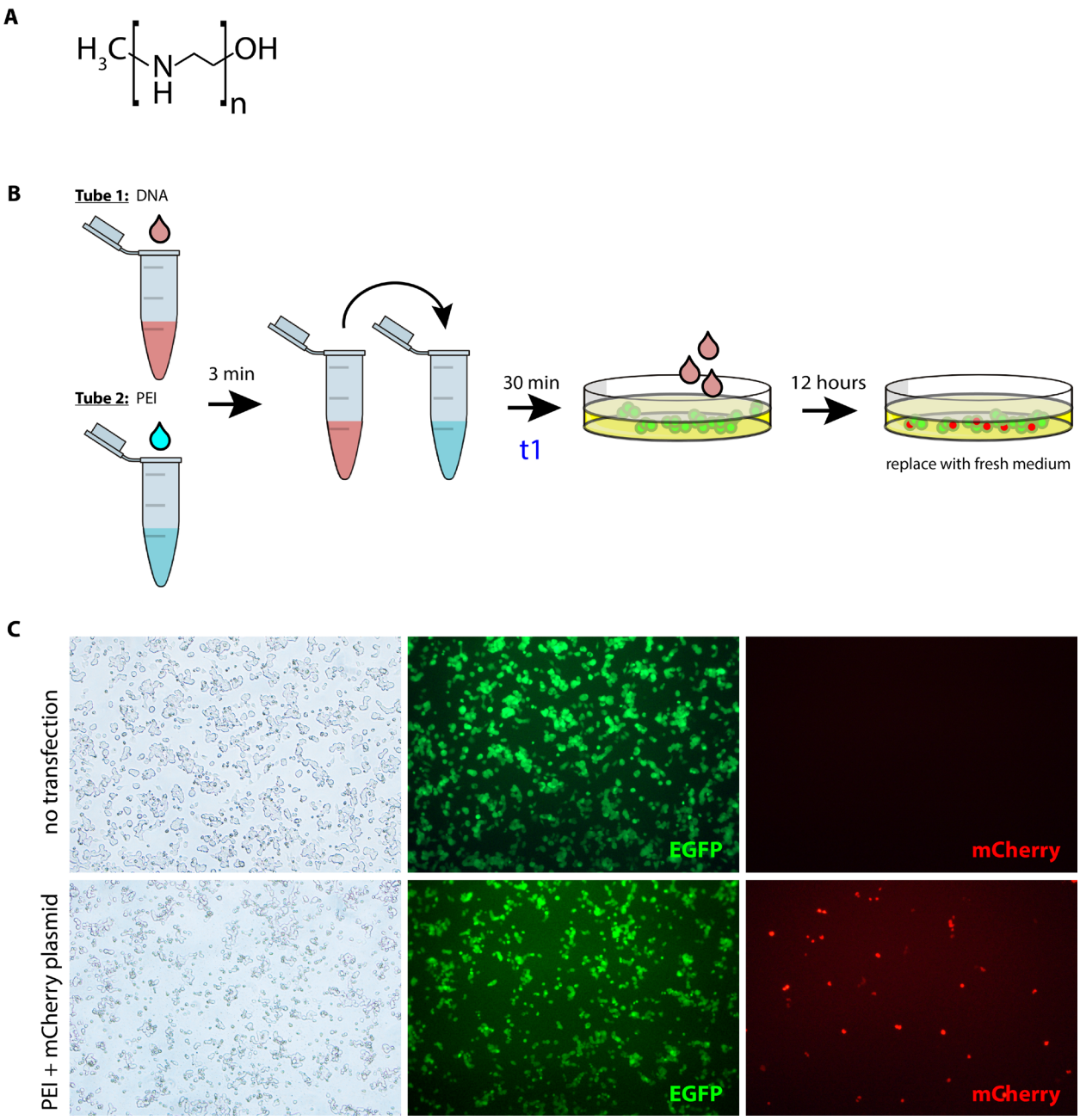

Figure 15 PEI can be used to transfect mSSCs

Chemical structure of PEI (A), standard PEI transfection protocol for HEK293T cells (B), the protocol was tested in CAG-EGFP mSSCs culture using pAAV-mCherry plasmid (C). Three days after transfection, total cells are visible by light microscopy in C (left panels) and by green color in C (middle panels); transfected cells are indicated by red color in C (Right panels).

The objective of this study was to optimize parameters to increase linear PEI transfection efficiency in mSSCs, after I confirmed that PEI can transfect mSSCs. I tested mSSC tolerance to PEI toxicity by exposing cultures to various PEI concentrations (0 M in IMDM or 150 mM NaCl, 0.375 mM, 0.75 mM, 1.5 mM and 3.75 mM in 150 mM NaCl) overnight. The viability of mSSCs (% of live cells /total number of cells) was assessed three days after exposure. Significant differences of cell viability are found between IMDM vs 1.5 mM ($p=0.001$); IMDM vs 3.75 mM ($p<0.0001$); 150 mM NaCl vs 1.5 mM PEI ($p=0.0026$); 150 mM NaCl vs 3.75 mM PEI ($p<0.0001$); 0.375 mM PEI vs 0.75 mM PEI ($p=0.0164$); 0.375 mM PEI vs 1.5 mM PEI ($p=0.0284$); 0.375 mM PEI vs 3.75 mM PEI ($p=0.0132$) (Fig. 16A). Therefore, I determined that 0.375 mM was the tolerable concentration for mSSCs. However, I proceeded the experiment with 2 PEI concentrations that resulted in the best cell viability, 0.375 mM and 0.75 mM PEI. Because exposure time also contributes to toxicity, I subsequently tested various incubation times (3 hrs, 6 hrs, and 12 hrs) with two different PEI concentrations, 0.375 and 0.75 mM; for both viability and transfection efficiency. I found no significant differences in complex incubation time among all conditions in terms of either viability and transfection efficiency (Fig. 16B, C). I chose 0.375 mM (5 μL of 7.5 mM PEI in 250 μL total volume in a 24-well) for 6 hours for the next parameter optimizations.

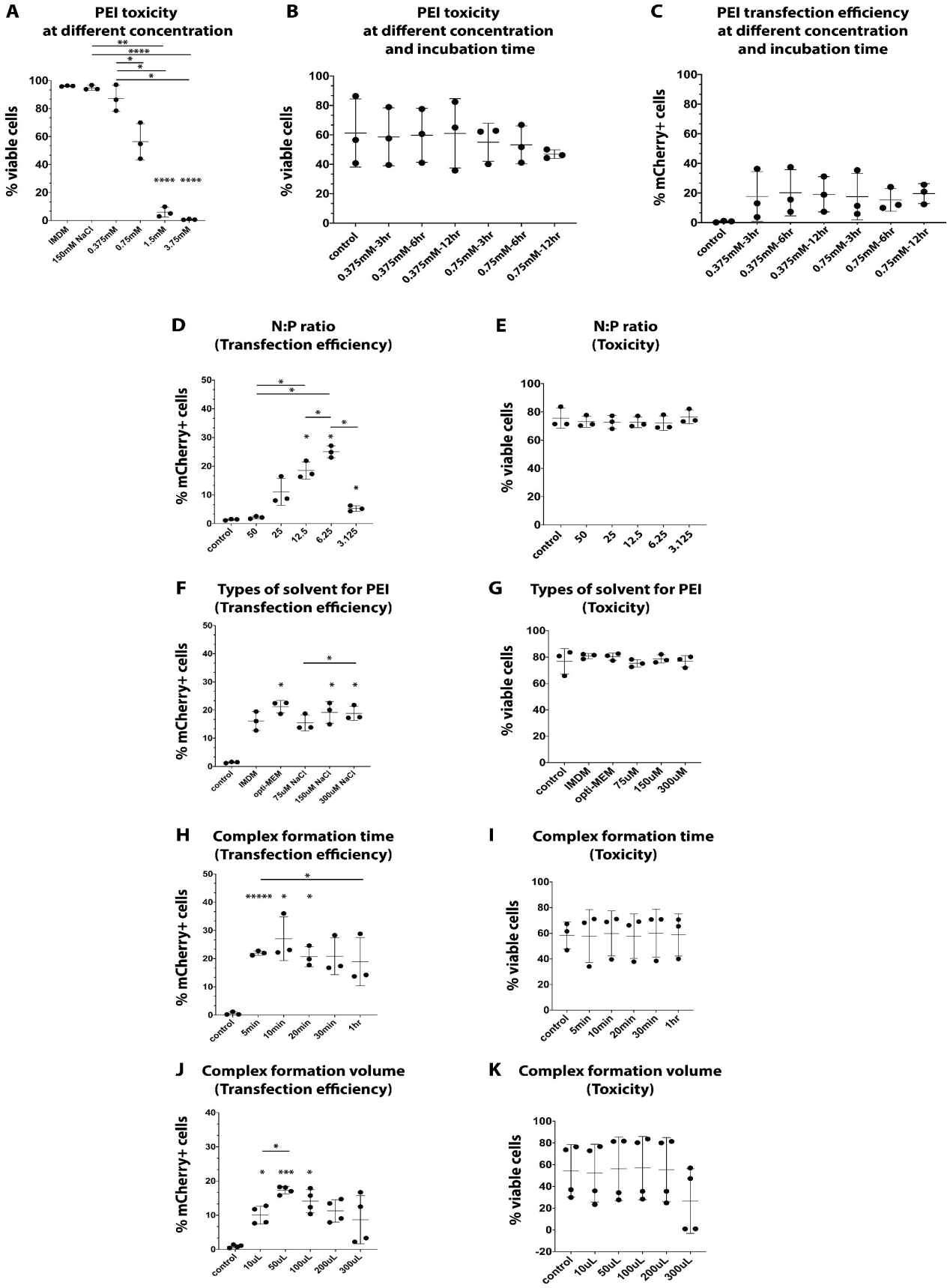
A
PEI toxicity
at different concentration
% viable cells
IMDM
150mM NaCl
0.375mM
0.75mM
1.5mM
3.75mM
B
PEI toxicity
at different concentration
and incubation time
% viable cells
control
0.375mM-3hr
0.375mM-6hr
0.375mM-12hr
0.75mM-3hr
0.75mM-6hr
0.75mM-12hr
C
PEI transfection efficiency
at different concentration
and incubation time
% mCherry+ cells
control
0.375mM-3hr
0.375mM-6hr
0.375mM-12hr
0.75mM-3hr
0.75mM-6hr
0.75mM-12hr
D
N:P ratio
(Transfection efficiency)
% mCherry+ cells
control
50
25
12.5
6.25
3.125
E
N:P ratio
(Toxicity)
% viable cells
control
50
25
12.5
6.25
3.125
F
Types of solvent for PEI
(Transfection efficiency)
% mCherry+ cells
control
IMDM
opti-MEM
75uM NaCl
150uM NaCl
300uM NaCl
G
Types of solvent for PEI
(Toxicity)
% viable cells
control
IMDM
opti-MEM
75uM
150uM
300uM
H
Complex formation time
(Transfection efficiency)
% mCherry+ cells
control
5min
10min
20min
30min
1hr
I
Complex formation time
(Toxicity)
% viable cells
control
5min
10min
20min
30min
1hr
J
Complex formation volume
(Transfection efficiency)
% mCherry+ cells
control
10uL
50uL
100uL
200uL
300uL
K
Complex formation volume
(Toxicity)
% viable cells
control
10uL
50uL
100uL
200uL
300uL

Figure 16 Stepwise optimization for PEI transfection protocol in mSSCs

Tolerance of mSSCs to different PEI concentrations (A), tolerance of mSSCs to 0.375 (10 μL of 7.5 mM PEI in 500 μL total volume), 0.75 mM PEI (20 μL of 7.5 mM PEI in 500 μL total volume) at different exposure time (3, 6, and 12 hours) (B); transfection efficiency (%mCherry-positive cells among all cells) using 0.15, 0.30 mM PEI with 1 ug DNA at different exposure time (C); transfection efficiency (D) and toxicity (E) in term of cell viability at different N:P ratio (nitrogen in PEI to phosphorus in DNA ratio); transfection efficiency (F) and toxicity in term of cell viability (G) using different solvents for PEI; transfection efficiency (H) and toxicity in term of cell viability (I) using different complex formation time; transfection efficiency (J) and toxicity in term of cell viability (K) using different complex formation volume. *Start indicates p-value of statistical significance compared to control (*p<0.05, **p<0.005, ***p<0.0005, ****p<0.00005, *****p<0.000005)*

Next, I optimized the molar ratio of nitrogen in PEI per phosphorus in DNA (N:P ratio). I kept our PEI amount fixed at its tolerable concentration (0.375 mM) and varied the DNA amounts. The N:P ratio can be calculated from amount of 7.5 mM PEI per well multiplied by 7.5 nmol/L (which is nitrogen content of PEI in 1 L of 7.5 mM PEI), divided by total DNA/well (μg) multiplied by 3 nmol (which is phosphorus/1μg DNA). I tested N:P ratios at 50, 25, 12.5, 6.25 and 3.125 (0.25, 0.5, 1, 2 and 4 μg of DNA per 10 μL of 7.5 mM PEI, respectively). I found that a N:P ratio of 12.5, 6.25 and 3.125 showed a significantly higher transfection efficiency than the control ($p<0.05$ all conditions) (Fig. 16D) while the viability was comparable among all conditions (Fig. 16E). Significant differences in transfection efficiency were observed in N:P=50 vs 12.5, 50 vs 6.25, 12.5 vs 3.125, and 6.25 vs 3.125 (all with $p<0.05$). Therefore, I proceeded the experiment with the N:P ratio of 6.25. Thus, a N:P ratio of 6.25 (2 μg of DNA per 10 μL of 7.5 mM PEI), a 0.375 mM PEI final concentration, and a six-hour incubation time was used the remainder of our study to balance toxicity and transfection capability.

The next parameter I optimized was the solvent (medium) in which the PEI/DNA complex forms (Fig. 16F). The standard HEK293T protocol was to resuspend PEI and DNA in 150 mM NaCl. In this experiment, I compared plain IMDM medium, Opti-MEM, 75 mM NaCl, 150 mM NaCl and 300 mM

NaCl. The control shown in the graph is non-transfection control in complete culture medium. Significance differences in viability were not observed; however, significant differences in transfection efficiency were seen in control vs opti-MEM, control vs 150 mM NaCl, control vs 300 mM NaCl, and 75 mM NaCl vs 300 mM NaCl (all with $p<0.05$) (Fig. 16F, G). Opti-MEM was chosen for the next parameter optimization because of the slightly higher mean in transfection efficiency.

Next, I optimized for the time/duration in which the PEI/DNA complex is allowed to form (complex formation time). I compared between 5, 10, 20, 30 minutes and 1 hour. No significant differences were observed in viability among incubation times (Fig. 16H, I). Transfection efficiency significant differences were seen in control vs 5 min ($p<0.000005$), control vs 10 min ($p<0.05$), control vs 20 min ($p<0.05$), and 5 min vs 1 hour ($p<0.05$). I chose 10 minutes because of its higher mean in transfection efficiency.

The last parameter I optimized was the volume in which the PEI/DNA complex is formed; I tested 10, 50, 100, 200 and 300 μL complex formation volumes (Fig. 16J, K). These are the total volumes for when PEI and DNA solutions were incubated together, thus PEI and DNA would be resuspended separately in half of the volume above. For example, 50 μL of complex formation volume means DNA and PEI were resuspended separately in 25 μL of Opti-MEM before mixing together to give a complex formation volume of 50 μL. Again, no significant differences in term of viability were seen (Fig. 16K). Significant differences in transfection efficiency were seen in control vs 10 μL ($p<0.05$), control vs 50 μL ($p<0.0005$), control vs 100 μL and 10 μL vs 50 μL ($p<0.05$) (Fig. 16J). Therefore, I chose 50 μL as the optimized complex formation volume.

Next, I compared our optimized PEI protocol to the standard protocol (HEK293T PEI transfection protocol), Lipofectamine Stem reagent transfection, and electroporation with a pAAV-CAG mCherry expression vector. Lipofectamine Stem reagent transfection was done according to the manufacturer's

protocol. For electroporation, six recommended conditions from the manufacturer were tested (Fig. 17A, B). No significant differences were seen across all the conditions either in terms of transfection efficiency or cell viability (Fig. 17C, D). The condition with the highest mean in transfection efficiency 125V; 5ms poring pulse was used in this comparison experiment.

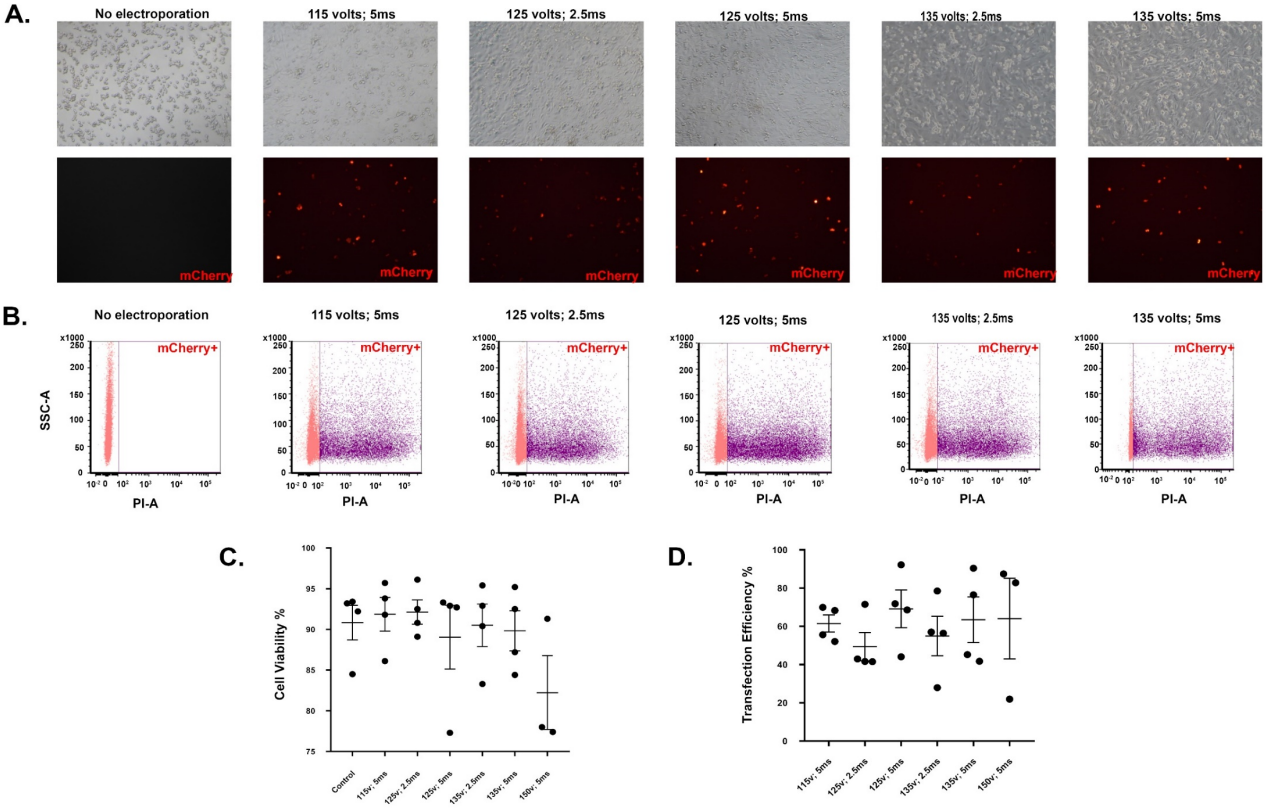

Figure 17 Optimization for electroporation conditions for mSSCs

Comparison of 6 electroporation conditions for mouse embryonic stem cells (mESCs) recommended from the manufacturer (A), flow cytometry showing transfection efficiency (mCherry-positive cells) (B), Cell ivability (%live cells/all cells) among all conditions (C), tansfection efficiency among all conditions (D).

To compare all the transfection method, the same amount of DNA (2 μg in a well of 24 well-plate with 250,000 cells or 8 μg for 1 million cells) was used in each protocol. The optimized PEI method for

mSSC transient transfection is summarized and shown in Fig. 18A. In brief, 2 μg DNA was resuspended in 25 μL Opti-MEM. In a separate tube, 10 μL of 7.5 mM PEI were resuspended in 25 μL of Opti-MEM to yield N:P ratio of 6.25. Each tube was resuspended and incubated for 3 min before mixing together to give a complex formation volume of 50 μL. The complex formation is then allowed for 10 min. The mixture was then added to the culture dropwise and incubated for 6 hours. (Fig. 18A) Red mCherry-positive cells were visible under fluorescence microscopy in all conditions, but Lipofectamine Stem reagent and optimized PEI conditions produced the highest transfection efficiencies (Fig. 18B). Quantification was done by flow cytometry. The gate was set sequentially for live cells (DAPI-negative cells) and then for mCherry-positive cells among live cells (Fig. 18C). The comparison was done by calculating the number of mCherry-positive live cells per 1,000 live cells input. Significant differences in mCherry-positive cells per 1,000 live cells input were seen in control vs Lipofectamine ($p<0.005$), control vs optimized PEI for mSSCs ($p<0.005$), standard PEI vs optimized PEI ($p<0.05$) and standard PEI vs lipofectamine ($p<0.05$) (Fig. 18D).

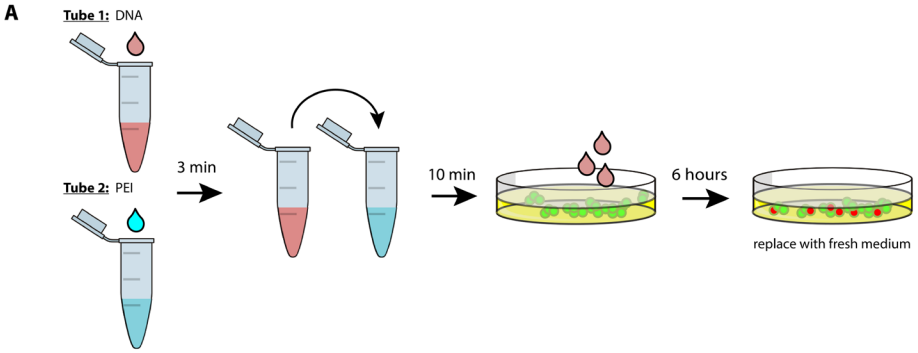
A
Tube 1: DNA
Tube 2: PEI
3 min
10 min
6 hours
replace with fresh medium

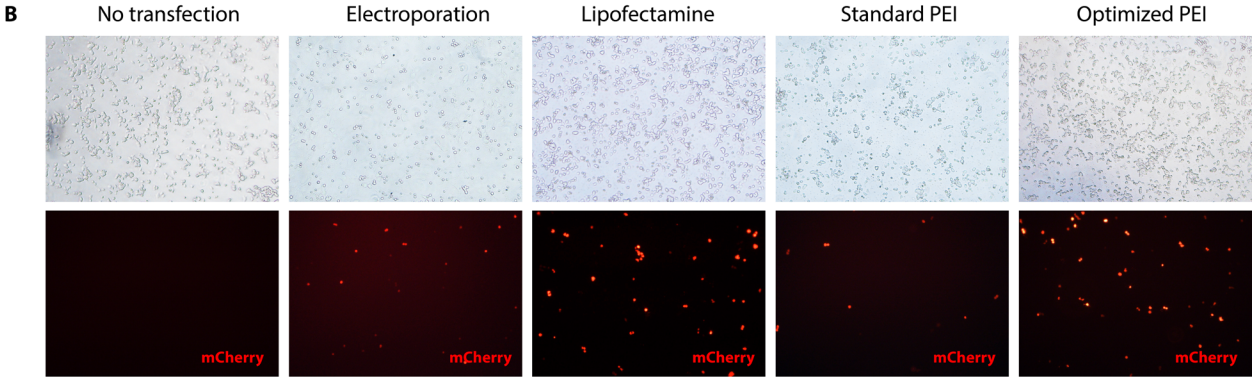
B
No transfection
Electroporation
Lipofectamine
Standard PEI
Optimized PEI
mCherry

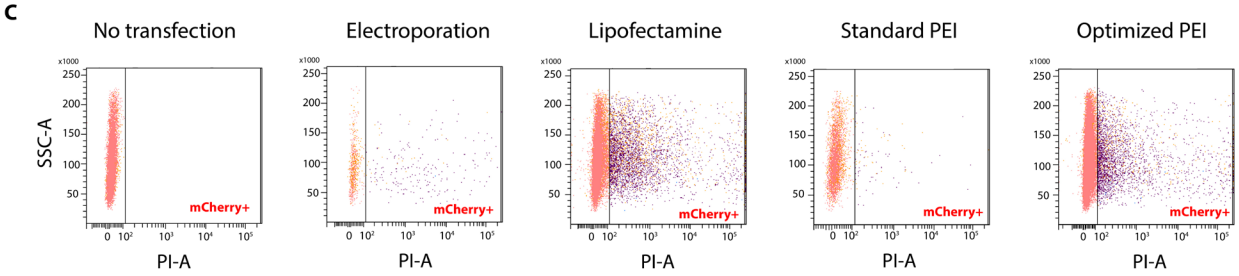
C
No transfection
Electroporation
Lipofectamine
Standard PEI
Optimized PEI
SSC-A
PI-A
mCherry+

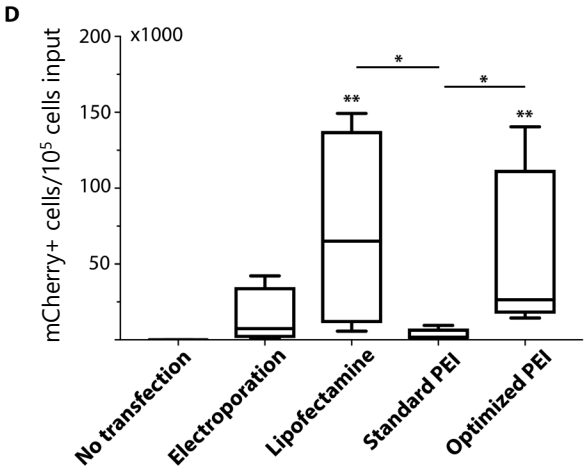
D
mCherry+ cells/10^5 cells input
x1000
No transfection
Electroporation
Lipofectamine
Standard PEI
Optimized PEI

Figure 18 Comparison of optimized PEI transfection protocol for mSSCs with other transient transfection methods known to work in mSSCs

Diagram summarizing optimized PEI transfection protocol for mSSCs (A). Bright field and red fluorescence images of mSSCs after being transfected with different methods (B). Quantification of mCherry-positive cells per 1,000 cells input at day 0 (D).

To test whether PEI-transfected mSSCs retained their stem cell properties to colonize mouse recipient testes, I transfected mSSCs derived from CAG-EGFP mice with pAAV-CAG-mCherry using our optimized PEI protocol. Three days after transfection, FACS-sorted mCherry-positive SSCs were transplanted into the testes of busulfan-treated nude mice, and testes were collected two months after transplantation (Fig. 19A, B). I did not observe any mCherry expression, which means the mCherry-plasmid was not integrated into the genome (Fig. 19C, D). To assess colonization, I only counted colonies which were EGFP-positive, ensuring the colonies came from our GFP mSSC cultures and were not endogenous. I found no significant differences in colonization between PEI-transfected and the non-transfected control mSSC cultures (Fig.19E). To show that the complete spermatogenesis came from transfected and transplanted cells, I co-stained the testicular tissue with VASA (indicating germ cells) and EGFP (indicating transplanted mSSCs) and found that colonies with complete spermatogenesis were also GFP-positive (Fig.19G, H, J, K, M, N, P, Q) compared to the non-transplanted control (Fig. 19F, I, L, O). Both control and transplanted testes exhibited tubules with VASA positive cells that were not EGFP positive. These represent recovering endogenous spermatogenesis after busulfan treatment. Overall, my results showed that PEI transfected mSSCs retained their stemness (ability to colonize and produce sperm), while there was no evidence of plasmid integration into the genome.

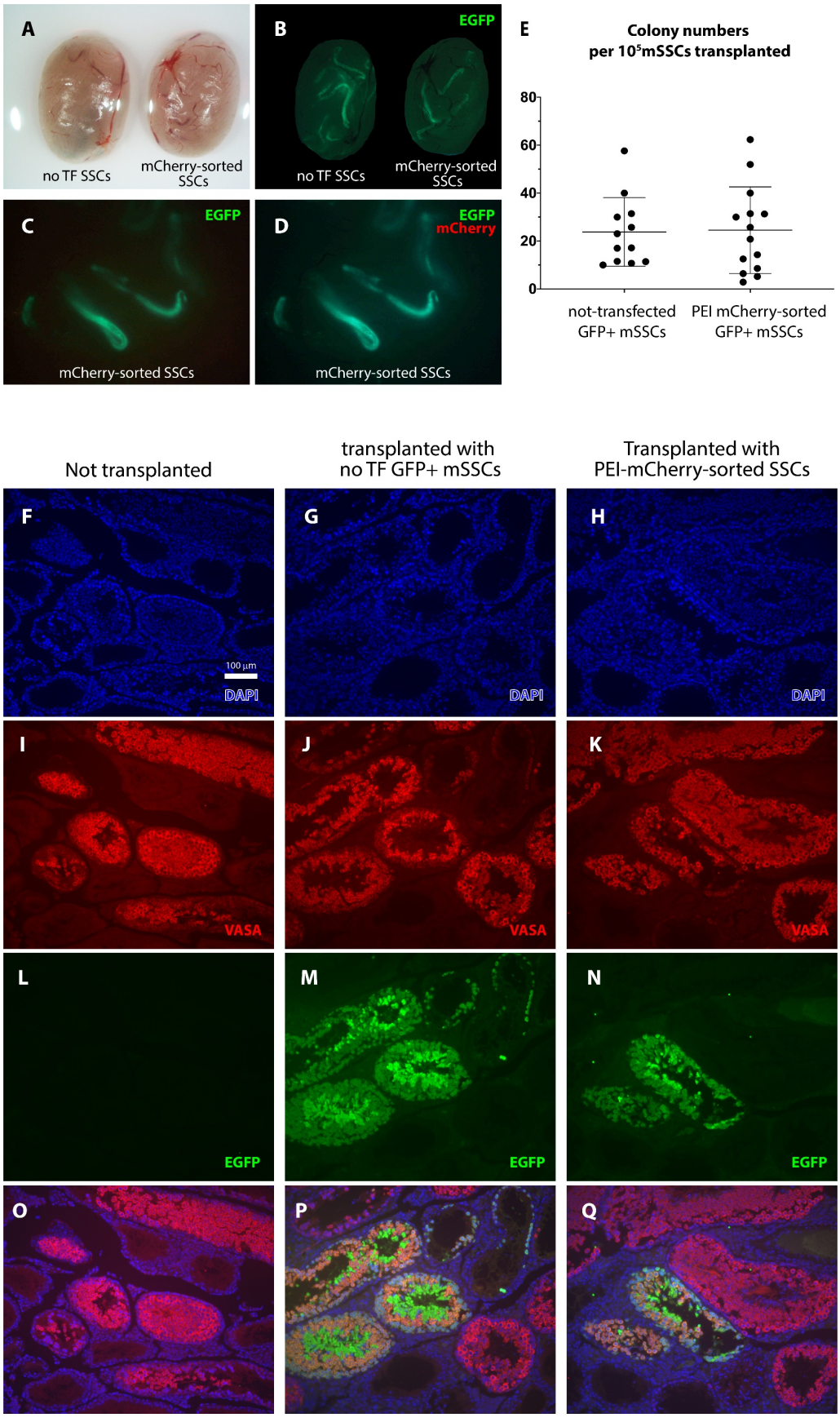
A
no TF SSCs
mCherry-sorted SSCs
B
EGFP
no TF SSCs
mCherry-sorted SSCs
C
EGFP
mCherry-sorted SSCs
D
EGFP
mCherry
mCherry-sorted SSCs
E
Colony numbers per 10⁵mSSCs transplanted
80
60
40
20
0
not-transfected GFP+ mSSCs
PEI mCherry-sorted GFP+ mSSCs
Not transplanted
transplanted with no TF GFP+ mSSCs
Transplanted with PEI-mCherry-sorted SSCs
F
100 µm
DAPI
G
DAPI
H
DAPI
I
VASA
J
VASA
K
VASA
L
EGFP
M
EGFP
N
EGFP
O
P
Q

Figure 19 PEI-transfected mSSCs were capable of colonization of seminiferous tubules and producing sperm.

Testis of Bulsulfan-treated nude mice injected with PEI-transfected mSSCs versus non-transfected control (A, B), mCherry-sort mSSCs under EGFP fluorescence (C) versus under EGFP/mCherry double filter (D). Quantification of colony numbers between PEI-transfected mSSCs versus non-transfected control (E). Cross section of seminiferous tubules transplanted with non-transplanted mSSCs (G, J, M, P) and PEI-transfected mSSCs (H, K, N, Q) compared to non-transplanted control (F, I, L, O).

4.1.4 **Discussion**

In this study I optimized a linear PEI transfection protocol for mSSCs that may be used for gene-targeting with limited or no random insertion into the genome, while mSSCs retain their potential to colonize the testes of busulfan-treated recipients. Because transfection often results in high variability, to best predict the transfection output, I performed at least three biological independent replicates per study. In each replicate, I included 2-3 internal replicates. Indeed, I saw variation in our results, which is likely because transfection is sensitive to environmental factors that are not easily controlled. From our observations, a major indicator of transfection efficiency was related to the health of the mSSCs which is influenced by their passage number, days after passage before transfection, slight differences in media conditions. This variability may have contributed to lack of significant differences for some the parameters I tested, which is why I continued in a stepwise fashion using the condition that tended to yield better results before proceeding to next steps.

Although few parameters alone showed a significant difference in transfection efficiency (PEI concentration, N:P ratio, and complex formation volume), the overall combination of our best conditions resulted in an optimized protocol that yields a significantly higher transfection efficiency than the standard PEI protocol. In addition, our optimized PEI protocol had a comparable transfection efficiency to the more expensive Lipofectamine Stem reagent protocol, and better transfection output compared to

electroporation, which is commonly used to transfect mSSCs. I report an optimized protocol for linear PEI transfection, which is both cost-effective and efficient for transfecting mSSCs.

Mouse SSC culture is largely used to understand gene function in stem cell maintenance and differentiation, and a common endpoint for studies is to transplant mSSCs into germ-cell depleted mice to evaluate their ability to colonize and differentiate. Thus, in addition to testing transfection efficiency, I also tested PEI transfected mSSC function by transplantation. Our findings show that PEI-transfection in mSSCs does not have a significant effect on colonization of recipient mouse testes.

I was unable to detect mCherry expression after transplantation, which indicates that our transfected plasmid did not integrate into the mSSC genome. Our optimized PEI protocol provides efficient transient transfection with no evidence of genome integration, which will make it amenable to gene-editing methods, like CRISPR/Cas9, where gene transfer expression needs to be robust and transient to limit the effects of genome integration or off-target effects.

4.1.5 **Conclusions**

CRISPR/Cas9 gene targeting in mouse spermatogonial stem cell (mSSC) culture is an important tool to study genes associated with spermatogenesis. It also has applications for producing genetically modified mouse lines and may have future applications for treating human infertility. Even with robust mSSC culture protocols and improved gene targeting efficiency of the mammalian genome following the introduction of the CRISPR/Cas9 system, gene targeting in mSSCs remains challenging. Transient transfection is an approach to introduce CRISPR/Cas9 components into target cells. Expression is typically transient, but sufficient to enable targeted genomic modification with CRISPR/Cas9. Random genomic integration after transient transfection is very rare and that may be important for both experimental and clinical applications. Polyethylenimine (PEI) is a cation complex capable of transiently

transfecting a wide range of mammalian cells but has not been shown to be applicable in mSSC culture. In this study, I optimized a transient transfection protocol using linear PEI (25kDa) in mSSC culture which resulted in successful transfection of a pAAV-CAG mCherry expression vector, while stem cells retained important properties of self-renewal, differentiation, and spermatogenesis.

4.1.6 **Acknowledgements**

Chatchanan Doungkamchan planned, did all the experiments except electroporation, analyzed the data and prepared the manuscript. Amanda Zielen performed electroporation and prepared the manuscript. Nilgun Yersel performed electroporation. Yi Sheng prepared pAAV-mCherry plasmid and advised on the project. Meena Sukhwani transplanted cells. Kyle E. Orwig advised on the project.

5.0 Germline gene editing restores spermatogenesis in a Tex11-D435fs mouse model of human azoospermia

5.1 Introduction

Azoospermia, a condition defined by complete absence of sperm in the ejaculate, affects approximately 1% of the male population worldwide [50, 52, 56]. Approximately 80-85% of azoospermic cases are classified as Non-obstructive azoospermia (NOA), whereas 15-20% of the cases are Obstructive azoospermia [52, 58, 59]. NOA is characterized by a failure of the testis to produce sperm, while the pathology in OA is an obstructive/obliterative lesion in male genital tracts that prevents sperm from being transported into the urethra [54]. OA is easily treated by testicular sperm extraction (TESE), a biopsy to collect sperm directly from the testis. Sperm recovery by TESE is successful in only 50% of NOA patients. There are no alternative fertility treatment options that would enable NOA patients with failed TESE to have a biological child. There are known causes to NOA such as Y-Chromosome micro deletion and aneuploidy, such as Klinefelter syndrome, which contributes to approximately 25% of all NOA cases [69, 70]. Other acquired causes include infection, trauma, medical treatments and undescended testes [56, 72]. Therefore, this leaves up to 75% of azoospermic cases that are unexplained or idiopathic [73]. Studies have identified single gene defects among the idiopathic azoospermic cases, including genes that are important for spermatogenesis, meiosis or DNA repair (reviewed in [50, 71, 82, 83, 85, 86]).

The number of single gene defects identified in idiopathic NOA patients are growing but the prognosis of NOA in terms of treatment outcome is approximately 50%, despite the microdissection Testicular sperm retrieval technique (discussed in Chapter 2). It is critical to develop new treatment especially for patients who fail testicular sperm retrieval. I hypothesize that gene targeting to convert a

mutated sequence to the wild-type sequence may restore gene expression of wild-type protein and hence restore spermatogenesis. Therefore, gene therapy may be the approach to improve prognosis in NOA patients caused by single gene defects.

The previous chapter focused on somatic (Sertoli) cell gene therapy to treat NOA. Although the therapy was performed around germ cells, it appeared that this therapy could be accomplished without germline modification or transmission to progeny. However, there are many single gene defects in germ cells that are associated with NOA, including mutations in TEX11 and SOHLH1 that will be addressed in my studies. Correction of these defects requires direct modification of the germ cells and those modifications could be passed to progeny. The main ethical concerns around germline gene therapy are the possibility that genome modification (on target or off target) could have unintended consequences for embryos or offspring that would become a permanent fixture in the family lineage. There are also concerns that germline gene editing could open a Pandora's box of possibilities for enhancement of intelligence, physical appearance or other characteristics [187, 188, 308]. However, a recent survey of US attitudes toward human genome editing revealed broad acceptance of somatic (64%) and germline (65%) gene editing for treatment of diseases, but lower acceptance for enhancements [309]. The US Academies of Science, Engineering and Medicine suggested that clinical trials of human genome editing could be initiated if technical challenges could be overcome, a comprehensive oversight framework is established that protects research subjects and their descendants and with the following considerations: 1) absence of reasonable alternatives; 2) restriction to treating a serious disease or condition; 3) restriction to editing genes that have been convincingly demonstrated to cause or to strongly predispose to that disease or condition; 4) restriction to converting such genes to versions that are prevalent in the population; 5) the availability of credible preclinical and/or clinical data on risks and potential health benefits of the procedures.

I propose a strategy for germline gene editing to treat NOA that involves converting disease-associated genetic variants to sequences that are common in the unaffected population and that this can be achieved with or without transmission to progeny. This can be achieved by CRISPR/Cas9-mediated gene editing in spermatogonial stem cells (SSC), *ex vivo*, followed by transplantation of gene corrected SSCs. Methods to culture mouse SSCs are well-established [276, 310] and critical to enable selection of precisely edited clones as well as test for off-target genomic modifications. Therefore, my studies will test both the technical feasibility and safety of germline gene editing to treat genetic male infertility.

In this chapter I used a mouse model of a human NOA-associated Tex11 mutation [130]. Tex11 mutations have been identified in a surprisingly high percentage of NOA patients [75, 76, 107]. Tex11 was shown in mice to interact with SYCP2, a component of the synaptonemal complex lateral elements [107]. Tex11-deficient spermatocytes exhibit loss of synapsis and crossover, which leads to meiotic arrest at the pachytene stage [107, 109]. Yatsenko and colleagues reported that Tex11 mutations alone contributed to 2.4% of all idiopathic NOA patients, and 15% of NOA with maturation arrest phenotype [76]. However, few of those mutations have been validated with a mouse model that exhibits the infertile phenotype. In this study we introduced a*Tex11-p.D435fs* (1258Ins(TT)), which was previously identified in an idiopathic NOA patient by Yang and colleagues and is characterized by a change of GATG to TTGGTA in exon 16 and results in a frameshift mutation at aspartic acid position 435 [73]. I generated the new Tex11-D435fs mouse model of human NOA to establish a causal relationship between this particular mutation and the NOA phenotype. I then used the model to demonstrate a germline gene editing strategy to repair the mutant allele and restore fertility; quantify the risk of off-target changes and demonstrate that germline gene editing can be achieved with or without transmitting the edit to the next generation.

5.2 Materials and methods

5.2.1 **Animals**

Animals were maintained and housed in the laboratory animal facility at Magee-Womens Research Institute. All study procedures were approved by the Institutional Animal Care and Use Committee of the University of Pittsburgh and Magee-Womens Research Institute. Procedures were performed in accordance with the NIH Guide for the Care and Use of Laboratory Animals (Assurance # 3654-01).

5.2.2 **Generating *Tex11-D435fs* mice**

The gRNA sequence "AATATGCTCCCTACAC" targets Tex11 and was designed by the program from Feng Zhang's lab (https://zlab.bio/guide-design-resources). The DNA template for sgRNA in vitro transcription was generated through PCR using the following primers: Forward 5' -TGTAATACGACTCACTATAGG AATATGCTCCCTACAC gttttagagctagaaatagc-3', and reverse 5' AAAAGCACCGACTCGGTGCC-3', using pSpCas9(BB)-2A-GFP (PX458) (Addgene 48138) as the template. The sgRNAs were synthesized by T7 in vitro transcription (MAXIscript™ T7 Transcription Kit, ThermoFisher), then purified using RNA Cleanup kit (Qiagen). The ssODN for 5.2.2 Generating Tex11-D435fs mice is GAATTTTGGAAAAATCTATGACTTTGTTGTTTTTTTTTAACTTTAG GTCCAAAAATATGCTCCCTACACTACAGTTATTCTCTGAAGTTGTATGAGTATGATA AAGCAGATCTGGATT and was ordered from Integrated DNA Technologies (Coralville, Iowa).

B6D2F1 (C57 BL/6J x DBA/2J F1) females (7-8 weeks old) were stimulated by intraperitoneal administration of 5 IU of PMSG (ProspecBio, Cat # HOR-272) at 3:30 pm on day 1, 5 IU of hCG (Sigma-Aldrich, Cat # CG5-1VL) 48 hours after PMSG injection on day 3. Then the females were mated to B6D2 F1 males. The embryos were collected from oviducts the following morning. After the cumulus cells were removed by incubation in 1% hyaluronidase in M2 medium, the embryos were cultured in KSOM medium at 5% CO_2 ,37° C until electroporation.

The reagents for embryo electroporation were mixed as follows in Opti-MEM medium: Cas9 protein 100 ng/µL (Alt.R S.p. Cas9 Nuclease 3NLS IDT Cat # 1074181); Tex11 sgRNA 200 ng/µL, Tex11 ssODN 200 ng/µL. The electroporation was performed using the Super electroporator NEPA21 type II and CUY 501-1-1.5 electrode (NEPA GENE Co. Ltd, Chiba, Japan) at these conditions: poring pulse (voltage 40 V, pulse length 2.5 ms, pulse interval 50 ms, number of pulses 4, decay rate 10%, polarity +); transfer pulse (voltage 7V, pulse length 50 ms, pulse interval 50 ms, number of pulses 5, decay rate 40%, polarity +/-). After electroporation, the embryos were washed two times in KSOM medium, then cultured in KSOM medium overnight at 5% CO_2, 37° C. On the following day, the two cell stage embryos were transferred to the oviducts of pseudopregnant CD1 females (0.5 dpc).

5.2.3 **Genotyping**

After litters were born, I used pup tails for DNA extraction at Day 5 of life. First, the tails were put in lysis buffer (100 mM NaCl, 10 mM TrisCl, pH 8 25 mM EDTA, pH 8 0.5% SDS) and agitated at 55 degrees Celsius overnight. Next, 100% Ethanol was added to the solution and the precipitated DNA was removed into a new tube in which 70% Ethanol was added. The tube was then centrifuged at full speed for 12 min. The supernatant was discarded. The DNA was dried for

about 30 minutes on a heat block which was set at 55 degrees Celsius and resuspended in nuclease free water.

PCR was done using LongAmp® Taq 2X Master Mix (m0287, New England Biolabs, MA, USA). Three forward primer sequences were used to distinguish between wild type and *Tex11* mutant mice. The first forward primer (Tex11-F1) was TGAAGGTATCTCCACTAGCATGG and will anneal to DNA of both *Tex11-D435fs* and WT mice. The second forward primer sequence (Tex11-WT F1) was GGTCCAAAAATATGCTGATG and will anneal with DNA from wild type mice only. The third forward primer (Tex11-Fm1) was TATGCTTTGGTACCCTACACTGG and will anneal to DNA from *Tex11-D435fs* mutant mice only. The same reverse primer sequence (Tex11-R1) was ACCTAAGTGCCACAGCAAAGAAC and was used for all PCR reactions. The PCR cycle was 95ºC for 10 minutes then 95ºC for 30s, annealing temperature for 20s, 72ºC for 50s for 30 cycles, then 72ºC for 10 minutes. For the annealing temperature, for forward primers one and two, the temperature used was 55 ºC. For the third forward primer to differentiate Tex+11 mutant mice, the annealing temperature was 57 ºC. PCR samples were run on a 1.5% agarose gel at 110 volts for 15 minutes and imaged for bands.

5.2.4 **Immunohistochemistry**

Mouse testis and epididymal tissues were removed from three *Tex11-D435fs* mutant mice and three wild type control DBA mice between 8-12 weeks of age. These tissues were fixed in 4% paraformaldehyde in Dulbecco's phosphate-buffered saline (DPBS) overnight at 4ºC. Tissues were washed with room temperature DPBS three to four times with at least 60-minute intervals between washes before processing for paraffin embedding. Tissue sections were collected on glass slides for immunohistochemistry.

Sections were warmed on a slide warmer for 5 minutes, and then deparaffinized with three washes of xylene, 10 minutes each. They were then hydrated in graded ethanol with two changes of 100% ethanol, followed by 95%, 80%, and 70% ethanol, each for 5 minutes. The slides were rinsed twice in distilled water and immersed in 97.5^{o}C sodium citrate antigen retrieval buffer solution for 40 minutes (10mM Sodium Citrate, 0.05% Tween-20, pH 6). After a cooling period of 20 minutes, the slides were rinsed in Phosphate Buffered Saline with Tween-20 (PBS-T) twice for two minutes each. Tissue sections were then permeabilized on a shaker for 30 minutes in a solution containing 100 mL 0.02% Triton X in 1x PBS. After two subsequent washes with PBS-T, sections were incubated with a blocking buffer (0.1% tween 20 and 10% donkey serum in PBS) for four hours at room temperature in a humidity chamber.

The following primary antibodies, diluted in blocking buffer, were used for immunofluorescence staining of the mouse testis tissue sections: rabbit anti-SALL4 (Abcam, diluted 1:800), rabbit anti-STRA8 (Abcam, diluted 1:200), rabbit anti-SYCP3 (Abcam, diluted 1:500), goat anti-TP1 (Abcam, diluted 1:1000), goat anti-ZIP4H/Tex11 (R&D Systems, diluted 1:100), mouse anti-DDX4 (Abcam, diluted 1:100). These primary antibodies were incubated with tissue sections overnight at room temperature in a humidified chamber. Isotype matched normal IgG controls were used on one tissue section on each slide instead of primary antibody as a negative control. After three two-minute washes with PBS-T, secondary donkey anti-rabbit (Invitrogen, diluted 1:100) or donkey anti-goat AlexaFluor-488 (Thermo Fisher, diluted 1:100) with donkey anti-mouse AlexaFluor-568 conjugated IgG (Invitrogen, diluted 1:100 in blocking buffer) were applied to the appropriate tissue sections and incubated at room temperature for two hours in a humidity chamber. Sections were washed with PBS-T three times for two minutes each and incubated in a humidified chamber for 15 minutes at room temperature with Vectashield

medium with 4',6-diamidino-2-phenylindole (DAPI) (Vector Labs) for fluorescence imaging. After two final washes for two minutes each in deionized water, the slides were mounted with Vectashield medium.

Imaging was performed on the Nikon Eclipse 90i fluorescence microscope, using an X-Cite 120 fluorescence light source, Nikon digital camera, and Nikon Eclipse 9i software. Stained tissue sections from three adult Tex11 mutant mice and three wild type controls were used for each co-staining experiment. For each tissue section, 100 circular tubules in cross-section were analyzed.

5.2.5 **Spermatogonial stem cell culture**

Tex11-D435fs heterozygous females were bred with DBA/2 WT mice. The heterozygous female pups were again bred to DBA/2 WT mice for 5 generations to obtain *Tex11-D435fs* with DBA/2 genetic background because SSC cultures from the DBA/2 strain are more robust than other strains. To establish an SSC culture, the protocol from Kanatsu-Shinohara and colleagues was followed with some modification [289]. In brief, testes from 6-9 day-old pups were digested with 0.25% trypsin and 1.2% w/v DNaseI. The digestion was stopped with knockout serum replacement. The testicular suspension was then washed followed by centrifugation at 600g for 7 min through a 30% Percoll cushion. The pellet was washed again in 1x DPBSS (Dulbecco's phosphate-buffered saline with 0.1% Fetal bovine serum, 10 mM HEPES, 10 mM sodium pyruvate, 1 mg/ml glucose and penicillin/streptomycin) and incubated with Thy1-antibody coated beads (CD90.2 MicroBeads, Miltenyi Biotech) for 1 hour, washed and run through a MACS column (Miltenyi Biotech). The Thy1-positive testicular cells were then eluted from the MACS column using 1x DPBSS, pelleted at 600g for 5 min, resuspended in IMDM/SFM and plated on

Mouse Embryonic Fibroblasts (MEF) feeder cells and were cultured for 4-6 passages before being used for gene targeting. The media for mSSCs was IMDM/SFM.

5.2.6 **Gene targeting**

Tex11-D435fs SSCs were plated onto mitotically inactivated mouse embryonic fibroblast (MEF) feeders in a 6 well-plate at 1 million cells/well in IMDM/SFM. The following morning, the media was changed into plain IMDM. Lipofectamine STEM reagent was used for transfection according to the manufacturer's protocol. I used 1.2 μg of sgTex11-D-P2/Cas9 plasmid and 2.3 μg of ssODN carrying WT sequence and 0.5 μg of pAAV-mCherry plasmid (total DNA amount =4 μg) with 10 μL of Lipofectamine STEM reagent (Invitrogen) to mark the transfected colony. One week after transfection, the mCherry-positive clones were identified under a fluorescence microscope. A glass pipet was used to pick and transfer positive colonies to a 96-well plate with MEF feeder. Each colony was grown separately in the 96-well plate for 7-14 days. When the colonies were sizable, few cells in a colony were picked for individual DNA extraction, and the colony genotyping was done after the DNA was unbiasedly amplified using single-cell whole genome amplification (Qiagen). The PCR genotyping includes DNA quality control PCR using F1R1 primers which bind to the common sequence in both WT and *Tex11-D435fs* original allele. And the second primer pair (Fm1, R1), which is specific to *Tex11-D435fs* allele, were used to identify unmodified clones. The clones positive for F1R1 but not for Fm1R1 pair were putative gene-corrected colonies and were further analyzed by Sanger sequencing to confirm the sequence. For Sanger sequencing, the F1R1 primer pair was used to amplify the region. The amplicons were purified using a DNA cleanup kit (Takara, Japan). The sequencing primers used were F1 and R1

(2 reactions for each sample.) The confirmed gene-corrected clones were propagated for another 3-6 passages before transplantation.

5.2.7 **Mouse SSC Transplantation**

Uncorrected and gene corrected SSC clones were transplanted into infertile W/Wv and busulfan-treated Tex11-D435fs male recipients. W mice were obtained from Jackson laboratory. The gene-corrected mSSCs were blown off from the feeder layers and subsequently digested briefly in 0.05% trypsin. The reaction was stopped by addition of KOSR and cells were washed with 1x PBS. The cells were counted and resuspended in IMDM/SFM medium with 10% trypan blue at 20 million cells/mL. The cells were injected in a volume of 3.5 uL into the testis of recipient mice via efferent ductules as described above. The unmodified clone was prepared the same way and was injected at the same volume/concentration into the contralateral testis of W mice.

5.2.8 **Sperm analysis**

To assess sperm production in both *Tex11-D435fs* mutant and wild type mice, the head of the epididymis was isolated for histological analysis and tail of the epididymis was dissected to collect sperm. In a two-centimeter dish, 60 μL of sterile, warm PBS was placed in the center of the dish. Subsequently, 2 mL of mineral oil was pipetted to surround the PBS. Sixty additional microliters of PBS (for a total of 120 microliters) was added to the small central droplet, and approximately 2 mL of additional mineral oil was added to cover the PBS. The tail of the epididymis was placed in the PBS droplet after it was cleaned of fat and extraneous tissue. It was snipped five times with a scissors to release the sperm, and then incubated at 37 ºC for 10 minutes.

The sperm from the droplet was then diluted in 90 µL of warm PBS in an Eppendorf tube. This dilution was performed for wild type mice only in anticipation that the *Tex11-D435fs* mice would have reduced or no sperm present. The sperm solution was further diluted by a factor of 10 in PBS and trypan blue to assess cell viability. Sperm were counted using a hemocytometer, with care taken to assess sperm morphology, motility, and progressive motility.

5.2.9 **Egg and Sperm collection**

B6D2F1 (C57 BL/6J x DBA/2J F1) females were superovulated by administration of PMSG (provide dose, ip) at 7 pm on day 1, and hCG (provide dose, ip) 48 hours later. The eggs were collected from the oviducts between14-15 hours after hCG injection, then cultured in 200 µl mHTF media (fertilization drops), to which L- glutathione reduced (GSH, final concentration 1mM) was added.

The cauda epididymides from each male mouse were removed, then placed into sperm dishes which contain 200 µl TYH+MBCD media, which was pre-equilibrated at 37°C, 5% CO_2 for at least 20 min. Each cauda epididymis was cut to release the sperm into the media. Then the sperm were incubated for 60 min (37 °C, 5% CO_2) for capacitation.

5.2.10 **IVF**

After the sperm have been incubated in TYH+MBCD media for 60 min, about 10 µl of sperm solution was added into the egg fertilization drops. The final concentration of sperm is no less than 1 x 10^6/ml. The fertilization dishes were placed in an incubator (37°C, 5% CO_2). If the sperm concentration was much less than 1 x 10^6 /mL, I collected the rest of the capacitated sperm

into a centrifuge tube from the sperm dish. The sperm solution were subjected to centrifugation at 300 g for 4 min, resuspended in mHTF, then added the additional sperm into the fertilization drops. Five to six hours after incubation, the eggs were washed three times with KSOM medium, then cultured overnight in KSOM. The next day, the 2-cell embryos were picked and transferred into the oviducts of pseudopregnant females.

5.2.11 **Piezo-assisted ICSI**

If sperm numbers were low, intracytoplasmic sperm injection (ICSI) was used instead of conventional IVF. Several microliters of sperm prepared from the "Sperm collection" were put into 1 ml TYH+MBCD medium, then passed through a syringe with a 23g needle a total of 15 times to detach the tails of the sperm. The sperm solution was pelleted at 400g for 4 min, and the majority of supernatant was removed, with only 10 μL left for resuspersion of sperm heads. Transfer of 1 μL of sperm heads and 5-10 eggs was performed into an injection drop. Subsequently, one or more sperm heads was drawn into the microinjection pipette. The egg was held by the holding pipette, with its spindle's position at 6 or 12 o'clock. The zona of egg was penetrated by applying piezo pluses with intensity at 3 or 4, frequency at 6. The injection pipette was slowly pushed through the ooplasm to the opposite pole of the egg and the sperm head was released. The injected eggs were allowed to recover at room temperature for 10 min, then returned into KSOM medium for culture in a CO_2 incubator. The next day, the 2-cell embryos were transferred to the oviducts of pseudopregnant females. If there were fewer than twenty 2-cells embryos, 2-cell CD-1 mouse embryos were co-transferred into the same female to increase the likelihood of pregnancy.

5.3 Results

5.3.1 *Tex11-D435fs* mice are infertile from NOA with maturation arrest phenotype

The testes of *Tex11-D435fs* mice (28.30±3.84 mg) were smaller than to wild-type (120.3±2.64 mg) (Fig. 20A and B; unpaired t-test p=0.0016). Histological analyses indicated a maturation arrest phenotype in *Tex11-D435fs* testis compared to wild-type (Fig. 20C and E. No elongated spermatids or sperm were seen in the lumen of the seminiferous tubules. Sperm were observed in the head of the epididymis of wild type mice but not Tex11-D435fs mice (Fig. 20D, F). Accordingly, no sperm were recovered from the tail of the epididymis of Tex11-435fs mice, whereas 8.60±4.37 million sperm were recovered per epididymis in the control group (p=0.0271, unpaired t-test) (Fig. 20G). When *Tex11-D435fs* male mice were bred with wild-type female, no offspring were produced compared to the average of 4.88± 3.64 pups/litter in WT (unpair t-test p<0.0001) (Fig. 20H). These data showed that the *Tex11-D435fs* were infertile with an NOA and maturation arrest phenotype, thus, validating the patient TEX11-D435fs azoospermia-associated variant [130].

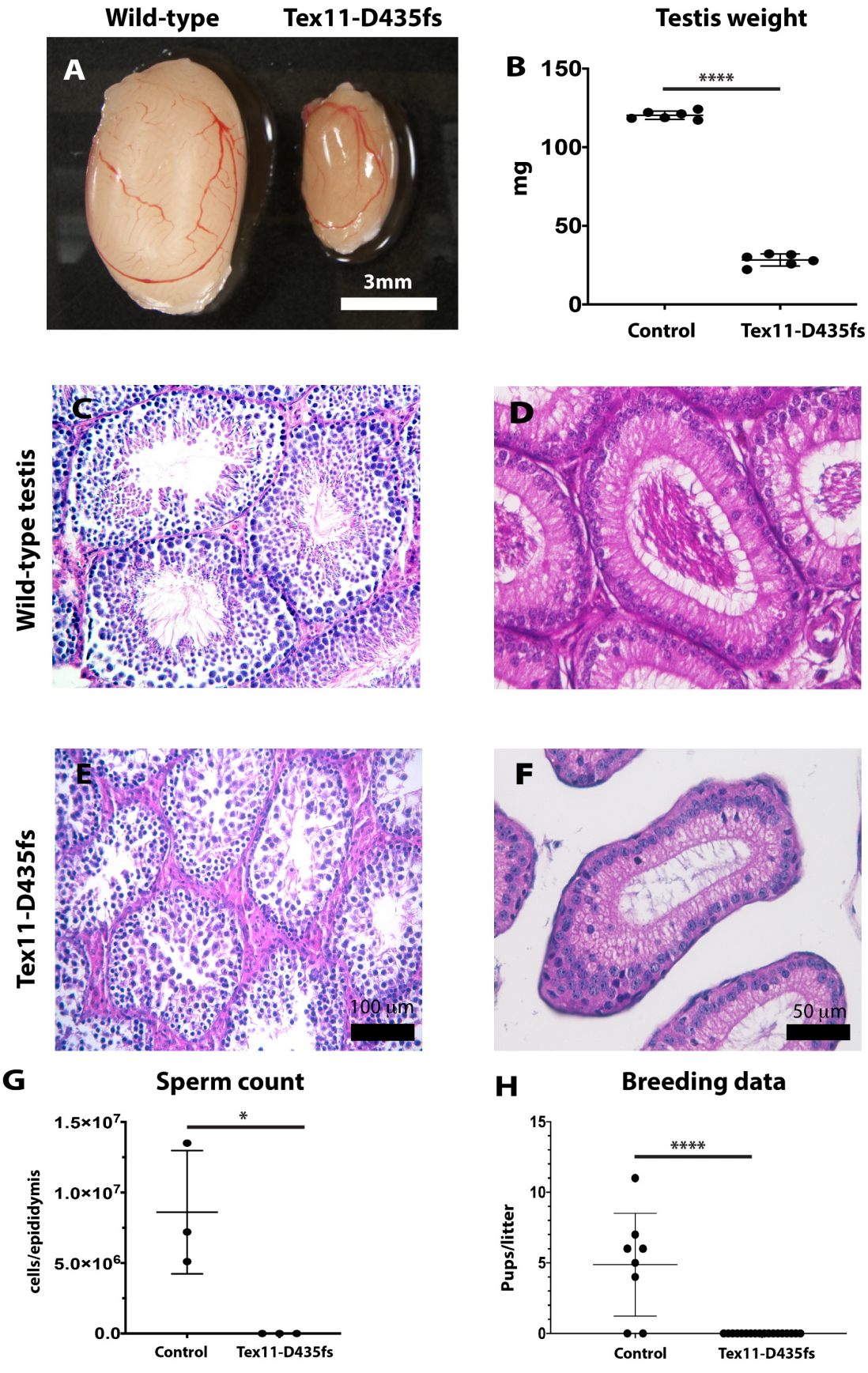
Wild-type
Tex11-D435fs
A
3mm
Testis weight
B
150
100
50
0
mg
****
Control
Tex11-D435fs
Wild-type testis
C
D
Tex11-D435fs
E
100 µm
F
50 µm
G
Sperm count
1.5×10^7
1.0×10^7
5.0×10^6
0.0
cells/epididymis
*
Control
Tex11-D435fs
H
Breeding data
15
10
5
0
Pups/litter
****
Control
Tex11-D435fs

Figure 20 Characterization of *Tex11-D435fs* mice

Macroscopic picture of testes from *Tex11-D435fs* mouse compared to WT (A). Testis weight (mg, B). Histology with H&E staining of seminiferous tubules (C, E) and H&E staining of the caput epididymis of WT and Tex11-D435fs mice (D, F). Sperm count per epididymis (G). The number of pups per litter after WT or *Tex11-D435fs* breeding with WT females (H).

To further characterize the maturation arrest phenotype, I stained the testicular tissues of Tex11-D435fs and WT mice with markers for various stages of germ cell differentiation. *Tex11-D435fs* testes contained multiple layers of VASA-positive germ cells (Fig. 21A, B), including SALL4-positive undifferentiated spermatogonia (Fig. 21C, D), STRA8-positive differentiating spermatogonia (Fig. 21E, F) and PIWIL1-positive spermatocytes (Fig. 21G, H). However, TP1-positive spermatids were rarely observed in *Tex11-D435fs* testes compared to wild-type control (Fig. 21I, J). This immunohistochemistry study therefore confirmed the phenotype of maturation arrest at the spermatocyte stage.

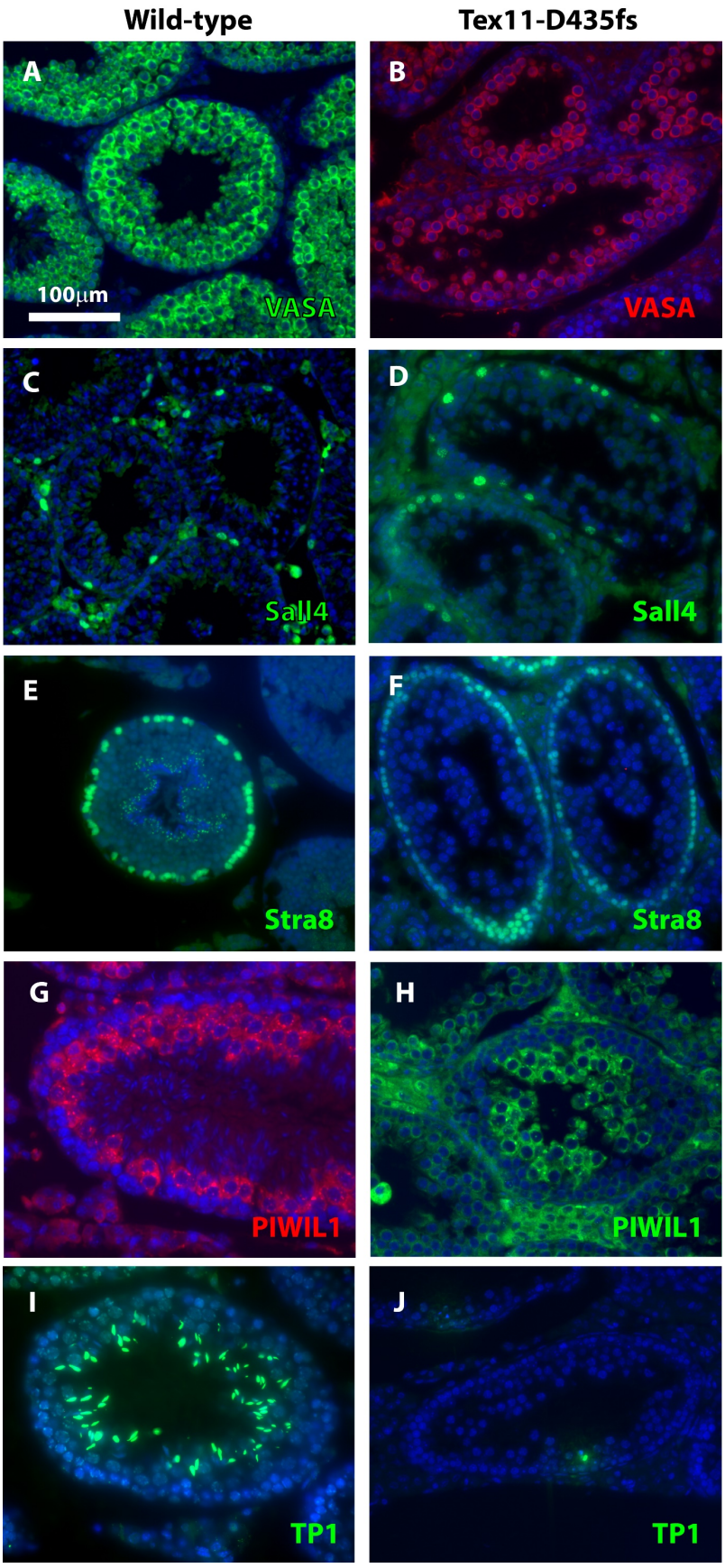
Wild-type
Tex11-D435fs
A
100μm
VASA
B
VASA
C
Sall4
D
Sall4
E
Stra8
F
Stra8
G
PIWIL1
H
PIWIL1
I
TP1
J
TP1

Figure 21 Characterization of maturation arrest phenotype in Tex11-D435fs mice

Immunohistochemistry for VASA (A, B), Sall4 (C, D), Stra8 (E, F), PIWIL1 (G, H), and TP1 (I, J) in *Tex11-D435fs* (B, D, F, H, J, L) compared to WT (A, C, E, G, I, K), *scale bar=100 μm*

5.3.2 Gene targeting using CRISPR/Cas9 and ssODN successfully reversed the mutated sequence in Tex11-D435fs mice to WT sequence

The sgRNAs were designed using Zhang's laboratory platform available on CRISPR.mit.edu. The targeted sequence was the mutant *Tex11-D435fs* sequence. Two candidate sgRNAs (Fig. 22A) were tested using Surveyor T7E1 assays in Neuro 2A cells (ATCC#CCL-131) to assess the ability to create DNA double-stranded breaks at the target locus in the mouse genome (Fig. 22B). Small-guide RNA-Tex11-D-P2 was selected for the downstream gene editing. Single-stranded Oligodinucleotide (ssODN) was the wild-type sequence with 60-bp nucleotide homology arms flanking each side of the target locus (Fig. 22A, see Appendix table 2 for sequence). sgRNA-Tex11-D-P2, ssODN and mCherry plasmid were co-transfected with Lipofectamine STEM reagent into *Tex11-D435fs* mSSC culture. A week after transfection the mCherry-positive colonies were picked and grown in a 96-well plate, genotyped and further expanded (Fig. 22C-E). PCRs with two sets of primers (Fig. 22A); 1 pair was specific to mutant allele (Fm1, R1) and the second pair was used as a quality control for DNA template (F1, R1). I screened a total of 115 clones and identified three clones that were negative for mutant allele by primer pair 1 (Fm1, R1) with positive quality control bands from primer pair 2 (F1, R1) (Fig. 22F). Sanger sequencing confirmed these clones to have gene-corrected wild-type sequence (clones 1A and 1D shown in Fig. 22H). PCR and Sanger sequencing for unmodified clone 10E are shown in Figure 26F and H. I chose clone 1D for functional testing by transplantation. To assess restoration of mRNA expression in clone

1D, I performed semi-quantitative PCR using primers specific for the Tex11-mRNA wild-type allele and confirmed expression (Fig. 22G).

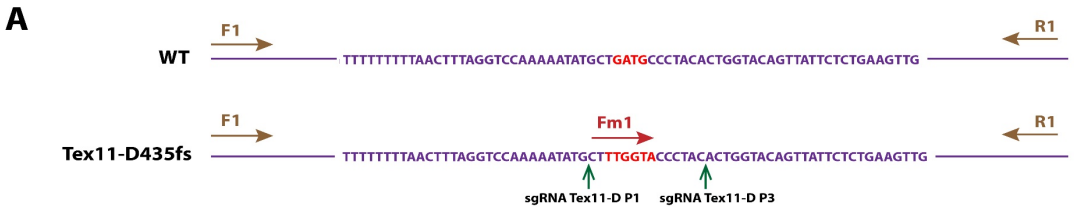
A
F1
R1
WT
TTTTTTTTTAACTTTAGGTCCAAAAATATGCTGATGCCCTACACTGGTACAGTTATTCTCTGAAGTTG
F1
Fm1
R1
Tex11-D435fs
TTTTTTTTTAACTTTAGGTCCAAAAATATGCTTTGGTACCCTACACTGGTACAGTTATTCTCTGAAGTTG
sgRNA Tex11-D P1
sgRNA Tex11-D P3

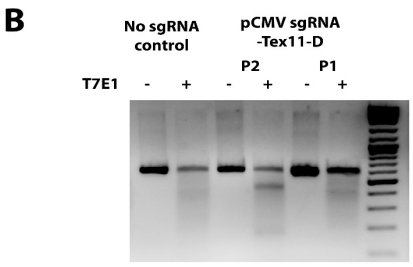
B
No sgRNA control
pCMV sgRNA -Tex11-D
P2
P1
T7E1
- + - + - +

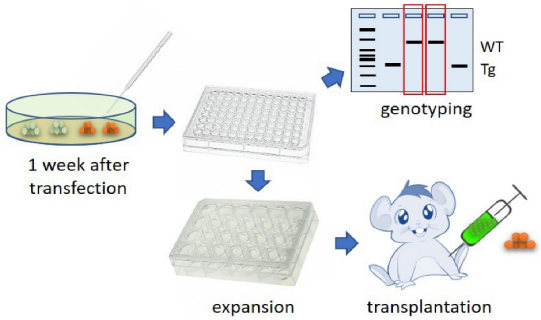
C
WT
Tg
genotyping
1 week after transfection
expansion
transplantation

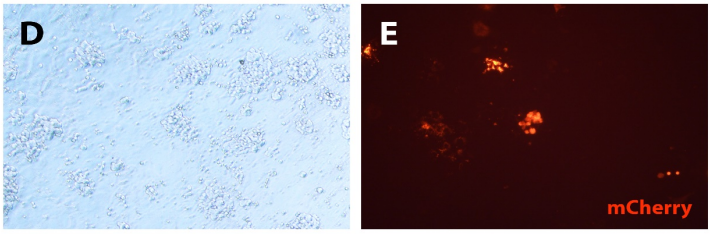
D
E
mCherry

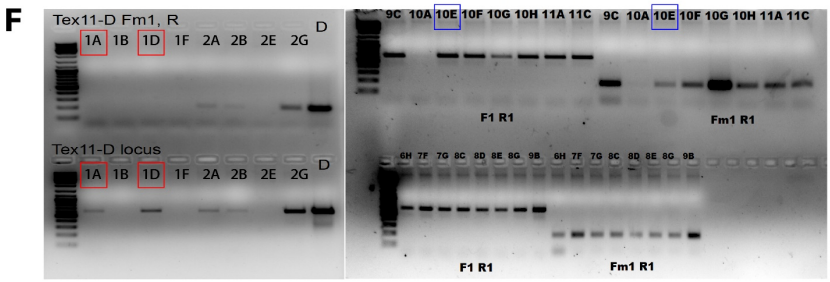
F
Tex11-D Fm1, R
1A 1B 1D 1F 2A 2B 2E 2G D
Tex11-D locus
1A 1B 1D 1F 2A 2B 2E 2G D
9C 10A 10E 10F 10G 10H 11A 11C
F1 R1
Fm1 R1
F1 R1
Fm1 R1

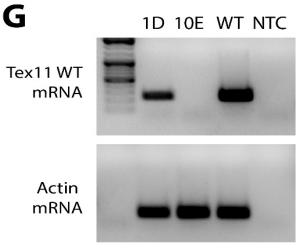
G
1D 10E WT NTC
Tex11 WT mRNA
Actin mRNA

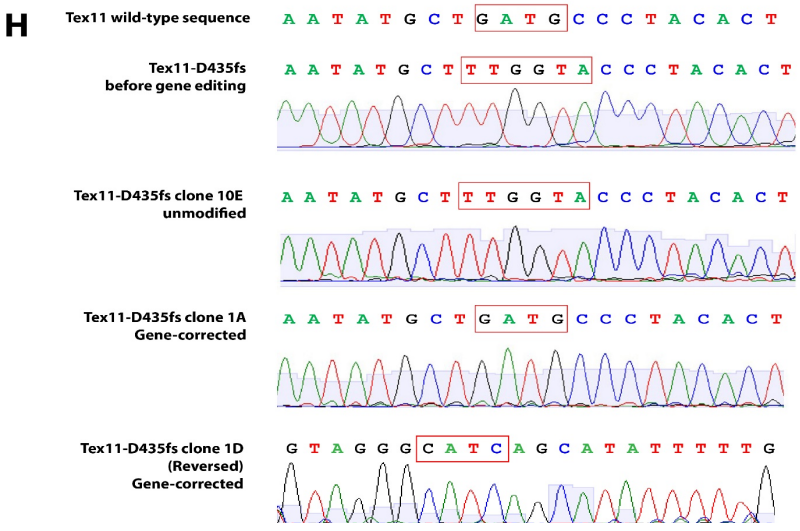
H
Tex11 wild-type sequence
A A T A T G C T G A T G C C C T A C A C T
Tex11-D435fs before gene editing
A A T A T G C T T T G G T A C C C T A C A C T
Tex11-D435fs clone 10E unmodified
A A T A T G C T T T G G T A C C C T A C A C T
Tex11-D435fs clone 1A Gene-corrected
A A T A T G C T G A T G C C C T A C A C T
Tex11-D435fs clone 1D (Reversed) Gene-corrected
G T A G G G C A T C A G C A T A T T T T T G

Figure 22 Gene targeting in *Tex11-D435fs* mSSCs

Targeted sequence at *Tex11-D435fs* locus compared to the WT sequence, where the DSBs were expected as a result of sgRNA *Tex11-D435fs* P1 or P2 and where the primers bind (A). T7E1 assay after transfecting Neuro2A cells with sgRNA *Tex11-D435fs* P1 or P2 (B). Diagram showing clonal selection, expansion and colony genotyping (C). *Tex11-D435fs* at 1 week after transfection with sgRNA *Tex11-D435fs* P2, ssODN and pAAV-CAG-mCherry (D, under bright field; E, under red fluorescence). Colony PCR showing gene-corrected clones (1A, 1D indicated in the red box) compared to transfected-but-not-gene-corrected clone (10E indicated in the blue box) (F). Quantitative PCR (qPCR) for Tex11-WT mRNA in gene-corrected clone 1D compared to transfected-but-not-gene-corrected clone 10E, with qPCR for actin mRNA as a control (G). Sanger sequencing to confirm the WT sequence in the gene-corrected clones (H).

5.3.3 Sperm were recovered from testes transplanted with gene-corrected *Tex11-D435fs* mSSCs

To assess the spermatogenic potential of gene-corrected clones, I transplanted the gene-corrected clones 1D into one testis of infertile W mice and transplanted the unmodified *Tex11-D435fs* SSCs into the contralateral side. At 4.5 months after transplantation, the testes transplanted with gene-corrected clones were larger in size (37.01±14.69 mg) than testes transplanted with unmodified *Tex11-D435fs* clones (16.10±3.47 mg) (Fig. 23A and B; one-tailed paired t-test p=0.0386)., I observed engraftment and colonization at 2.5 months after transplantation from both sides with complete spermatogenesis through elongated spermatids observed only on the testis transplanted with gene-corrected clones (Fig. 23C and F). Sperm were observed in both the caput (Fig. 23D, G) and the cauda epididymis of testes transplanted with gene corrected clones, but not from testis transplanted with unmodified Tex11-D435fs clones (Fig. 23E, H). Sperm counts were 2.75±1.12 million sperm/epididymis in testes transplanted with gene corrected clones compared

to 0 from testes transplanted with unmodified clones (Fig. 23I; one-tailed paired t-test p=0.0254). Epididymal sperm from W recipient testes transplanted with gene corrected SSCs were used to fertilize the WT eggs by IVF and ICSI (Fig. 23J shown 2-cell embryos from IVF). ICSI fertilization rates were 18.5% (10 2-cell embryos per 54 oocytes injected) and 23.25% (10 2-cell embryos per 43 oocytes injected) with 1 live offspring born from transferring 10 embryos at 2-cell stage (Fig. 23K in circle). The IVF fertilization rates were 37.5% (163 2-cell embryos per 435 oocytes injected) and 89.3% (287 2-cell embryos per 342 oocytes injected). Total of 158 2-cell embryos were transferred into 5 pseudopregnant females and 46 live-born offspring were born as a result. Similarly, 172 4-cell embryos were transferred into 7 pseudopregnant females and 47 offspring were born. The offspring will be genotyped to assess Tex11 allele. Three male and three female offspring will be grown and bred to normal female mice to assess their fertility status and their offspring development and fertility.

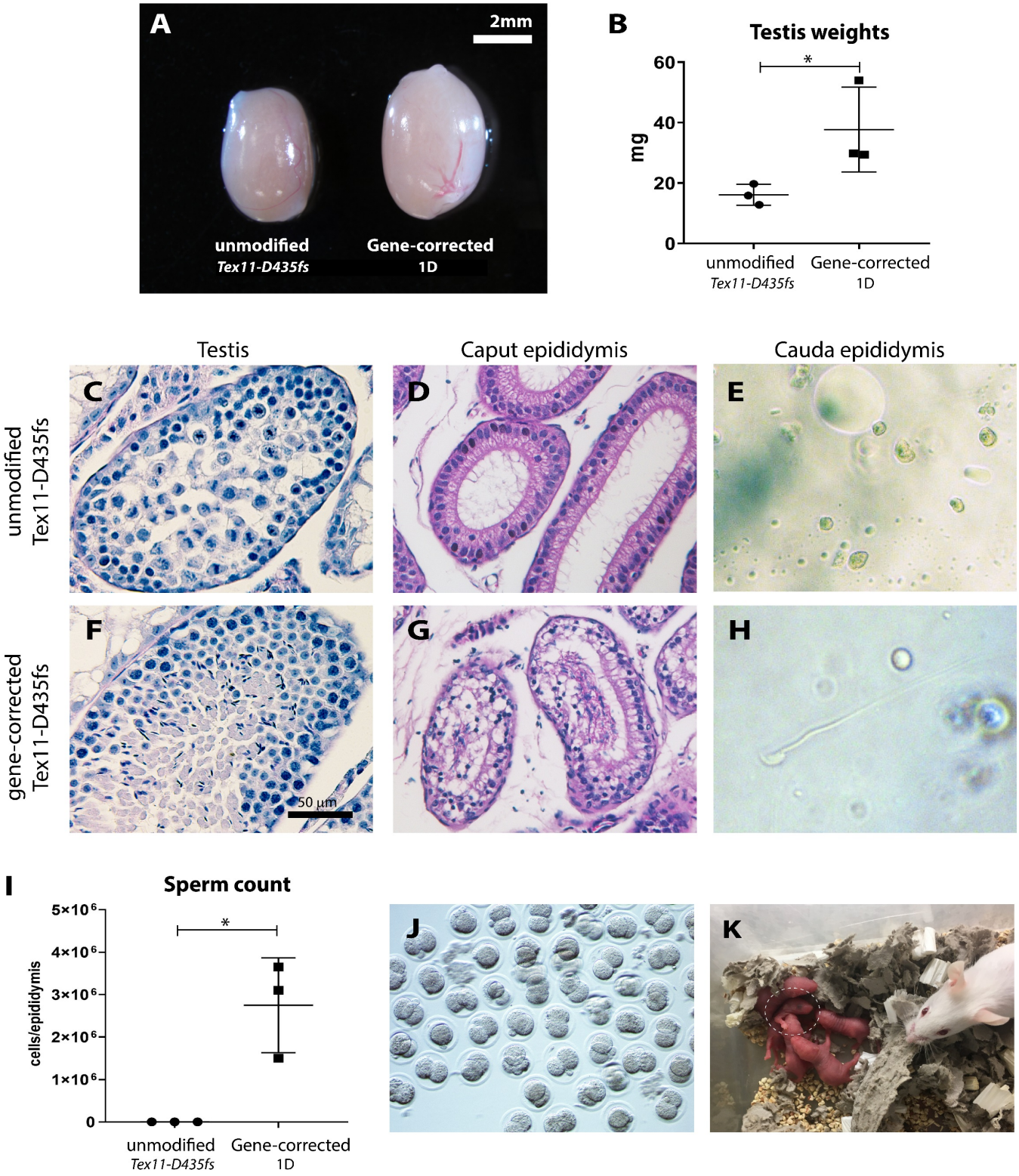

Figure 23 transplantation of gene-corrected 1D mSSC clone into germ cell-depleted W/Wv mice resulted in fertilizing -capable sperm

Macroscopic images of W/Wv testes transplanted with unmodified non-transfected *Tex11-D435fs* mSSCs versus the contralateral side that were transplanted with the gene-corrected 1D mSSC clone (A). Testis weights were quantified from the 3 animals (B). Histology with H&E staining for testis (C, F), caput epididymis (D, G). Triturated cell cells from cauda epididymis (E, H) under bright field. Sperm count per one cauda epididymis from gene-corrected 1D mSSC clone compared to the unmodified clone (I). Two-cell embryos from IVF using sperm from the side transplanted with 1D mSSC clone (J) were transferred to pseudopregnant femailes and produced live offspring (K).

5.4 Discussion

In this study, a new mouse model of human azoospermia with a *Tex11-D435fs* mutation was generated. *Tex11-D435fs* males exhibited NOA with a maturation arrest phenotype and no sperm were observed in the testis or the head or tail of the epididymis. Breeding with wild-type females confirmed that Tex11-D435fs mice were infertile. Histological analysis of *Tex11-D435fs* mouse testes revealed that germ cell maturation arrest occurred at the spermatocyte stage, which corresponds to the phenotype found in the human patient [130]. Conversion of the mutant sequence to the sequence that is common in wild type mice using CRISPR/Cas9-mediated germline gene editing released the maturation arrest and complete spermatogenesis ensued. Thus, I concluded that *Tex11-D435fs* is causative for azoospermia with maturation arrest phenotype in mice and men.

The purpose of this study was to demonstrate that ex vivo CRISPR/Cas9 gene editing followed by transplantation of spermatogonial stem cells (SSCs) is an effective and safe way to treat male infertility. Tex11-D435fs is a good model to test this approach because with maturation arrest at the spermatocyte stage, mutant mice have SSCs in their testes. This phenotype also created a challenge because all SSC niches were occupied by resident germ cells. Therefore, similar to bone marrow transplantation, an ablative chemotherapy treatment was needed to remove

endogenous germ cells and create space for engraftment of gene-corrected SSCs. Systemic chemotherapy treatments have myriad side effects that must be managed clinically by a combination of dose optimization, palliative treatments and treatments of symptoms (e.g., anemia, leukopenia, gut flora support, etc) [311]. In the current study, we found that treatment of Tex11-D435fs mice with 32 mg/kg busulfan eliminated most or all endogenous germ cells and did not require additional supportive treatments. For future clinical application, targeted radiation of the testis is an alternative approach to remove endogenous germ cells that would avoid some of the systemic side effects [312, 313].

Mouse SSC culture is well established and was critical to the success of this study [276, 310]. Most reports on the clinical application of germline gene editing focus on the editing of zygotes [314-316], which can have varied and unpredictable outcomes, including no edit, one allele with correct edit, two alleles with correct edit, one or two alleles with incorrect edits (insertions/deletions), heterozygous edits and mosaic edits. There are only a limited number of zygotes available per cycle, so few chances to get the correct edit(s). Screening embryos prior to transfer would be indirect via trophectoderm biopsy followed by preimplantation genetic diagnosis (PGD). In, contrast, SSCs grow in colonies that can be picked, expanded clonally and subjected to genomic analyses to characterize on-target and off-target edits before transplantation. The number of clones that can be analyzed is virtually unlimited and mosaicism is not an issue because fertilization is from a single sperm.

The potential for off-target editing by CRISPR/Cas9 can occur in regions with similar sequence to the sgRNA. The tolerance for mis-match can be up to 3-5 nucleotides, especially in sequences further away from the PAM sequence [130]. In germline gene therapy, it is important to confirm accurate editing at the target locus and fully characterize off-target editing events. I use

next-generation whole genome sequencing to compare the sequence between the original unmodified sequence and the gene-corrected clone. This experiment is underway.

Many labs have reported progress with human SSC culture (reviewed in [317]) but so far it has been difficult to identify conditions to maintain and expand hSSCs that can be independently replicated among laboratories. If human SSC cultures cannot be established, in vitro germ cell technologies may provide an alternative. I describe this approach in Chapter 5.

5.5 Conclusion

There are important ethical, legal and society concerns about the safety, feasibility, and appropriate applications of germline gene editing. Leading societies recommend that clinical application of germline gene editing should be approached with caution and within a robust regulatory framework and only after safety and feasibility have been established. Selection of diseases that would be most appropriate targets of germline gene editing will be a challenge. For germ cell mutations that cause NOA, germline gene editing is the only approach to cure. I demonstrated that germline gene editing to treat NOA is feasible by converting a mutant Tex11 sequence to a sequence that is common in the wild type population. Recipients produced sperm that were competent to fertilize wild type oocytes with or without transmission of the genetic modification to offspring. Offspring will carry the original mutation and/or wild type sequence meaning that the approach is essentially without footprint. It is important to fully characterize any off-target edits and those experiments are underway.

5.6 Acknowledgements

Chatchanan Doungkamchan planned and carried out gene therapy experiments and prepared the manuscript. Kyle Orwig planned, advised, and prepare the manuscript. Emily Barnard performed immunohistochemistry and prepared the manuscript. Yi Sheng performed IVF/ICSI and advised on the experiments. Meena Sukhwani treated the recipients with Busulfan and transplanted SSCs into the recipients. Sarah Steimer performed fertility assessment, animal breeding and colony maintenance. Nijole Pollock designed sgRNAs for Tex11-D435fs for generating mouse model. Alexander Yatsenko advised on the project.

6.0 Germline gene therapy in an azoospermic mouse model with a large deletion without germline transmission

6.1 Introduction

Genetic defects, such as large deletions, are commonly identified diseases caused by defects in single genes, including azoospermia. One such instance of this, a 99-kb large deletion in *Tex11*, was observed in two instances among fifteen unrelated, idiopathic NOA cases screened by array Comparative Genomic Hybridization (aCGH), for a total of 13.3 % (2/15) of cases screened in the initial study [76]. As mentioned previously, successful germline gene therapy without a footprint may be possible in cases with small mutations; however, this approach is much less efficient for large deletions. With large deletions, the genetic information needed for the transgene cassette becomes larger as well, minimizing the efficiency of homologous recombination [318, 319]. Compared to a HR efficiency of approximately 20% when using ssODN shorter than 200 bp [320], long DNA donor templates result in an efficiency as low as 5% when the donor size is 8 kb, including homology arms [321]. These numbers were produced from studies performed in cell lines or pluripotent stem cell lines, where the transfection efficiency is much higher than in mSSCs. When the efficiency is too low, it is not possible to screen colonies without selection markers. For this reason, transgenes with selection cassettes are required for gene therapy in large deletion cases.

The idea of gene therapy in the germline is highly controversial in the scientific community and society in general. The main reason is for fear that transgenes may cause unknown interactions with the genome, possibly causing deleterious effects on embryonic development and

future health [187]. In this study, I proposed an approach to restore expression using a transgene cassette to restore spermatogenesis in Sohlh1 KO mice with a large deletion, without transgene transmission to the next generation.

6.2 Materials and methods

6.2.1 **Animal**

Animals were bred and housed in the animal facility at Magee-Womens Research Institute. All study procedures were approved by the Institutional Animal Care and Use Committee of the University of Pittsburgh and Magee-Womens Research Institute. Procedures performed were in accordance with the NIH Guide for the Care and Use of Laboratory Animals (Assurance # 3654-01). Sohlh1-heterozygous animals were gifts from Dr. Rajkovic. Heterozygous females were bred to DBA/2 males for 5-6 generations to obtain Sohlh1-KO mice with DBA/2 background. Once the DBA/2 background was achieved, the colony was maintained by breeding heterozygous males with heterozygous females.

6.2.2 **Donor template plasmid construction**

PUC 19 plasmid was used as a backbone for making PGK-Puromycin-T2A-mCherry-sv40polyA fragment. PCR was performed to amplify PGK-Puromycin and mCherry-sv40polyA fragments separately. The fragments were ligated into pUC19 plasmid with GeneArt Seamless assembly kit (Invitrogen). The positive colonies were confirmed by sequencing. Then, the Sohlh1-

cDNA was amplified from a Sohlh1-cDNA plasmid and was ligated into an pU6-(BbsI) CBh-Cas9-T2A-BFP-P2A-Ad4E4orf6 plasmid (Addgene #64220). The plasmid 64220 with Sohlh1 cDNA was then digested with NheI and AflII to yield Sohlh1 cDNA-P2A fragment. PUC19-PGK-Puromycin-T2A-mCherry was amplified by PCR and digested with NheI and AflII and was used for ligation with the digested Sohlh1-cDNA-P2A. The positive colonies which now contained PGK-Puromycin-T2A-Sohlh1 cDNA-P2A-mCherry-sv40polyA, was amplified by PCR with primers bearing recognition site for PmeI on the 5' end and SalI on the 3' end. The PCR amplicon was digested with PmeI and SalI enzymes and was used to ligate with a plasmid with Rosa26 homology arm pDonor MCS Rosa26 that was digested with the same enzyme (Addgene #37200). The final plasmid was sent to confirm the sequence by Sanger sequencing. The plasmid was digested with SapI /KpnI to linearize the plasmid before use as a donor DNA template.

6.2.3 **Immunohistochemistry**

Tissue for immunofluorescence staining was fixed overnight in 4% paraformaldehyde (PFA) followed by washes with 1x PBS every hour for 4 hours. For H&E staining, the tissues were fixed in Buins solution overnight followed by several washes in 70% ethanol. The fixed tissue was sent to Magee-Women's Research Institute Histology Core for paraffin embedding, sectioning and H&E staining. The sections that were fixed with 4% PFA were then used for immunohistochemistry as previously described in Chapter 4.2. Briefly, the sections were deparaffinized in xylene and rehydrated in ethanol solution at decreasing concentrations. Sections were then boiled in Citrate antigen retrieval buffer for 30 minutes, after which they were washed with 1x PBS and blocked with blocking buffer for at least 4 hours before incubating with primary antibody overnight at 4^{o}C. After primary antibody incubation, sections were washed and

incubated in secondary antibody for 1 hour. Sections were subsequently washed and mounted with Vectashield mounting medium containing DAPI for nuclear visualization. The concentration of primary and secondary antibodies can be found in Appendix table 1.

6.2.4 **Spermatogonial stem cell culture**

The protocol to establish an SSC culture is described and was followed with some modification. In brief, testes from genotyped *Sohlh1-KO* 6-9 day-old mouse pups were removed. The tunica was subsequently removed, and the testes were digested with 0.25% trypsin and 1.2% w/v DNaseI. The reaction was stopped with knockout serum replacement (KOSR). Percoll separation was performed to separate germ cells from somatic cells and debris and pelleted. The pellet was incubated with Thy1-antibody coated antibody beads for 1 hour, washed, and separated via MACS column. The Thy1-positive testicular cells were pelleted, washed and then plated on Mouse Embryonic Fibroblast (MEF) feeder cells. The mSSCs were cultured for 4-6 passages before being used for gene targeting to remove any remaining testicular somatic cells. The media used for mSSC culture was IMDM/SFM supplemented with Synthechol (Sigma), human GDNF (Preprotech), and human bFGF (Preprotech).

6.2.5 **Gene targeting**

Mouse spermatogonial stem cells were dissociated with 0.05% Trypsin. The digestion was stopped with KOSR and the SSCs were washed with plain IMDM media. The SSCs were counted and plated at 1 million cells per a well on MEFs on a 6-well plate coated with 0.1% gelatin. The following day, transfection performed using lipofectamine STEM reagent according to

manufacturer's protocol with modifications. Five hundred micrograms of each plasmid (sgRosa26-60 and -65) and 2 μg of donor template were used. All DNA components were mixed in 50 uL of Opti-MEM, and 10 uL of Lipofectamine were mixed with 40 μL of Opti-MEM in a separate tube. Each tube was mixed and allowed to sit for 3 minutes. The DNA mix was transferred into the Lipofectamine tube, mixed, and incubated at room temperature for 20 minutes. While incubating, the mSSCs were washed with plain IMDM once and 1 mL of plain IMDM was put into each well. Then the DNA/Lipofectamine mix was added into the well dropwise and incubated for 5 hours. The well was washed with plain IMDM once and replaced with full IMDM/SFM media supplemented with GDNF, bFGF, and synthechol.

6.2.6 **Colony selection and expansion**

Approximately 7-10 days post-transfection, transfected wells were dissociated with Trypsin and plated into a new 6-well plate at 200,000 cells/well. When transferred to a new plate, puromycin was added to the media at a final concentration of 0.15 mM. The transfected SSCs were cultured in puromycin media for 10-14 days. Puromycin-resistant colonies were then picked and transferred to a 96-well plate coated with MEF. Seven to ten days after colony selection, colonies were picked for colony genotyping. DNA from single colonies were amplified using a Repli-G whole genome amplification kit for PCR genotyping. The clones that were positive via PCR screening were selected for expansion and propagated for confirmation tests and transplantation.

6.2.7 **Colony PCR**

There are three pairs of primers used to assess insertion into the Rosa26 locus. The primer that detects the 5' site of insertion starts at the Rosa26 region outside of the homology arm (Rosa26 P1 Fwd), while the reverse primer starts at the PGK promoter (PGK RV1). The primer pair to detect 3' site of insertion uses a forward primer from the mCherry sequence (mCherry 3P Fwd2), while the reverse primer binds to the outside region of the homology arm (Rosa26 P2). The Rosa26 surveyor F and R primers are used as DNA quality control primers and were used to distinguish WT from the inserted allele. The PCR was done using LongAmp buffer. The PCR conditions were as follows: 95°C for 10 minutes, 30 cycles of 95°C for 20 seconds, annealing temperature for 20 seconds (56.9°C for Rosa26 P1+PGK RV1, 56.4°C for mCherry 3P Fwd2+ Rosa26 P2, and 59.3°C for Rosa26 surveyor F and R), 72°C for 30 seconds, then a final extension of 72°C for 10 minutes. The amplicons were visualized on 1.5% agarose gel and ethidium bromide. The clones that were positive for PCR at both the 5' and 3' insertions were confirmed with Sanger sequencing. Primer sequences can be found in Appendix B.

6.2.8 **Mouse SSC Transplantation**

The gene-corrected mSSCs were blown off of the feeder layers and digested briefly in 0.05% trypsin. The reaction was stopped by KOSR, after which cells were washed with 1x PBS. The cells were counted and resuspended in IMDM/SFM medium with 10% trypan blue at 20 million cells/mL as described in the previous section. The cells were injected into the testis of recipient mice via the efferent ductules at 3.5 uL. The *Sohlh1-KO* recipient mice were treated with Bulsulfan at 6 weeks old at 44 mg/kg. The Bulsulfan-treated *Sohlh1-KO* mice were used as

recipients for transplantation at 4 weeks post- Bulsulfan treatment. The assessment of engraftment and spermatogenesis was performed 4.5-5 months after transplantation.

6.3 Results

6.3.1 *Sohlh1-KO* testis showed maturation arrest phenotype at undifferentiated spermatogonia

To confirm the phenotype of *Sohlh1-KO* male mice, I stained testicular cross sections from *Sohlh1-KO* testis with Sohlh1 antibody. No Sohlh1-positive cells were observed in the seminiferous cross sections of *Sohlh1-KO* mice compared to wild-type (Fig. 24G, J). H&E staining was used to assess histology. In *Sohlh1-KO* testis, only a single layer of germ cells on the basement membrane was observed with no spermatocytes, spermatids or sperm (Fig. 24C), whereas, normal-appearing seminiferous tubules with sperm in the lumen was observed in *Sohlh1*$^{-/+}$ testis (Fig. 24A, B). Immunohistochemistry for VASA showed multiple layers of germ cells in both *Sohlh1*$^{-/+}$ and wild-type testes (Fig. 24D, E), whereas, rare VASA-positive germ cells are seen on the basement membrane of Sohlh1-KO testis (Fig. 24F). Immunohistochemistry showed no positive cells for STRA8, which is a marker for differentiated spermatogonia in *Sohlh1-KO* testis (Fig. 24I, L). On the contrary, Sall4-positive undifferentiated spermatogonia were still visible on the basement membrane of *Sohlh1-KO* testis (Fig. 24H, K). This confirmed a maturation arrest phenotype at the undifferentiated spermatogonia stage in the *Sohlh1-KO* mouse model used in this study. More importantly, the result suggested that spermatogonial stem cell (SSCs) culture can be established from residual undifferentiated spermatogonia present in the testis of *Sohlh1-KO* testes.

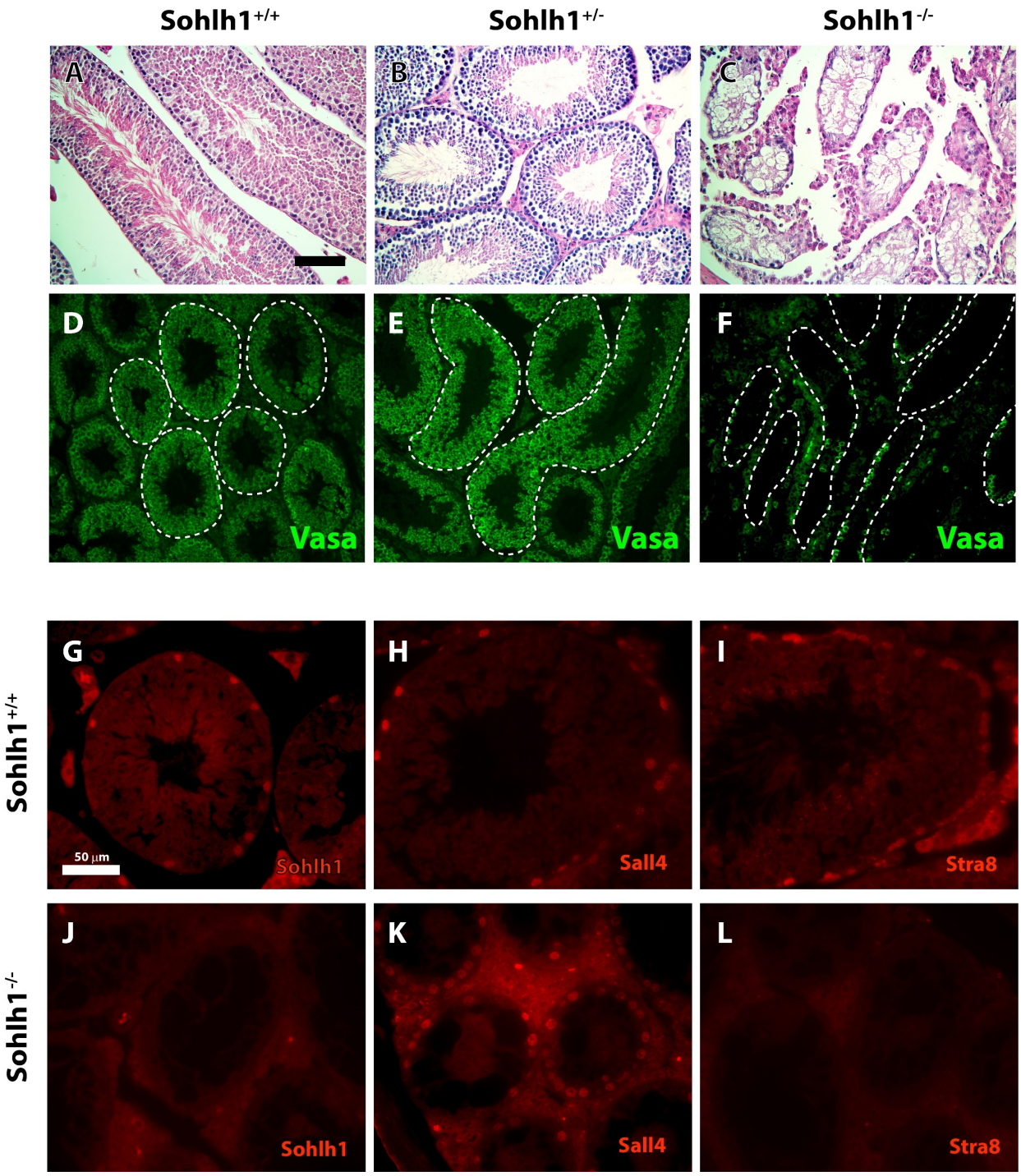

Figure 24 Characterization of *Sohlh1-KO* mouse that were used for gene therapy.

Histology (H&E staining) for testis cross section from Sohlh1+/+ (A), Sohlh1+/- (B) and Sohlh1-/- (C). Immunohistochemistry for VASA, pan-germ cell marker (D-F). Immunohistochemistry for Sohlh1 (G, J), for Sall4 (H, K) and Stra8 (I, L). *scale bar = 50 μm*

6.3.2 **Gene targeting in Sohlh1-KO mSSCs**

SgRNA was designed with Feng Zhang's laboratory platform at CRISPR.mit.edu. Three sgRNAs, sgRNA-Rosa26-45, 60 and 65 were ligated into pENTR-Cas9-EGFP plasmids (Fig. 25B) and tested in Neuro2A cells for efficiency to create DSBs. All sgRNA showed similar DSB efficiency by T7E1 assay (Fig. 25C). The donor template comprised approximately 1 kb of both homology arms flanking both sides. The cassette consisted of PGK-Puromycin-T2A-Sohlh1 cDNA-P2A-mCherry. The plasmid construct was tested in Neuro2A cells. mCherry-positive Neuro2A cells were observed, showing in-frame sequence until mCherry, the most distal part of the cassette (Fig. 25D). Sanger sequencing was done to confirm the cassette sequence. The total length, including homology arms, was 5.5 kb. The sgRNA-Rosa26-45, 60 and 65 and donor templates were used in different combinations to transfect Neuro2A cells to determine the optimal grouping for gene editing. All combinations were shown to result in desired insertion at the Rosa26 locus; however, I chose to proceed with the condition with sgRNA-Rosa26 -60, -65, and the donor template (Fig. 25E), which was used for *Sohlh1-KO* mSSCs transfection.

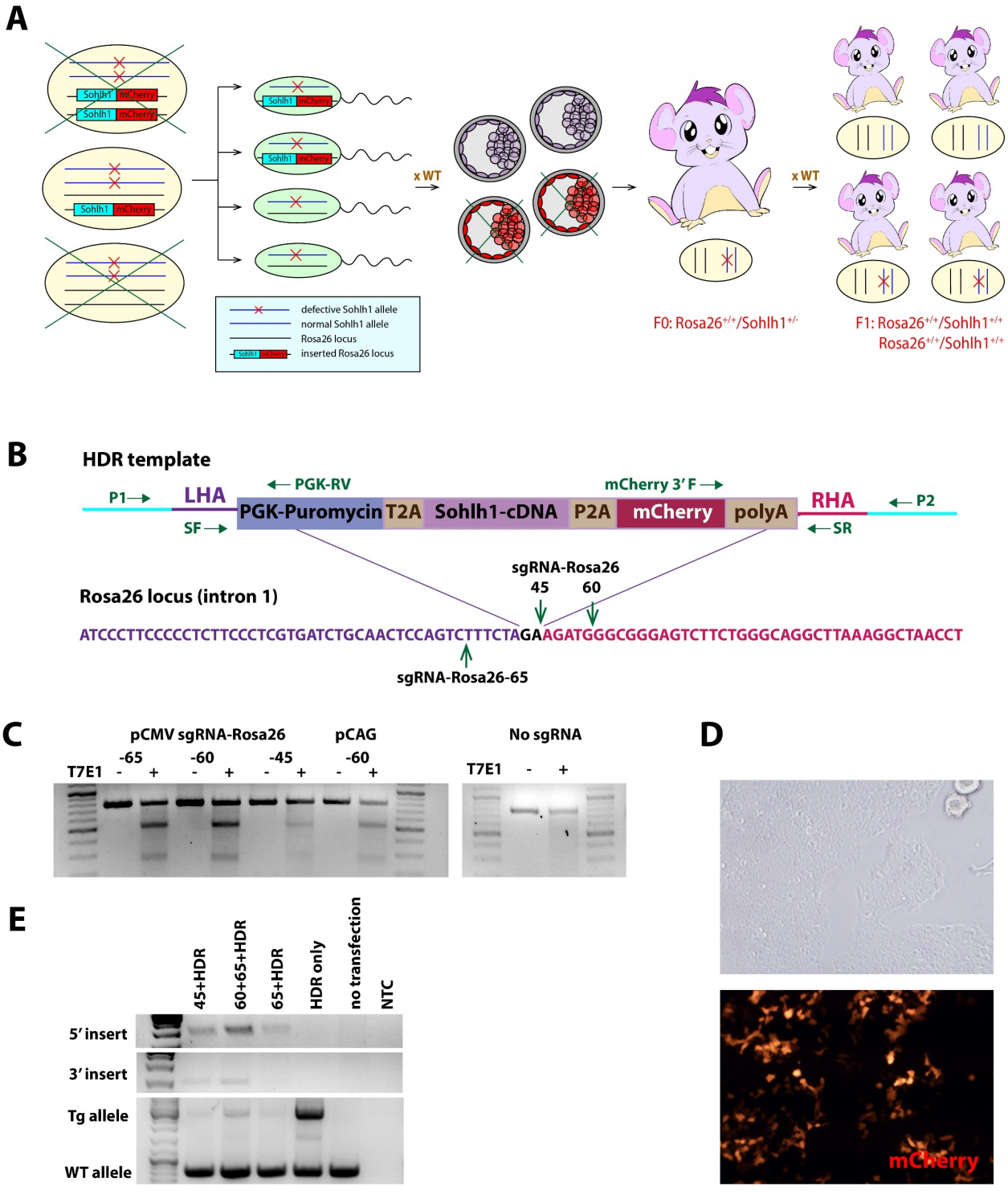

Figure 25 Gene targeting in a model with a large deletion.

Diagram showing the possibility of using germline gene therapy for large deletions without germline transmission (A). Small guided RNAs and HDR template sequences targeting Rosa26 locus (B), T7E1 assay in Neuro2A cells (C),

Testing of donor plasmid expression in Neuro2A cells (D), Testing of sgRNAs/Donor template combination in Neuro2A cells for gene targeting in Sohlh1-KO mSSCs (E).

Seven to ten days post-transfection into *Sohlh1-KO* mSSCs, Puromycin selection was initiated at 0.15 μM for ten to fourteen days (Fig. 26A, B). Puromycin-positive colonies were picked and transferred to a 96 well plate for colony genotyping (Fig. 26C). Colony genotyping for insertion of the transgene at the Rosa26 locus utilized 2 pairs of primers to detect insertion at the 5' site (Rosa26 P1, PGK RV1) and at the 3' site (mCherry Fwd2, Rosa26 P2). Genotyping was performed for all Puromycin-resistant clones (Fig. 26D). The clones that were positive at both 5' and 3' insertion sites and were also positive for the WT allele of Rosa26 ($Rosa26^{Tg/WT}$) were expanded for transplantation (colony 1-7, Fig. 26D). Semi-quantitative PCR using mRNA as the PCR templates showed expression of Sohlh1 mRNA in gene-corrected clones 1-7 compared to unmodified KO, heterozygous and WT mSSC clones (Fig. 26E). No Reverse Transcriptase (RT) control samples were used to show that the amplification was not a result of residual DNA template (Fig. 26E). Transplantation was performed for clones 1 and 7. The animal will be sacrificed for sperm assessment at 5 months post-transplantation.

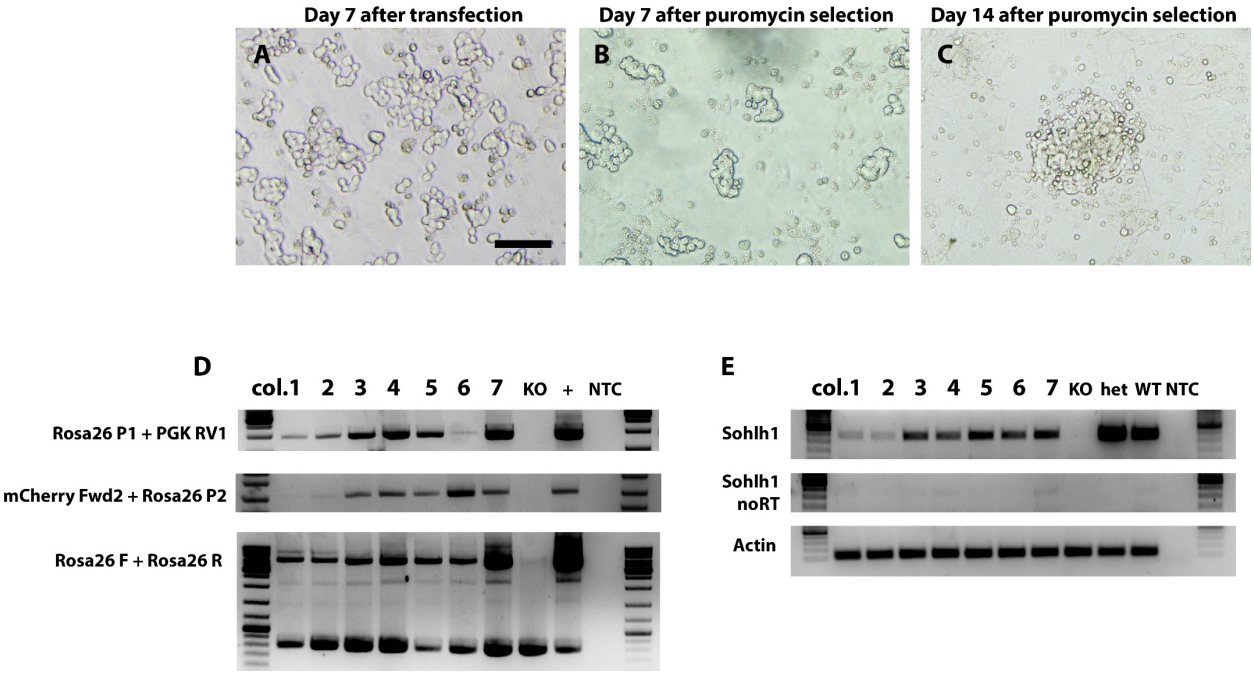

Figure 26 Gene targeting at Rosa26 locus in *Sohlh1-KO* mSSCs

Sohlh1-KO mSSCs at 7 days after transfection with sgRNA plasmids, DNA donor template (A), at 7 days (B) and 14 days (C) after 0.15 μM Puromycin selection. PCR genotyping for Puromycin-resistant clones (D). Quantitative PCR for *Sohlh1* mRNA in Puromycin-resistant clones (E). *Sohlh1* no RT=*Sohlh1* mRNA template with noRT in the cDNA conversion reaction, used as a control for residual genomic DNA.

6.3.3 *Sohlh1-KO* recipient mice required Bulsulfan treatment prior to transplantation

Although *Sohlh1-KO* testis have rare germ cells, there were no engraftments following transplantation with CAG-EGFP mSSCs (Fig. 27A-H). I hypothesized that the niche on the basement membrane was fully occupied by Sohlh1-deficient undifferentiated spermatogonia. *Sohlh1*$^{-/+}$ mice were subsequently treated with varying dosages of Bulsulfan (38, 44, 46 mg/kg) to remove residual germ cells. Mice were unable to tolerate 46 mg/kg, whereas one of the four mice treated with the lowest dose still produced offspring. *Sohlh1*$^{-/-}$ mice were treated with 44 mg/kg Bulsulfan, after which depletion of VASA-positive *Sohlh1*-deficient germ cells was seen (Fig. 27I-

P). When transplanted with WT GFP-mSSCs, Bulsulfan-treated *Sohlh1-KO* showed successful engraftment of GFP-positive colonies and full spermatogenesis (Fig. 27K-P).

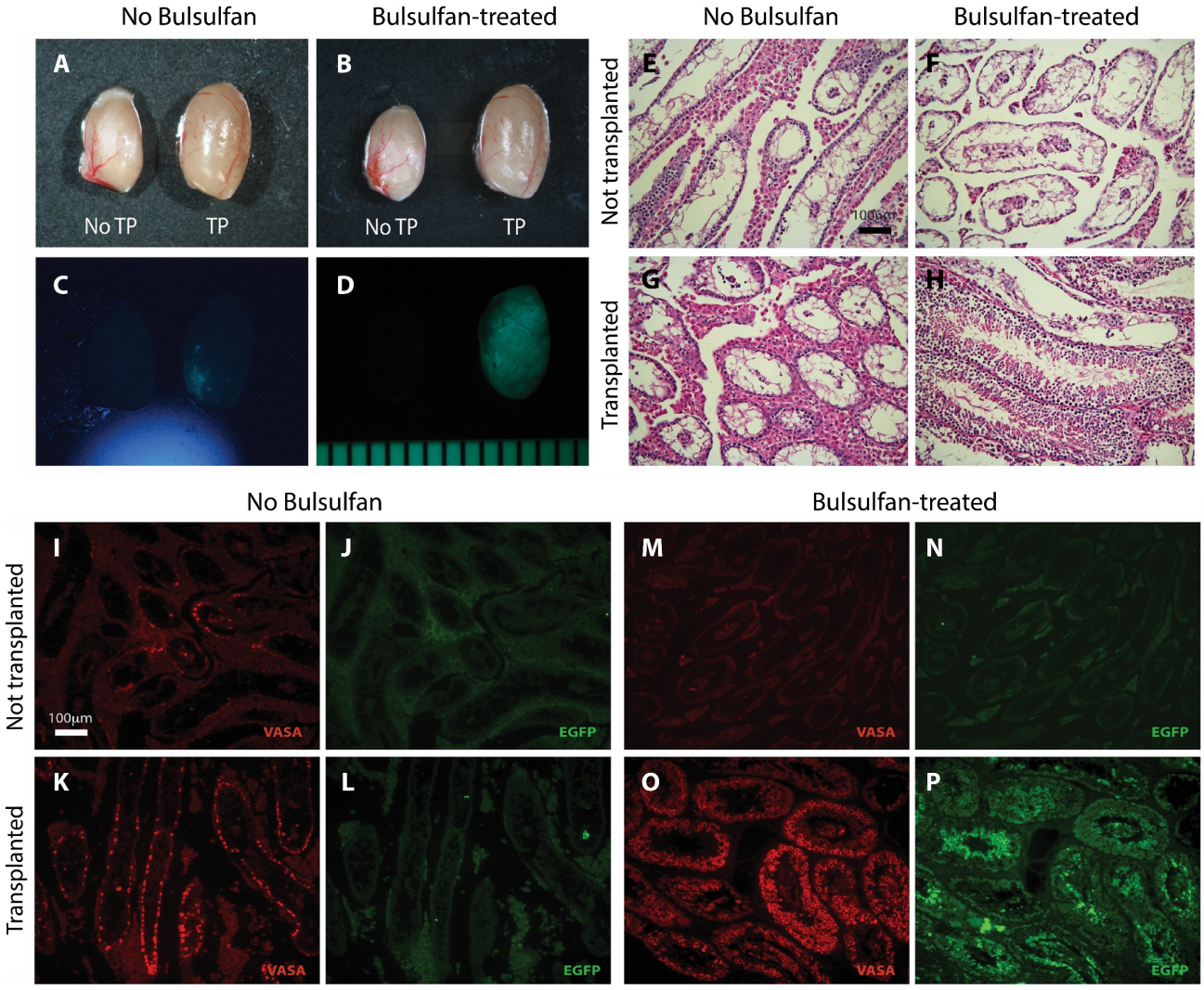

Figure 27 Transplantation of CAG-EGFP mSSCs into Sohlh1-KO recipients, with or without 44 mg/kg Bulsulfan treatment

Gross picture of *Sohlh1-KO* testis not treated with Bulsulfan, with and without transplantation with CAG-EGFP mSSCs (A), *Sohlh1-KO* testis treated with Bulsulfan, with and without transplantation with CAG-EGFP mSSCs (B). *TP =transplantation.* Histology with H&E of the seminiferous tubules from *Sohlh1-KO* mice transplanted with CAG-EGFP mSSCs with or without Bulsulfan treatment (E-H). Immunohistochemistry for VASA and EGFP in Sohlh1-KO recipients not treated (I-L) or treated with Bulsulfan (M-P) with and without transplantation.

6.4 Discussion

In this study, I showed that it is possible to insert a large therapeutic transgene with antibiotic selection cassette in a "Safe Harbor" Rosa26 locus of mouse SSCs. I identified SSCs with one WT Rosa26 allele and one Rosa26 allele containing transgene expressing a functional Sohlh1 cDNA and a puromycin resistance cassette ($Rosa26^{Tg/WT}$) and confirmed expression of Sohlh1 mRNA. Finally, I optimized busulfan treatment conditions to remove endogenous germ cells from Sohlh1 KO mouse testes and create space for engraftment transplanted SSCs. This progress lays the foundation for future studies to transplant $Sohlh1^{Tg/WT}$ SSCs into busulfan-treated Sohlh1 KO infertile males.

Similar to the previous chapter, this study raises concerns about germline gene editing and potential for transfer of on-target or off-target edits and/or foreign DNA to the next generation. In future studies, I would plan to use Southern blot and/or whole genome sequencing to screen for clones with random insertion of the transgene or for other off-target insertions or deletions. Using my experimental design with heterozygous expression of the therapeutic transgene in SSCs, I expect that half of the sperm from gene-corrected transplanted cells will be transgenic (Sohlh1-, Rosa26Tg), whereas the other half will be WT and transgene-free at the Rosa26 locus (Sohlh1-, Rosa26WT) (Fig. 29A, column 2). Consequently, when fertilizing WT female gametes, half of the resultant embryos will be transgene-free (Fig. 2A, column 3). In the clinic, prenatal genetic diagnosis (PGD) could then be used to select against transgene-positive embryos so that only transgene-free embryos (Sohlh1-/+, Rosa26WT/WT) are used. The resultant offspring would be 100% heterozygous Sohlh1, because they will inherit a functional copy of Sohlh1 from their mothers, and WT at the Rosa26 locus (Sohlh1-/+, Rosa26WT/WT) and they will be fertile (Fig. 29A, columns 4 and 5). Using this approach, it is theoretically possible to correct the infertile

phenotype in the patient and progeny will be fertile even without transgene transmission because they will inherit a functional copy of the transgene from their mothers.

The other concern with this approach was the promoter used to drive gene expression, as a silenced or overactive promoter could disrupt spermatogenesis. In this study, I chose the PGK promoter because 1) it was shown in a previous study to successfully drive gene expression in mSSC culture [322] and 2) the size is small compared to other ubiquitous promoters, such as CAG [323], which decreases overall template DNA size, and thus increasing the chance for more efficient transfection. In this study, Puromycin-resistant clones emerged after 10-14 days of Puromycin selection, indicating that there was transgene integration into the genome and PGK successfully drove the expression of the Puromycin-resistance gene. However, I did not observe mCherry-positive clones, possibly because the copy number of mCherry protein was too low, and thus too dim, to be seen under the microscope. To assess expression level of the cassette, I used quantitative PCR to quantify *Sohlh1* mRNA expression and found that *Sohlh1* mRNA was detectable in gene-corrected clones compared to the unmodified clone, indicating activity of the PGK promoter. Optimization of Western blot to detect the expression of the cassette at protein level is underway.

Because expression of Sohlh1 is limited to undifferentiated spermatogonia, there is a concern that expression in another germ cell types driven by the PGK promoter or even abnormal expression level in the appropriate germ cells may disrupt spermatogenesis. However, previous studies showed that the *Sohlh1-KO* maturation arrest phenotype can be rescued when the Sohlh1-mCherry transgene was driven by the strong, ubiquitous CAG promoter expressed outside of *Sohlh1* locus [324]. CAG is a ubiquitous promoter with high expression activity in germ cells. The only difference between CAG and PGK is that PGK is not as strong promoter as CAG [325], which

could pose a problem. If PGK driven Sohlh1 clones do not regenerate spermatogenesis, I would consider using the CAG promoter.

6.5 Conclusion

Avoiding germline transmission when performing gene therapy for azoospermia due to large deletions may appear impossible, as a transgene selection cassette is an essential component for gene therapy; however, in this study, I proposed a method for germline gene therapy that avoids germline transmission when combined with PGD for selection of unmodified embryos. Off-target assessment by whole genome sequencing is underway. Assessment of spermatogenesis will be performed at 5 months post-transplantation. If spermatogenesis is restored, IVF/ICSI/PGD will be completed to confirm fertility and embryo viability.

6.6 Acknowledgements

Chatchanan Doungkamchan planned, performed the experiments, and prepared the manuscript. Kyle E. Orwig planned, advised, and prepared the manuscript. Yi Sheng performed ICSI/IVF and advised on experiments. Meena Sukhwani transplanted mSSCs and treated the Sohlh1-KO with Bulsulfan. Sarah Steimer performed fertility assessment, bred animals, and maintained the animal colony.

7.0 Gene therapy approach for azoospermia with Sertoli cell-only syndrome through iPSCs and PGCLC differentiation

7.1 Introduction

In previous chapters, I have shown different approaches to gene therapy in Sertoli cells and germ cells, which are the cells from which the defect originates. Fixing the mutation inside defective cells seems reasonable; however, as mentioned in an earlier chapter, 30-40% of azoospermic cases present as Sertoli cell-only syndrome, in which no germ cells are seen in testicular tissue (Chapter 2). Additionally, culture techniques for human spermatogonia are still not robust [326-329]. In this chapter, I propose an approach to germline gene therapy through induced pluripotent stem cells (iPSCs) [330] to circumvent the current limitations surrounding human spermatogonial culturing and the cases with no germ cells to culture, edit or serve as a source of spermatogenesis.

It is possible to produce patient-specific iPSCs from a skin biopsy or blood sample. Methods to culture and gene edit human iPSCs are already well-established. Therefore, an infertility-associated mutation in patient iPSCs could be corrected with CRISPR/Cas9 gene editing, clonally expanded and then sequentially differentiated to Epiblast-like cells (EpiLCs) and primordial germ cell-like cells (PGCLCs) [165, 166, 331]. Gene-corrected PGCLCs could then be transplanted into patient testes for regeneration of spermatogenesis, as previously described for mice [163].

In this chapter, I demonstrate this approach in *Sohlh1*-KO mice, the same model used in the previous chapter. I derived iPSCs from testicular fibroblasts of *Sohlh1*-KO mice which were

then used for gene-targeting. To demonstrate the feasibility of PGCLC derivation from iPSCs, I tested this PGCLC protocol in Lentivirus-derived wild-type (WT) iPSCs, that were derived from the MEF of WT male mice [332]. PGCLCs were then transplanted into the testes of busulfan-treated nude mice, and sperm were recovered three months later for IVF/ICSI. PCR was used to distinguish the origin of sperm from either the nude recipient or from the PGCLCs. I found that 1 out of 8 embryos were WT, meaning that the sperm was not from the nude mice recipients. This showed that iPSCS can be derived from testicular fibroblasts, gene-edited, and then induced into sperm-producing PGCLCs.

7.2 Materials and methods

7.2.1 **Fibroblasts derivation from testes**

Testes were retrieved from 6-9-day-old Sohlh1-KO pups. The tunica albuginea was removed, and the testes were digested with 0.25% Trypsin and 1.2% w/v DnaseI. The digestion was stopped with KOSR. The suspension of testicular cells was then separated using Percoll solution. The resultant pellet was then incubated with Thy1-antibody-coated beads for 1 hour to enrich for undifferentiated germ cells. The pellet was washed and was fractionated through a MACS column. The cells that ran through the column (Thy1-negative, non-germ cells) were collected, pelleted, and resuspend with 15% FBS in DMEM media for fibroblast culturing. The fibroblasts were then used for iPSC transformation after 3-4 passages.

7.2.2 **iPSC derivation**

Induced pluripotent stem cells were derived by 2 different methods: 1) Lentivirus, which resulted in integration of genetic materials OSKM (Oct4, Sox2, Klf4, Myc) [330] into the genome, and 2) Sendai virus, which resulted in no integration of OSKM factors into the genome. Lentivirus was made using the lentivirus OSKM plasmid (addgene#20328) [333] and was used to infect MEF feeder cells at a MOI of 50. Three days after colonies started to form, individual colonies were selected and expanded. Characterization of iPSCs for pluripotency was done around passages 6-10. For Sendai virus, commercially available Cytotune V.2.1 Sendai virus kit (Invitrogen) was used to transform WT MEF and testicular cells derived from Sohlh1-KO testis according to the manufacturer's protocol.

7.2.3 **iPSC culture maintenance**

iPSCs were maintained on MEF feeders in iPSC media (DMEM [Invitrogen] with 15% KSR, 0.1 mM Non-essential amino acids (NEAA), 1 mM sodium pyruvate, 0.1 mM 2-mercaptoethanol,100 U/ml penicillin, 0.1 mg/ml streptomycin, and 2 mM L-glutamine) supplemented with LIF (1000 u/ml). The media was changed daily, and cells were passaged every 2-4 days [332].

7.2.4 **Colony staining for pluripotency markers**

Putative iPSC colonies were tested for pluripotency markers alkaline phosphatase (SCR0004, Millipore, Germany) Oct-4, Sox2, DPPA-4 and SSEA-1 (SCR007, Millipore,

Germany). Staining was performed according to the manufacturer's protocol with each marker in a 96-well plate.

7.2.5 **Teratoma assay**

After being tested for pluripotency markers, putative iPSCs were digested with TrypLExpress enzyme (Gibco) and washed with 1x PBS. Cells were resuspended at 1-2 million cells/mL, after which 15-30 μL were injected into the interstitial space of immune-deficient SCID mouse testes [334]. Three to four replicates were performed for each clone. After 6-8 weeks, tissues were collected and sent for histology at the Histology Core at Magee-Womens Research Institute for paraffin embedding, sectioning and Hematoxylin/Eosin staining. Tri-lineage differentiation to endodermal, mesodermal and ectodermal tissues was confirmed by a pathologist.

7.2.6 **Karyotyping**

Cells were plated at a concentration of 50,000 cells per well in a 6-well plate coated with matrigel. The cells were allowed to grow for one to two days until undifferentiated colonies were visible. The cells were dissociated by TrypLE enzyme, collected, and counted. One million cells were pelleted and sent to the mouse karyotyping laboratory at Magee-Women's Hospital. The G-banding was performed as previously described. The picture of chromosome spread was created using a Nikon microscope and Nikon Eclipse 2i software. Twenty chromosome spreads were taken per clone for evaluation of aneuploidy. Counting was completed using Nikon Eclipse A software.

7.2.7 **Gene targeting in iPSCS**

IPSCs were plated on Matrigel at 50,000 cells/well in a 6-well plate. iPSCs were grown until colonies formed, usually about one to two days. Cells were collected using TrypLE enzyme. The digestion was stopped with KOSR and cells were subsequently washed with 1x PBS. The second wash was performed with Opti-MEM media. The cells were counted and resuspended in Opti-MEM at 1,000,000 cells in 100 μL of Opti-MEM. Small-guided RNA and Cas9 protein were incubated for ten minutes, then the linearized donor template for Sohlh1 gene editing (described in chapter 4.3) was added to the mixture. The donor template/sgRNA/Cas9-RNPs was transferred into the cell suspension and to the cuvette. The mixture was electroporated at 125 V for 2.5 seconds. The cells were re-plated in MEF-coated plates with media changes daily. Visible colonies formed after 4-5 days. PCR reaction for the insertion allele was used for positive colony screening (explained in Chapter 4.3).

7.2.8 **EpiLC and PGCLC inductions**

PGCLC induction was performed as previously described. Briefly, iPSCs were grown and maintained in N2B27 medium with 2i (CHIR99021, 3mM: Stemgent; PD0325901, 0.4mM: Stemgent, San Diego, CA) and LIF (1000 u/mL) on mouse embryonic fibroblast (MEFs) feeders. Before EpiLC induction, iPSCs were dissociated with TrypLE, washed, and plated on a poly-L-ornithine (0.01%; Sigma) and laminin (10 ng/mL; BD Biosciences) coated dish to adapt cells to feeder-free conditions. After iPSCs adapted to feeder-free conditions, they were dissociated with TrypLE and plated in a 12-well plate coated with human plasma fibronectin (16.7mg/mL) at 100,000 cells/well in N2B27 medium containing activin A (20 ng/mL), bFGF (12 ng/mL), and

KOSR (1%). Media was changed daily. At day 3, PGCLC induction was initiated with EpiLCs dissociation via TrypLE. Cells were counted and then plated in a low-cell-binding U-bottom 96-well plate (NUNC) at 1,000 cells/well. Media was serum-free (GK15; GMEM [Invitrogen] containing 15% KSR, 0.1 mM NEAA, 1 mM sodium pyruvate, 0.1 mM 2-mercaptoethanol,100 U/ml penicillin, 0.1 mg/ml streptomycin, and 2 mM L-glutamine) in addition to cytokines BMP4 (500 ng/ml; R&D Systems), LIF (1000 u/ml; Invitrogen), SCF (100 ng/ml; R&D Systems), BMP8b (500 ng/ml; R&D Systems), and EGF (50 ng/ml; R&D Systems). Cells were incubated in these conditions for three to four days [163, 332].

7.2.9 **FACS**

After PGCLC induction, cell clumps were pooled and dissociated with TrypLE according to the protocol. Cells were washed with DMEM/F12 supplemented with 0.1% BSA and collected after centrifugation. The pellet was resuspended with anti-Integrin-β3 antibody (BioLegend) and anti-SSEA1 antibody (eBioscience) conjugated with PE and Alexa Fluor 647, respectively. After antibody incubation, cells were washed with 1x PBS supplemented with 0.1% BSA for FACS sorting. Negative control cells were unstained. Cells were sorted and analyzed on a flow cytometer (ARIA II; BD Biosciences). The double-positive cells were counted and resuspended in plain GMEM media with 10% Trypan blue at 20 million cells/mL for transplantation.

7.2.10 **Transplantation**

Cells were injected into the seminiferous tubules of nude mice at 3.5 uL per testis. Three months after injection, sperm were collected from the nude mice for ICSI. Eight embryos were collected for genotyping the following day.

7.2.11 **Genotyping of embryos**

The embryos were individually digested, and genomic DNA was amplified by PCR. PCR served to differentiate sperm origin between the nude mice and iPSCs (WT at nude locus). I used F1 and R1 to amplify the sequence common between WT and nude alleles, after which the amplicon was sent for Sanger sequencing for allele identification.

7.3 Results

7.3.1 **iPSCs were successfully derived from Wild-type and Sohlh1-KO testicular fibroblasts**

I tested two methods of iPSC derivations: 1) stable and 2) transient expression of OSKM (Oct-4, Sox2, Klf4, Myc) factors. For the stable expression approach, I used a Lentivirus harboring an OSKM plasmid to infect Mouse Embryonic Fibroblasts (MEF). For the transient OSKM expression transfection, I used the Sendai virus iPSC induction kit available commercially (Cytotune Sendai iPSCs V2.1, Invitrogen) to reprogram MEF and Sohlh1-KO testicular fibroblasts

according to the manufacturer's protocol. The resulting colonies were individually expanded and characterized by pluripotency and karyotyping.

7.3.2 **iPSCs tests for pluripotency**

Three clones from each cell type and reprogramming method (MEF-Lenti, MEF-Sendai, and Sohlh1-Sendai) were tested for pluripotency. Morphology of derived iPSCs showed round, packed and dome-like appearances (Fig. 28B), resembling that of mouse embryonic stem cells compared to non-reprogrammed fibroblasts from the same animal (Fig. 28A, B). Shown in Fig. 1A, B is a clone derived from Sohlh1-KO testicular fibroblast by Sendai virus (Sohlh1-Sendai), after which I performed in situ immunostaining for pluripotency markers (Alkaline phosphatase, SSEA1, Sox2, Oct4, Nanog and DPPA2). All pluripotency markers were positive for each of the nine derived iPSC clones (3 clones for MEF-Lenti, 3 for MEF-Snedai and 3 for Sohlh1-Sendai). Shown in Fig. 1C-H is a clone from MEF-Sendai derivation. Two clones from each derivation method were chosen for teratoma assay, the ultimate test for pluripotency, which assesses the ability of the cells to generate three germ layers. I found that all 6 clones (2 clones from MEF-Lenti, 2 from MEF-Sendai and 2 from Sohlh1-Sendai) could produce teratomas consisting of tissues from all three germ layers. Shown in Fig. 28I-K is the same clone from Solhlh1-Sendai with skeletal muscle, which represents mesodermal origin (Fig. 28I), neuronal tissue for ectoderm (Fig. 28J) and respiratory epithelium for endoderm (Fig. 28K). These three tests showed that iPSCs derived by each method retained their pluripotency. Next, I performed karyotyping by G-banding. Preliminary karyotyping showed 81.2% of tested Sohlh1-Sendai clone were euploid. Shown in fig. 28L-N are examples of karyotyping spreads from the aforementioned Sohlh1-Sendai clone.

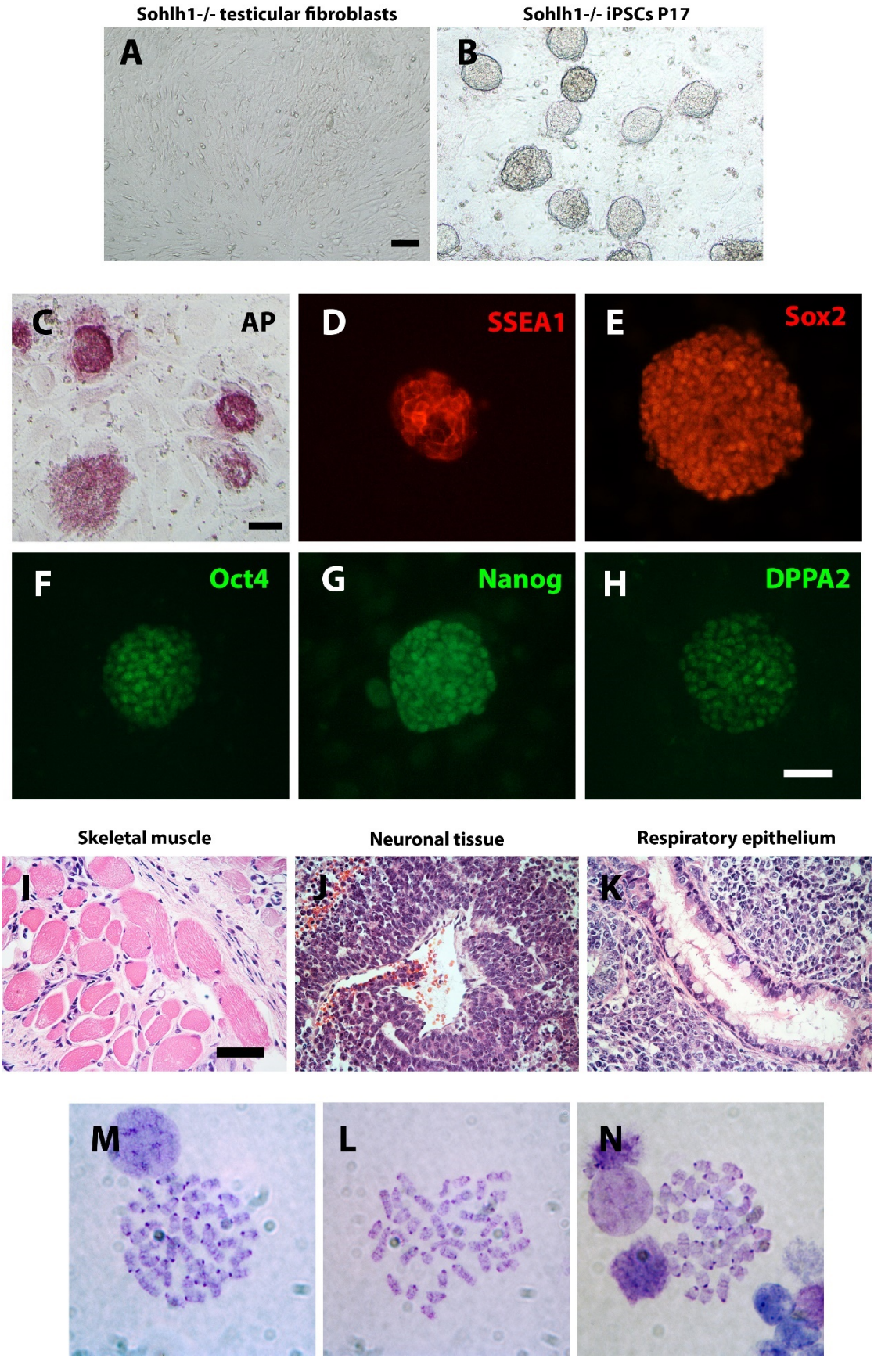
Sohlh1-/- testicular fibroblasts
Sohlh1-/- iPSCs P17
A
B
C
AP
D
SSEA1
E
Sox2
F
Oct4
G
Nanog
H
DPPA2
Skeletal muscle
Neuronal tissue
Respiratory epithelium
I
J
K
M
L
N

Figure 28 Characterization of Sohlh1-/- iPSCs dervied by Sendai virus infection.

Morphological comparison between non-reprogrammed and reprogrammed Sohlh1-/- fibroblasts (A, B). In-well staining for pluripotency markers alkaline phosphatase (AP) (C), SSEA-1 (D), Sox2 (E), Oct4 (F), Nanog (G), DPPA2 (H). Teratoma assay showing H&E staining from teratoma obtained from injection of Sohlh1-/- iPSCs into the testis of SCID mice (I-K). Preliminary karyotyping by in-house G-banding of Sohlh1-/- iPSCs (M-N).

7.3.3 **Gene targeting in Sohlh1-Sendai iPSCs**

I performed gene targeting in Sohlh1-Sendai iPSCs by electroporation with sgRNA-Rosa26-60, 65 in the form of RNA and Cas9 protein. The CRISPR/Cas9 components were transfected by electroporation with the CRISPR/Cas9 Ribonucleoprotein (RNP) complex. At seven to ten days, electroporated iPSCs were passaged onto new MEF feeders with media containing 0.15 μM Puromycin for Puromycin selection. At seven days after Puromycin treatment, Puromycin-resistant clones were seen (Fig. 29A, B) compared to zero colonies present in the non-transfection control iPSCs (Fig. 29C). PCR was performed to identify insertion and showed that electroporated Sohlh1-KO miPSCs were positive for transgene insertion at the Rosa26 locus in both replicates, compared to the non-transfected control (Fig. 29D). These data showed that gene targeting was feasible in iPSCs from Sohlh1-deficient mice.

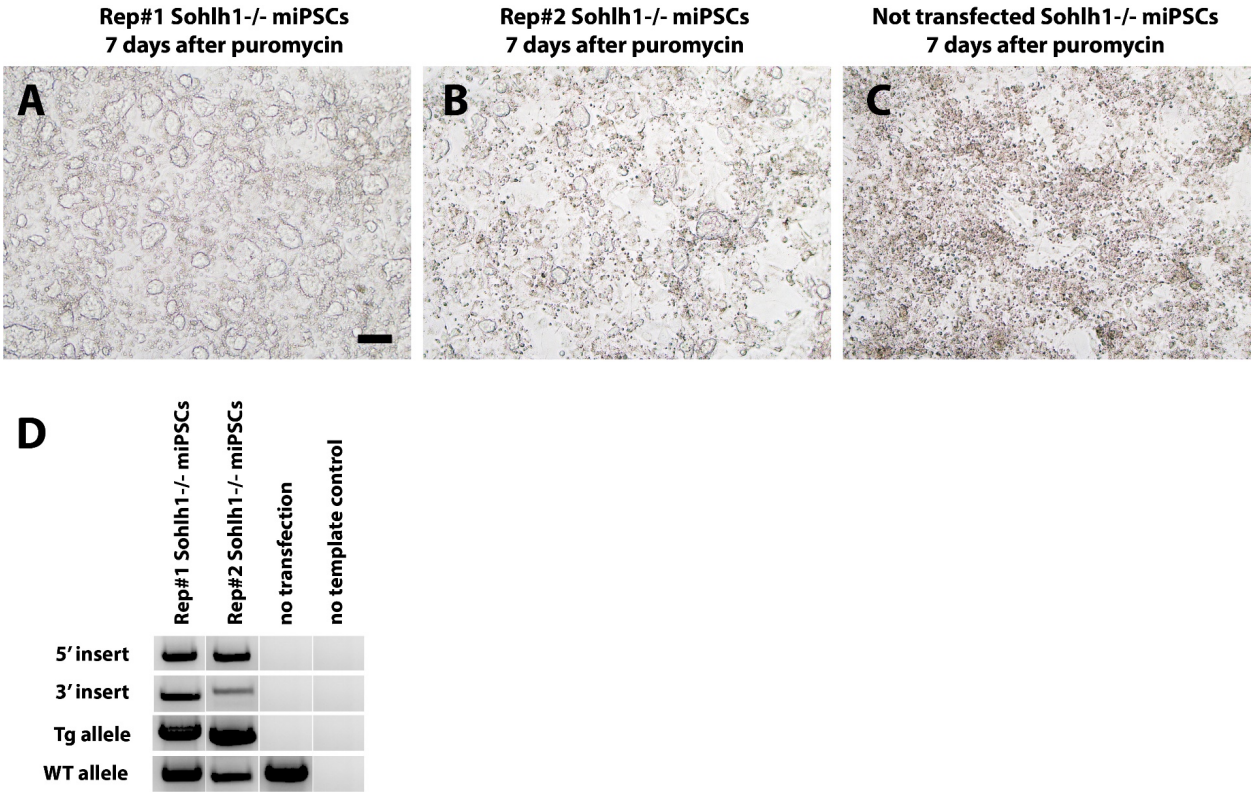

Figure 29 Gene targeting at Rosa26 locus in Sohlh1-/- iPSCs.

Sohlh1-/- iPSCs at 7 days after Puromycin selection at 0.15 μM, showing replicate #1 (A) and replicate #2 (B) compared to non-transfected Sohlh1-/- iPSCs at 7 days into Puromycin selection at the same concentration (C). PCR screening for transgene insertion at Rosa26 locus using Puromycin-resistant replicate #1 and #2 compared to non-transfected control and no template control (D). *miPSCs=mouse induced pluripotent stem cells*

7.3.4 **PGCLCs induction in lentiviral-derived WT iPSCs line**

I used the protocol studied by Hayashi and colleagues for in vitro oocyte derivation through EpiLCs and PGLCL induction for PGCLC derivation [332]. According to the initial study by Hayashi and colleagues, PGCLC induction was only successful in iPSC clones derived with stable expression of OSKM factors. Therefore, I tested the same protocol with MEF-Lenti iPSCs that were derived in-house. The iPSCs were transferred from feeders to ornithine-coated plates for

feeder-free condition adaptation, and the media was changed to N2B27 media with 2i+LIF. Cell morphology changed to flatter, wider-spread colonies than was seen when feeders were present; however, colony formation was still observed (Fig. 30A). After EpiLC induction, the morphology of the cells changed into flat, cobblestone like-shapes, which resembled that of fibroblasts. This matches the morphology reported in Hayashi's study (Fig. 30B). PGCLC induction was performed and clumps of cells were observed, as indicated in the protocol (Fig. 30C). Cell clumps were digested and stained for SSEA-1 and ITGB6, known surfaced markers for PGCs. FACS was used to select for SSEA-1/ITGA6 double positive cells for transplantation (Fig. 30G-I). The negative control gate was set based on unstained cells (Fig.30D-F). FACS showed 16.5% double-positive cells among live cells which were then transplanted into the seminiferous tubules of Bulsulfan-treated Nude mice. At 3 months post-transplantation, sperm were recovered from the tail of the epididymis and were used for ICSI. To distinguish the origin of sperm from any possible residual sperm in nude mice, I used Sanger sequencing of the Foxn1 gene, at which a frame-shift deletion is causative for the nude phenotype (GGGCG→ GGCG; Fig. 30J). Among 8 embryos tested, I found 1 embryo (embryo 8) with the wild-type sequence (Fig. 30L), as opposed to seven with a heterozygous nude genotype (Fig. 30K). This indicates that the sperm origin for embryo 8 was from iPSCs, and not from a nude mouse, meaning that transplanted PGCLCs were able to differentiate and give rise to sperm.

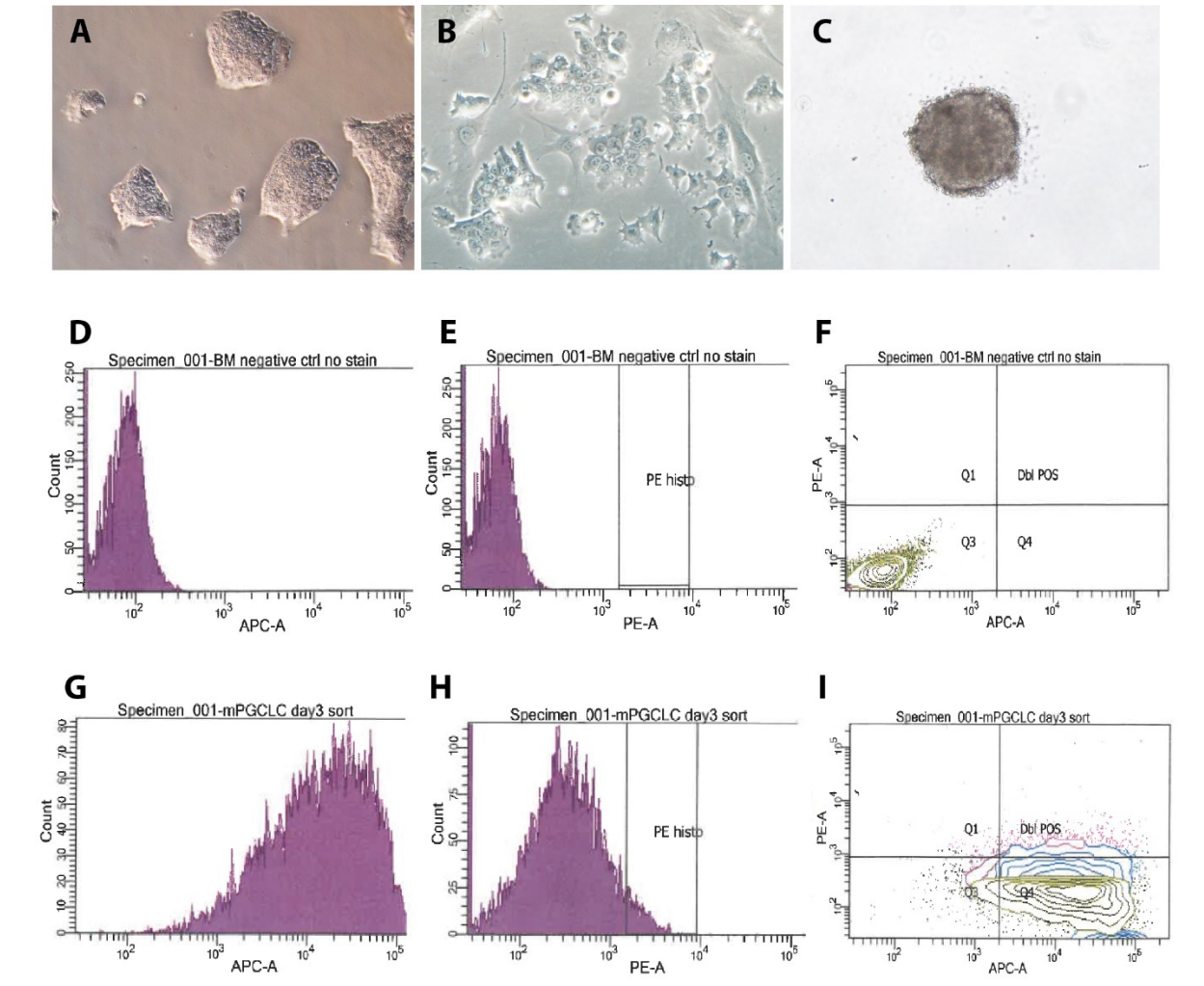

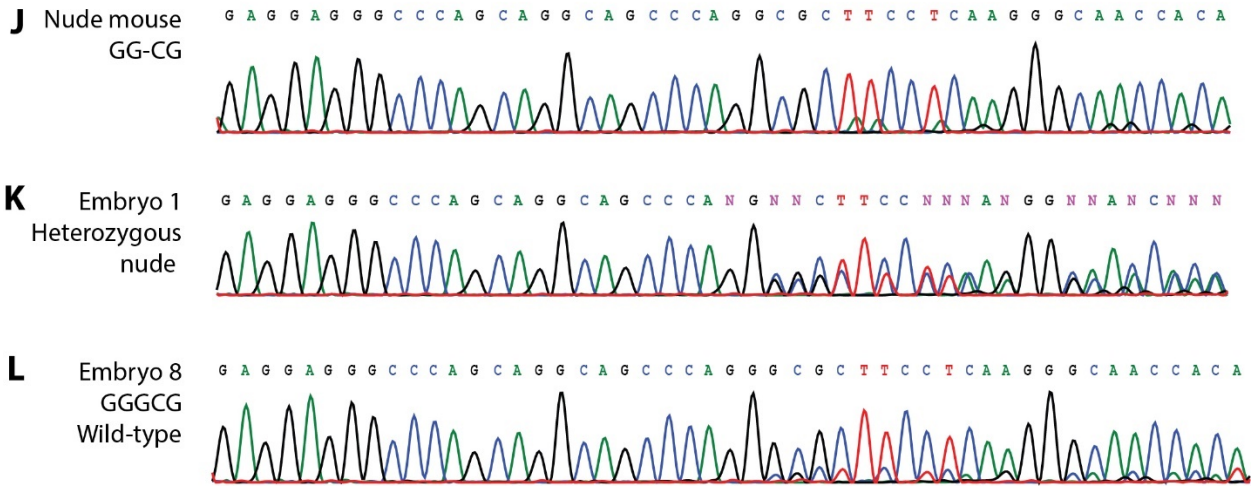

Figure 30 PGCLC derivation using Lentiviral-derived WT iPSCs from MEF (MEF-Lenti iPSCs).

MEF-Lenti iPSCs plated onto the L-ornithine-coated plate when adjusted into the feeder-free condition (A). At 2 days after EpiLC induction (B). At 3 days after PGCLC induction (C). The PGCLC clumps were digested and stained for ITGB6 and SSEA1 using ITGB-6-PE and SSEA-1-APC antibodies. FACS was used to isolate for double-positive cells (G-I). Negative control gates were set using unstained control (D-F). Sanger sequencing of embryos resulting from ICSI using sperm from ITGB6+/SSEA1+ cells transplantation into homozygous nude mice. Sequence of the nude mouse at Foxn1 locus showed 1 bp deletion (GG-CG). Embryo1 born from residual sperm of nude mice showed heterozygous nude/WT when fertilized with WT egg (K). Embryo8 showed WT sequence (GGGCG as opposed to GG-CG) (L), showing that the origin of sperm was not from the nude recipient.

7.4 Discussion

In this study I demonstrate an approach for germline gene therapy in azoospermia with no germ cells (SCO). However, there are still limitations to this approach. First, PGCLC transplantation could give rise to tumors from residual contaminated pluripotent cells. Secondly, because the outcome of gonadal fate induction from iPSCs also depends on donor genetic background, translation to human might exhibit different, unreliable outcomes [335]. Finally, since the risk of teratoma formation is high when transplanted into recipients, our only option to avoid this risk may be by deriving gametes entirely in vitro as previously described in mice [168, 170]. Current studies in rodents only showed spermatid-like cells, which morphologically resemble round spermatids, as the most advanced haploid cells derivable in vitro from PGCLCs. Although Round Spermatid Injection (ROSI) is efficient in rodents, it is not widely practiced in because of poor pregnancy rates and embryo outcome [336, 337].

Another significant limitation to any experiment involving human germ cell derivation from pluripotent cells is the functional testing of sperm generated *in vitro*. Most reproductive

scientists agree that the best way to show sperm functionality is to fertilize an egg, and to produce viable, healthy offspring. However, none of these approaches are allowed in humans. Xenotransplantation of human SSCs into nude mice or monkey testis are shown to result in colonization, and therefore, might be used to assess the potential of *in vitro*- derived human PGCLCs or SSCs to engraft the testis.

7.5 Conclusions

I provided an alternative approach to germline gene editing for azoospermia in Sertoli cell only syndrome, as spermatogonial stem cell culture may not be feasible for gene targeting in this population. In our approach, I demonstrated gene targeting in iPSCs derived from *Sohlh1-KO* mice. EpiLC and PGCLC induction protocols were tested in WT iPSCs derived from MEF via stable expression of OSKM factors. Sperm that originated from PGCLCs was evidenced after transplantation of these cells into nude testis, validating my approach for PGCLC induction. This study demonstrates another strategy to treat azoospermia, particularly for patients with Sertoli cell only syndrome. However, years of additional studies are needed to demonstrate that this approach is reproducible and safe in mice; can be translated to higher animal models and eventually to human cells.

7.6 Acknowledgements

Chatchanan Doungkamchan planned, optimized the gene therapy and tested the iPSCs and PGCLC induction protocols and analyzed the data. Kien Tran performed pluripotency characterizations, PGCLC induction and analysis of transplanted PGCLCs. Yi Sheng made Lentivirus and performed ICSI. Meena Sukwani transplanted iPSCs into SCID mice and PGCLCs into Nude mice. Kyle Orwig advised on the project.

8.0 Concluding remark

Gene therapy is a promising approach to correct the disease phenotype related to single gene defects. Azoospermia is one of the diseases with a wide array of single gene defects identified in Sertoli cells and germ cells, both of which are known to play important role in spermatogenesis. This study showed that Sertoli cell gene therapy can be done by injecting adenovirus carrying therapeutic vector into the lumen of the seminiferous tubules. This approach was shown to successfully restored the expression of the defective gene in the Sertoli cells and spermatogenesis without modifying germline. For germline gene therapy, both small mutations and large deletions were correctable by CRISPR/Cas9 and donor DNA template in the spermatogonial stem cells obtained from the testis of azoospermic animals. The gene therapy for small mutations in germ cells was done by converting the mutated sequence to the wild-type sequence which was successfully demonstrated in the mice with *Tex11-D435fs* mutation. The gene therapy for large deletions in germ cells was also demonstrated in *Sohlh1*-KO mice by inserting a transgenic cassette containing *Sohlh1*-cDNA and puromycin-resistant gene into the Rosa26 locus. The mRNA of *Sohlh1* was detected in the gene-corrected clones. The heterozygous clones for transgene were selectively expanded and transplanted to the Bulsulfan-treated Sohlh1-KO mice to allow the chance of recovering transgene-free sperm. Prenatal genetic diagnosis will be used to selected for the transgene-free embryos for implantation to avoid germline transmission. In human, where spermatogonial stem cell technique is not well-established, gene therapy in iPSCs and PGCLC induction serve as an alternative approach to correct single gene defects related to NOA. In conclusion, this study showed that gene therapy for azoospermia related to single genes defects is possible for Sertoli cell and germ cell defects without germline transmission.

Appendix A Antibodies

Appendix table 1 Antibodies used in gene therapy study

antibody	Host species	Catalog number	Supplier	concentration
Immunofluorescence staining				
Primary antibodies				
Androgen receptor (AR)	Rabbit	SC-816	Santa Cruz	1:100
EGFP	Goat	NB100-1770	Novus	1:200
Sox9	Rabbit	AB5535	Millipore/Fisher	1:200
Vasa	Rabbit	ab13840	Abcam	1:200
CD68	Rabbit	ab125212	Abcam	1:200
CD66b	Rabbit	ab197678	Abcam	1:50
CD3	Rabbit	ab16669	Abcam	1:50
SALL4	Rabbit	AB29112	Abcam	1:800
STRA8	Rabbit	AB49602	Abcam	1:200
SYCP3	Rabbit	AB15093	Abcam	1:500
H2AX	Rabbit	AB11174	Abcam	1:100
PIWIL1	Goat	AF6548	R&D Systems	1:200
TP1	Goat	AB73135	Abcam	1:1000
ZIP4H/Tex11	Goat	AF5627	R&D Systems	1:100
DDX4	Mouse	AB27591	Abcam	1:100
Secondary Antibodies				
Alexa 488 donkey anti-goat	Donkey	A-11055	Life technologies	1:200
Alexa 568 donkey anti-rabbit	Donkey	A10042	Life technologies	1:200
Streptavidin-conjugated Alexa 488	-	S11223	Life technologies	1:200
Alexa 488 donkey anti-rabbit	Donkey	A21206	Invitrogen	1:100
Alexa 568 donkey anti-mouse	Donkey	A10037	Invitrogen	1:100
chromogenic immunostaining				
Primary antibodies				
Androgen Receptor (AR)	Rabbit	M4070	Spring Biosciences	1:400
Phosphoglycerate Kinase 1 and 2 (PGK1/2)	Rabbit	SC-28784	Santa Cruz	1:400
Secondary antibodies				
ImmPRESS VR Anti-Rabbit IgG HRP Polymer Detection Kit	Horse	MP-6401-15	Vector Laboratories	N/A

Appendix B primers/oligos sequences

Appendix table 2 primers/oligos sequences used in this study

oligos	sequences
For SCARKO genotyping	
EF1a-7	ACGTGAGGCTCCGGTGCCCGTCAG
GFP-6	CGCTTTACTTGTACAGCTCGT
Rosa26-F	GTGTTCGTGCAAGTTGAGTCC
Rosa26-R	TAAAGACATGCTCACCCGAGTTTTA
P1	CAGCACCCTACACTAGAATACTG
P2	AATGACCTGAGAGTGCTTCCTCC
P3	AGGGCACAGAGTAAGCAGTTTGC
P4	TCCAGATGTAGGACAGACCTTCC
Cre-F	TGGTTTCCCGCAGAACCTGAAG
Cre-R	GAGCCTGTTTTGCACGTTCACC
For Tex11-D435fs generation	
sgRNA-Tex11-WT	AATATGCTGATGCCCTACAC(TGG)
ssODN WT-to-D435fs	GAATTTTGGAAAAATCTATGACTTTGTTGTTTTTTTTTAACTTT AGGTCCAAAAATATGCTTTGGTACCCTACACTGGTACAGTTAT TCTCTGAAGTTGTATGAGTATGATAAAGCAGATCTGGATT
For Tex11 Genotyping/Gene therapy experiment	
Tex11-F1	TGAAGGTATCTCCACTAGCATGG
Tex11-R1	ACCTAAGTGCCACAGCAAAGAAC
Tex11-Fm1	TATGCTTTGGTACCCTACACTGG
Tex11-WT F1	GGTCCAAAAATATGCTGATG
Tex11-WT mRNA F1	GGTCCAAAAATATGCTGATG
Tex11-WT mRNA RV1	GCATCACCCTCCATGATTGC
sgRNA-Tex11-D-P2 (antisense)	AGAATAACTGTACCAGTGTA (GGG)
ssODN D435fs-to-WT (antisense)	AATCCAGATCTGCTTTATCATACTCATACAACTTCAGAGAATA ACTGTACCAGTGTAGGGCATCAGCATATTTTGGACCTAAAGTT AAAAAAAAACAACAAAGTCATAGATTTTTCCAAAATTC
For Sohlh1-KO colony genotyping	
Rosa26 P1	CTACTGTGTTGGCGGACTGG

PGK RV1	TTTGAAGCGTGCAGAATGC
mCherry 3P Fwd2	GAGATCAAGCAGAGGCTGAA
Rosa26 P2	AAGACAACAAACACCTGAACTTTG
Rosa26 Surveyor F	GTGTTCGTGCAAGTTGAGTCCAT
Rosa26 Surveyor R	TAAAACTCGGGTGAGCATGTCTTTA
For Sohlh1-KO gene targeting at Rosa26 locus	
sgRNA-Rosa26-60	AGTCTTTCTAGAAGATGGGC (GGG)
sgRNA-Rosa26-65 (antisense)	GTCTTTCTAGAAGATGGGCG (TGG)
For Sohlh1-KO genotyping	
Sohlh1-KO-geno-G1	GAGTCTCTGGCATTACGGGAT
Sohlh1-KO-geno-G2	CTGAGTCTCAGCCTGAGGAG
Sohlh1-KO-geno-HPRT2	GCAGTGTTGGCTGTATTTTCC
Sohlh1-KO-geno-G3	CTGGAGCCCAAGAAGACAAG

Bibliography

1. Hofmann, M.C., *Gdnf signaling pathways within the mammalian spermatogonial stem cell niche.* Mol Cell Endocrinol, 2008. **288**(1-2): p. 95-103.

2. Oatley, J.M. and R.L. Brinster, *The germline stem cell niche unit in mammalian testes.* Physiol Rev, 2012. **92**(2): p. 577-95.

3. Russell, L.D., et al., *Mammalian Spermatogenesis*, in *Histological and Histopathological Evaluation of the Testis*, L.D. Russell, et al., Editors. 1990, Cache River Press: Clearwater, FL. p. 1-40.

4. Oatley, J.M., et al., *Colony stimulating factor 1 is an extrinsic stimulator of mouse spermatogonial stem cell self-renewal.* Development, 2009. **136**(7): p. 1191-1199.

5. Yoshida, S., M. Sukeno, and Y. Nabeshima, *A vasculature-associated niche for undifferentiated spermatogonia in the mouse testis.* Science, 2007. **317**(5845): p. 1722-6.

6. Jan, S.Z., et al., *Molecular control of rodent spermatogenesis.* Biochimica et biophysica acta, 2012. **1822**(12): p. 1838-50.

7. Tadokoro, Y., et al., *Homeostatic regulation of germinal stem cell proliferation by the GDNF/FSH pathway.* Mech Dev, 2002. **113**(1): p. 29-39.

8. Kanatsu-Shinohara, M., et al., *Anchorage-independent growth of mouse male germline stem cells in vitro.* Biol Reprod, 2006. **74**(3): p. 522-9.

9. Kubota, H., M.R. Avarbock, and R.L. Brinster, *Growth factors essential for self-renewal and expansion of mouse spermatogonial stem cells.* Proc Natl Acad Sci U S A, 2004. **101**(47): p. 16489-94.

10. Meng, X., et al., *Regulation of cell fate decision of undifferentiated spermatogonia by GDNF.* Science, 2000. **287**(5457): p. 1489-93.

11. He, Z., et al., *Gdnf upregulates c-Fos transcription via the Ras/Erk1/2 pathway to promote mouse spermatogonial stem cell proliferation.* Stem Cells, 2008. **26**(1): p. 266-78.

12. Wu, X., et al., *The POU domain transcription factor POU3F1 is an important intrinsic regulator of GDNF-induced survival and self-renewal of mouse spermatogonial stem cells.* Biology of Reproduction, 2010. **82**(6): p. 1103-11.

13. Grisanti, L., et al., *Identification of spermatogonial stem cell subsets by morphological analysis and prospective isolation.* Stem Cells, 2009. **27**(12): p. 3043-52.

14. Naughton, C.K., et al., *Glial cell-line derived neurotrophic factor-mediated RET signaling regulates spermatogonial stem cell fate.* Biol Reprod, 2006. **74**(2): p. 314-21.

15. Suzuki, H., et al., *The heterogeneity of spermatogonia is revealed by their topology and expression of marker proteins including the germ cell-specific proteins Nanos2 and Nanos3.* Dev Biol, 2009. **336**(2): p. 222-31.

16. Hai, Y., et al., *The roles and regulation of Sertoli cells in fate determinations of spermatogonial stem cells and spermatogenesis.* Semin Cell Dev Biol, 2014. **29**: p. 66-75.

17. Griswold, M.D., *The central role of Sertoli cells in spermatogenesis.* Semin Cell Dev Biol, 1998. **9**(4): p. 411-6.

18. Ramaswamy, S. and G.F. Weinbauer, *Endocrine control of spermatogenesis: Role of FSH and LH/ testosterone.* Spermatogenesis, 2014. **4**(2): p. e996025.

19. Wang, R.-S., et al., *Androgen Receptor in Sertoli Cell Is Essential for Germ Cell Nursery and Junctional Complex Formation in Mouse Testes.* Endocrinology, 2006. **147**(12): p. 5624-5633.

20. Huckins, C., *The spermatogonial stem cell population in adult rats. I. Their morphology, proliferation and maturation.* Anat Rec, 1971. **169**(3): p. 533-57.

21. Oakberg, E.F., *Spermatogonial stem-cell renewal in the mouse.* Anat.Rec., 1971. **169**(3): p. 515-531.

22. de Rooij, D.G., *Spermatogonial stem cell renewal in the mouse. I. Normal situation.* Cell Tissue Kinet, 1973. **6**(3): p. 281-7.

23. Phillips, B.T., K. Gassei, and K.E. Orwig, *Spermatogonial stem cell regulation and spermatogenesis.* Philos Trans R Soc Lond B Biol Sci, 2010. **365**(1546): p. 1663-78.

24. de Rooij, D.G. and M.D. Griswold, *Questions About Spermatogonia Posed and Answered Since 2000.* Journal of Andrology, 2012. **33**(6): p. 1085-1095.

25. Clermont, Y. and C.P. Leblond, *Differentiation and renewal of spermatogonia in the monkey, Macacus rhesus.* Am J Anat, 1959. **104**: p. 237-73.

26. Clermont, Y., *Two classes of spermatogonial stem cells in the monkey (Cercopithecus aethiops).* Am J Anat, 1969. **126**(1): p. 57-71.

27. Fayomi, A.P. and K.E. Orwig, *Spermatogonial stem cells and spermatogenesis in mice, monkeys and men.* Stem Cell Res, 2018. **29**: p. 207-214.

28. Busada, J.T. and C.B. Geyer, *The Role of Retinoic Acid (RA) in Spermatogonial Differentiation.* Biol Reprod, 2016. **94**(1): p. 10.

29. Chapman, K.M., et al., *NRG1 and KITL signal downstream of retinoic acid in the germline to support soma-free syncytial growth of differentiating spermatogonia.* Cell Death Discovery, 2015. **1**: p. 15018.

30. Besmer, P., et al., *The kit-ligand (steel factor) and its receptor c-kit/W: pleiotropic roles in gametogenesis and melanogenesis.* Dev Suppl, 1993. **Suppl**: p. 125-37.

31. Ohta, H., et al., *Regulation of proliferation and differentiation in spermatogonial stem cells: the role of c-kit and its ligand SCF.* Development, 2000. **127**(10): p. 2125-31.

32. Filipponi, D., et al., *Repression of kit expression by Plzf in germ cells.* Mol Cell Biol, 2007. **27**(19): p. 6770-81.

33. Gassei, K. and K.E. Orwig, *SALL4 expression in gonocytes and spermatogonial clones of postnatal mouse testes.* PLoS ONE, 2013. **8**(1): p. e53976.

34. Hobbs, R.M., et al., *Functional antagonism between Sall4 and Plzf defines germline progenitors.* Cell Stem Cell, 2012. **10**(3): p. 284-98.

35. Lovelace, D.L., et al., *The regulatory repertoire of PLZF and SALL4 in undifferentiated spermatogonia.* Development, 2016. **143**(11): p. 1893-1906.

36. Ballow, D., et al., *Sohlh1 is essential for spermatogonial differentiation.* Developmental Biology, 2006. **294**(1): p. 161-7.

37. Barrios, F., et al., *SOHLH1 and SOHLH2 control Kit expression during postnatal male germ cell development.* Journal of Cell Science, 2012. **125**(Pt 6): p. 1455-64.

38. Valli, H., et al., *Spermatogonial Stem Cells and Spermatogenesis*, in *Knobil and Neill's Physiology of Reproduction*, T.M. Plant and A.J. Zeleznik, Editors. 2015, Elsevier: San Diego. p. 595-635.

39. de Rooij, D.G. and J.A. Grootegoed, *Spermatogonial stem cells.* Curr Opin Cell Biol, 1998. **10**(6): p. 694-701.

40. Handel, M.A. and J.C. Schimenti, *Genetics of mammalian meiosis: regulation, dynamics and impact on fertility.* Nat Rev Genet, 2010. **11**(2): p. 124-36.

41. Zickler, D. and N. Kleckner, *Meiotic chromosomes: integrating structure and function.* Annu Rev Genet, 1999. **33**: p. 603-754.

42. Cohen, P.E., *Meiosis Overview*, in *Reference Module in Biomedical Sciences*. 2018, Elsevier.

43. Baudat, F., Y. Imai, and B. de Massy, *Meiotic recombination in mammals: localization and regulation.* Nat Rev Genet, 2013. **14**(11): p. 794-806.

44. Deng, W. and H. Lin, *miwi, a murine homolog of piwi, encodes a cytoplasmic protein essential for spermatogenesis.* Dev Cell, 2002. **2**(6): p. 819-30.

45. Thomson, T. and H. Lin, *The biogenesis and function of PIWI proteins and piRNAs: progress and prospect.* Annu Rev Cell Dev Biol, 2009. **25**: p. 355-76.

46. Meistrich, M.L., et al., *Roles of transition nuclear proteins in spermiogenesis.* Chromosoma, 2003. **111**(8): p. 483-8.

47. Yu, Y.E., et al., *Abnormal spermatogenesis and reduced fertility in transition nuclear protein 1-deficient mice.* Proc Natl Acad Sci U S A, 2000. **97**(9): p. 4683-8.

48. Shirley, C.R., et al., *Abnormalities and reduced reproductive potential of sperm from Tnp1- and Tnp2-null double mutant mice.* Biol Reprod, 2004. **71**(4): p. 1220-9.

49. Zegers-Hochschild, F., et al., *International Committee for Monitoring Assisted Reproductive Technology (ICMART) and the World Health Organization (WHO) revised glossary of ART terminology, 2009∗.* Fertility and Sterility, 2009. **92**(5): p. 1520-1524.

50. Agarwal, A., et al., *A unique view on male infertility around the globe.* Reprod Biol Endocrinol, 2015. **13**: p. 37.

51. Grimes, D.A. and L.M. Lopez, *"Oligozoospermia," "azoospermia," and other semen-analysis terminology: the need for better science.* Fertil Steril, 2007. **88**(6): p. 1491-4.

52. Esteves, S.C., *Clinical Management of infertile men with nonobstructive azoospermia.* Asian Journal of Andrology, 2015. **17**: p. 459-470.

53. Cooper, T.G., et al., *World Health Organization reference values for human semen characteristics.* Human Reproduction Update, 2010. **16**(3): p. 231-245.

54. Jungwirth, A., et al., *European Association of Urology Guidelines on Male Infertility: The 2012 Update.* European Urology, 2012. **62**(2): p. 324-332.

55. World Health, O., *[Laboratory manual of the WHO for the examination of human semen and sperm-cervical mucus interaction].* Ann Ist Super Sanita, 2001. **37**(1): p. I-XII, 1-123.

56. Gudeloglu, A. and S.J. Parekattil, *Update in the evaluation of the azoospermic male.* Clinics, 2013. **68**(Suppl 1): p. 27-34.

57. Lee, J.Y., et al., *Role of Genetics in Azoospermia.* Urology, 2011. **77**(3): p. 598-601.

58. McLachlan, R.I., et al., *Histological evaluation of the human testis—approaches to optimizing the clinical value of the assessment: Mini Review.* Human Reproduction, 2007. **22**(1): p. 2-16.

59. Kim, E.D., et al., *Testis Biopsies Frequently Demonstrate Sperm in Men With Azoospermia and Significantly Elevated Follicle-Stimulating Hormone Levels.* The Journal of Urology, 1997. **157**(1): p. 144-146.

60. Jarvi, K., et al., *CUA Guideline: The workup of azoospermic males.* Can Urol Assoc J, 2010. **4**(3): p. 163-7.

61. Hamada, A.J., S.C. Esteves, and A. Agarwal, *A comprehensive review of genetics and genetic testing in azoospermia.* Clinics (Sao Paulo), 2013. **68 Suppl 1**: p. 39-60.

62. Schlegel, P.N., *Causes of azoospermia and their management.* Reprod Fertil Dev, 2004. **16**(5): p. 561-72.

63. Gil Salom, M., *[Spermatic recovery techniques for intracytoplasmic spermatozoid injection (ICSI) in male infertility].* Arch Esp Urol, 2004. **57**(9): p. 1035-46.

64. Su, L.M., et al., *Testicular sperm extraction with intracytoplasmic sperm injection for nonobstructive azoospermia: testicular histology can predict success of sperm retrieval.* J Urol, 1999. **161**(1): p. 112-6.

65. Schlegel, P.N., *Testicular sperm extraction: microdissection improves sperm yield with minimal tissue excision.* Hum Reprod, 1999. **14**(1): p. 131-5.

66. Schlegel, P.N. and P.S. Li, *Microdissection TESE: sperm retrieval in non-obstructive azoospermia.* Hum Reprod Update, 1998. **4**(4): p. 439.

67. Schlegel, P.N., et al., *Testicular sperm extraction with intracytoplasmic sperm injection for nonobstructive azoospermia.* Urology, 1997. **49**(3): p. 435-40.

68. Robin, G., et al., *[Assessment of azoospermia and histological evaluation of spermatogenesis].* Ann Pathol, 2010. **30**(3): p. 182-95.

69. Reijo, R., et al., *Diverse spermatogenic defects in humans caused by Y chromosome deletions encompassing a novel RNA-binding protein gene.* Nat Genet, 1995. **10**(4): p. 383-93.

70. Van Assche, E., et al., *Cytogenetics of infertile men.* Hum Reprod, 1996. **11 Suppl 4**: p. 1-24; discussion 25-6.

71. Massart, A., et al., *Genetic causes of spermatogenic failure.* Asian J Androl, 2012. **14**(1): p. 40-8.

72. AUA, *The Evaluation of the Azoospermic Male: Best Practice Statement.* 2011. **Male Infertility**: p. 4-25.

73. Yang, F., et al., *TEX11 is mutated in infertile men with azoospermia and regulates genome-wide recombination rates in mouse.* EMBO Molecular Medicine, 2015. **7**(9): p. 1198-1210.

74. Choi, Y., et al., *Mutations in SOHLH1 gene associate with nonobstructive Azoospermia.* Human Mutation, 2010. **31**(7): p. 788-793.

75. Sha, Y., et al., *A novel TEX11 mutation induces azoospermia: a case report of infertile brothers and literature review.* BMC Med Genet, 2018. **19**(1): p. 63.

76. Yatsenko, A.N., et al., *X-Linked TEX11 Mutations, Meiotic Arrest, and Azoospermia in Infertile Men.* New England Journal of Medicine, 2015. **372**(22): p. 2097-2107.

77. Gottlieb, B., et al., *The androgen receptor gene mutations database: 2012 update.* Hum Mutat, 2012. **33**(5): p. 887-94.

78. Ropke, A., et al., *Comprehensive sequence analysis of the NR5A1 gene encoding steroidogenic factor 1 in a large group of infertile males.* Eur J Hum Genet, 2013. **21**(9): p. 1012-1015.

79. Bashamboo, A., et al., *Human Male Infertility Associated with Mutations in NR5A1 Encoding Steroidogenic Factor 1.* The American Journal of Human Genetics, 2010. **87**(4): p. 505-512.

80. Maor-Sagie, E., et al., *Deleterious mutation in SYCE1 is associated with non-obstructive azoospermia.* J Assist Reprod Genet, 2015. **32**(6): p. 887-91.

81. Ben Khelifa, M., et al., *A MEI1 homozygous missense mutation associated with meiotic arrest in a consanguineous family.* Hum Reprod, 2018. **33**(6): p. 1034-1037.

82. Ghieh, F., et al., *Genetic defects in human azoospermia.* Basic Clin Androl, 2019. **29**: p. 4.

83. Krausz, C. and A. Riera-Escamilla, *Genetics of male infertility.* Nat Rev Urol, 2018. **15**(6): p. 369-384.

84. Lin, Y.-N. and M. Matzuk, *Genetics of Male Fertility*, in *Human Fertility*, Z. Rosenwaks and P.M. Wassarman, Editors. 2014, Springer New York. p. 25-37.

85. Kathleen, H., et al., *Mendelian genetics of male infertility.* Annals of the New York Academy of Sciences, 2010. **1214**(1): p. E1-E17.

86. Walsh, T.J., R.R. Pera, and P.J. Turek. *The genetics of male infertility*. in *Seminars in reproductive medicine*. 2009. © Thieme Medical Publishers.

87. Tamowski, S., K.I. Aston, and D.T. Carrell, *The use of transgenic mouse models in the study of male infertility.* Syst Biol Reprod Med, 2010. **56**(3): p. 260-73.

88. Soumillon, M., et al., *Cellular source and mechanisms of high transcriptome complexity in the mammalian testis.* Cell Rep, 2013. **3**(6): p. 2179-90.

89. Jamsai, D. and M.K. O'Bryan, *Mouse models in male fertility research.* Asian J Androl, 2011. **13**(1): p. 139-51.

90. Nef, S. and L.F. Parada, *Hormones in male sexual development.* Genes Dev, 2000. **14**(24): p. 3075-86.

91. Wilson, J.D., J.E. Griffin, and D.W. Russell, *Steroid 5 alpha-reductase 2 deficiency.* Endocr Rev, 1993. **14**(5): p. 577-93.

92. Bennett, N.C., et al., *Molecular cell biology of androgen receptor signalling.* Int J Biochem Cell Biol, 2010. **42**(6): p. 813-27.

93. Walker, W.H., *Non-classical actions of testosterone and spermatogenesis.* Philos Trans R Soc Lond B Biol Sci, 2010. **365**(1546): p. 1557-69.

94. Zhou, Q., et al., *Localization of androgen and estrogen receptors in adult male mouse reproductive tract.* J Androl, 2002. **23**(6): p. 870-81.

95. Tsai, M.-Y., et al., *Differential effects of spermatogenesis and fertility in mice lacking androgen receptor in individual testis cells.* Proceedings of the National Academy of Sciences, 2006. **103**(50): p. 18975-18980.

96. Johnston, D.S., et al., *Murine germ cells do not require functional androgen receptors to complete spermatogenesis following spermatogonial stem cell transplantation.* Endocrinology, 2001. **142**(6): p. 2405-8.

97. Plant, T.M., S. Ramaswamy, and K. De Gendt, *Spermatogenesis, Endocrine Control of*, in *Reference Module in Biomedical Sciences*. 2016, Elsevier.

98. Chakraborty, P., et al., *Androgen-Dependent Sertoli Cell Tight Junction Remodeling Is Mediated by Multiple Tight Junction Components.* Molecular Endocrinology, 2014. **28**(7): p. 1055-1072.

99. De Gendt, K., et al., *A Sertoli cell-selective knockout of the androgen receptor causes spermatogenic arrest in meiosis.* Proc Natl Acad Sci U S A, 2004. **101**(5): p. 1327-32.

100. Chang, C., et al., *Infertility with defective spermatogenesis and hypotestosteronemia in male mice lacking the androgen receptor in Sertoli cells.* Proceedings of the National Academy of Sciences of the United States of America, 2004. **101**(18): p. 6876-6881.

101. O'Hara, L., et al., *Autocrine androgen action is essential for Leydig cell maturation and function, and protects against late-onset Leydig cell apoptosis in both mice and men.* Faseb j, 2015. **29**(3): p. 894-910.

102. Wang, Z.Q., et al., *Gain-of-function mutation of KIT ligand on melanin synthesis causes familial progressive hyperpigmentation.* Am J Hum Genet, 2009. **84**(5): p. 672-7.

103. O'Hara, L. and L.B. Smith, *Androgen receptor roles in spermatogenesis and infertility.* Best Pract Res Clin Endocrinol Metab, 2015. **29**(4): p. 595-605.

104. Hiort, O., et al., *Significance of mutations in the androgen receptor gene in males with idiopathic infertility.* J Clin Endocrinol Metab, 2000. **85**(8): p. 2810-5.

105. Sinnecker, G.H.G., et al., *Functional assessment and clinical classification of androgen sensitivity in patients with mutations of the androgen receptor gene.* European Journal of Pediatrics, 1996. **156**(1): p. 7-14.

106. Ghadessy, F.J., et al., *Oligospermic infertility associated with an androgen receptor mutation that disrupts interdomain and coactivator (TIF2) interactions.* J Clin Invest, 1999. **103**(11): p. 1517-25.

107. Yang, F., et al., *Meiotic failure in male mice lacking an X-linked factor.* Genes & Development, 2008. **22**(5): p. 682-691.

108. Wang, P.J., et al., *An abundance of X-linked genes expressed in spermatogonia.* Nat Genet, 2001. **27**(4): p. 422-6.

109. Adelman, C.A. and J.H. Petrini, *ZIP4H (TEX11) deficiency in the mouse impairs meiotic double strand break repair and the regulation of crossing over.* PLoS Genet, 2008. **4**(3): p. e1000042.

110. Blatch, G.L. and M. Lassle, *The tetratricopeptide repeat: a structural motif mediating protein-protein interactions.* Bioessays, 1999. **21**(11): p. 932-9.

111. Suzuki, H., et al., *SOHLH1 and SOHLH2 coordinate spermatogonial differentiation.* Developmental Biology, 2012. **361**(2): p. 301-12.

112. Mehta, A. and J.E. Haber, *Sources of DNA double-strand breaks and models of recombinational DNA repair.* Cold Spring Harb Perspect Biol, 2014. **6**(9): p. a016428.

113. Zhou, B.B. and S.J. Elledge, *The DNA damage response: putting checkpoints in perspective.* Nature, 2000. **408**(6811): p. 433-9.

114. WareJoncas, Z., et al., *Precision gene editing technology and applications in nephrology.* Nat Rev Nephrol, 2018. **14**(11): p. 663-677.

115. Doudna, J.A. and E. Charpentier, *Genome editing. The new frontier of genome engineering with CRISPR-Cas9.* Science, 2014. **346**(6213): p. 1258096.

116. Sternberg, S.H. and J.A. Doudna, *Expanding the Biologist's Toolkit with CRISPR-Cas9.* Mol Cell, 2015. **58**(4): p. 568-74.

117. Ran, F.A., et al., *Genome engineering using the CRISPR-Cas9 system.* Nat Protoc, 2013. **8**(11): p. 2281-2308.

118. Makarova, K.S., et al., *A putative RNA-interference-based immune system in prokaryotes: computational analysis of the predicted enzymatic machinery, functional analogies with eukaryotic RNAi, and hypothetical mechanisms of action.* Biol Direct, 2006. **1**: p. 7.

119. Barrangou, R., et al., *CRISPR provides acquired resistance against viruses in prokaryotes.* Science, 2007. **315**(5819): p. 1709-12.

120. Sapranauskas, R., et al., *The Streptococcus thermophilus CRISPR/Cas system provides immunity in Escherichia coli.* Nucleic Acids Res, 2011. **39**(21): p. 9275-82.

121. Barrangou, R. and L.A. Marraffini, *CRISPR-Cas systems: Prokaryotes upgrade to adaptive immunity.* Mol Cell, 2014. **54**(2): p. 234-44.

122. Bolotin, A., et al., *Clustered regularly interspaced short palindrome repeats (CRISPRs) have spacers of extrachromosomal origin.* Microbiology, 2005. **151**(Pt 8): p. 2551-2561.

123. Mojica, F.J.M., et al., *Intervening Sequences of Regularly Spaced Prokaryotic Repeats Derive from Foreign Genetic Elements.* Journal of Molecular Evolution, 2005. **60**(2): p. 174-182.

124. Jinek, M., et al., *A Programmable Dual-RNA–Guided DNA Endonuclease in Adaptive Bacterial Immunity.* Science, 2012. **337**(6096): p. 816-821.

125. Brouns, S.J., et al., *Small CRISPR RNAs guide antiviral defense in prokaryotes.* Science, 2008. **321**(5891): p. 960-4.

126. Fu, Y., et al., *High-frequency off-target mutagenesis induced by CRISPR-Cas nucleases in human cells.* Nat Biotechnol, 2013. **31**(9): p. 822-6.

127. Hsu, P.D., et al., *DNA targeting specificity of RNA-guided Cas9 nucleases.* Nat Biotechnol, 2013. **31**(9): p. 827-32.

128. Nishimasu, H., et al., *Crystal structure of Cas9 in complex with guide RNA and target DNA.* Cell, 2014. **156**(5): p. 935-49.

129. Jinek, M., et al., *Structures of Cas9 endonucleases reveal RNA-mediated conformational activation.* Science, 2014. **343**(6176): p. 1247997.

130. Zhang, X.H., et al., *Off-target Effects in CRISPR/Cas9-mediated Genome Engineering.* Mol Ther Nucleic Acids, 2015. **4**: p. e264.

131. Kim, D., et al., *Evaluating and Enhancing Target Specificity of Gene-Editing Nucleases and Deaminases.* Annu Rev Biochem, 2019. **88**: p. 191-220.

132. Singh, P., J.C. Schimenti, and E. Bolcun-Filas, *A Mouse Geneticist's Practical Guide to CRISPR Applications.* Genetics, 2015. **199**(1): p. 1-15.

133. Nagano, M., et al., *Lentiviral vector transduction of male germ line stem cells in mice.* FEBS Lett, 2002. **524**(1-3): p. 111-5.

134. Hamra, F.K., et al., *Production of transgenic rats by lentiviral transduction of male germ-line stem cells.* Proc Natl Acad Sci U S A, 2002. **99**(23): p. 14931-6.

135. Takehashi, M., et al., *Adenovirus-mediated gene delivery into mouse spermatogonial stem cells.* Proc Natl Acad Sci U S A, 2007. **104**(8): p. 2596-601.

136. Watanabe, S., et al., *Adeno-associated virus-mediated delivery of genes to mouse spermatogonial stem cells.* Biol Reprod, 2017. **96**(1): p. 221-231.

137. Platt, R.J., et al., *CRISPR-Cas9 knockin mice for genome editing and cancer modeling.* Cell, 2014. **159**(2): p. 440-55.

138. Honaramooz, A., et al., *Adeno-associated virus (AAV)-mediated transduction of male germ line stem cells results in transgene transmission after germ cell transplantation.* FASEB J, 2008. **22**(2): p. 374-82.

139. Thomson, J.A., et al., *Embryonic stem cell lines derived from human blastocysts.* Science, 1998. **282**(5391): p. 1145-7.

140. Toyooka, Y., et al., *Embryonic stem cells can form germ cells in vitro.* Proc Natl Acad Sci U S A, 2003. **100**(20): p. 11457-62.

141. Clark, A.T., et al., *Spontaneous differentiation of germ cells from human embryonic stem cells in vitro.* Hum Mol Genet, 2004. **13**(7): p. 727-39.

142. Geijsen, N., et al., *Derivation of embryonic germ cells and male gametes from embryonic stem cells.* Nature, 2004. **427**(6970): p. 148-54.

143. Hubner, K., et al., *Derivation of oocytes from mouse embryonic stem cells.* Science, 2003. **300**(5623): p. 1251-6.

144. Daley, G.Q., *Gametes from embryonic stem cells: a cup half empty or half full?* Science, 2007. **316**(5823): p. 409-10.

145. Hooley, R.P., et al., *Intra-testicular injection of adenoviral constructs results in Sertoli cell-specific gene expression and disruption of the seminiferous epithelium.* Reproduction, 2009. **137**(2): p. 361-70.

146. Handel, M.A., J.J. Eppig, and J.C. Schimenti, *Applying "gold standards" to in-vitro-derived germ cells.* Cell, 2014. **157**(6): p. 1257-61.

147. Nayernia, K., et al., *Stem cell based therapeutical approach of male infertility by teratocarcinoma derived germ cells.* Hum Mol Genet, 2004. **13**(14): p. 1451-60.

148. Guan, K., et al., *Pluripotency of spermatogonial stem cells from adult mouse testis.* Nature, 2006. **440**(7088): p. 1199-1203.

149. Kee, K., et al., *Bone morphogenetic proteins induce germ cell differentiation from human embryonic stem cells.* Stem Cells Dev, 2006. **15**(6): p. 831-7.

150. West, F.D., et al., *KIT ligand and bone morphogenetic protein signaling enhances human embryonic stem cell to germ-like cell differentiation.* Hum Reprod, 2010. **25**(1): p. 168-78.

151. Tilgner, K., et al., *Isolation of primordial germ cells from differentiating human embryonic stem cells.* Stem Cells, 2008. **26**(12): p. 3075-85.

152. Bucay, N., et al., *A novel approach for the derivation of putative primordial germ cells and sertoli cells from human embryonic stem cells.* Stem Cells, 2009. **27**(1): p. 68-77.

153. Park, T.S., et al., *Derivation of primordial germ cells from human embryonic and induced pluripotent stem cells is significantly improved by coculture with human fetal gonadal cells.* Stem Cells, 2009. **27**(4): p. 783-95.

154. Kee, K., et al., *Human DAZL, DAZ and BOULE genes modulate primordial germ-cell and haploid gamete formation.* Nature, 2009. **462**(7270): p. 222-5.

155. Aflatoonian, B., et al., *In vitro post-meiotic germ cell development from human embryonic stem cells.* Hum Reprod, 2009. **24**(12): p. 3150-9.

156. West, F.D., et al., *Enrichment and differentiation of human germ-like cells mediated by feeder cells and basic fibroblast growth factor signaling.* Stem Cells, 2008. **26**(11): p. 2768-76.

157. Tilgner, K., et al., *Expression of GFP under the control of the RNA helicase VASA permits fluorescence-activated cell sorting isolation of human primordial germ cells.* Stem Cells, 2010. **28**(1): p. 84-92.

158. Eguizabal, C., et al., *Complete meiosis from human induced pluripotent stem cells.* Stem Cells, 2011. **29**(8): p. 1186-95.

159. Medrano, J.V., et al., *Divergent RNA-binding proteins, DAZL and VASA, induce meiotic progression in human germ cells derived in vitro.* Stem Cells, 2012. **30**(3): p. 441-51.

160. Easley, C.A.t., et al., *Direct differentiation of human pluripotent stem cells into haploid spermatogenic cells.* Cell reports, 2012. **2**(3): p. 440-6.

161. Ohinata, Y., et al., *A signaling principle for the specification of the germ cell lineage in mice.* Cell, 2009. **137**(3): p. 571-84.

162. Hayashi, K. and M.A. Surani, *Self-renewing epiblast stem cells exhibit continual delineation of germ cells with epigenetic reprogramming in vitro.* Development, 2009. **136**(21): p. 3549-56.

163. Hayashi, K., et al., *Reconstitution of the mouse germ cell specification pathway in culture by pluripotent stem cells.* Cell, 2011. **146**(4): p. 519-32.

164. Nakaki, F., et al., *Induction of mouse germ-cell fate by transcription factors in vitro.* Nature, 2013. **501**(7466): p. 222-6.

165. Sasaki, K., et al., *Robust In Vitro Induction of Human Germ Cell Fate from Pluripotent Stem Cells.* Cell Stem Cell, 2015. **17**(2): p. 178-94.

166. Irie, N., et al., *SOX17 is a critical specifier of human primordial germ cell fate.* Cell, 2015. **160**(1-2): p. 253-68.

167. Hayashi, K., et al., *Offspring from oocytes derived from in vitro primordial germ cell-like cells in mice.* Science, 2012. **338**(6109): p. 971-5.

168. Zhou, Q., et al., *Complete Meiosis from Embryonic Stem Cell-Derived Germ Cells In Vitro.* Cell Stem Cell, 2016. **18**(3): p. 330-40.

169. Morohaku, K., et al., *Complete in vitro generation of fertile oocytes from mouse primordial germ cells.* Proc Natl Acad Sci U S A, 2016. **113**(32): p. 9021-6.

170. Hikabe, O., et al., *Reconstitution in vitro of the entire cycle of the mouse female germ line.* Nature, 2016. **539**(7628): p. 299-303.

171. Hayashi, K. and M. Saitou, *Perspectives of germ cell development in vitro in mammals.* Anim Sci J, 2014. **85**(6): p. 617-26.

172. Brons, I.G.M., et al., *Derivation of pluripotent epiblast stem cells from mammalian embryos.* Nature, 2007. **448**(7150): p. 191-U7.

173. Han, D.W., et al., *Epiblast Stem Cell Subpopulations Represent Mouse Embryos of Distinct Pregastrulation Stages.* Cell, 2010. **143**(4): p. 617-627.

174. Kojima, Y., et al., *The Transcriptional and Functional Properties of Mouse Epiblast Stem Cells Resemble the Anterior Primitive Streak.* Cell Stem Cell, 2014. **14**(1): p. 107-120.

175. Smith, A.G., et al., *Inhibition of pluripotential embryonic stem cell differentiation by purified polypeptides.* Nature, 1988. **336**(6200): p. 688-90.

176. Williams, R.L., et al., *Myeloid leukaemia inhibitory factor maintains the developmental potential of embryonic stem cells.* Nature, 1988. **336**(6200): p. 684-7.

177. Hayashi, K., et al., *Dynamic equilibrium and heterogeneity of mouse pluripotent stem cells with distinct functional and epigenetic states.* Cell Stem Cell, 2008. **3**(4): p. 391-401.

178. Ying, Q.L., et al., *The ground state of embryonic stem cell self-renewal.* Nature, 2008. **453**(7194): p. 519-U5.

179. Tesar, P.J., et al., *New cell lines from mouse epiblast share defining features with human embryonic stem cells.* Nature, 2007. **448**(7150): p. 196-U10.

180. Guo, G., et al., *Klf4 reverts developmentally programmed restriction of ground state pluripotency.* Development, 2009. **136**(7): p. 1063-1069.

181. Okita, K., T. Ichisaka, and S. Yamanaka, *Generation of germline-competent induced pluripotent stem cells.* Nature, 2007. **448**(7151): p. 313-U1.

182. Takahashi, K., et al., *Induction of Pluripotent Stem Cells from Adult Human Fibroblasts by Defined Factors.* Cell, 2007. **131**(5): p. 861-872.

183. Yamashiro, C., et al., *Generation of human oogonia from induced pluripotent stem cells in vitro.* Science, 2018. **362**(6412): p. 356-360.

184. Durruthy Durruthy, J., et al., *Fate of induced pluripotent stem cells following transplantation to murine seminiferous tubules.* Hum Mol Genet, 2014. **23**(12): p. 3071-84.

185. Sosa, E., et al., *Differentiation of primate primordial germ cell-like cells following transplantation into the adult gonadal niche.* Nat Commun, 2018. **9**(1): p. 5339.

186. Cyranoski, D., *The CRISPR-baby scandal: what's next for human gene-editing.* Nature, 2019. **566**(7745): p. 440-442.

187. Wolf, D.P., P.A. Mitalipov, and S.M. Mitalipov, *Principles of and strategies for germline gene therapy.* Nat Med, 2019. **25**(6): p. 890-897.

188. National Academies of Sciences, E. and Medicine, *International Summit on Human Gene Editing: A Global Discussion*, ed. S. Olson. 2015, Washington, DC: The National Academies Press. 8.

189. Chan, S., et al., *Genome Editing Technologies and Human Germline Genetic Modification: The Hinxton Group Consensus Statement.* Am J Bioeth, 2015. **15**(12): p. 42-7.

190. National Academies of Sciences, E., and Medicine, *Human Genome Editing: Science, Ethics, and Governance*. 2017, Washington, DC: The National Academies Press.

191. Ormond, K.E., et al., *Human Germline Genome Editing.* Am J Hum Genet, 2017. **101**(2): p. 167-176.

192. Lander, E.S., et al., *Adopt a moratorium on heritable genome editing.* Nature, 2019. **567**(7747): p. 165-168.

193. Devroey, P., et al., *Pregnancies after testicular sperm extraction and intracytoplasmic sperm injection in non-obstructive azoospermia.* Hum Reprod, 1995. **10**(6): p. 1457-60.

194. Bernie, A.M., et al., *Comparison of microdissection testicular sperm extraction, conventional testicular sperm extraction, and testicular sperm aspiration for nonobstructive azoospermia: a systematic review and meta-analysis.* Fertil Steril, 2015. **104**(5): p. 1099-103 e1-3.

195. Ishikawa, T., et al., *Learning curves of microdissection testicular sperm extraction for nonobstructive azoospermia.* Fertil Steril, 2010. **94**(3): p. 1008-11.

196. Tsujimura, A., et al., *Conventional multiple or microdissection testicular sperm extraction: a comparative study.* Hum Reprod, 2002. **17**(11): p. 2924-9.

197. Kahraman, S., et al., *Fertility with testicular sperm extraction and intracytoplasmic sperm injection in non-obstructive azoospermic men.* Hum Reprod, 1996. **11**(4): p. 756-60.

198. Mulhall, J.P., et al., *Presence of mature sperm in testicular parenchyma of men with nonobstructive azoospermia: prevalence and predictive factors.* Urology, 1997. **49**(1): p. 91-5; discussion 95-6.

199. Ezeh, U.I., H.D. Moore, and I.D. Cooke, *A prospective study of multiple needle biopsies versus a single open biopsy for testicular sperm extraction in men with non-obstructive azoospermia.* Hum Reprod, 1998. **13**(11): p. 3075-80.

200. Seo, J.T. and W.J. Ko, *Predictive factors of successful testicular sperm recovery in non-obstructive azoospermia patients.* Int J Androl, 2001. **24**(5): p. 306-10.

201. Friedler, S., et al., *Outcome of first and repeated testicular sperm extraction and ICSI in patients with non-obstructive azoospermia.* Hum Reprod, 2002. **17**(9): p. 2356-61.

202. Bettella, A., et al., *Testicular fine needle aspiration as a diagnostic tool in non-obstructive azoospermia.* Asian J Androl, 2005. **7**(3): p. 289-94.

203. Koscinski, I., et al., *Seminal haploid cell detection by flow cytometry in non-obstructive azoospermia: a good predictive parameter for testicular sperm extraction.* Hum Reprod, 2005. **20**(7): p. 1915-20.

204. Nagata, Y., et al., *Seminal plasma inhibin-B level is a useful predictor of the success of conventional testicular sperm extraction in patients with non-obstructive azoospermia.* J Obstet Gynaecol Res, 2005. **31**(5): p. 384-8.

205. Ramasamy, R., N. Yagan, and P.N. Schlegel, *Structural and functional changes to the testis after conventional versus microdissection testicular sperm extraction.* Urology, 2005. **65**(6): p. 1190-4.

206. Hauser, R., et al., *Comparison of efficacy of two techniques for testicular sperm retrieval in nonobstructive azoospermia: multifocal testicular sperm extraction versus multifocal testicular sperm aspiration.* J Androl, 2006. **27**(1): p. 28-33.

207. Vernaeve, V., et al., *How successful is repeat testicular sperm extraction in patients with azoospermia?* Hum Reprod, 2006. **21**(6): p. 1551-4.

208. Colpi, G.M., et al., *Microsurgical TESE versus conventional TESE for ICSI in non-obstructive azoospermia: a randomized controlled study.* Reprod Biomed Online, 2009. **18**(3): p. 315-9.

209. Ghalayini, I.F., et al., *Clinical comparison of conventional testicular sperm extraction and microdissection techniques for non-obstructive azoospermia.* J Clin Med Res, 2011. **3**(3): p. 124-31.

210. Nowroozi, M.R., et al., *In Vitro Colonization of Human Spermatogonia Stem Cells: Effect of Patient's Clinical Characteristics and Testicular Histologic Findings.* Urology, 2011. **78**(5): p. 1075-1081.

211. Weedin, J.W., et al., *Early Versus Late Maturation Arrest: Reproductive Outcomes of Testicular Failure.* The Journal of Urology, 2011. **186**(2): p. 621-626.

212. Dadkhah, F., et al., *Optimal number of biopsies and impact of testicular histology on the outcome of testicular sperm extraction.* Urol J, 2013. **10**(1): p. 795-801.

213. Sacca, A., et al., *Conventional testicular sperm extraction (TESE) and non-obstructive azoospermia: is there still a chance in the era of microdissection TESE? Results from a single non-academic community hospital.* Andrology, 2016. **4**(3): p. 425-9.

214. Caroppo, E., et al., *Testicular histology may predict the successful sperm retrieval in patients with non-obstructive azoospermia undergoing conventional TESE: a diagnostic accuracy study.* J Assist Reprod Genet, 2017. **34**(1): p. 149-154.

215. Maglia, E., et al., *Clinical comparison between conventional and microdissection testicular sperm extraction for non-obstructive azoospermia: Understanding which treatment works for which patient.* Arch Ital Urol Androl, 2018. **90**(2): p. 130-135.

216. Okada, H., et al., *Conventional versus microdissection testicular sperm extraction for nonobstructive azoospermia.* J Urol, 2002. **168**(3): p. 1063-7.

217. Liberati, A., et al., *The PRISMA statement for reporting systematic reviews and meta-analyses of studies that evaluate healthcare interventions: explanation and elaboration.* BMJ, 2009. **339**: p. b2700.

218. Nyaga, V.N., M. Arbyn, and M. Aerts, *Metaprop: a Stata command to perform meta-analysis of binomial data.* Arch Public Health, 2014. **72**(1): p. 39.

219. Tournaye, H., et al., *Are there any predictive factors for successful testicular sperm recovery in azoospermic patients?* Hum Reprod, 1997. **12**(1): p. 80-6.

220. Silber, S.J., et al., *The use of epididymal and testicular spermatozoa for intracytoplasmic sperm injection: the genetic implications for male infertility.* Hum Reprod, 1995. **10**(8): p. 2031-43.

221. Ferras, C., et al., *AZF and DAZ gene copy-specific deletion analysis in maturation arrest and Sertoli cell-only syndrome.* Mol Hum Reprod, 2004. **10**(10): p. 755-61.

222. Altuner, D., et al., *The effect of mirtazapine on cisplatin-induced oxidative damage and infertility in rat ovaries.* ScientificWorldJournal, 2013. **2013**: p. 327240.

223. El-Haggar, S., et al., *Fine needle aspiration vs. mTESE in non-obstructive azoospermia.* Int J Androl, 2008. **31**(6): p. 595-601.

224. Song, S.H., et al., *Natural course of severe oligozoospermia in infertile male: influence on future fertility potential.* J Androl, 2010. **31**(6): p. 536-9.

225. Kalsi, J., et al., *In the era of micro-dissection sperm retrieval (m-TESE) is an isolated testicular biopsy necessary in the management of men with non-obstructive azoospermia?* BJU Int, 2012. **109**(3): p. 418-24.

226. Berookhim, B.M., et al., *Microdissection testicular sperm extraction in men with Sertoli cell-only testicular histology.* Fertil Steril, 2014. **102**(5): p. 1282-6.

227. Cetinkaya, M., et al., *Evaluation of Microdissection Testicular Sperm Extraction Results in Patients with Non-Obstructive Azoospermia: Independent Predictive Factors and Best Cutoff Values for Sperm Retrieval.* Urol J, 2015. **12**(6): p. 2436-43.

228. Enatsu, N., et al., *Predictive factors of successful sperm retrieval on microdissection testicular sperm extraction in Japanese men.* Reprod Med Biol, 2016. **15**(1): p. 29-33.

229. Binsaleh, S., D. Alhajeri, and K. Madbouly, *Microdissection testicular sperm extraction in men with nonobstructive azoospermia: Experience of King Saud University Medical City, Riyadh, Saudi Arabia.* Urol Ann, 2017. **9**(2): p. 136-140.

230. Eken, A. and F. Gulec, *Microdissection testicular sperm extraction (micro-TESE): Predictive value of preoperative hormonal levels and pathology in non-obstructive azoospermia.* Kaohsiung J Med Sci, 2018. **34**(2): p. 103-108.

231. Yu, Y., et al., *Heterogenicity of testicular histopathology and tubules as a predictor of successful microdissection testicular sperm extraction in men with nonobstructive azoospermia.* Medicine (Baltimore), 2018. **97**(22): p. e10914.

232. Amer, M.K., et al., *Can spermatozoa be retrieved in non-obstructive azoospermic patients with high FSH level?: A retrospective cohort study.* Andrologia, 2019. **51**(2): p. e13176.

233. Chan, P.T.K. and P.N. Schlegel, *Nonobstructive azoospermia.* Current Opinion in Urology, 2000. **10**(6): p. 617-624.

234. Silber, S.J., et al., *Distribution of spermatogenesis in the testicles of azoospermic men: the presence or absence of spermatids in the testes of men with germinal failure.* Human Reproduction, 1997. **12**(11): p. 2422-2428.

235. Aiman, J., et al., *Androgen insensitivity as a cause of infertility in otherwise normal men.* N Engl J Med, 1979. **300**(5): p. 223-7.

236. Xu, J., et al., *A novel functional variant in Wilms' Tumor 1 (WT1) is associated with idiopathic non-obstructive azoospermia.* Mol Reprod Dev, 2017. **84**(3): p. 222-228.

237. Massin, N., et al., *Healthy birth after testicular extraction of sperm and ICSI from an azoospermic man with mild androgen insensitivity syndrome caused by an androgen receptor partial loss-of-function mutation.* Clinical Endocrinology, 2012. **77**(4): p. 593-598.

238. Mirfakhraie, R., et al., *A Novel Mutation in the Transactivation-Regulating Domain of the Androgen Receptor in a Patient With Azoospermia.* Journal of Andrology, 2011. **32**(4): p. 367-370.

239. Baltimore, D., et al., *A prudent path forward for genomic engineering and germline gene modification.* Science, 2015. **348**(6230): p. 36-38.

240. Porteus, M.H. and C.T. Dann, *Genome editing of the germline: broadening the discussion.* Mol Ther, 2015. **23**(6): p. 980-2.

241. Kanatsu-Shinohara, M., et al., *Adenovirus-mediated gene delivery and in vitro microinsemination produce offspring from infertile male mice.* Proc Natl Acad Sci U S A, 2002. **99**(3): p. 1383-8.

242. Ikawa, M., et al., *Restoration of spermatogenesis by lentiviral gene transfer: offspring from infertile mice.* Proc Natl Acad Sci U S A, 2002. **99**(11): p. 7524-9.

243. Yomogida, K., Y. Yagura, and Y. Nishimune, *Electroporated transgene-rescued spermatogenesis in infertile mutant mice with a sertoli cell defect.* Biol Reprod, 2002. **67**(3): p. 712-7.

244. Zazo Seco, C., et al., *Allelic Mutations of KITLG, Encoding KIT Ligand, Cause Asymmetric and Unilateral Hearing Loss and Waardenburg Syndrome Type 2.* Am J Hum Genet, 2015. **97**(5): p. 647-60.

245. Fleischman, R.A., et al., *Deletion of the c-kit protooncogene in the human developmental defect piebald trait.* Proc Natl Acad Sci U S A, 1991. **88**(23): p. 10885-9.

246. Lee, C.S., et al., *Adenovirus-Mediated Gene Delivery: Potential Applications for Gene and Cell-Based Therapies in the New Era of Personalized Medicine.* Genes Dis, 2017. **4**(2): p. 43-63.

247. Cohen, C.J., et al., *The coxsackievirus and adenovirus receptor is a transmembrane component of the tight junction.* Proc Natl Acad Sci U S A, 2001. **98**(26): p. 15191-6.

248. Ogawa, T., et al., *Transplantation of testis germinal cells into mouse seminiferous tubules.* Int J Dev Biol, 1997. **41**(1): p. 111-22.

249. Yoshida, N. and A.C. Perry, *Piezo-actuated mouse intracytoplasmic sperm injection (ICSI).* Nat Protoc, 2007. **2**(2): p. 296-304.

250. Walker, W.H., et al., *Restoration of spermatogenesis and male fertility using an androgen receptor transgene.* PLoS One, 2015. **10**(3): p. e0120783.

251. Meng, J., et al., *Androgens regulate the permeability of the blood-testis barrier.* Proc Natl Acad Sci U S A, 2005. **102**(46): p. 16696-700.

252. Brinster, R.L. and J.W. Zimmermann, *Spermatogenesis following male germ-cell transplantation.* Proc Natl Acad Sci U S A, 1994. **91**(24): p. 11298-302.

253. Brinster, R.L. and M.R. Avarbock, *Germline transmission of donor haplotype following spermatogonial transplantation.* Proc Natl Acad Sci U S A, 1994. **91**(24): p. 11303-7.

254. Kerr, J.B., et al., *Response of the seminiferous epithelium of the rat testis to withdrawal of androgen: evidence for direct effect upon intercellular spaces associated with Sertoli cell junctional complexes.* Cell Tissue Res, 1993. **274**(1): p. 153-61.

255. Creasy, D.M., *Pathogenesis of male reproductive toxicity.* Toxicol Pathol, 2001. **29**(1): p. 64-76.

256. Meng, J., et al., *Sertoli cell-specific deletion of the androgen receptor compromises testicular immune privilege in mice.* Biol Reprod, 2011. **85**(2): p. 254-60.

257. Lakschevitz, F.S., et al., *Identification of neutrophil surface marker changes in health and inflammation using high-throughput screening flow cytometry.* Exp Cell Res, 2016. **342**(2): p. 200-9.

258. Pulford, K.A., et al., *Distribution of the CD68 macrophage/myeloid associated antigen.* Int Immunol, 1990. **2**(10): p. 973-80.

259. Kung, P., et al., *Monoclonal antibodies defining distinctive human T cell surface antigens.* Science, 1979. **206**(4416): p. 347-9.

260. Bergelson, J.M., et al., *Isolation of a common receptor for Coxsackie B viruses and adenoviruses 2 and 5.* Science, 1997. **275**(5304): p. 1320-3.

261. Tomko, R.P., R. Xu, and L. Philipson, *HCAR and MCAR: the human and mouse cellular receptors for subgroup C adenoviruses and group B coxsackieviruses.* Proc Natl Acad Sci U S A, 1997. **94**(7): p. 3352-6.

262. Roelvink, P.W., et al., *The coxsackievirus-adenovirus receptor protein can function as a cellular attachment protein for adenovirus serotypes from subgroups A, C, D, E, and F.* (0022-538X (Print)).

263. Mirza, M., et al., *Coxsackievirus and adenovirus receptor is up-regulated in migratory germ cells during passage of the blood-testis barrier.* Endocrinology, 2007. **148**(11): p. 5459-69.

264. Wang, C.Q.F., et al., *Coxsackie and adenovirus receptor (CAR) is a product of Sertoli and germ cells in rat testes which is localized at the Sertoli-Sertoli and Sertoli-germ cell interface.* Experimental cell research, 2007. **313**(7): p. 1373-1392.

265. Sharma, A., et al., *Adenovirus receptors and their implications in gene delivery.* Virus research, 2009. **143**(2): p. 184-194.

266. Sharma, P., et al., *Accessibility of the coxsackievirus and adenovirus receptor and its importance in adenovirus gene transduction efficiency.* J Gen Virol, 2012. **93**(Pt 1): p. 155-8.

267. Zhang, Y. and J.M. Bergelson, *Adenovirus receptors.* J Virol, 2005. **79**(19): p. 12125-31.

268. Stephen, S.L., et al., *Chromosomal Integration of Adenoviral Vector DNA In Vivo.* Journal of Virology, 2010. **84**(19): p. 9987-9994.

269. Yang, Y., et al., *Immune responses to viral antigens versus transgene product in the elimination of recombinant adenovirus-infected hepatocytes in vivo.* Gene Ther, 1996. **3**(2): p. 137-44.

270. Yang, Y., Q. Su, and J.M. Wilson, *Role of viral antigens in destructive cellular immune responses to adenovirus vector-transduced cells in mouse lungs.* J Virol, 1996. **70**(10): p. 7209-12.

271. Thomson, B.J., *Viruses and apoptosis.* Int J Exp Pathol, 2001. **82**(2): p. 65-76.

272. Sultana, T., et al., *Mice depleted of the coxsackievirus and adenovirus receptor display normal spermatogenesis and an intact blood-testis barrier.* Reproduction, 2014. **147**(6): p. 875-83.

273. Su, L., D.D. Mruk, and C.Y. Cheng, *Regulation of the blood-testis barrier by coxsackievirus and adenovirus receptor.* Am J Physiol Cell Physiol, 2012. **303**(8): p. C843-53.

274. Ehrhardt, A., H. Xu, and M.A. Kay, *Episomal persistence of recombinant adenoviral vector genomes during the cell cycle in vivo.* J Virol, 2003. **77**(13): p. 7689-95.

275. Hazra, R., et al., *Elevated expression of the Sertoli cell androgen receptor disrupts male fertility.* Am J Physiol Endocrinol Metab, 2016. **311**(2): p. E396-404.

276. Kanatsu-Shinohara, M., et al., *Functional assessment of self-renewal activity of male germline stem cells following cytotoxic damage and serial transplantation.* Biol Reprod, 2003. **68**(5): p. 1801-7.

277. Kanatsu-Shinohara, M., et al., *Genetic and epigenetic properties of mouse male germline stem cells during long-term culture.* Development, 2005. **132**(18): p. 4155-63.

278. Miyamoto, T., et al., *Single-nucleotide polymorphisms in HORMAD1 may be a risk factor for azoospermia caused by meiotic arrest in Japanese patients.* Asian journal of andrology, 2012. **14**(4): p. 580.

279. Song, B., et al., *Association of genetic variants in SOHLH1 and SOHLH2 with non-obstructive azoospermia risk in the Chinese population.* European Journal of Obstetrics & Gynecology and Reproductive Biology, 2015. **184**: p. 48-52.

280. Chen, S.R. and Y.X. Liu, *Regulation of spermatogonial stem cell self-renewal and spermatocyte meiosis by Sertoli cell signaling.* Reproduction, 2015. **149**(4): p. R159-67.

281. Ali, R.H., et al., *Exome sequencing revealed a novel biallelic deletion in the DCAF17 gene underlying Woodhouse Sakati syndrome.* Clinical genetics, 2016. **90**(3): p. 263-269.

282. Ayhan, Ö., et al., *Truncating mutations in TAF4B and ZMYND15 causing recessive azoospermia.* Journal of medical genetics, 2014. **51**(4): p. 239-244.

283. Gershoni, M., et al., *A familial study of azoospermic men identifies three novel causative mutations in three new human azoospermia genes.* Genetics in Medicine, 2017. **19**(9): p. 998-1006.

284. Okutman, O., et al., *Exome sequencing reveals a nonsense mutation in TEX15 causing spermatogenic failure in a Turkish family.* Human molecular genetics, 2015. **24**(19): p. 5581-5588.

285. Arafat, M., et al., *Mutation in TDRD9 causes non-obstructive azoospermia in infertile men.* Journal of Medical Genetics, 2017. **54**(9): p. 633-639.

286. Kherraf, Z.E., et al., *SPINK2 deficiency causes infertility by inducing sperm defects in heterozygotes and azoospermia in homozygotes.* EMBO molecular medicine, 2017. **9**(8): p. 1132-1149.

287. Al-Agha, A.E., et al., *Primary ovarian insufficiency and azoospermia in carriers of a homozygous PSMC3IP stop gain mutation.* The Journal of Clinical Endocrinology & Metabolism, 2018. **103**(2): p. 555-563.

288. Oatley, J.M., et al., *Identifying genes important for spermatogonial stem cell self-renewal and survival.* Proc Natl Acad Sci U S A, 2006. **103**(25): p. 9524-9.

289. Kanatsu-Shinohara, M., et al., *Improved serum- and feeder-free culture of mouse germline stem cells.* Biol Reprod, 2014. **91**(4): p. 88.

290. Sato, T., et al., *Genome Editing in Mouse Spermatogonial Stem Cell Lines Using TALEN and Double-Nicking CRISPR/Cas9.* Stem Cell Reports, 2015. **5**(1): p. 75-82.

291. Tamm, C., S.P. Galitó, and C. Annerén, *A comparative study of protocols for mouse embryonic stem cell culturing.* PloS one, 2013. **8**(12).

292. Kanatsu-Shinohara, M., et al., *Production of knockout mice by random or targeted mutagenesis in spermatogonial stem cells.* Proc Natl Acad Sci U S A, 2006. **103**(21): p. 8018-23.

293. Kanatsu-Shinohara, M., S. Toyokuni, and T. Shinohara, *Genetic selection of mouse male germline stem cells in vitro: offspring from single stem cells.* Biology of reproduction, 2005. **72**(1): p. 236-240.

294. Werth, S., et al., *A low molecular weight fraction of polyethylenimine (PEI) displays increased transfection efficiency of DNA and siRNA in fresh or lyophilized complexes.* J Control Release, 2006. **112**(2): p. 257-70.

295. Hsu, C.Y. and H. Uludag, *A simple and rapid nonviral approach to efficiently transfect primary tissue-derived cells using polyethylenimine.* Nat Protoc, 2012. **7**(5): p. 935-45.

296. Lungwitz, U., et al., *Polyethylenimine-based non-viral gene delivery systems.* Eur J Pharm Biopharm, 2005. **60**(2): p. 247-66.

297. Wightman, L., et al., *Different behavior of branched and linear polyethylenimine for gene delivery in vitro and in vivo.* J Gene Med, 2001. **3**(4): p. 362-72.

298. Boussif, O., et al., *A versatile vector for gene and oligonucleotide transfer into cells in culture and in vivo: polyethylenimine.* Proc Natl Acad Sci U S A, 1995. **92**(16): p. 7297-301.

299. Sonawane, N.D., F.C. Szoka, Jr., and A.S. Verkman, *Chloride accumulation and swelling in endosomes enhances DNA transfer by polyamine-DNA polyplexes.* J Biol Chem, 2003. **278**(45): p. 44826-31.

300. Godbey, W.T., K.K. Wu, and A.G. Mikos, *Tracking the intracellular path of poly(ethylenimine)/DNA complexes for gene delivery.* Proc Natl Acad Sci U S A, 1999. **96**(9): p. 5177-81.

301. Kopatz, I., J.S. Remy, and J.P. Behr, *A model for non-viral gene delivery: through syndecan adhesion molecules and powered by actin.* J Gene Med, 2004. **6**(7): p. 769-76.

302. Akinc, A., et al., *Exploring polyethylenimine-mediated DNA transfection and the proton sponge hypothesis.* J Gene Med, 2005. **7**(5): p. 657-63.

303. Grandinetti, G. and T.M. Reineke, *Exploring the mechanism of plasmid DNA nuclear internalization with polymer-based vehicles.* Mol Pharm, 2012. **9**(8): p. 2256-67.

304. Han, X., et al., *The heterogeneous nature of polyethylenimine-DNA complex formation affects transient gene expression.* Cytotechnology, 2009. **60**(1-3): p. 63.

305. Clamme, J.P., J. Azoulay, and Y. Mely, *Monitoring of the formation and dissociation of polyethylenimine/DNA complexes by two photon fluorescence correlation spectroscopy.* Biophys J, 2003. **84**(3): p. 1960-8.

306. Kunath, T., et al., *Transgenic RNA interference in ES cell-derived embryos recapitulates a genetic null phenotype.* Nat Biotechnol, 2003. **21**(5): p. 559-61.

307. Derouazi, M., et al., *Serum-free large-scale transient transfection of CHO cells.* Biotechnol Bioeng, 2004. **87**(4): p. 537-45.

308. Collins, M. and A. Thrasher, *Gene therapy: progress and predictions.* Proceedings of the Royal Society B: Biological Sciences, 2015. **282**(1821).

309. Scheufele, D.A., et al., *U.S. attitudes on human genome editing.* Science, 2017. **357**(6351): p. 553-554.

310. Kubota, H., M.R. Avarbock, and R.L. Brinster, *Culture conditions and single growth factors affect fate determination of mouse spermatogonial stem cells.* Biol Reprod, 2004. **71**(3): p. 722-31.

311. Hermann, B.P., et al., *Spermatogonial Stem Cell Transplantation into Rhesus Testes Regenerates Spermatogenesis Producing Functional Sperm.* Cell Stem Cell, 2012. **11**(5): p. 715-726.

312. Shetty, G., et al., *Hormone suppression with GnRH antagonist promotes spermatogenic recovery from transplanted spermatogonial stem cells in irradiated cynomolgus monkeys.* Andrology, 2013. **1**(6): p. 886-898.

313. Shetty, G., et al., *Effect of hormone modulations on donor-derived spermatogenesis or colonization after syngeneic and xenotransplantation in mice.* Andrology, 2018.

314. Ma, H., et al., *Correction of a pathogenic gene mutation in human embryos.* Nature, 2017. **548**: p. 413.

315. Raposo, V.L., *Gene Editing, the Mystic Threat to Human Dignity.* J Bioeth Inq, 2019. **16**(2): p. 249-257.

316. Kang, H.S., et al., *Transcription Factor GLIS3: A New and Critical Regulator of Postnatal Stages of Mouse Spermatogenesis.* Stem Cells, 2016.

317. David, S. and K.E. Orwig, *Spermatogonial Stem Cell Culture in Oncofertility.* Urol Clin North Am, 2020. **47**(2): p. 227-244.

318. Chu, V.T., et al., *Increasing the efficiency of homology-directed repair for CRISPR-Cas9-induced precise gene editing in mammalian cells.* Nat Biotech, 2015. **33**(5): p. 543-548.

319. Maruyama, T., et al., *Increasing the efficiency of precise genome editing with CRISPR-Cas9 by inhibition of nonhomologous end joining.* Nat Biotech, 2015. **33**(5): p. 538-542.

320. Chen, F., et al., *High-frequency genome editing using ssDNA oligonucleotides with zinc-finger nucleases.* Nat Methods, 2011. **8**(9): p. 753-5.

321. Rong, Z., et al., *Homologous recombination in human embryonic stem cells using CRISPR/Cas9 nickase and a long DNA donor template.* Protein Cell, 2014. **5**(4): p. 258-60.

322. Sato, T., et al., *In vitro sperm production from mouse spermatogonial stem cell lines using an organ culture method.* Nat Protoc, 2013. **8**(11): p. 2098-104.

323. Qin, J.Y., et al., *Systematic comparison of constitutive promoters and the doxycycline-inducible promoter.* PLoS One, 2010. **5**(5): p. e10611.

324. Suzuki, H., C.T. Dann, and A. Rajkovic, *Generation of a germ cell-specific mouse transgenic cherry reporter, Sohlh1-mCherryFlag.* Genesis, 2013. **51**(1): p. 50-58.

325. Hong, S., et al., *Functional analysis of various promoters in lentiviral vectors at different stages of in vitro differentiation of mouse embryonic stem cells.* Mol Ther, 2007. **15**(9): p. 1630-9.

326. Kubota, H. and R.L. Brinster, *Technology Insight: in vitro culture of spermatogonial stem cells and their potential therapeutic uses.* Nature Clinical Practice Endocrinology & Metabolism, 2006. **2**(2): p. 99-108.

327. Goharbakhsh, L., et al., *Isolation and culture of human spermatogonial stem cells derived from testis biopsy.* Avicenna J Med Biotechnol, 2013. **5**(1): p. 54-61.

328. Kokkinaki, M., A. Djourabtchi, and N. Golestaneh, *Long-term culture of human SSEA-4 positive spermatogonial stem cells (SSCs).* Journal of stem cell research and therapy, 2011. **S2**: p. 003.

329. Medrano, J.V., et al., *Human spermatogonial stem cells display limited proliferation in vitro under mouse spermatogonial stem cell culture conditions.* Fertil Steril, 2016.

330. Takahashi, K. and S. Yamanaka, *Induction of pluripotent stem cells from mouse embryonic and adult fibroblast cultures by defined factors.* Cell., 2006. **126**(4): p. 663-676.

331. Irie, N. and M.A. Surani, *Efficient Induction and Isolation of Human Primordial Germ Cell-Like Cells from Competent Human Pluripotent Stem Cells.* Methods Mol Biol, 2017. **1463**: p. 217-226.

332. Hayashi, K. and M. Saitou, *Generation of eggs from mouse embryonic stem cells and induced pluripotent stem cells.* Nat Protoc, 2013. **8**(8): p. 1513-24.

333. Carey, B.W., et al., *Reprogramming of murine and human somatic cells using a single polycistronic vector.* Proc Natl Acad Sci U S A, 2009. **106**(1): p. 157-62.

334. Wesselschmidt, R.L., *The teratoma assay: an in vivo assessment of pluripotency.* Methods Mol Biol, 2011. **767**: p. 231-41.

335. Ramathal, C., et al., *Fate of iPSCs derived from azoospermic and fertile men following xenotransplantation to murine seminiferous tubules.* Cell Rep, 2014. **7**(4): p. 1284-97.

336. Vloeberghs, V., G. Verheyen, and H. Tournaye, *Intracytoplasmic spermatid injection and in vitro maturation: fact or fiction?* Clinics, 2013. **68**: p. 151-156.

337. Tanaka, A., et al., *Fourteen babies born after round spermatid injection into human oocytes.* Proc Natl Acad Sci U S A, 2015. **112**(47): p. 14629-34.